R. & M. No. 2906
(15,152)
A.R.C. Monograph

MINISTRY OF SUPPLY

AERONAUTICAL RESEARCH COUNCIL
REPORTS AND MEMORANDA

The Spinning of Model Aircraft and the Prediction of Full-Scale Spin and Recovery Characteristics

BY

G. E. PRINGLE, Ph.D., and D. J. HARPER, B.Sc.

LONDON: HER MAJESTY'S STATIONERY OFFICE

PRICE £1 15*s* 0*d* NET

MINISTRY OF SUPPLY

AERONAUTICAL RESEARCH COUNCIL

REPORTS AND MEMORANDA

The Spinning of Model Aircraft and the Prediction of Full-Scale Spin and Recovery Characteristics

By

G. E. PRINGLE, Ph.D. and D. J. HARPER, B.Sc.

LONDON: HER MAJESTY'S STATIONERY OFFICE
1956

Printed and published by
HER MAJESTY'S STATIONERY OFFICE
To be purchased from
York House, Kingsway, London W.C.2
423 Oxford Street, London W.1
P.O. Box 569, London S.E.1
13A Castle Street, Edinburgh 2
109 St. Mary Street, Cardiff
39 King Street, Manchester 2
Tower Lane, Bristol 1
2 Edmund Street, Birmingham 3
80 Chichester Street, Belfast
or through any bookseller

Printed in Great Britain

CONTENTS

LIST OF TABLES

LIST OF ILLUSTRATIONS

LIST OF ILLUSTRATIONS—*continued.*

LIST OF ILLUSTRATIONS—*continued.*

The Spinning of Model Aircraft and the Prediction of Full-Scale Spin and Recovery Characteristics

By

G. H. PRINGLE, Ph.D. *and* D. J. HARPER, B.Sc.

COMMUNICATED BY THE PRINCIPAL DIRECTOR OF SCIENTIFIC RESEARCH (AIR), MINISTRY OF SUPPLY

*Reports and Memoranda No. 2906**
March, 1952

Summary.—The report discusses some technical aspects of a long series of tests made with dynamic scale model aircraft in the Royal Aircraft Establishment Vertical Tunnel for the purpose of studying their spinning characteristics. Data accumulated up to the end of 1947 are included, and mention is made, where appropriate, of any further work done up to the end of 1949. The central problem is that of drawing valid conclusions regarding the full-scale spin and recovery; with this in mind there is some discussion of the sensitivity of the spinning model to applied forces including those that upset the spin to produce recovery and those that alternatively generate a new spin. The difference between model- and full-scale spins is analysed with a view to correcting the model data, and some attention is given to power-on spins. A chapter is given to special aspects of the spin of tailless aircraft, and another to safety devices.

CHAPTER I

Introduction

In 1939 it was already thought possible to predict from a careful inspection of design, the probable spinning characteristics of any conventional type of aeroplane. A casual examination of the problem might therefore suggest that for practical purposes all the designer had to do, to ensure safety in spinning, was to provide an ample margin of those quantities which previous experience had shown to be favourable. (By ' safety ' we mean, the ability to recover from a spin at will, and ' favourable ' implies favouring recovery and not the continuance of spinning.) A closer examination soon disappoints such a belief. When an aeroplane has been designed to satisfy the requirements of ordinary flight, there may be quite a small margin of variation within which the essential external form and control surfaces can be adjusted in any efforts to meet a secondary requirement. Spinning, for better or worse, has receded into the background as a tactical manœuvre, but the possibility of a spin occurring accidentally during other manœuvres is too dangerous to ignore. The task of the designer and technician is therefore that of trying to meet certain requirements in the spinning behaviour of the aeroplane, without appreciably upsetting the stability in ordinary flight, or the aircraft's weight or performance. That trend in design which makes the stabilising and control surfaces as small as possible consistent with stability, is broadly contrary to the principles of design likely to result in a satisfactory recovery from spins, and so the requirements for safety are likely to be met, if at all, with only small margins in hand. In these circumstances the closest possible estimate of full-scale behaviour in the spin is necessary, and it is needed before actual flight trials, if possible even before the construction of the aircraft. What we now know as the design criteria for good recovery from spins are inadequate, in that their guidance can at most separate the very good from the very bad spinning types, whilst leaving a substantial doubt about cases near the borderline of safety. It is believed that a

*R.A.E. Report Aero. 2456—received 26 August, 1952.

somewhat finer mesh is provided by the tunnel tests which provide the subject matter of much of this account, and which are established as a routine method of investigation. In these tests the motion of a spinning aircraft is simulated by a model loaded to a state of dynamical similarity, the flight of which is studied as it freely spins in a vertically ascending wind stream. The information obtained in this way can never replace flight trials as the final test of the aircraft's behaviour, but owes its importance to the fact that it can be obtained in advance.

The primary task of model-spinning research has therefore been the routine testing of new designs. This does not apply equally to all new designs, but only to those that are most likely to spin in the course of their duties. The emphasis at present is rather upon accidental spins of short duration and on the need for pilots to be free to practise safely, during their training on aerobatic types of aircraft, the technique of recovery from such spins. Heavy aircraft are excluded from consideration, not so much because spins are unknown in operations, for unfortunately they are liable to occur during evasive manœuvres, but rather because the risk of structural failure or of uncontrollable stick forces usually overshadows the purely aerodynamic information that model tests are normally capable of giving. These points explain some of the reasons for the official policies on spinning expressed in Ministry of Supply Air Publication 970 (A.P. 970), where above a certain all-up weight the spinning requirements are relaxed unless the aircraft is a fighter, when it is obvious that its duties are such that the ability to recover from spins is desirable.

As with all tunnel tests, the real difficulty lies in the evaluation of the results, since at the outset the degree of applicability to full-scale conditions is quite unknown. The data of routine model tests are material for very instructive statistical investigations into their relation to full-scale trials, and one aim of research is to review this relationship and revise the conclusions as more data accumulate. Such an approach can give an empirical basis for working rules and procedure, but not a close insight into the underlying physical situation, and we are therefore impelled to seek improvement in the prediction of full-scale behaviour through a better tunnel technique which will give the fullest possible realism to the model tests. One avenue to this is simply the improvement of equipment and the increase of the Reynolds numbers of tests, but an equally fruitful one is the analysis of the aerodynamic forces in such a way as to expose the principal effects of scale. As a way to understanding the fundamentals of the spin, the rolling balance is probably unrivalled, and its replacement by the free-spinning tunnel was a move in favour of short-term research slightly to the detriment of long-range objectives.

As it is, the information given to designers must seem sometimes nebulous, sometimes even misleading. If it were not so, model-spinning research would hold no serious problems; therefore no attempt is made to present it as a closed chapter of achievement, but rather as an unfinished one.

The accurate prediction of spinning behaviour is, of course, only one side of the task. Another side is to ascertain, on each type considered, what is the best method of attempting recovery. Naturally there is an initial bias in favour of a standard method for all aircraft, but if the trend of design is unfavourable to good recovery then it is incumbent on us to examine all methods of control that may seem promising, even at the expense of uniformity of flight procedure. This does not commit the Royal Air Force in any way but such issues of policy are of course ultimately subject to knowledge of the facts.

A further set of problems arises in the consideration of safety in spinning in the wider sense including structural safety and manageable control forces. To investigate structural safety demands a rather detailed knowledge of the distribution of aerodynamic forces on the aircraft and also of the kinematics of spinning. This investigation was never a primary aim of free-model tests, but the accumulation of observations on which to base some of the simple dynamical formulae used in strength calculations has become a part of the tunnel work, and could be a more vital part if rolling balance and static model tests were included. But in no case can the prediction of flight characteristics rest with a knowledge that recovery is aerodynamically a possibility, if there is a substantial doubt that the aircraft may break before the attempt can be made, or during the recovery itself. Fortunately this has only rarely been a real danger on aerobatic aircraft, but the possibility of trouble has occasionally seemed ominously near. The prediction of the kinematics of the spin is discussed in Chapter V, and the control forces are referred to in Chapter VI. Control forces in the spin have not been the subject of research in this country, but information from the United States has helped to tide over the difficult period between the introduction of heavy fighters and the development of power assistance for controls.

This account surveys the work done on these and associated problems at the R.A.E. during the period beginning in mid-1939 and ending in mid-1947. Where further work has been done which amplifies or modifies the conclusions reached, brief mention is made of it, and references given where possible.

At the beginning of the period, emphasis was placed upon the prolonged spin in order that pilots should be able to practise spinning on all aerobatic types of aircraft; the incipient spin (2 turns) was covered by the argument that if recovery was possible from a spin of n turns, then recovery would also be possible from spins of less than n turns. The emphasis has gradually shifted until, at the time of publication, most aircraft are only required to recover from the incipient spin and we are really only trying to make the aircraft recover under these conditions. Unfortunately, very little investigation has been made into this complex initial motion, and as little experimental work has been done, this account concentrates on the prolonged, or steady spin. Where it is pertinent, comment has been made on the incipient spin aspects.

The subsequent chapters are intended to show bias towards fundamentals, but the main effort in the work of the vertical tunnel was dominated in recent years by the routine aspect; so to conclude this introduction, the following is a list of models made and tested in the period 1939–1947. The models are listed in order of testing.

TABLE I.I

List of Models Tested in the Vertical Tunnel, 1939 to 1947

Type	Contractor	R.A.E. Report No. or other Reference	Date of Report	Author(s) of Report
Tornado, Typhoon ..	Hawker	B.A. 1554 and Aero. 1819 ..	Oct. 1939 May 1945	— Pringle, V. G. Warren.
S.23/37	General Aircraft ..	B.A. 1560	Nov. 1939	—
Australian Trainer ..	—	B.A. Deptl. Note Wind Tunnels 394	June 1939	Finn. —
M.18	Phillips & Powis ..	B.A. 1611	July 1940	Finn, Bigg.
T4/39	Airspeed	Aero. 1734	Feb. 1942	—
F18/39	Martin-Baker	B.A. 1591	Apl. 1940	—
Tourist	Gloster	Aero. 1909	Jan. 1944	Pringle, H. G. Alston.
P.V. Trainer	Percival	Aero. 1731	Feb. 1942	—
Proctor	Percival	B.A. 1635	Oct. 1940	—
Moth Minor	De Havilland	Unreported ..	—	—
Firefly	Fairey	Aero. 2286	Aug. 1948	Tatchell.
F9/40	Gloster	B.A. 1636	Oct. 1940	Finn, R. P. Alston, Francis.
M.20/2	Phillips & Powis ..	B.A. 1673	Apl. 1941	H. G. Alston, Finn.
A.S. 49	Airspeed	B.A. 1693	July 1941	Pringle, H. G. Alston.
Beaufighter	Bristol	Aero. 1684	Oct. 1941	—
Welkin	Westland	Aero. 1739	Mar. 1942	—
F7/41	Vickers	Aero. 1832	June 1943	Pringle, V. G. Warren.
Vampire	De Havilland	Aero. 1939	Apl. 1944	Pringle, V. G. Warren.
Messenger	Miles	Aero. 1805	Mar. 1943	—
Meteor	Gloster	Aero. 2343	Nov. 1949	Harper, Dennis.
Tempest	Hawker	Aero. 1917	Feb. 1944	—
Ace	Gloster	Unreported ..	—	—
TX3/43 Glider	General Aircraft ..	Unreported ..	—	—
G.A.L.56 Glider ..	General Aircraft ..	—	—	—
Hornet	De Havilland	Aero. 2203	June 1947	Pringle, Harper.
Fury, Sea Fury ..	Hawker	Aero. 2273 ..	July 1948	Tatchell, Harper.
Mosquito	De Havilland	Unreported ..	—	—
Spearfish	Fairey	Unreported ..	—	—
E1/44	Gloster	Unreported ..	—	—
Libellula	Miles	Unreported ..	—	—
A.W.52G	Armstrong Whitworth	Unreported ..	—	—
E6/44	Saunders-Roe	Unreported ..	—	—
Attacker	Supermarine	Unreported ..	—	—
Fighter A	—	Aero. 2262	Apl. 1948	Harper, Pringle.
Prentice	Percival	Aero. 2298	Nov. 1948	Harper.
D.H.108	De Havilland	Aero. 2305	Dec. 1948	Harper.
Balliol	Boulton-Paul	Aero. 2253	Mar. 1948	Tatchell, Pringle.
Athena	A. V. Roe	Aero. 2267	May 1948	Tatchell, Pringle.
Fighter B	—	Aero. 2271	June 1948	Harper.

CHAPTER II

The Preparation of Dynamic Models

2.1. **General Requirements.**—A freely flying model is said to reproduce the motions of the full-scale aircraft when all the angles are unchanged, *i.e.*, when the flight paths are geometrically similar and the attitudes of the model and the aircraft (as defined by angles of incidence, bank and sideslip) are identical.

To achieve this, the ratio of inertia force to aerodynamic force must be kept the same when going from model- to full-scale, or

$$Mg : ML/T^2 : \rho V^2 L^2 f(R) . \quad .. \quad (2.1)$$

From the first ratio

$$L_m/T_m^{\,2} = L_a/T_a^{\,2} \quad .. \quad .. \quad (2.2)$$

where suffices m and a relate to model and aircraft respectively.

Now $nL_m = L_a$.

Therefore $n^{1/2}T_m = T_a \quad .. \quad .. \quad .. \quad (2.3)$

and, since $V \equiv L/T$, $n^{1/2}V_m = V_a$ . .. .. (2.4)

Now from (2.1)

$$\frac{\rho_m V_m^{\,2} L_m^{\,2} f(R_m)}{\rho_a V_a^{\,2} L_a^{\,2} f(R_a)} = \frac{M_m L_m/T_m^{\,2}}{M_a L_a/T_a^{\,2}} = \frac{M_m}{M_a} \quad \text{(from 2.2).}$$

Now $V_m^{\,2}/V_a^{\,2} = 1/n$ and $L_m^{\,2}/L_a^{\,2} = 1/n^2$.

Therefore

$$\frac{M_m}{M_a} = \frac{1}{n^3}\frac{\rho_m f(R_m)}{\rho_a f(R_a)}$$

or, if $\rho_a/\rho_m = \sigma_a$ (the relative air density of test),

$$n^3 M_m = \frac{M_a f(R_m)}{\sigma_a f(R_a)} .$$

Thus we see that the mass of the model, besides being 'to scale' (giving the same density of material as the aircraft at ground level), must also be adjusted to take account of the difference between the air densities in the model- and full-scale tests. It would also be possible to allow for Reynolds number effects by adjusting the density of the model, as the equation indicates, but for one thing. Equation (2.1) implicitly assumes that the direction of the resultant aerodynamic force and its point of application are unchanged by Reynolds number effects. This is unlikely over the large range of Reynolds number involved (*see* Fig. 7.18), although a simplifying assumption commonly made in spinning theory is that the resultant force is normal to the wing chord at incidences well above the stall. For this reason, and because of the time involved in making changes in the density of a model without altering its radii of gyration, it is not considered a satisfactory way of allowing for scale effects, and we write

$$n^3 M_m = M_a/\sigma_a .$$

Radius of gyration is proportional to n in the same way as other lengths.

We have therefore the following set of ratios:—

Parameter	*Dimension*	*Model/full-scale values*
Length	L	$1/n$
Mass	M	$1/n^3\sigma_a$
Time	T	$1/n^{1/2}$
Linear Velocity ..	L/T	$1/n^{1/2}$
Angular Velocity ..	$1/T$	$n^{1/2}$
Moment of Inertia	ML^2	$1/n^5\sigma_a$

In addition, of course, the centre of gravity should be in the correct position on the model, although accuracy of vertical position is not of great importance.

These ratios, then, ensure that the inertia forces and moments are to scale, *i.e.*, that, brought to non-dimensional coefficients (dividing by $\rho V^2 L^2$ for forces or $\rho V^2 L^3$ for moments), they will have the same numerical values as for the full-scale aircraft if the spins are geometrically similar.

To ensure that the aerodynamic forces and moments are correct is much more difficult because of the appearance of very large scale effects. Chapter VII deals with method of allowing for these, providing that forces and moments, particularly those resulting from control deflections, of the right order are obtained on the model. The models have therefore been made to scale as accurately as possible, whilst any very small details have been omitted. Details such as propellers (usually windmilling, and not dynamically to scale), undercarriages and flaps where appropriate are represented, but ducts and radiators, for instance, are left solid as it is practically impossible to ensure representative flow through them. Correct balancing of the controls is not reproduced as hinge moments have not been measured on free-spinning models; only major balance areas such as horn balances are reproduced as these might affect the control moment on the aircraft as a whole.

A third property required of the model is that it shall be robust. In the vertical tunnel nets are suspended at a distance of about 6 in. from the walls and there are safety nets across the tunnel above and below the working-section. Models frequently hit the nets at comparatively high speeds, either during the dive after recovery or as a result of hitting the side net while spinning and then diving down the tunnel. Frequent damage and repair not only causes considerable delay in the test programme, but also tends to alter the behaviour of the model. Thus strength of construction is an important consideration.

2.2. **Materials.**—Robustness is best obtained by making the model as nearly solid as possible; this also helps to ensure not only accuracy of manufacture but

also minimum changes of shape due to shrinkage, etc. The main material used is therefore balsa wood. A good medium-density balsa wood combines a sufficiently low density with adequate strength for most purposes and it is only necessary to protect sharp edges and to strengthen thin surfaces. Silk is used for protective purposes, and birch or pine spars are used to add strength to fins, tailplanes, etc. The control lines are made of thread with small lengths of rubber inserted so that the tensions in the lines are adjustable. Other lengths of rubber are used to ensure that the controls move positively when the delay mechanism (Fig. 4.9) releases the tensions in the control lines.

On the nowadays rare occasions when it is necessary to lighten a solid model in order to obtain the correct loading, holes are drilled or cut in the parts requiring lightening, and are covered with thick tissue paper stretched tightly over them.

2.3. **Methods of Construction.**—For the purposes of this description it is assumed that the model is of a fairly high density so that no lightening of components is necessary. Fig. 2.1 shows two views of a typical model, with the main features of the construction indicated.

2.3.1. **Fuselage.**—The fuselage is shaped in two halves divided by the plane of symmetry. This method is adopted because a ' tunnel ' is required running aft along the fuselage centre-line from the nose of the model. This ' tunnel ' houses a piece of lead (the counterpoise weight) which is used to adjust the centre of gravity position and must be accurately cut and smoothly finished or the counterpoise either becomes immovable or becomes loose and moves under gravity forces while the model is being tested.

It is also usual to hollow out a certain amount of the rear fuselage ahead of the tail unit to ensure that some weighting of the fuselage will be necessary. Before the two halves are glued together, hardwood fin post and tailplane spars are jointed into the rear fuselage if they are considered necessary.

Small blocks of pine each with three holes about 0·03 in. in diameter are inserted in the sides of the fuselage on the centre-line. These are used in the determination of the c.g. position, the central hole being placed at the anticipated aftmost position of the full-scale c.g. and the other two representing extreme fore-and-aft limits.

The delay mechanism is housed in the fuselage, usually with the top left uncovered, although with the larger models it has been possible to enclose the mechanism completely, usually in the cabin. Where part of the mechanism is exposed, it is usual to place it in the plane of symmetry above the wing and aft of the cabin, where this is possible, thus, it is hoped, minimising its aerodynamic interference effects.

A nose-block of pine is made to fit in the front of the ' tunnel '; this also serves to mount the propeller where there is one. The block is a push fit and is not fixed; this enables the position of the counterpoise continually to be checked. Exposed parts of the fuselage, such as the nose just aft of the nose-block, and the cockpit canopy, are usually covered with silk as they are subject to considerable rubbing along the tunnel safety nets.

2.3.2. **Wings.**—The construction of the wings depends on the number of dihedral changes along the span. The aim is to keep the grain of the wood parallel to the leading and trailing edges as much as possible; thus the construction consists basically of two pieces for each wing joined together along a spanwise vertical plane. Any joints for dihedral changes are strengthened by the insertion of short ' spars ' and the centre-section of the wing where it is enclosed by the fuselage is left rectangular in section so that an accurate and strong joint may be made with the fuselage. After small pieces of pine have been set into the wing tips in line with the c.g. to take the wire spikes on which the externally applied moment-vanes (*see* Chapter VII) are mounted, and the wing-fuselage junction fillets have been shaped, a strip of silk $\frac{3}{8}$-in. to $\frac{1}{2}$-in. wide is glued along the leading edge, round the tip and along the trailing edge of the wing including the fillet. This encloses the actual edge of the wood and is stuck to the top and bottom surfaces on either side of it.

2.3.3. **Tail unit.**—The method of construction here is very similar to that for the wings except that it sometimes happens that the tailplane has to be made in two halves; the inboard end of each half is then left rectangular in section and is let into the fuselage, the same method being adopted with the fin. Where necessary, a spanwise spar of birch is enclosed in the tailplane and fin at about half chord. The edges are protected by silk strips.

2.3.4. **Control surfaces.**—Only that part of the control aft of the hinge-line is represented except when a large horn balance is used. The main part of the control is made of balsa and the horn is either balsa, or more likely, pine, which is glued and bound on with silk. A small piece of thread is attached from the leading edge of the horn to the corresponding point on the tailplane or fin. This thread is long enough to permit full and free control movement, but prevents the safety net from becoming firmly caught in the horn.

Silk tape is used for the hinges of the controls. Pairs of strips are used, one of which crosses from the top of the control to the under-surface of the aerofoil, and *vice versa*. Fig. 2.2 shows diagrammatically how they are arranged. The longer the control span, the more pairs of strips must be used. The leading edge of the control is chamfered to allow the correct angular movements, and small ' stops ' of pine are glued to the top and bottom surfaces of both the aerofoil and the control to give exact limits to the angular displacement.

2.3.5. **Details.**—With such details as undercarriages, slats, flaps, propellers, etc., one of the main considerations is strength. Undercarriages are usually made of pine, the wheel and leg being integral, and the leg is let into the full thickness of the wing. Thin balsa sheet glued to the undercarriage is used for the doors. Slats are made of pine or birch and are to scale and have a correct width

of slot, and usually mounted on thin birch ribs let into the wing leading edge. Flaps are made of balsa and mounted on birch stays or balsa blocks. Propellers are seldom dynamically to scale though the diameter and solidity are correct; they are made of mahogany and have a thickened section to give added strength. They are mounted on a dural tube or a piece of dowel projecting from the nose-block, or nacelle, and are kept in place by a non-rotating pine spinner fixed to this spindle.

2.4. **Choice of Scale for Models.**—Two limitations of the tunnel restrict the choice of scale for the model. The more important is the maximum tunnel speed available, which must not be exceeded by the maximum rate of descent of the model (*i.e.*, that reached at the point of recovery), and which is about 55 ft/sec, that is, the drag at 55 ft/sec must be greater than the weight.

Now $C_D = w_a/\frac{1}{2}\rho_a V_a^2$.

From section 2.1,

$$V_a^2 = nV_m^2.$$

Therefore $$n = \frac{2}{C_D \rho V_m^2} \frac{w_a}{\sigma_a}$$

We may either assume a minimum drag coefficient from the data given in Chapter V, or we may proceed directly to the scale by examining the scales and relative wing loadings, w/σ, of previous models. Fig. 2.3 shows the scales of a representative selection of models plotted against w/σ where σ is the relative density at the height of the full-scale test. The extreme limit of scale is given by $n = 0{\cdot}3w/\sigma$, corresponding to a minimum drag coefficient of 0·9, but such a large scale leads inevitably to difficulties of operation due to the vertical acceleration of the model during recovery, when the model speed becomes greater than the maximum tunnel speed; a better choice is obtained by using the more average value of n given by $n = 0{\cdot}4w/\sigma$, corresponding to a minimum drag coefficient of about 0·7. These expressions only apply, of course, to the present Vertical Tunnel; a higher tunnel speed will enable larger models to be used.

The second limitation on scale is the actual size of the model in relation to the tunnel diameter. It has been found that models of span greater than about $2\frac{1}{2}$ ft tend to become unmanageable in that they hit the side nets so often as to make it impossible to obtain results. With a better velocity distribution it might be that somewhat larger models could be used but it seems unlikely that model spans much greater than one-quarter the tunnel diameter will be feasible. With models which have oscillatory spins, the ratio of model span to tunnel diameter must be even smaller.

2.5. **The Loading of Dynamic Models.**—In order to represent the aircraft at altitude the relative densities $W/\rho Ss$ must be the same model-scale as full-scale. Since the density of the air in the tunnel cannot be reduced, the mass of the model is increased instead, in the ratio $1/\sigma$. The radii of gyration are unchanged, being a geometrical property of the aircraft and the inertias are therefore also increased by $1/\sigma$.

The model centre of gravity position is obtained by balancing the model about two axes parallel to the y-axis and in the xy and yz-planes. No attempt is made to reproduce the correct vertical position; it must naturally be fairly close to the full-scale position and the difference is not thought to have any significant effect on the model behaviour; the correct fore-and-aft position is obtained by adjusting the position of the counterpoise weight in the nose.

Lead weights are placed in the model at suitable positions, usually in the wing tips on the y-axis, and in the rear fuselage on the x-axis. The mass of each piece is then adjusted until the correct model moments of inertia (determined as described below) are obtained and the correct weight is finally made up by loading the model at the centre of gravity.

2.6. **Measurement of Moments of Inertia of Models.**—The moments of inertia of a model about the x- and y-axes are determined by observing its period when swinging as a compound pendulum about parallel axes. In the case of the z-axis a bifilar suspension is used. The distance between the swinging axis and the centre of gravity is made equal to the correct scaled radius of gyration, which ensures that the period of oscillation is a minimum when the model radius of gyration has been adjusted to its correct value by adjusting the lead weights.

The moment of inertia thus measured contains the moment of the air pressures on the model caused by its acceleration through the air; this is normally referred to as the 'virtual' moment of inertia. Attention was first directed to the importance of this additional moment in spinning work by Wright[1] in 1930, though the principle was already well known. Various methods of estimating the virtual moments are available; the most direct for ordinary model work is to use the fact that the virtual moment is directly proportional to the density of the surrounding medium. By obtaining the periods of swing T_1 and T_2 in gases of density ρ_1 and ρ_2 we find that the virtual moment is proportional to $(T_1^2 - T_2^2)/(\rho_1 - \rho_2)$. Apparatus exists in the Vertical Tunnel for swinging the model first in air and then in hydrogen, the density of which can be measured simultaneously with the time of swing.

A number of models have been swung in this way and it has become possible to collect the measurements of the virtual moments of inertia and relate them to the geometrical characteristics of the model. This has been done using American data[2] (1941) on the additional mass effect of plates, and obtaining expressions with empirical constants. Figs. 2.4 to 2.6 show the measured virtual moments plotted against the virtual moments calculated from

$$\Delta A = 19\bar{c}S\{0{\cdot}6 + 0{\cdot}04A_1\}\{1 - 0{\cdot}133(\theta - 1)\}4s^2 \text{ slug ft}^2 \times 10^{-5}$$

$$\Delta B = 20\bar{c}Sl_E^2 \text{ slug ft}^2 \times 10^{-5}$$

and $$\Delta C = 8sSl_R^2 \text{ slug ft}^2 \times 10^{-5},$$

where c, s, S are the wing mean chord, semi-span and area, A_1 and θ are the wing aspect and taper ratios, and

l_E and l_R are the distances between the nose of the aircraft (excluding the spinner) and the elevator (or elevon) and rudder hinges, respectively, all model-scale.

Although there is considerable scatter, this is probably due at least equally to errors of measurement as to inadequacy of the above expressions, for the difference between times T_1 and T_2 is very small, on the average about 1 per cent, often less, and it is only possible to measure T to about $\pm \frac{1}{4}$ per cent so that the measurements may easily show errors of 50 per cent. This is confirmed by the few cases where two or more determinations of the virtual moments have been made; the points are joined by vertical lines in the figures and show considerable scatter. However, the virtual moments are a small proportion of the total inertia, usually less than 5 per cent, so that an error of 50 per cent in the virtual moment is of minor importance; the majority of the points are less in error than this and so the above expressions form a useful means of estimating the virtual moments. It is, however, probably necessary to measure the virtual moments for unconventional aircraft as they may not fit the expressions satisfactorily, though a few points for tailless aircraft with swept-back wings are shown in Figs. 2.4 and 2.5, and agree reasonably well.

It is sometimes of importance to know the inclination of the x-principal axis of inertia to the wing chord. This is done by freely supporting the model in a horizontal plane by pivots in the blocks used for finding the centre of gravity. The pivots, and thus the model, are then rotated rapidly about a space vertical axis in the plane of symmetry and intersecting the pivot axis. Since the definition of a principal axis is that Σmxz shall be zero, the principal axis will assume a horizontal position under these conditions, and the inclination of the wing chord may then be measured.

2.7. **Acknowledgement.**—Practically all the models tested since the Vertical Tunnel was erected have been made by Mr. A. Hart of 40 Dept., R.A.E., and the authors wish, on behalf of all who have worked in the Vertical Tunnel, to express their appreciation of his work. His accuracy of construction, readiness to repair badly damaged models and ingenuity when confronted with difficult constructional problems have contributed very considerably to the smooth and successful running of the work in the Tunnel.

CHAPTER III

Models in the Steady Spin

3.1. **Introduction.**—In the previous chapter measures were described for reproducing in a model the loading conditions of a full-scale aeroplane. Let us now study the spin from various aspects. The most natural course is to concentrate on the problem of recovery from the spin, as this is the main object of all spinning work. As will be seen in Chapter IV, much remains to be discovered about the mechanism of recovery, and the field is open for further research. Also, in Chapter VII we shall give reasons why it is insufficient to regard the model as dispensing with the need for a detailed understanding of the processes and magnitudes involved. It therefore seems desirable to accumulate aerodynamic data of every kind relevant to the spin, if we are to understand the details of model behaviour. Some of these data are necessary for the prediction of full-scale characteristics other than recovery from the spin, as we shall see in Chapter V.

We may begin the record of measurements in the usual way by referring to lift and drag of models; the pitching moment is dealt with separately in Chapter V.

3.2. **Lift, Drag and Normal Force on Spinning Models.**—It is one of the initial assumptions of the simple theory of spinning that the resultant aerodynamic force on the aircraft lies in the plane of symmetry, *i.e.*, the side force is negligible. Under these conditions the lift force is balanced by the centrifugal force arising from the rotation, and the drag force is balanced by the weight of the aircraft. A more accurate description of the forces, allowing for side force is given by Gates and Bryant[3] (1926), and enables us to evaluate corrections to the simpler theory.

Fig. 3.1 is a spherical diagram reproduced from Ref. 3 and shows the relationship of the geometrical quantities defining the attitude of the aircraft.

Since θ, the pitch, and φ, the bank angle defining the wind axes are nearly right-angles, it is usually convenient to concentrate on the smaller angles:

θ_y inclination of the 'outer' span above the horizon

$\gamma = \pi/2 - \theta_1$. γ is the angle between relative wind and vertical

β sideslip angle.

Gates and Bryant point out that the frame of the wind axes x, y, z of the aircraft can be fitted into the frame z_0AB of the spin when the following are known:

(*a*) θ_1 the pitch of the helical path ($\gamma = \pi/2 - \theta_1$)

(*b*) β the angle of sideslip

(*c*) the direction of the resultant aerodynamic force referred to x, y, z,

for these are equivalent to fixing P and G in both frames.

The information (c) is comprised in the incidence α, and ε, the inclination of the resultant aerodynamic force to the plane of symmetry, if it is assumed that the aerodynamic force in the plane of symmetry is normal to the chord.

The force equations take the form (in wind axes):

x-axis $\quad \frac{1}{2}\rho V^2 C_D = w \sin\theta + wvr/g$

y-axis $\quad \frac{1}{2}\rho V^2 C_Y = -w \cos\theta \sin\varphi + wur/g$

z-axis $\quad \frac{1}{2}\rho V^2 C_L = \mathrm{w} \cos\theta \cos\varphi + w(uq - vp)/g$

Hence, if we require to compare lift and drag data measured statically with data obtained from observations of the free spin, it may sometimes be necessary to allow for the presence of a small gravity component in the lift equation, and for a small centrifugal component in the drag equation. But p, q and r are components in wind axes of the spin rotation Ω, and r cannot be appreciable except for spins in which the lift axis is inclined to the horizon; that is if both θ and φ are appreciably less than 90 deg, which in practice seldom occurs. The relative importance of the second term of the equation of drag is indicated by the ratio

$$\frac{vr}{g \sin\theta} = \frac{\beta\Omega V \sin\theta}{g \sin\theta}$$

where θ_z is the inclination of Oz (Fig. 3.1) below the horizon, and is, as pointed out above, almost always small.

Apart from this usually negligible correction we may write

$$\frac{1}{2}\rho V^2 C_D = w \sin\theta$$

$$\frac{1}{2}\rho V^2 C_Y = -w \cos\theta \sin\varphi$$

$$\frac{1}{2}\rho V^2(\sqrt{C_D{}^2 + C_Y{}^2}) \simeq w \text{ if } \varphi \simeq 90 \text{ deg.}$$

If therefore, it is required to estimate V from a knowledge of w and the force coefficients, it is noted that the appropriate combination of coefficients in the last equation is at least not less than C_D, and only differs from it by a term in C_Y which, from the nature of the spin, may usually be neglected. The estimate of V may thus tend to be rather higher than the actual value.

Postponing the problem of how the true drag coefficient depends on the spin parameters, we first require some knowledge of the first term in the analysis of drag, that is, the drag measured in static tests. It is natural that no facilities exist for the accurate measurement of this quantity on actual dynamic models. However, it has been found useful to make cruder measurements with the simplest kind of apparatus; this is readily placed in the vertical tunnel and the observations are rapidly made. Sketches in Fig. 3.2 show the arrangement of the balance and the methods of using it to measure lift, drag and normal force.

3.3. **Static Drag.**—Specimen results of drag measurements are given in Fig. 3.3. One of the points of interest is whether it is a reasonable approximation to regard the drag as the same function of incidence for all types when confining the discussion to incidences well above the stall: in many ways this would simplify the evaluation of characteristics of the spin. These measurements show that for the models tested the assumption is hardly justified, although it becomes more reasonable as an approximation for the larger incidences. Various factors probably influence the situation (apart from rotational effects which are discussed in Chapter V), and probably the most important are:

(a) Drag contribution of fuselage

(b) Effect of propellers.

At higher incidences the drag will be more dominated by the wing contribution and so proportionately less variation is to be expected. It is seen that the tailless and propellerless models in Fig. 3.3 have less drag than the others.

3.4. **Static Chordwise and Normal Forces.**—In spinning work it is often more natural to resolve the forces in body axes rather than in wind axes. Lift and drag tend to be of the same order of magnitude and are often regarded simply as components of the normal force neglecting the chordwise component of the resultant aerodynamic force which is always much smaller. Thus in the simple theory of spinning we have the equilibrium expressed in Fig. 3.4.

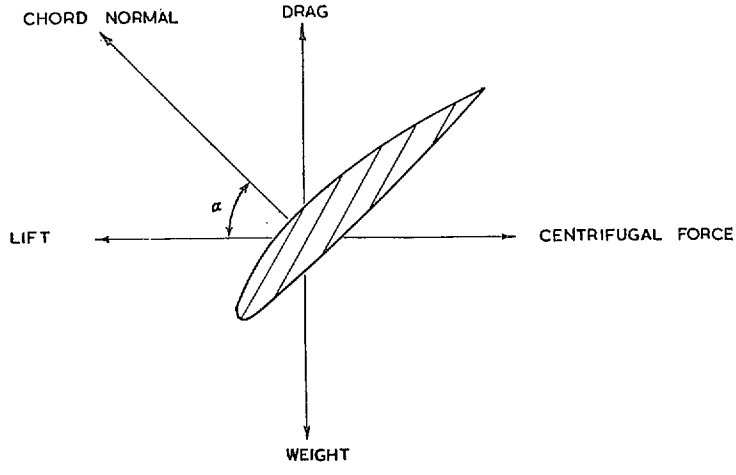

FIG. 3.4. Balance of forces in steady spin; simple theory.

The chordwise force owes its importance not so much to any disturbance of the simple force equations but to its indirect effect on the aerodynamic yawing moments. It was therefore thought to merit investigation with greater accuracy than the other quantities, and with due attention to the effects of scale. This investigation is described in Chapter VII.

The normal force was measured on a few models concurrently with drag. It, too, may be expected to show scatter between different types; in particular it is known that the propeller exerts forces in its own plane corresponding to the 'lift' or 'fin' effect, and these may be a noticeable contribution.

The results given in Fig. 3.5 show that the normal force is fairly consistent between two widely different types in the region well above the stall and has slightly higher values in that region than those for a flat plate.

3.5. **Static Lift: Effect of Maximum Lift on Recovery.**—Although the maximum lift coefficient does not play a very striking role in spinning theory, it is one of the respects in which models notably fail to reproduce conditions at higher Reynolds numbers. Therefore the question is often asked as to whether this seriously matters in model spinning tests. It is the lift values near the stall which are the most likely source of trouble, and the measurements of Fig. 3.6 show that models vary very considerably in their maximum lift coefficients. This variation is evidently partly due to the wing sections, the thicker wings having the higher maxima.

The highest lift encountered in these tests was on the *Prentice*, giving $C_{L\max} \sim 1{\cdot}3$ at a Reynolds number of 50,000. Evidently if this could be artificially reduced by 'spoilers' we should be able to investigate directly whether the high maximum lift was affecting the spin and recovery appreciably. Fig. 3.7 shows the large loss of lift observed when thick wires are attached to the upper wing surface; the greatest part of the loss comes from the root. Above $\alpha = 25$ deg the loss is much smaller altogether. Comparative tests of the recovery from the spin are given in Fig. 3.8 and show practically no difference in recovery between high and low $C_{L\max}$ conditions.

3.6. **Spanwise Variation of Geometrical Incidence.**—The experimental result given in the previous paragraph is less surprising when we examine the distribution of geometrical incidence along the aircraft span. It is sometimes assumed that in the spin the 'rising' or 'leading' wing tip is unstalled. Examination of model data shows that this is only likely to be true in most cases for quite steep spins and is certainly untrue for flat spins.

Some photographic records were made of the behaviour of smoke generated at the wing tip of the *Prentice* model at two different incidences in the spin; these showed reversed flow over the upper wing surface at the higher incidence; at the lower incidence the photographs showed approximately chordwise flow. This result was confirmed with observations of the behaviour of light cotton tufts stuck to the wing surface, Fig. 3.9.

The variation of geometrical incidence along the span is from $\alpha' = (\alpha - \arctan \lambda)$ at the 'rising' wing tip to $\alpha'' = (\alpha + \arctan \lambda)$ at the 'falling' wing tip, where $\lambda = \Omega s/V$.

It is, of course, well known that λ is related in a complex manner to α, through the pitching-moment equation, and therefore no simple rule is likely to be found. However, it is of some interest to consider how the resulting values of α' stand in relation to the stalling angle, and how they vary with α. Some representative values are given in Fig. 3.10 for different types. It is unfortunate that our records are fewest in the lower incidence range, but it is evident that roughly

$$\alpha' \simeq \tfrac{3}{4}\alpha$$

and therefore there is every reason to expect the wing to be fully stalled in the incidence range beginning quite close above the incidence for 'straight' stalls. For aircraft with moderate values of λ this would be so above $\alpha \sim 30$ deg, but as the figure shows, for some aircraft with large values of λ, the 'rising' wing may be unstalled at values of α up to over 50 deg. We conclude that only in very steep or very fast spins is there any likelihood of an unstalled wing tip.

3.7. **Range of Values of γ.**—It is a usual assumption of spinning theory that the spiral pitch θ_1 of the flight path is nearly 90 deg and that $\gamma = \pi/2 - \theta_1$ is small. As this quantity is not observed except in cinematograph records, it may be conveniently obtained by an approximate calculation.

We note that if the aerodynamic resultant force is normal to wing chord

$$\text{Lift/Drag} = \cot \alpha = R\Omega^2/g .$$

But $$\sin \gamma = R\Omega/V .$$

Therefore $$\sin \gamma = \frac{g \cot \alpha}{\Omega V} .$$

This formula gives γ in terms of quantities observed in the tunnel. If, however, we require to predict γ without recourse to observations it is more convenient to put

$$V = (2w/\rho C_D)^{1/2}$$

and $$\sin \gamma = \frac{g \cot \alpha}{\Omega} (\rho C_D/2w)^{1/2}.$$

These formulae enable us to see how γ will vary under different conditions. As α increases, $\cot \alpha$ decreases, and Ω increases. The slight increase in $C_D^{1/2}$ will not in general prevent γ from falling off rapidly at the higher incidences. At low incidence γ may become more appreciable and some values calculated from observations of model spins are given in Fig. 3.11.

3.8. **Effect of Lift Devices on the Spin and Recovery.**—In the past a number of tests of model aircraft were made with slots, both fixed and automatic. These usually showed a considerable effect, but the effect was always greatest when only one slot was opened. Hence it seems that it is due not to the direct effect on the lift, drag and

pitching moment of the model, but to the asymmetric moment of the slots. This in turn is due to their aerodynamic influence in retarding the stall of the wing. Because of this asymmetric effect the slot is an alternative, but not so controllable, device to the wing-tip vane for studying the ease of recovery from spins.

With wing flaps the position is different. These are always placed at or near the wing root, and are therefore less likely to generate large asymmetric moments even if opened on only one side of the aircraft. This location of flaps has, however, a very important effect on the airflow past the tail in the spin. Fig. 3.12 shows an example of this in the case of the *Firefly* 4, where smoke produced in the flap wake impinges on the tail even at moderately high incidences. That there is consequently a serious loss of control power in recovery is shown in Fig. 3.13, in that recovery from an established spin has become more difficult. In the same connection it is worth recalling a test by Finn and Stephens[4] in 1936 on a model *Hurricane*, in which they showed that recovery from a spin with flaps up could be expedited by lowering the outer split flap but that use of the inner, or even both, was adverse.

Some attention has also been given to the use of a different kind of lift flap, the leading-edge type. Applied to the Fighter A model these gave a large increment of lift in the range of incidences above the stall of the unflapped wing (Fig. 3.14). A number of experiments on the recovery of this model showed that the effect is similar to that obtained from slots, *i.e.*, it is most marked when the flaps are used differentially. The effect is then quite large and approximately corresponds to a ' negative drag ' of the flap, based on its own area, of the order $C_D = 0{\cdot}75$.

3.9. **Effect of Dive Brakes on the Spin.**—In some aircraft dive brakes (drag flaps) would be available to assist recovery from the spin if this were likely to be efficacious, and some interest was therefore taken in them during model tests. Usually these flaps are designed for high diving speeds and the area is too small to exert much influence on the fully stalled wings at the relatively low spinning speeds. The effect on recovery is also so small as to be only just detectable by the usual methods, and is sometimes slightly beneficial (*e.g.*, *Balliol*) and sometimes slightly adverse (*e.g.*, *Meteor*, Fighter B) to recovery. The interest in their effect is now concentrated more on whether they will hinder rather than hasten recovery, for as operating altitude increases so it becomes necessary. to limit the speed in the dive after recovery, and it may be necessary to open the dive brakes during the spin or at least when recovery action is taken. As the recovery usually deteriorates as the altitude is increased, any further deterioration due to having the dive brakes open is to be deprecated.

3.10. **Rudder Power in the Spin.**—Without rolling-balance tests, it is extremely difficult to assess the moments generated by the controls. In a few cases, however, the rudder yawing moments, $\overline{n'\zeta}$, have been estimated directly. This can be done in free-spinning model tests by measuring α and λ as functions of the yawing moment applied to the aircraft by means of a wing-tip vane. The tests can be made for different rudder positions and also varying amounts of elevator shielding. Fig. 3.15 shows the results of the measurements on three models, with the rudder deflected to the full extent in both pro-spin and anti-spin directions. It is sometimes assumed that the rudder power is proportional to the ' unshielded area ', and this assumption is the basis of Fig. 3.16, where $\overline{n'\zeta}$ is half the yawing moment difference between the positions of extreme deflection, A_R is the area of the rudder which, with certain reasonable assumptions about the spreading of the tailplane and wing wakes (*see* also Chapter VI), is left unshielded and l'' is the distance between the centroid of this area and the centre of gravity of the aircraft. Evidently the proportion is only a rough one, justified only as a convenient approximation. To obtain a better estimate, a mean line represented by $n'\zeta = 0{\cdot}7A_R l''/2Ss$ may be used, as this passes through the points shown in Fig. 3.16.

CHAPTER IV

Recovery from the Spin, and Control Effectiveness

4.1. **Kinematics of Rotation of Solid Bodies.**—Before entering on a discussion of the effectiveness of the controls in a spin, and of the best ways of using them to recover, it is useful to note some kinematic features of the rotation of solid bodies which have an indirect bearing upon the subject.

It is essential to the geometry of angular displacements that the result of successive rotations about different axes depends generally on the order in which they are performed, as may be seen by reference to Donkin's theorem[5]. This theorem states that two successive displacements represented on a unit sphere by great circle arcs AB, BC are equivalent to a rotation $2XY$ where X and Y are the middle points of AB and BC. If AB is a roll about the chord axis, BC a yaw about the chord-normal, then the result is equivalent to $2XY$ (Fig. 4.1). This is different from the result of the same rotations in the opposite order. Equally important is the fact that the performance of pure rolling and yawing motions has resulted in a change of pitch. If, as in Fig. 4.1, the wings are level at A and again at C then the chord lies along the line of greatest slope of the wing plane. From A to B the chord does not change slope; hence at C the slope is greater than at A, *i.e.*, the incidence is less. The amount can be calculated from the formula

$$\sin \alpha_2 = \sin \alpha_1 \cos \theta, \text{ where } AB = \theta \quad .. \quad (4.1)$$

If the sequence were reversed we should have

$$\sin \alpha_2 = \frac{\sin \alpha_1}{\cos \theta}$$

representing an increase of incidence.

It is remarkable that a reduction of incidence can be made without ever having a pitching angular velocity in body axes; it is a reminder that the study of the spin cannot be completed by exclusive concentration on angular velocities and their integrals. Another way of expressing this is to say that the infinitesimal angular displacements from a given attitude are not exact differentials, and the finite or integrated movements in going from one attitude to another depend on the route from start to finish as well as on the end points of the route themselves.

It is doubtful whether considerations of this sort have been consciously applied to the problem of recovery from the spin. They may, however, underlie some aspects of recovery technique, for instance, that known as 'pump-handling' of the controls, whereby the pilot, perhaps as last resort, attempts to upset the equilibrium of a bad spin by coarse use of the controls, either singly or together in phase or out of phase. Thus a quickly executed roll of 20 deg, corrected by yawing until the wings are level could effect a change of attitude of the order of 5 deg. It does not, however, bestow any angular momentum about the pitch axis.

4.2. **Analysis of Some Simple Recovery Motions.**—The procedure just mentioned may be usefully applied in the consideration of tilt in the recovery. If BC were, for instance, an anti-spin yawing rotation, AB would represent outward tilt. In what follows it will be seen that there is much to be said about the role of tilt in the dynamics of spinning, as has indeed been long recognised. It is therefore a useful preliminary to examine the conditions which hold when no tilt is allowed to develop from beginning to end. That this is by no means typical of the recoveries of models is quite evident in watching them; the case of zero tilt is simply a basis of comparison.

Consider therefore the case where the wings are level and there is zero initial pitching angular velocity q. We have to consider what relations governing p, q and r* will ensure that

$$\theta_y \equiv 0.$$

Changing to horizontal and vertical axes in the plane of symmetry (Fig. 4.2) we obtain the two components

$$\left.\begin{aligned} \Omega &= p \cos \alpha + r \sin \alpha \\ \dot{\theta}_y &= p \sin \alpha - r \cos \alpha \end{aligned}\right\} \quad .. \quad .. \quad (4.2)$$

The condition for wings to remain level is

$$\alpha = \arctan \frac{r}{p}.$$

Differentiating this we obtain

$$q = \dot{\alpha} = \frac{\dot{p}r - r\dot{p}}{p^2 + r^2}. \quad .. \quad .. \quad .. \quad (4.3)$$

To obtain some information on the dynamical aspect of this relationship we may consider various cases in which the time-graphs of p and r are assumed, so that equation (4.3) leads to a definite variation of q also. These values are then inserted in Euler's equations for the moments: (*N.B.*—in this Chapter all moments are about body axes)

$$\left.\begin{aligned} L &= A\dot{p} - (B - C)qr \\ M &= B\dot{q} - (C - A)rp \\ N &= C\dot{r} - (A - B)pq \end{aligned}\right\} \quad .. \quad .. \quad (4.4)$$

in which each equation contains an acceleration term as well as the usual centrifugal term. We note that in the steady spin L, M and N are just sufficient to balance the centrifugal moments and that of these only the pitching component is other than zero; so the aerodynamic rolling and yawing moments are each balanced out.

It is convenient for practical purposes to adopt the approximation

$$C \simeq A + B \quad .. \quad .. \quad .. \quad .. \quad (4.5)$$

*Rates of rotation in body axes; the primes are omitted in this Chapter.

in consequence of which Euler's equations become, approximately

$$\left.\begin{aligned} \frac{L}{A} &= \dot{p} + qr \\ \frac{M}{B} &= \dot{q} - rp \\ \frac{N}{C} &= \dot{r} - \frac{(A-B)}{C} pq \end{aligned}\right\} \quad \ldots \quad \ldots \quad (4.6)$$

4.2.1. **Case I.**—We now consider a type of recovery in which the assumptions are as follows :

(i) Steady spin at 60 deg incidence with level wings

(ii) Wings remain level

(iii) p remains constant

(iv) r decreases linearly to zero in a time equal to some constant times the period τ of the steady spin.

These assumptions bear some resemblence to the full-scale case considered by Bryant and Jones[6] (1932).

In Fig. 4.3 one mass distribution is represented with times of recovery T varying from one-half to twice the period of the steady spin. In Fig. 4.4 the last diagram of Fig. 4.3 is repeated on a larger scale to include two other loading conditions, one with $A < B$ and one with $A > B$. From this diagram it is seen that this inertia difference, which in steady spins is only of significance if combined with a definite tilt angle, is here significant because q is non-zero even with zero tilt. Even for this rather artificial type of recovery, therefore, the moments required are more easily provided by the rudder if A exceeds B. To convert these figures to ordinary coefficients, based on the initial velocity (not the instantaneous velocity), we have

$$\bar{n} = \frac{N}{C\Omega_0^2 \lambda_0^2 \mu i_o}$$

from which it seems that the advantage of large A over the case $A = B$ can be of the order of 5 units, or more for faster recovery. The fast recoveries are, however, unlikely, because even the slowest case considered ($T = 2\tau$) would require about 15 units of rudder moment to initiate it, if $\mu = 40$. From this it is at once obvious, by considering the available rudder moments, why recoveries in less than one turn of the spin are unusual on heavily loaded aircraft. It is pointed out that in Fig. 4.3 the spin would cease rather before $r = 0$ because the incidence would be reduced to below the stall.

The magnitudes of the required moments calculated as described above give a clue to the occurrence of other types of recovery. These values are of course not simply the moments generated by the controls, but the total resultant aerodynamic moments, and to obtain a knowledge of the control moments would entail a full analysis of each individual case. It is interesting that at least a small anti-spin rolling moment is permissible; some of this would in practice be contributed by variations in $\overline{lpv}$ apart from aileron deflections. A moderate use of aileron moment may however be admitted.

The graph of $M/B\Omega_0^2$ shows initially a small increase of moment above that required to balance the steady centrifugal moment. Thereafter the aerodynamic moment required slowly falls off in spite of the acceleration in pitch; this is because the centrifugal term itself falls off rapidly. This in turn points to the requirement of a small initial elevator movement followed by a very cautious use of elevator, for even with elevator fully up, the decrease of tail moment with decreasing incidence is quite slow, as may be seen from Fig. 5.12 in the next Chapter; more is required for a quick recovery than for a slow one, and the more so as $\overline{mq}$ terms would then be larger. If the orthodox method of recovery is followed, in which the elevator is used, however cautiously, there is an obvious likelihood that q will exceed the very moderate values assumed here, and the consequences of this must be ascertained. This is dealt with in section 4.3 below, but first we must briefly consider another type of recovery.

4.2.2. **Case II.**—The assumptions made for the recovery shown in Fig. 4.5 are

(i) Steady spin at 60 deg incidence with wings level, as before

(ii) Wings remain level

(iii) p decreases linearly to zero in twice the time taken by r

(iv) r decreases, as before, linearly to zero in time $T = \tau/2$, τ or 2τ.

From Fig. 4.5 it is evident that in comparison with Case I, the increase in q is delayed, in that it does not attain such large values at first, but it later becomes larger and overtakes Case I. L is on the whole numerically larger, permitting a greater employment of the ailerons against the spin. N is unchanged but more rudder power might be required to counteract the adverse aileron yawing moment. The sharpest contrast appears in the curves of M, where the drop towards the end of recovery is less marked and even, for the fastest recovery, gives place to a sharp rise. It would therefore appear that the permissible amount of elevator deflection is in some measure associated with the amount of the other control deflections, being greater for large rudder and aileron movements than for small, and greater for effective rudders than for ineffective, other things being equal.

4.3. **Effects of Control Movements on Recovery.**—In the above calculations we have seen that on the simplest showing, the three moments are closely interwoven, but that apart from minor corrections to the yawing moment curves, the moments of inertia enter chiefly in a relation of proportionality of L, M and N to A, B and C respectively, if the recovery follows a prescribed course in a given time, as equation (4.6) shows.

The primary effect of a movement of each control is to initiate an angular acceleration about the appropriate axis, if it is deflected during the steady spin. In the case of ailerons there is a yawing component to be considered as well as the rolling moment, as shown in Fig. 4.6,

taken from biplane data[7] (1932). A similar consideration also applies to the elevators, for here there is often a change in rudder moment due to elevator deflection as the degree of shielding varies.

We can never neglect a further complication which we may call the secondary effect of each control movement. This is most easily thought of in relation to the steady spin as consisting of the moments generated about the other axes in the new steady spin resulting when a given moment is applied. The secondary effect of a rolling moment l is principally a yawing moment which has been given the approximate value $-lv_v/\lambda_v$ (*see* Chapter VII, section 7.5.4); the secondary effect of a yawing moment n is a rolling moment given by $-n\lambda_v/v_v$, assuming that m_v can be neglected, as is probably not always so.

It is implicit in the method of deriving these expressions that the relevant primary moment will move the aircraft into the attitude of a new equilibrium, *e.g.*, outwards tilt with $B > A$ to counterbalance an anti-spin rudder moment, inwards tilt with $A > B$. In actual fact, of course, the initial effect must be such as to produce inwards sideslip in both cases. Here we refer again to equations (4.2). Any factor which brings the axis of rotation closer to the chord-normal will produce an outward sideslip. This can occur either because p has become too small in relation to r, as is a possible temporary condition through the use of anti-spin aileron deflection or through excessive use of the elevators. Anti-spin rudder deflection alone should however at first produce inwards sideslip, although it seems quite probable that the disturbance to the centrifugal pitching moment may soon reverse this condition. The conflict is between derivatives of different orders with respect to time, as may be seen by expressing the initial motion in infinite series as

$$p = p_0 + p_1 t + p_2 t^2 + \ldots$$
$$q = q_0 + q_1 t + q_2 t^2 + \ldots$$
$$r = r_0 + r_1 t + r_2 t^2 + \ldots \quad .$$

Then in the steady spin, Euler's equations become

$$L_0 = -(B - C)q_0 r_0$$
$$M_0 = -(C - A)r_0 p_0$$
$$N_0 = -(A - B)p_0 q_0 .$$

On applying an additional yawing moment N, say, we find

$$p_1 = 0, \quad q_1 = 0, \quad r_1 = N/C$$
$$p_2 = \frac{(B - C)}{2A}(q_0 r_1 + r_0 q_1) \simeq 0$$
$$q_2 = \frac{(C - A)}{2B}(r_0 p_1 + p_0 r_1) \simeq \frac{p_0 N}{2C}$$
$$r_2 = \frac{(A - B)}{2C}(p_0 q_1 + q_0 p_1) = 0 .$$

Thus in slow recoveries there is a possibility that the quadratic term $q_2 t^2$ may overtake what is required for level wings, so that the effect of rudder deflection could be the opposite of what would at first seem natural, and outward sideslip would result. Very roughly this condition, neglecting terms higher than t^2 is

$$t > 2^{1/2}/\Omega_0$$

i.e., it requires a rotation of at least $2^{1/2}$ radians at the steady-spin rotation rates.

To pursue this matter further in the same direction it would be necessary to adopt the methods of Bryant and Jones (*l.c.*). It seems probable, however, that the immediate effect of anti-spin rudder deflection is to retard r and to cause θ_y to increase. In such a case the secondary effect is initially an anti-spin rolling moment irrespective of the sign of v_v and only in slow recoveries is it likely that the previous formula $-n\lambda_v/v_v$ holds good, for here the instantaneous condition of the aircraft approximates more closely to a state of equilibrium and all the time derivatives become less important.

In the R.A.E. method of studying models it is the slow recoveries which receive most attention; hence 'equilibrium' theory has a wider relevance than in full-scale practice. Evidence of this is that increase of A almost always favours recovery in the routine tests, in agreement with what would be expected from the formula $-n\lambda_v/v_v$; it does not follow that the same is true in quick recoveries.

4.4. **Summary of Control Effectiveness in Recovery.**—The established principles underlying the technique of spin recovery are well summarized by Bryant and Jones in Ref. 6 as a result of a number of calculations of specimen recoveries. They conclude that, to quote from their report:

(*a*) Sideslipping in a spin introduces a rolling moment (chord axes) which is large even for a small angle of sideslip, and any factor which produces a pure rolling couple against the spin will, in general, be nullified by a change in sideslip;

(*b*) Sideslipping also introduces a yawing moment which may be of either sign for either direction of sideslip, but is invariably small. Hence, any factor which can provide a moderate yawing couple for recovery will not be counteracted by changes in sideslip;

(*c*) It thus appears that the rudder is by far the most effective control for the purpose of recovery from an established spin; and

(*d*) Ailerons do not assist recovery by virtue of their rolling couple; their influence in assisting or retarding recovery will be governed by the yawing moment they produce.

(*e*) Reversal of the elevators without other control movements may lead to another and faster steady spin more stable than the original, and possibly even at a higher incidence. It is probably better to reverse the rudder in a flat spin before moving the stick, and to move the latter when the rate of spin is observed to fall off.

These authors emphasize that the rolling moment due to sideslip is always a stabilizing factor in the spin.

We now consider these conclusions, which were only intended to apply when B exceeds A, a condition which happened to be satisfied by most of the aircraft then current, to see in what measure they need to be revised in order to cover all types of aircraft.

In particular, there seems no reason to call (*a*) in question. In the case of (*b*) we have to note that, as we saw in section 4.3, $\overline{n\zeta}$ may be ' controlled ' by an inertia term if v_v is positive; this also reduces the secondary rolling moment. It is fundamental to conclusion (*b*) that $\overline{n\zeta}$ is enhanced by the unstable directional stability of aircraft with B large.

In more recent years, aircraft with A larger than B have come increasingly into the field. Accordingly it has become increasingly necessary to revise in such cases all the above conclusions. In theory we have the possibility that both rolling and yawing moments can be strongly ' controlled ' by the inertia terms arising in sideslip, thus leading to an exceptionally stable spin. Conclusion (*c*) would than also require some modification in that the rudder would tend to become ineffectual on such aircraft, as would the ailerons. This would of course render it all the more necessary to find the best way of using the controls.

Consider then the use of elevator alone. The major objection is that the elevator power may be insufficient to overcome the centrifugal pitching moment. Another objection clearly brought out in Bryant and Jones' calculations and confirmed in practice, is the risk of a second fast spin developing as a result of outwards sideslip. This risk is clearly diminished as A increases, as is shown in Fig. 4.7, and for a particular value of A recovery by elevator alone becomes certain by reason of the changed shape of the curve. Calculations on the steady spin in fact give a conservative idea of the point at which this danger disappears, for if a position of spin equilibrium does not exist with elevators down, there can be no risk of entering it, whereas an equilibrium may exist in theory without necessarily being entered in practice.

Irving and Batson[8] (1932) in fact concluded that for monoplanes with A large, good recovery by elevators alone is indicated. The same idea has been illustrated in the U.S.A. by an attractive statistical analysis of model test results by Neihouse[9] (1942), reproduced in Fig. 4.8.

Irving and Batson also concluded that with $(A - B)$ positive it was advantageous for a monoplane to have l_v small. We may also note that the danger of a second spin seems to be less, from Fig. 4.7, if the rudder is used than if not; moreover it is of course found in model tests that recovery by elevator alone can be prevented by applying pro-spin yawing moments.

Conclusion (*d*) also needs some revision in view of the increased importance of the secondary moments. When pro-spin ailerons are applied a direct yawing moment $-\overline{n\xi}$ arises irrespective of the sign of v_v, but the secondary yawing moment arising from the direct rolling moment is, as seen in section 4.3, dependent on the sign of v_v. That this asymmetric effect may easily be the larger of the two moments is brought out by the analysis of Ref. 9 and is discussed again in the next section.

The primary and secondary effects of each control movement are now summarised in the following table, with the most favourable cases heavily under-ruled. It should be noted that the secondary yawing moments due to aileron deflections change sign with v_v strictly, and not $(A - B)$. Chapter VII, section 7.5.4, shows that generally $(A - B)$ must be slightly negative for v_v to be zero.

TABLE IV.I

Effects of Control Deflections

N.B.—Rotations and moments are about body axes.

Control	$A < B$	$A > B$
Anti-spin rudder deflection.	Initial motion reduces r. Inward tilt develops anti-spin $\overline{ni}$. Secondary anti-spin rolling moment.	Initial motion reduces r. Tilt develops controlling pro-spin $\overline{ni}$. Secondary anti-spin rolling moment.
Downward elevator deflection.	Tends to reduce incidence. May cause positive $\overline{n\eta}$. Promotes outward tilt and pro-spin $\overline{lv}$, $\overline{li}$ and $\overline{ni}$.	Tends to reduce incidence. May cause positive $\overline{n\eta}$. Promotes pro-spin $\overline{lv}$ and $\overline{li}$ but anti-spin $\overline{ni}$.
Anti-spin aileron deflection.	Initial motion reduces p. Outward tilt develops controlling $\overline{lv}$ and $\overline{li}$. Secondary pro-spin yawing moment. Pro-spin $n\xi$.	Initial motion reduces p. Outward tilt develops controlling $\overline{lv}$ and $\overline{li}$. Secondary anti-spin yawing moment. Pro-spin $\overline{n\xi}$.
Pro-spin aileron deflection.	Initial motion increases p. Inward tilt develops controlling $\overline{lv}$ and $\overline{li}$. Secondary anti-spin yawing moment. Anti-spin $\overline{n\xi}$.	Initial motion increases p. Inward tilt develops controlling $\overline{lv}$ and $\overline{li}$. Secondary pro-spin yawing moment. Anti-spin $\overline{n\xi}$.

4.5. **Model Data on Control Effectiveness.**—It is pertinent to enquire how far these conclusions go towards accounting for the observed data for models like the *Wellesley*, or more recently the *Typhoon*, on both of which aircraft there were cases of difficulty in recovery or failure to recover in full-scale. Model tests indicated extremely effective elevators, rudder quite adequately effective, and at least on the *Typhoon* the ailerons acted positively, so that if put against the spin they assisted recovery.

Fig. 4.9a shows a model rigged for such tests in which the escapement mechanism releases the controls simultaneously.

4.5.1. **Ailerons.**—Fig. 4.10 gives results obtained by Pringle and Warren[10] (1945) on the recovery of the *Typhoon* model loaded so that i_A, i_B, i_C were 0·082, 0·063, 0·134 respectively. These curves show that on a scale of yawing moments the effect of aileron deflections was ' positive ' either when used fixed or when operated as part of the recovery action, according to the table:

TABLE IV.II

Aileron Effectiveness on the Typhoon Model

Use of Ailerons		Effect on Recovery
Spin	Recovery	
Central	Against Spin	$4\frac{1}{2}$ units better
With	Against Spin	3 units better
With	Central	$1\frac{1}{2}$ units worse
With	With Spin	$2\frac{1}{2}$ units worse

From these results it seems that the increased disturbance of the spin obtained by full travel in the second case relative to the first is offset by the adverse effect on the steady spin of the initial pro-spin position. This is consistent with the third result where the same travel is used as in the first but from a less favourable starting point.

Amongst other examples of ' positive ' ailerons are the *Meteor* 2, *Welkin* and G.A. TX.3/43, where v_η is positive, while the *Magister* and Fighter B (where $A < B$) are cases where aileron settings with the spin were favourable to recovery. These results agree broadly with the results of the N.A.C.A. analysis[9] and indicate that the secondary yawing moment is the dominant effect of aileron deflections. (Not to be confused with the yawing moment due to aileron deflection $\overline{n\xi}$.)

4.5.2. **Rudder and elevators.**—Turning now to the other controls on the *Typhoon* we have Fig. 4.11 showing that the restriction of rudder movement is slightly more adverse to recovery than is that of the elevator. Both controls are still effective however, and full reversal of both appears to be required for satisfactory recovery. In at least one reported case, difficulty in recovery in a *Typhoon* was actually associated with excessive stick forces which prevented forward stick movement.

In the case of the *Wellesley*, where the ratio of B/A was considerably less than for the *Typhoon*, the rudder movement became relatively unimportant, and a large stick movement was vital for recovery. On the other hand, a number of models, *e.g.*, *Firefly*, *Miles* M.28, *Tempest*, *Fury*, *etc.*, for which $A < B$, suffered little or no deterioration of recovery due to restriction of elevator movement, and this even improved recovery in some cases.

The following table shows the effect of limiting the the rudder and elevator movements for recovery, for the *Typhoon* and *Wellesley*.

TABLE IV.III

Rudder and Elevator Effectiveness on Typhoon and Wellesley

Model	Controls for recovery		Threshold yawing moment, $10^3 C_n'$
	Rudder	Elevator	
Typhoon ..	Reversed	Down	19
		Central	15
		Up	11
	Central	Down	13
Wellesley ..	Reversed	Down	47
		Central	20
		Half up	12
		Up	0
	Unmoved	Down	>36

4.6. **Timing of Control Movements.**—4.6.1. **Ailerons.**—Section 4.5.1. gives an example of the way in which timing of control movements can be important; the deflection of ailerons beforehand is not equivalent to deflection during recovery action, though it is usually qualitatively similar. Reference to Figs. 4.3 and 4.5 will provide one reason for this, in that the rolling moments only vary slowly in the first part of the recovery. Also in Table IV.1 when $A < B$ and we consider using pro-spin ailerons, the conflicting transient term is removed if we deflect them first before making the main recovery effort. Such effects have been indequately studied on full-scale monoplanes, probably because of the chance of aileron snatch or unpleasant control forces. The usually dangerous effect of 'crossed' ailerons on conventional designs is, however, a well-founded tradition.

4.6.2. **Elevators.**—An even more important case of delayed control movement is that enjoined in the standard technique for recovery, in which the elevators are purposely held up until the rudder has had time to take effect. One reason is the avoidance of outward sideslip, as we have already sufficiently emphasized. But this is probably only a secondary reason; the main one is that on very many designs of empennage the downward elevator deflection increases the area of rudder blanketed by the tailplane wake. The diagrams of Fig. 4.12 are a sufficient illustration of this.

Both full-scale and model evidence corroborate this idea. The *Seafire* 15 was a notable instance in which ordinary use of elevator led to a dangerous flat spin. Eventually, even before the rudder size was increased to improve this design, recovery was shown to be possible by skilful piloting in which only the minimum use was made of the elevator. Even on the *Typhoon* model, where the unshielded area of rudder was much less drastically reduced by downward movement of the elevator, there was a measurable improvement (of 3 units) in the model recovery when the elevator was delayed until after the rudder had been moved. The experiments were done by making minor adjustments to the rigging of the model controls. A much more satisfactory arrangement was introduced by Mrs. H. G. Alston on the larger models; this was a double mechanism, shown installed in a model in Fig. 4.9b, which releases the rudder and elevator separately at an interval which can be adjusted over an adequate range. A number of models has been tested with this mechanism, and the *Firefly* is an outstanding example of the effect of the delay on the threshold of recovery (Fig. 4.13). The full-scale tests also indicated that the aircraft was sensitive to the timing of the elevator.

4.7. **Best Use of Controls.**—Summing up, we can say that the ailerons should be deflected before the main recovery effort, the direction depending broadly on the sign of $(A - B)$.

The best timing of the elevator varies between two extremes; on one hand are the *Seafire* 15, the *Firefly* and others, where delay is essential to recovery, and where full elevator movement may not be necessary (although this is probably desirable in the closing stages of the recovery in order to prevent a further stall and spin in the opposite direction); on the other hand are aircraft like the *Wellesley* and *Typhoon*, where the full elevator movement is essential but the delay between the rudder and elevator movements is of minor importance. Between these extremes there are cases where the optimum amount of elevator movement is less than the full downward travel, *e.g.*, the *Master*, and can be obtained by comparative model tests. There is another group of designs like the M20/2 and *Hornet*, in which the shielding of the rudder is not influenced by elevator position; because of this and the near equality of A and B the timing of the elevator is of slight importance.

On all designs, of course, full rudder reversal is the primary control movement for recovery; though it may not be sufficient of itself to ensure recovery, without it recovery in most cases is likely to be impossible.

CHAPTER V

Prediction of Spin Characteristics

5.1. **Reasons Why Knowledge is Required.**—Structural safety can usually be ensured in spinning without designing specifically for it, but it is necessary to give some consideration to the tail loads, especially if the aerodynamic tail loads are to be combined with the loads due to a tail parachute. Their formulation demands a knowledge of the rates of descent in the spin and especially in the steepest spins that can occur.

A further need for information occurs in the cases of twin-engined aircraft and jet aircraft. The possibility exists of high rates of rotation giving rise to excessive loads on the engines and mountings.

Three main methods of predicting the spin characteristics are available. They are

(i) Detail calculation for each individual aircraft

(ii) A statistical comparison of the known characteristics of previous aircraft

(iii) Individual model measurements.

Method (i) requires detailed knowledge of the aerodynamic forces acting on the aircraft, which is not available. Methods (ii) and (iii) on the other hand may be used in conjunction with each other to make use of all the available model and full-scale data.

5.2. **Rates of Descent.**—One of the important characteristics of the spin in practice is the rate of loss of height. Usually there is some altitude, not precisely known, which is insufficient for recovery. Any excess above the minimum is available in an emergency for the pilot to attempt recovery, but to convert the excess into a duration of time we require the rate of descent. Rate of descent and aircraft speed are very nearly equal and usually it is unnecessary to distinguish between them, though we may sometimes do so. Strictly speaking, if V_H is rate of loss of height and V_a is the aircraft speed or velocity of the c.g., then

$$V_H = V_a \cos \gamma$$

and as we have seen in Chapter III, γ is usually less than 5 deg, so that the two quantities differ by less than one per cent, though the difference becomes larger at small incidences.

V_a is a very important quantity for another reason. It is the starting point in calculations of the stresses and the control forces on the aircraft. A knowledge of its probable values is therefore essential on this ground alone before spinning tests can be safely undertaken.

The equation of forces resolved along the flight path gives us that

$$\tfrac{1}{2}\rho V_a^2 C_D = w \cos \gamma$$

therefore

$$\tfrac{1}{2}\rho V_H^2 C_D = w \cos^3 \gamma .$$

The major variable determining V_a or V_H is therefore the wing loading w; the second in order of importance is C_D; ρ is only of importance if true speeds rather than indicated speeds are required,which is not so in calculating stresses.

In the simple theory of spinning C_D is equated to $C_z \cos \alpha$ where C_z is the normal force coefficient and is, of course, mainly due to the wings of the aircraft. C_z is, of course, a function of incidence, and we shall see that C_D is also a function of rate of rotation, but to a limited extent and it only becomes appreciable in fast spins. For very fast spins the aircraft is increasingly supported by the wing tips, and also, though to a lesser extent, by the tail, in such a way that the rate of descent is materially reduced and the stresses become appreciably redistributed.

5.2.1. **Variation of C_D with incidence.**—A number of measured values of C_D of models in free spinning are plotted in Fig. 5.1. These values are based on the rate of descent V_H, and neglect the effect of γ; they also include the drag of the vanes used to apply moments to the models as it is by no means certain that this should be subtracted. In any case, the error due to both these causes is hardly likely to be more than 5 per cent, the actual drag being less than that estimated, and as the measurement of tunnel speed (giving V_H) is subject to random variations of 3 per cent, this error is neglected. In this figure no attempt has been made to indicate any functional dependence on rotation; the points lie fairly close to a curve expressing dependence to the first order on incidence alone. This brings out the important fact that the rate of descent is primarily determined by the incidence, or attitude, of the aircraft. To a fairly good approximation we can therefore put

$$C_D = 0{\cdot}025\alpha - 0{\cdot}1$$

or, if we wish to define an upper limit to the possible rate of descent,

$$C_D = 0{\cdot}0166\alpha .$$

5.2.2. **Effect of rotation on C_D.**—A slight refinement of these expressions may be obtained by an application of simple strip-theory to the rotating wing. On the assumption of a linear relationship between α and C_D for the wing element we find practically no first-order sensitivity of the wing-drag coefficient to λ, for the drag of one element will be as much less than the mean on one side as it is greater on the other. The only appreciable contribution comes from the higher local air speed at the wing tips, and is of second order in λ.

For a straight trapezoidal wing with root chord θc_0 and tip chord c_0, consider the element at $y = \beta s$ from the plane of symmetry, as in Fig. 5.2:

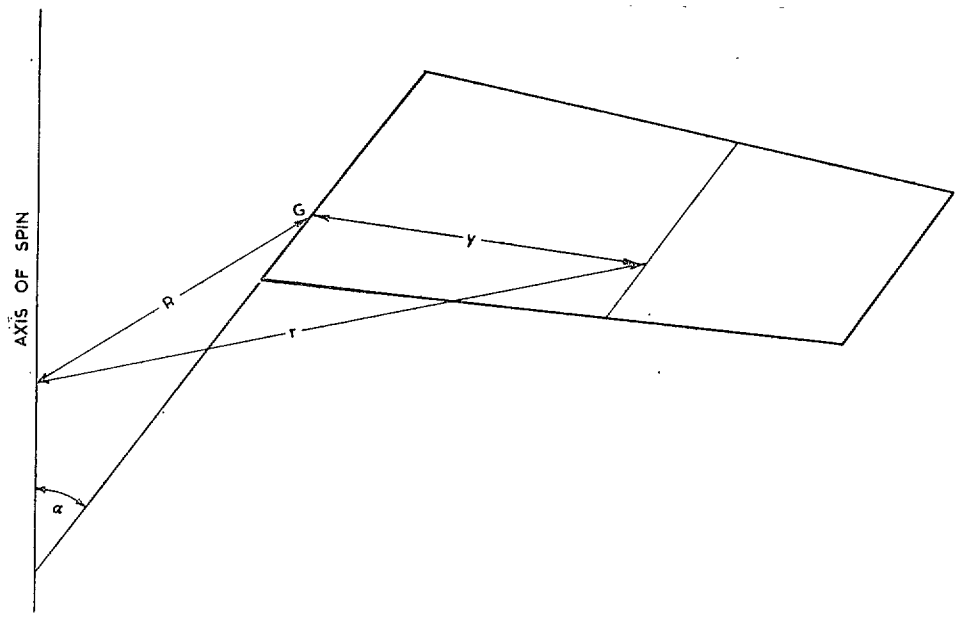

FIG. 5.2. Geometry of trapezoidal wing for strip-theory calculations.

Then the local air speed may be written as

$$\begin{aligned} V^2 &= V_H^2 + \Omega^2 r^2 \\ &= V_H^2 + \Omega^2(R^2 + y^2) \\ &= V_G^2 + \Omega^2 y^2 \\ &= V_H^2(sec^2\gamma + \lambda^2\beta^2) . \end{aligned}$$

In order to apply our assumptions about the drag to the actual wing, we need also to consider the vectorial distribution of lift and drag. A linear C_D may be regarded as one component of a normal force C_z which is a function of α; the comparatively small chordwise force will shift the direction of the resultant force C_R to some inclination $f(\alpha)$ near the normal. To obtain overall drag we require the vertical component. The local contribution of the element is $C_{R(\alpha + \arctan\beta\lambda)} \cos [f(\alpha) - \alpha]$. Taking the mean for positive and negative values of β, this reduces very nearly to $C_{R(\alpha)} \cos [f(\alpha) - \alpha]$ or $C_{D(\alpha)}$. The mean drag is therefore only increased by the factor $(\sec^2\gamma + \beta^2\lambda^2)$. Now put

$$\text{local chord} = c_0(\beta + \theta - \beta\theta) .$$

The mean drag coefficient is then given by integration along the span from $y = 0$ to s; we get

$$\begin{aligned} \frac{C_D(\lambda)}{C_D(0)} &= \frac{\int_0^1 (sec^2\gamma + \beta^2\lambda^2)(\beta + \theta - \beta\theta)\, d\beta}{\int_0^1 (\beta + \theta - \beta\theta)\, d\beta} \\ &= \sec^2\gamma + \lambda^2 \frac{(\theta + 3)}{6(\theta + 1)} . \quad .. \quad .. \quad (5.1) \end{aligned}$$

In Fig. 5.3 we use the approximation $\sec^2\gamma = 1$, but it may be remarked that strictly $\gamma \to 90$ deg as $\lambda \to 0$ in free spins, but only very slowly. The figure shows that this factor is not very sensitive to taper ratio θ; it also shows that in very fast spins a rise in drag coefficient over the static value of about 20 per cent is to be expected, and hence a correspondingly lower rate of descent.

In Figs. 5.4 and 5.5 an attempt has been made to analyse the effects on drag on the *Wellesley* and the *Prentice* models to show the increase of drag due to rotation as well as to incidence, and the tail drag is also shown as an independent variable. The measurements are here corrected for the drag of any vanes mounted on the models, and the points have been grouped together to obtain curves for mean values of λ. In the case of the *Wellesley* the measured drag does not exceed the estimate by very much, but for the *Prentice* the difference is considerably greater. That this is likely to be so in most cases may be seen by a comparison of Figs. 3.3 and 5.1. In Fig. 5.1, the average drag coefficient at 60 deg incidence is 1·4 and the average value of λ is about 0·35. In Fig. 3.3, at 60 deg the average static drag coefficient is 1·1. There is thus at this moderate value of λ, an increase in drag due to spinning of about 25 per cent on the average (allowing for the vane drag included in Fig. 5.1) compared with an estimated increase of not more than 5 per cent (Fig. 5.3) and the *Wellesley* and *Prentice* models are seen to be below average in this range.

It thus appears that a first-order term is present to which the simple strip-theory gives no clue. It may be that the wing stall is advanced on both wings simultaneously by the rotation, leading to higher drag coefficients, and if this is so we should expect $\overline{n'p}$ to be affected by the same mechanism.

5.3. **Rates of Rotation of Spinning Models :—Simple Theory.**—It is shown in Chapter III that in the steady spin there is a broad relationship between the wing-tip incidence and the mean incidence, for models. This relationship, if it could be accurately established, would

be sufficient to relate λ to α and hence to predict a curve of spinning rates of rotation. Such data are necessary for the investigation of the strength of the aircraft in the spin. Generally no difficulty is found in meeting the requirements in the cases of light or single-engined aircraft, but there is a serious possibility of inadequate strength of twin-engined aircraft under the sideways centrifugal loads on the engines; in turbine engines there are also the internal loads due to the gyroscopic moments to be catered for.

In 1943 a note by Pringle[11] was issued on ' Rates of turning in the spin of twin-engined types '. One unforeseen consequence of this wording was to create the impression of a fundamental division in spinning behaviour between single- and twin-engined types. It is emphasized that any such differences probably go no deeper than the largely known effects of mass distribution, and possibly minor effects due to the propellers and engine nacelles.

The immediate difficulty of applying model data is that for each model there is not one rate of rotation but a variety, obtained as a function of the applied yawing moment. In selecting a particular yawing moment as the appropriate value, we by-pass the problem of scale effect which only a thorough full-scale investigation could solve fully. For the moment, however, if we try to relate λ to n' we find on the whole that the differences between individual models are larger than the observed variation for a given model over a moderate range of C_n' apart from one or two exceptional cases. Figs. 5.6 and 5.7 show that on the average λ lies between 0·2 and 0·4 and that therefore a mean value of 0·3 or 0·35 could be adopted for stressing, provided that suitable safety factors were used. If the applied yawing moment is limited to an arbitrary value of 15, the upper limit of 0·35 is reasonable. Fig. 5.6 shows the normal gradual rise of λ with n' for single-engined aircraft, Fig. 5.7 is a similar diagram for twin-engined types, and Fig. 5.8 gives the observed data for a few types in which λ appears to jump discontinuously to a higher range of values.

In adopting a standard or average value of λ, it is necessary, in order to obtain Ω, to combine it with a formula for rate of descent; in the note[11] referred to this was

$$V_E\sigma^{1/2} = 27w^{1/2}$$

which corresponds to a drag coefficient $C_D = 1{\cdot}15$. Combining this with $\lambda = 0{\cdot}35$, and $\sigma = 0{\cdot}629$ (corresponding to 15,000 ft, the equivalent altitude of most of the model tests), we find

$$\Omega = 12w^{1/2}/s \text{ at } 15{,}000 \text{ ft.} \quad .. \quad (5.2)$$

It was also considered desirable that if measurements of the steady spin were to be used as the basis of prediction, a further factor of about 1·3 should be applied to cover any higher rates likely to be reached during recovery or during the entry to spins with abnormal virtual accelerations.

The formula just given did not provide a satisfactory basis of prediction. It was perhaps inevitable that greater accuracy should be in demand in cases where the margin of strength was small. In fact, equation (5.2) often gives an overestimate and the scatter in relation to model measurements is large. This fact is brought out by the diagram of Fig. 5.9 in which values measured at $10^3C_n' = 15$ are plotted against those calculated using equation (5.2).

5.4. **More Detailed Investigation of Rate of Rotation.**— Variation of Ω as $w^{1/2}/s$ is only the simplest of possible dimensional formulae, and to achieve any notable improvement it would seem necessary to make fully detailed calculations of the balance of moments. This is hardly practicable at present because of our ignorance of the full-scale moments. However it is possible to make a somewhat closer estimate if we carry the calculation only as far as its first stage, at which λ is estimated as a function of α through the balance of pitching moments. The completion of the process by solving the asymmetric equations is replaced by an arbitrary estimate of α. This arbitrary assumption of α is in accordance with the practice of considering at least two stressing cases, one a steep spin at 30 deg incidence and one a flatter spin at 60 deg incidence, so that the probable range is covered. This process has been checked by comparison with model data[12] (Pringle, 1945).

Qualitatively the kinds of data to be explained are those of Figs. 5.6 to 5.8; in Fig. 5.10 we have a selection of data—those most accurately measured—plotted against α. An analysis is required which will account for a function, with a minimum near 45-deg incidence, depending on c.g. position, inertia and elevator position for a given model, and also varying from model to model. It has long been realised that the pitching-moment equation is not a simple matter, for A. V. Stephens showed in 1932[13] that for the *Bristol Fighter* ' the approximation $\overline{m\alpha} + \overline{mi} = 0$ only applies at incidences below 45 deg and that the rotation of the aeroplane must have considerable effect upon the balance of pitching moments at higher incidences '.

The pitching-moment equation is as follows for the steady spin:

$$\overline{m\alpha} + \overline{m\eta} + \overline{mv} + \overline{mp} + \overline{mq} + \overline{mi} = 0\,. \quad (5.3)$$

In Ref. 12 it was proposed to ignore $\overline{mv}$, $\overline{mp}$ and $\overline{mq}$. The grounds for doing so are that $\overline{mv}$ has been shown to become appreciable only when the sideslip angle of the tail is of the order of 15 deg or more[3]. Assuming that the physical cause of $\overline{mp}$ is similar, and that it results from the effects of local tail sideslip we may neglect both in that fairly wide category of spins for which the angle is below 15 deg. If that angle is exceeded $\overline{mpv}$ is probably only of the order of 0·0005. $\overline{mq}$ is only appreciable if there is appreciable tilt, and observations of models again show a wide category of spins in which the tilt is very small.

We may now express $\overline{m\alpha}$ and $\overline{m\eta}$ jointly through the wing and tail normal force coefficients and their respective centres of pressure. For a monoplane we have some early data in Fig. 5.11, and Fig. 5.12 gives some measurements of tail normal forces in straight flight. It is intended to leave the wing force coefficient C_z and the tail force coefficient C_z' as symbols for the present, however. Let h_1 denote the centre-of-pressure coefficient for the wing relative to the centre of gravity, and the tail volume coefficient

$$\overline{V} = S'x'/S\bar{c}\,.$$

We also define α^x as the setting of the wing chord relative to the longitudinal principal axis of inertia. Then

$$\overline{mi} = \tfrac{1}{2}b\lambda^2 \sin 2\overline{\alpha - \alpha^x}. \quad .. \quad .. \quad (5.4)$$

In most cases α^x is between 2 deg and 7 deg and is generally not negligible.

We shall next assume that the only important contributions to $\overline{m\alpha}$ and $\overline{m\eta}$ are those of the wing alone and the horizontal tail surfaces. There is some reason to allow also for a contribution from the propeller or propellers; this in turn is of two parts, $\overline{m\alpha_P} + \overline{mg}$, say, where the first is due to propeller fin effect, the normal destabilising term also found at low incidence, and the second is the gyroscopic term dependent upon sense of rotation.

Now writing $C_D = C_z \sin\alpha$ and C_z' for the tail normal force coefficient the pitching equation may be reduced to

$$\frac{1}{2g}\left(\frac{S\overline{k_G^2 - k_A^2}}{S'x'}\sin 2\overline{\alpha - \alpha^x} - \frac{x'^2\sin^2\alpha}{\mu S}C_z'\right)\Omega^2 - \frac{h_1}{\overline{V}\sin\alpha} = \frac{C_z'}{C_D} \quad .. \quad .. \quad (5.5)$$

in which the second term inside the bracket arises from a small correction for the difference between aircraft velocity and local relative velocity at the tail. The equation may be abbreviated in the form

$$C_D F(\Omega, \alpha) \equiv \Omega^2(K_1 \sin 2\overline{\alpha - \alpha^x} - K_2 \sin^2\alpha) - \frac{K_3}{\sin\alpha} = C_z'(\alpha, \eta)\,. \quad .. \quad (5.6)$$

This indicates that Ω should tend to show a minimum at or near the incidence of 45 deg, as we saw was actually the case, in Fig. 5.10.

From tunnel tests we have some data to check the validity of the assumptions made, and this is done in Fig. 5.13 by plotting the measurements in such a form that the ordinates would be equal to C_z' if all the assumptions are correct. To achieve this, equation (5.5) is multiplied throughout by C_D. In doing this we inevitably introduce a rather large scatter associated with the accuracy with which it is possible to measure C_D. However, selecting only those points for which the most careful measurements were made, it is possible to detect a general agreement between different types of aircraft as well as the trend of the variation with α, and also the clear separation between points for ordinary spins and those with the elevator down. Whether the empirical curves so obtained closely follow the typical course of C_z' as measured for different elevator positions at high incidences may be judged by comparison with Fig. 5.12, two curves of which are transferred to Fig. 5.13. The qualitative agreement as to the order of magnitude is satisfactory, but there are both a considerable scatter of the measured points, and a marked difference in slope of C_z' against α compared with the curves of Fig. 5.12. To attempt an accurate check a number of other variables would of course have to be taken into account, but it is evident that there is a fair measure of agreement between different aircraft types, and this presentation does introduce order into the apparently disconnected series of data in Fig. 5.10 and allows a useful approach to the prediction of Ω.

5.4.1. **Causes of scatter.**—The general scatter of the points in Fig. 5.13 is probably attributable to a number of causes besides experimental error. They are listed in probable order of magnitude:

(i) Variation of C_z', *e.g.*, due to sideslip at the tail, tail design, body and wing interference, and elevator angle (Bamber and Zimmerman[14], 1933)

(ii) Error in assuming that the whole drag is due to the wings

(iii) Varying propeller effects

(iv) Neglect of variations of body pitching moment from type to type.

Nevertheless, taking the empirical curve as representative, it is noted that the quantity required to calculate Ω is really C_z'/C_D. In view of the second-order term in C_D depending on Ω^2 we would not expect C_z'/C_D to be a universal function of α for different aircraft or for different loading conditions of the same aircraft. This is brought out by plotting the left-hand side of equation (5.5) as it stands, thus introducing another cause of scatter in exchange for that due purely to error in measuring C_D; the result is in fact a poorer separation of spins with and against the elevator. The points of Fig. 5.13 are generally within 0·1 indicating an error of Ω^2 of 10–15 per cent; this becomes less when Ω^2 is larger, and is reasonably satisfactory for stressing purposes.

5.4.2. **General trend of curves.**—In Fig. 5.13 the empirical curves have markedly greater slopes than those obtained in the direct measurements of tailplane force, although it seems probable (*see* also Fig. 5.14) that a complete investigation would show the curves flattening out at high incidence. This larger slope may be due to any or all of the following:

(i) *The moment of the z component of body force.*—The discrepancy is of order, for high incidence,

$$\Delta C_z' = 0{\cdot}2$$

or

$$\Delta m = 0{\cdot}2 \times \bar{V}/A_1, \sim 0{\cdot}02\,.$$

Now we should expect the body damping moment to be of order $\lambda\Delta m$, i.e., if $\lambda = 0{\cdot}5$, of order 0·010. This is in

fact the case[15] (Irving, 1933), and in some degree confirms the partial explanation in terms of body moment.

(ii) *Wake effects on the tailplane.*—At lower incidences, where the empirical curves lie below the measured values, it seems probable that not only does the body pitching moment decrease notably, but that a definite interference effect of the wings and body, influencing the direction and speed of local flow over the tail should become apparent (*see* also Fig. 6.3). This would tend to reduce the apparent C_z'. Conversely, at higher incidences, a blockage effect increasing the local air speed would tend to increase the apparent C_z'.

(iii) *Errors in the assumed centre-of-pressure positions.*—The error in the wing centre-of-pressure position is likely to have the larger effect, for as Fig. 5.11 shows, the distance of the centre of pressure aft of the c.g. may increase by as much as $0{\cdot}1\bar{c}$ in the spinning range, thus increasing the apparent C_z'.

(iv) *Propeller effects.*—In the case of the *Spearfish*, the points calculated from the measurements appeared at first to be unduly low on Fig. 5.13. This result could be due to the up elevator angle being — 30 deg, and to propeller effects. That the latter could be appreciable may seen be from Fig. 5.14 where the function $C_DF(\Omega, \alpha)$ is estimated for the *Spearfish* and the *Sea Fury* for different conditions of propeller rotation. In this figure we see that the propeller rotating 'with' the spin has little effect but that rotation 'against' the spin leads to lower apparent values of C_z' at low incidences, and an increased slope. These results are clearly due to the two terms $\overline{ma_p}$ and $\overline{mg}$, where $\overline{ma_p}$ tends to reduce the apparent C_z' irrespective of the direction of rotation and $\overline{mg}$ tends to increase the apparent C_z' when the propeller is rotating 'with' the spin, and *vice versa.*

5.5. **Spinning Against the Controls.**—From the typical calculations given in Chapter IV we expect to find that reversal of elevator to recover, especially if accompanied or preceded by reversal of the rudder into the anti-spin position, will lead to a steeper spin than the original one if recovery fails to occur. This is the typical behaviour in model-spinning tests with applied pro-spin yawing moments sufficiently large to prevent recovery. It is easy to appreciate that such steepening is not universal, especially where the rudder is badly shielded by the downward elevator movement, or for some reason the slope of $\overline{n'p}$ is insufficient. In some cases it is observed that the non-recovery does take the form of a flatter, not a steeper spin. In either case, however, the rate of rotation tends to be high. One reason for this is the presence of the term in $\sin 2\overline{\alpha - \alpha^x}$ in equation (5.5) which tends to make the angular velocity a minimum near 45 deg incidence, so that very steep and very flat spins both tend to be fast. A second reason is that C_z' is an increasing function of η. The typical cases in Fig. 5.10 show that the question whether putting the stick forward accelerates the spin in the event of non-recovery, can only be answered with certainty if the steady spin is at an incidence of about 45 deg. In any other case it depends on the incidence in the initial steady spin. Examples of both kinds are known from model data; the following cases illustrate the point. In each case the rudder is also reversed for recovery; this, of course, generally tends to reduce the rate of rotation.

TABLE V.I

Effect of Control Reversal on Spin Parameters

Aircraft	$10^3C_n'$	Elevator Position (deg)	Ω (radn/sec)	α (deg)
Spearfish	13	Up 30 Down 15	2·02 2·29	60 54
Fighter A	4	Up 25 Down 15	3·59 2·82	75 60
Prentice (Design) ..	41	Up 26½ Down 22½	3·09 2·95	72 54
Gloster E1/44	15	Up 25 Down 20	2·35 3·05	56 39

As far as the strength of the aircraft is concerned, it is important only that we know the maximum rate of rotation and the incidence at which it occurs, and the maximum may therefore be treated as independent of the steady rate of spin rotation. The practice of applying a safety factor to the steady rate to cover the maximum is

only justifiable when speaking of a given incidence, but does not strictly cover the variable incidence in the free spin and recovery.

5.6. **Applicability to Full-Scale.**—We have already seen that earlier work on the comparison of model and full-scale data showed that the model measurements of $\overline{m\alpha}$ balanced the full-scale $\overline{mi}$ only at moderate incidences, and that the discrepancy increased progressively with increasing incidence. There is some reason to regard this discrepancy as being due to the effects of sideslip and rotation, in exactly the same way as we found in free-model tests; and there is no particular reason to distrust the free-model indications of the relationship between Ω and α. Owing to its importance in strength requirements, however, this has been the subject of a controversy which can be only finally settled by many more full-scale measurements than have yet been made.

Only one or two isolated cases may be mentioned. The chief uncertainty lies in the failure to relate measured full-scale rates of rotation to incidences. This may be overcome to a certain extent as suggested in section 5.3, by relating the measured full-scale rates of rotation to the model rates measured with an applied yawing moment which is constant from model to model.

The *Prentice* has been observed by eye witnesses both in flat and steep spins, respectively fast and slow. The slower rate measured from the ground was 2·6 radn/sec and agrees well with the value of 2·35 radn/sec measured for the model, loaded to represent the full-scale aircraft, at 15 units of applied yawing moment. For the *Harvard* the rate of rotation measured in a number of full-scale spins by means of the R.A.E. spin recorder was 3·0 radn/sec, which compares with 2·8 radn/sec in the model tests at 15 units of applied yawing moment; comparative figures for the *Meteor* 4 are 1·8 radn/sec full-scale and 2·25 radn/sec model-scale.

In this connection we expect, however, that there will always be a probable discrepancy of more than 5 per cent if we admit that the estimation of $(C - A)$ has a probable error of 10 per cent, for Ω varies, to a first approximation as $w^{1/2}/(C - A)^{1/2}$ on a given aircraft.

5.7. **Use of Formula to Predict Ω.**—To obtain a working formula for obtaining Ω we may neglect the term in C_z' inside the brackets in equation (5.5) as it is of minor importance in the normal range of loading; we then have:

$$\frac{1}{2g}\left(\frac{S\overline{k_c^2 - k_A^2}}{S'x'}\sin 2\overline{\alpha - \alpha^x}\right)\Omega^2 - \frac{h_1}{\overline{V}\sin\alpha} = \frac{C_z'}{C_D}. \quad .. \quad (5.7)$$

TABLE V.II

Rates of Rotation of Spinning Models

Aircraft	Model-test results		$\Omega_D = \left[\frac{60S'x'}{S(k_c^2 - k_A^5)}\right]^{1/2}$ at $\alpha = 60$ deg	$\Omega = \frac{12w^{1/2}}{s}$
	α (deg)	Ω (radn/sec)		
Spitfire 1	53	2·4	2·55	3·15
Typhoon	60	2·85	2·5	3·65
Firefly 4	67	2·55	2·5	3·7
Beaufighter	60	2·35	2·5	2·65
Mosquito	61	2·8	2·7	2·85
Vampire 3	43	2·5	2·45	3·35
Tempest 5	64	2·8	2·75	3·55
Tempest 2	64	2·75	2·5	3·55
Ace	57	2·45	2·6	4·15
Sea Fury	60	2·9	2·9	4·1
Fury	60	2·7	2·6	3·8
Hornet	52	2·9	2·85	3·5
Spearfish	61	2·1	2·15	2·5
E1/44	53	2·1	2·3	4·55
E6/44	45	1·35	2·05	3·1
Attacker	48	1·75	2·6	4·6
Fighter B	63	2·3	2·15	3·7
Meteor 4	55	2·25	2·25	4·15
Magister	55	2·5	2·3	2·25
Harvard	66	2·75	2·7	2·6
Prentice	60	2·35	2·45	1·75
Athena	64	2·55	2·4	3·1
Balliol	68 (80)	2·8 (4·2)	2·4	3·25

For a new aircraft, k_A, k_c, S, S', $\bar{V}$, x' and α^x are known or may be calculated. Knowing the centre of gravity position, h_1 may be obtained from Fig. 5.11 for the incidence under consideration, and C_z' and C_D may be obtained from Figs. 5.13 and 5.1 respectively. As mentioned earlier, it is usual to consider two cases, 60 deg incidence with the elevators up, and 30 deg incidence with the elevators down. The latter case covers the established spin against full elevator, which probably will only occur in very bad spins. We may therefore take $C_z' = 0{\cdot}65$ and $0{\cdot}7$ (allowing for some decrease of slope as indicated by the straight-flight measurements) respectively and $C_D = 1{\cdot}4$ and $0{\cdot}65$ respectively at these two incidences.

To simplify the matter still further, we may also assume average values for α^x, h_1 and $\bar{V}$ and we then have

$$\Omega_D = \left[\frac{60S'x'}{S(k_c^2 - k_A^2)}\right]^{1/2} \text{ radn/sec at 60-deg incidence, elevators up, .. (5.8)}$$

and

$$\Omega_D = \left[\frac{120S'x'}{S(k_c^2 - k_A^2)}\right]^{1/2} \text{ radn/sec at 30-deg incidence, elevators down. .. (5.9)}$$

The second case is an extreme, in all probability a factor of $1{\cdot}5$ on Ω_D^2 at 60 deg will be sufficient to cover the speeding up normally encountered in recovery.

Applying the first of these expressions to a number of models tested we obtain the rates of rotation shown in Table V.II. For comparison, the rates of rotation and incidences measured on the models with pro-spin yawing moments of 15 units applied, and the rates estimated using equation (5.2), are also given.

The average predicted rate of rotation, $2{\cdot}48$ radn/sec agrees very well with the average of the measured values, which is $2{\cdot}46$ rads sec, and the standard deviation of the prediction is $0{\cdot}28$ radn/sec or 11 per cent, which, when all the possible causes of scatter are remembered, is very reasonable. The average of the rates predicted by equation (5.2) is $3{\cdot}37$ radn/sec which confirms that in general this expression considerably overestimates.

The average measured incidence is just under 60 deg and it is thus reasonable to combine the predicted rate of rotation with this incidence.

A satisfactory estimate of the spin conditions for stressing may thus be obtained by using equation (5.8), or if a slightly finer mesh is required, equation (5.6) may be used.

CHAPTER VI

Prediction of Recovery Characteristics

6.1. **Methods of Prediction.**—Although model tests are practicable and often useful it has for some time been a question whether they could be anticipated by some simple ' design criterion '. By this we mean, the attempt to apply past experience, especially results of model tests, to some simple inequality which discriminates success from failure in recovery. This must always be an important aim of spinning research, for it helps the designer to incorporate features, in a new aircraft, which will give good recovery characteristics.

Two main suggestions for achieving this are to be examined. The first was made by Irving[8] and was to make spinning calculations as a routine on each type. This implies solving the moment equations and producing graphs of unbalanced yawing moment against incidence for the aeroplane spinning with elevators either up or down and rudder central. From such curves we can see whether the aircraft is likely to spin flat and whether it can remain in a stable spin against the controls. Two major difficulties arise against this procedure:

(*a*) Incomplete data on aerodynamic derivatives

(*b*) Most data apply to model scale and the applicability to full scale is to some extent unknown.

The second objection does not hold if we are content to predict model results only, but the first is more serious. The rolling balance work done by Irving, Batson and Warsap[16] in 1935 went far to remove the difficulty, but some gaps remain; for example, we require a knowledge of how design factors affect $\overline{l'v}$ and $\overline{n'v}$ in the conditions relevant to the spinning of monoplanes.

In 1937 a notable attempt was made by Finn to take a short cut to the end[17]. At that time it was known that the major variables determining recovery were:

(i) The inertia difference $(C - A)$

(ii) The contribution of body and tail to the moment $\overline{n'p}$ (rudder central)

(iii) The yawing moment due to rudder deflection

(iv) C.G. position.

In this anaysis it was decided to neglect all secondary factors, even the inertia difference $(A - B)$, as most of the previous model tests had shown that $(C - A)$ is much the more important, probably because, through its direct effect on λ, it indirectly affects the body-damping contribution; the relative importance is brought out, for example, in a research by Francis[18] (1936). The inertia difference coefficient $(C - A)/\rho Ss^3$ was therefore taken as an independent variable. The ' body damping ' and ' rudder power ' were not estimated as aerodynamic coefficients at a particular α and λ but were represented by geometrical ratios derived by simple rules from the design of the side elevation of the aeroplane. The

feasibility of this is shown by the rough proportionality demonstrated in the report already quoted[16] from which the body damping is evidently determined at a given α and λ chiefly by the weighted side area $\int nhx^2\,dx$ where h is the depth of body in side view and x is the distance measured along the body axis from the c.g. A further weight factor n is inserted in the integrand to allow for tail interference, and has the value 2 for areas below the tailplane and 0 for areas blanketed by the tailplane wake. (For this purpose we take the wake as spreading out at 15 deg on either side of a mean angle of 45 deg so that the shielded area is defined by lines at 60 deg to the tailplane chord at the leading edge and 30 deg at the trailing edge.) The rest of the side area has a factor of 1.

The rudder power is represented by the product of the unshielded rudder area and its leverage about the c.g.

These parameters are plotted against b, and it is evident that the models having low values are on the whole those which fail in free-spinning tests under standard conditions. In fact a rough separation could be achieved by means of straight lines representing a minimum standard. A fairly good separation was also obtained by using a single parameter, the product of the other two ; this feature was abandoned by Tye and Fagg[19] (1940) in their extension of the enquiry to include full-scale aircraft.

No extravagant claims were made for these aerodynamic criteria of recovery. At first only a minimum standard was laid down but with the reservation ' there is a wide band of values of the damping-power factor within which ability or failure to pass the required standard is governed by secondary factors not included in this analysis ', and again ' in general, the designer should aim at providing about twice the minimum value '. In Ref. 19 the authors tried to improve the separation into two distinct categories by some refinements of procedure. One of these was the introduction of a weight factor n of $-\frac{1}{4}$ for shielded areas of fin and rudder, whereas for areas of rudder below the tailplane, allowing for the leakage through the elevator cutaway, the factor was reduced from 2 to $1\frac{1}{2}$. These authors also investigated whether the separation was improved by considering spins at 60 deg, as it has usually been held that a good damping at 60 deg was desirable in order to prevent the flat spin. However, the separation was not thereby improved.

6.2. **Advantages and Disadvantages of Present Design Criteria.**—The design criteria in this form have been of undoubted value in giving a rough indication of spinning characteristics, with a minimum of effort. The designer, however, requires a finer mesh, and in the aircraft of today he is often obliged to work either distinctly below the minimum requirements, or else in that wide band where ability to recover is determined by secondary factors omitted from the simple analysis. To be of real value, aerodynamic criteria must be accurate enough to make the error in either parameter significantly less than the range of variation which the designer is prepared to contemplate. If a factor of 2 is dismissed as insignificant, the designer may be asked to provide twice as much side area as is strictly necessary; such a requirement becomes an absurdity. But it is just here that the present criteria fail, for there is no explicit allowance for the effect of body section in assessing the damping. The tests of Ref. 16 show that body damping can vary from 10 units to 35 units purely by variation from a section with a rounded top to a section with a rounded bottom and flat top.

The present criteria can in fact only be a reasonable guide within a fairly narrow range of variation of design, and we are faced with the problem of increasing not only the accuracy but the scope of the predictions. Tye and Fagg stated that damping and rudder power should both reach minimum standards, and left them as separate parameters, whilst recognising that a deficiency in either might be to some extent made good by a surplus in the other; this introduces a considerable factor of human judgement into the method and detracts from its value. The procedure of multiplying the parameters, on the other hand, is lacking in theoretical justification.

It is not surprising that the present criteria have sometimes proved misleading, especially for cases near the proposed borderline, *e.g.*, amongst the outwardly similar types, *Typhoon* and *Tempest*, only the *Typhoon* has given trouble, but they have similar parameters (both slightly below the borderline). The *Spitfire* lies considerably low on the graph but has proved satisfactory in flight. Again, the changes in the parameters of the *Seafire* 15 to make it satisfactory were much less in practice than the present requirements indicated.

The test of a criterion of recovery is not in the clean separation of past cases into two categories, though it should do this, but in predicting the future recovery of new designs. It is here that new difficulties are met. In particular, the aerodynamic data may lie outside the range already covered whether in wing-loading, inertia coefficients or such details as body section. It is here that an over simplified theory breaks down. In the analysis of Ref. 19 the mean wing loading was about 21 lb/ft^2 and there were few aircraft with circular body-sections. In more recent fighters and high-altitude aircraft the tendency has been to higher wing loadings and to circular body sections.

6.3. **Classification of Sources of Error.**—In effect the criteria are a crude application of the yawing moment equation, and express a form of the inequality

$$\overline{n'\zeta} + \overline{n'p} \lesssim 0 \quad .. \quad .. \quad .. \quad (6.1)$$

for a particular incidence, namely 45 deg; but by keeping the parameters separate we help to ensure that flat spins are excluded if the damping is sufficiently large.

Assuming that this is the theoretical background, we may estimate the approximate ' scatter ' caused by the many simplifying assumptions implicit in the present procedure, and also the reduction in scatter to be expected if we improve the procedure.

Sources of error may be placed in four classes :

6.3.1. **Errors in estimating body and tail yawing moments due to roll.**—We call the contribution of the body and tail to $\overline{n'p}$ (model) $\overline{n'p}_B$ at a given α.

In the first place, the use of b as independent variable implies that λ is a function of b. In the previous Chapter a method is given for estimating Ω^2, the result of which gives after some reduction,

$$\lambda^2 = \frac{2}{A_1 b \sin 2\overline{\alpha - \alpha^x}} \left\{ \overline{V} C'_z + \frac{h_1 C_D}{\sin \alpha} \right\} . \quad .. \quad (6.2)$$

At a given incidence this may determine λ^2 to about 15 per cent standard deviation; if all the variables except b are given constant values the variation is likely to increase to about 22 per cent standard deviation. These errors exclude any error in estimating b itself. Allowing even 10 per cent standard deviation in b, the figures for λ^2 increase to 18 per cent and 24 per cent. The full formula for λ^2 does in fact allow for variations in c.g. position, affecting the balance of pitching moments, whereas in the present procedure c.g. position only affects the value of the damping through the geometrical body-damping ratio and is therefore inadequately represented.

Secondly, the assumption that body damping is a function of ' body damping ratio ' is untrue unless we incorporate a weight factor (ε, say) to cover the effect of body section. The values appropriate to $\alpha = 60$ deg and $\alpha = 45$ deg are approximately as given in the following table, in which we take

$$\overline{n'p}_B = \varepsilon\lambda \left(\frac{\int hx^2 \, dx}{4Ss^2} \right) . \quad .. \quad .. \quad (6.3)$$

TABLE VI.I

Effect of Body Section on Damping in Roll

Body cross-section	ε (60 deg)	ε (45 deg)
Circular (pointed profile)	0·6	0·6
Rectangular	2·4	1·5
Elliptical	2·9	2·1
Round top, flat bottom	0·9	1·1
Round top, flat bottom + strakes ..	2·1*	1·7*
Round bottom, flat top	3·3	2·5
Round bottom, flat top + strakes ..	4·7*	3·5*
Fin — Free	3·8	1·5 (1½)
Fin — Under tailplane	7·6	3·0 (3)
Fin — Above tailplane	−0·95	−0·38 (−0·4)
Rudder under tailplane	+5·7	+2·25 (+2)

* Depending on width of strakes, this is for $0 \cdot 014 l''$. (l'' = c.g. to rudder post.)

In neglecting ε altogether there is a possibility of about $\pm$ 70 per cent error in the damping coefficient; if we use ε and assume that $n'p_B$ is always the same function of λ and body-damping ratio, the error becomes of order $\pm$ 20 per cent but depends upon the range of λ, and the range of variation of body plan-form.

Two difficulties arise in assigning a value of ε to a given body section. One is that the circular section was only investigated with ' pointed ' profiles, which is not typical of modern fuselages. Another difficulty is that of interpolating between circular and elliptical or circular and rectangular sections, even assuming that the figure of 0·6 is correct. This can only be a matter of judgement at present and it is difficult to assign ε impartially.

It seems desirable to modify the factors used by Tye and Fagg for the empennage contribution to body-damping ratio and it is suggested that the values in the brackets in Table VI.I should be used. A further error creeps in if, as seems convenient, we neglect the effect of body section on the empennage contribution; this error is about 20 per cent of the body contribution; depending on the magnitude of λ.

Since the body contribution to body-damping ratio is usually from one-third to one-half of the total due to body and empennage, we may reasonably expect the total damping to be in error by about 18 per cent if ε and the proposed new factors for the empennage are used, and otherwise by about 50 per cent if the previous empennage factors only are used.

Wing interference seems to be relatively unimportant, in that it appears to be fairly constant in going from the high to low positions relative to the body, and therefore neglect of it is likely to give at most a constant error which will not increase the final ' scatter '. From this there is however an important exception. In some cases the wing wake partly envelopes the fin and rudder, and

in such cases it seems natural to exclude the shielded area from the integral of the body damping ratio, although this point has not been adequately investigated experimentally.

6.3.2. **The inertia yawing moment.**—We now consider a second type of error. The inequality (6.1) cannot be significant in the spin without the inertia term and it should be replaced by the following:

$$\overline{n'\zeta} + \overline{n'p_B} + \overline{n'p_W} + \overline{n'i} \lesssim 0 \quad . \quad . \quad . \quad . \quad (6.4)$$

The inertia term may be of the order of 5 units and of either sign. This is hardly a negligible contribution. In the analysis of R. & M. 1810[17] the omission of this term was based on evidence in which only a limited range of $(A - B)$ was admitted. To cover present requirements a wider variation is necessary, and the effect on the balance of yawing moments may be seen by reference to the data obtained by Francis (*loc. cit.*) or to Fig. 4.7.

6.3.3. **Wing contribution and sideslip effects.**—In considering $\overline{n'p_W}$, the wing contribution, the procedure entailed by the use of the inequality (6.4) would be equivalent to allowing only a functional dependence on λ at a given α. The question then to be considered is whether any other major factors affect it. There is some evidence, not yet sufficiently explored by rolling balance tests, that thickness ratio is an important parameter and that Reynolds number may also be involved. Naturally, wing plan-form and taper would be expected to exert an influence.

The sideslip term $\overline{n'v}$ is neglected; some evidence suggests that it is small in the spin; in any event, its variation from type to type is unlikely to be important in producing ' scatter '.

6.3.4. **Scale effects.**—The question of scale effects and applicability to full-scale arises throughout this discussion. It was a merit of the procedure of R. & M. 1810[17] and the work of Tye and Fagg[19] that they could be applied separately to model- and full-scale results and a mean borderline found. It was less satisfactory to find that the borderlines so chosen have a constant separation, though this may point to inadequate representation of scale effects during model tests.

The chief source of error due to scale effect probably lies in the values of ε for the calculation of $\overline{n'p_B}$. The measurements were made under conditions more nearly representative of full-scale although the actual Reynolds number was low. Thus, we would expect more scatter from this cause in an analysis of model results than full-scale. An example of this is the *Prentice*[20] (Harper, 1948), where at model-scale the fuselage (a square surmounted by a semicircle in section) evidently gave a very much greater damping moment than would be indicated by the factor ε of 1.1, and the addition of strakes had little effect.

6.4. **Suggestions for a Criterion of Recovery.**—To remedy the drawbacks associated with a large scatter, it is suggested that a criterion should be sought with explicit recognition of the yawing-moment equation as its basis; the prospect of improved accuracy depending on the closeness with which the real aerodynamic derivatives are established. Then, as the majority of the available information at present is on models, the criterion should be capable of overall check against model tests, and there would be no attempt to reach a full-scale answer of the kind on which model tests throw no further light. At present there is no method of showing which is to be preferred when model-test results conflict with the criteria. Instead we need information on scale effects applicable to either free-spinning models or to design calculations.

At the moment the most practicable improvements would probably be as follows:

(*a*) To base an estimate of aerodynamic derivatives on a simple formula for λ

(*b*) To estimate $\overline{n'\zeta}$, $\overline{n'p_B}$ and $\overline{n'i}$ by simple rules; especially to use ε, but neglecting the effect of plan-form on ε

(*c*) To neglect $\overline{n'v}$ and the shielding of the body by the wing, but to allow for the shielding of the fin and rudder by the wing as well as by the tailplane

(*d*) To calculate the unbalanced yawing moment and plot it as a function of t/c. This is justified by experimental evidence that over a wide range of λ, $\overline{n'p_W}$ has a flat maximum and is therefore mainly a function of α, *i.e.*, for a given wing it is constant for a constant α.

This procedure, followed for a particular incidence, gives a set of ordinates with which the measured threshold applied yawing moment model-scale should be strongly correlated. It would also be reasonable to expect the points to be separated, according to the ability or failure of the full-scale aircraft to recover from spins, by some curve crudely representing the full-scale $\overline{n'p_W}$, which includes wing-body interference. This may, however, prove to be otherwise if $\overline{\Delta n'p}$ is largely determined by other parameters, *e.g.*, the precise Reynolds number.

Such a programme is limited, falling short of the ' spinning diagram ' which might be a later development. It abolishes the two-fold criterion, but so far does not properly distinguish between aircraft whose full-scale failure is in the form of flat spins and those where it is in the form of steep spins. Finally, it attempts to answer the question ' Is a spin against the controls possible? ' rather than ' Can such a spin be avoided in practice by using the correct technique for recovery? ', and it is therefore possibly somewhat pessimistic.

There is some justification, apart from economy of effort, for choosing say 45 deg as the crucial incidence, for there the rate of rotation tends to have a minimum value. The danger of loss of fin efficiency increases as α decreases due to the wing wake, but most cases of failure in recovery have been associated with spins which have appeared to be fairly flat.

6.5. **Application to Full-scale Data.**—A preliminary attempt to apply these suggestions gave the data in Fig. 6.1. The formula adopted for λ is simply

$$\lambda = (1{\cdot}3/A_1 b)^{1/2} \quad .. \quad .. \quad .. \quad (6.5)$$

which is obtained from equation (6.2) and represents the spin parameter for spins with the following assumed data:

Elevator Position :—Fully down		C_z'	0·9
Incidence	45 deg	h_1	0·12
α^x	$3\frac{1}{2}$ deg	C_D	1·0
$\bar{V}$	0·5		

Since $\overline{n'i}$, though not negligible, is a smaller contribution than the others, we may use constant derivatives $\overline{l'p}$ and $\overline{l'v}$ in calculating it, in default of more detailed information.

$$\overline{n'i} = c\lambda^2 \cos\alpha \,.\, \theta_y$$

where

$$\theta_y = -\frac{\overline{l'p} - C_L l_v/2\mu\lambda}{l_v + a\lambda^2 \sin\alpha}.$$

Then if we take

$$\overline{l'p} \simeq -0{\cdot}07\lambda$$
$$l_v \simeq -0{\cdot}26$$
$$C_L \simeq +1{\cdot}0$$

it follows that

$$\overline{n'i} = \frac{c(-0{\cdot}07\lambda + 0{\cdot}13/\mu\lambda)}{(1 + 0{\cdot}28A_1)b + c}.$$

Finally $\overline{n'\zeta}$ is represented by the unshielded rudder volume coefficient; the available information on this shows a fair variation from type to type, but in the absence of detailed measurements we write

$$\overline{n'\zeta} = A_R \frac{l''}{2Ss}.$$

The area A_R is that left unshielded by the tailplane and wing, at 45 deg incidence, when the elevator is neutral, assuming as usual that the wakes spread out 15 deg on either side of the free-stream direction.

6.6. **Notes on the Suggested Criterion.**—6.6.1. **Effect of wing taper.**—In looking for evidence of flow conditions strongly influenced by the nose bluntness or thickness ratio of the wing section, it is reasonable first to examine the effect of taper of the plan-form. To do so we must first make some assumption about the effect of local incidence on C_X; the simplest is that

$$\Delta C_X = \beta C_{X0}$$

say, for a wing with constant thickness ratio, where $\beta = y/s$ and where ΔC_X is the asymetric part of C_X from which $\overline{n'p_W}$ arises. Then the local element of wing, having chord length $c_0(\beta + \theta - \beta\theta)$, gives a yawing moment

$$\tfrac{1}{2}\rho V^2 \,.\, \Delta C_X yc\, dy$$
$$= \tfrac{1}{2}\rho V^2 \,.\, \beta C_{X0} \,.\, \beta s^2 c_0(\beta + \theta - \beta\theta)\, d\beta$$

provided we neglect the effect of rotation in increasing the local air speed.

Therefore $$\overline{n'p_W} = \frac{C_{X0}}{(1+\theta)} \int_0^1 \beta^2(\beta + \theta - \beta\theta)\, d\beta$$
$$= \tfrac{1}{4} C_{X0} \left(1 + \frac{\theta}{3}\right) \Big/ (1 + \theta).$$

We do not know how C_X varies with t/c but there is some reason to think that it becomes small for low thickness ratios. If, for example, it becomes zero at the wing tip a further factor $(1 - \beta)$ in the integrand would approximately allow for this, and the term involving θ would become $(1 + \frac{2}{3}\theta)/(1 + \theta)$. Hence in ignorance of the real relationship between θ and t/c we may tentatively assume that the factor lies between these two, say $(1 + \frac{1}{2}\theta)/(1 + \theta)$. Such a factor does not noticeably improve the ' separation ' in Fig. 6.1 and it is therefore ignored for the present.

It has been emphasized that the suggested criterion should best apply to model data. However, the mutual compatability of data appears to be better, on the present hypothesis of a wing-thickness parameter affecting $\overline{n'p_W}$, for full-scale than for model data. For example, we see now that the full-scale behaviour of the aircraft is consistent with the data in every case except that of the *Mentor*, although there is some scattering of the ' borderline ' cases. We are, however, still in some difficulty to explain the free-model data on the *Wellesley*, M.18, and *Prentice*. One possibility is that the scale effects in some cases become exceptionally large when λ is large, but this and other possibilities can only be elucidated by further detailed measurements on rotating wings.

6.6.2. **Wing-body interference.**—The available model evidence[15, 16] would suggest that the addition of the monoplane wing to a body and empennage makes about 10 units difference to the damping moment. This effect is more or less independent of the height at which the wing is inserted, and cannot be allowed for by simply excluding that part of the body which is ' shielded ' by the wing wake. More detailed data would be of value here, but it may reasonably be supposed that wing-body interference is the main contribution to the apparent wing yawing moment in Fig. 6.1. Furthermore, the data on the effect of a wing on the body appear to conflict with what is known of the effect of tailplane wake on the fin and rudder, and to follow different rules.

6.6.3. **The crucial incidence in the spin.**—Reference to Fig. 4.7 gives no confirmation of the idea of choosing a crucial incidence, unless c is above a certain negative value; in which case the crucial incidence might seem to be between 20 deg and 30 deg. However, the unbalanced yawing moment with rudder central is only one side of the equation: the other is the available rudder power. It seems probable that rudder power as a function of incidence is widely variable from type to type, owing to the different relative layout of wing tailplane and rudder.

Examples are given in Fig. 6.2 of variation of unshielded rudder area as a function of incidence. It is assumed that the wing and the tailplane shed wakes spreading out at 15 deg on either side of the direction of the free

stream. The area of unshielded rudder may thus either increase or decrease with incidence and on the M20/2 shows a pronounced maximum at about 55 deg, below which the rudder is progressively enveloped by the wing wake. It is therefore probable that different types will vary as to the incidences at which the rudder is adequate to provide a moment large enough to upset the spinning equilibrium.

To examine this question in more detail, it would be necessary to allow for the effect of wing interference on the empennage even when no wake envelopes the fin. Irving and Batson found only a small interference effect on the damping. Two simple experiments bear on the same point. One was the observation of tufts at three different points on the fin of a stationary *Tempest* model from which the tailplane had been removed. The flow direction was deflected from the main stream by the combined action of the wing and body to a maximum extent of more than 10 deg in the manner shown in Fig. 6.3. This deflection of the flow and the associated velocity field must influence the curve of $\overline{m\alpha}$, though it does not go far towards explaining the anomalies in the estimation of tail normal-force coefficients from measurements of free spins (Chapter V).

A second experiment was a pitot-traverse downstream of two models without rotation. On the Fighter A (Fig. 6.4) various modifications of the kind usually found advantageous had proved ineffectual and it was supposed that this might be due to a wing wake reducing the fin efficiency. A pitot-traverse at 30 deg incidence showed that the wing and tailplane wakes were practically contiguous and that enlargement of the fin in this region would not be likely to improve recovery. On the *Mosquito* traverses were done at 30 deg and 60 deg incidence (Fig. 6.5) and the results showed that the wakes tended to separate at higher incidences in the region of the fin. All three results are broadly consistent with the assumption that the wakes spread out at angles of $\pm$ 15 deg to the main stream; certainly this assumption is close enough at 45 deg incidence.

A further difficulty in assigning a crucial incidence is that the shielding of the rudder by the tailplane is often dependent on the elevator position. The wake becomes wider when the elevator is moved down, and this may diminish the area of unshielded rudder. This is so for the *Typhoon*, *Spitfire* and many other types, but not for the M20/2, *Mosquito* or other designs where the fin and rudder are set well forward of the tailplane.

6.7. **The Possibility of an Incipient Spin Standard.**—It has been pointed out that recovery from incipient or two-turn spins may be possible with a lower standard of design than is required for sustained spins. This is a matter on which model tests can shed very little light, and the full-scale data are hardly exhaustive, but because fighter aircraft are nowadays only required to recover from two-turn spins, it seems desirable that some indication of the standard of design required should be formulated. A number of aircraft, *e.g.*, *Firefly*, *Sea Fury*, *Seafire*, *Vampire*, etc., have successfully recovered from two-turn spins although their spinning criteria were below those required for recovery from sustained spins and although the model recoveries in terms of applied yawing moment were relatively poor. A satisfactory relaxed standard may be found when we have attained a reliable rule for sustained spins. In the meantime it might be of some guidance to use a lower criterion on the lines of the one suggested in section 6.4; perhaps using 30 deg instead of 45 deg as the crucial incidence, since the incidence appears to increase as the spin proceeds and does not usually reach normal spinning values in the first two turns.

6.8. **The Prediction of Control Forces.**—Although the speeds in the spin are fairly low and are comparable with stalling speeds, there is a risk of large control forces, especially in the case of the elevator and, to a lesser extent, the ailerons, because of the large deflections required. It is therefore of importance to estimate these forces for heavy aircraft before undertaking full-scale trials. Unfortunately, an accurate calculation could only be made with the use of data which at present only the tests themselves can provide.

The estimate is based on three items:

(i) The air speed in the steady spin

(ii) Variation of the speed during recovery

(iii) Hinge-moment coefficients as a function of α and η.

Only (iii) can be obtained from wind-tunnel tests. The steady air speed can be estimated as indicated in the previous chapter. The least certain factor is (ii) and it is also a rather important factor because the highest speeds are reached in this phase of the manoeuvre combined with large hinge moment coefficients. An upper limit can be given for the aircraft speed as a function of incidence but there is at present no means of estimating the lowest relevant incidence. A lower limit is obtained by assuming the speed to remain constant at its value for the steady spin, and the upper limit by assuming the speed at any incidence in the recovery to be that which would be attained in a steady spin at that incidence.

We have in this country few data on which to base a prediction of elevator forces, and it is usual to use N.A.C.A. data on elevator hinge moments[21] (Sears and Hoggard, 1942).

An estimation of the stick forces may then be made as shown in Fig. 6.6. The speed as a function of incidence is obtained from the drag coefficient, which is drawn in Fig. 6a to cover rates of descent slightly higher than the average (Fig. 5.1). Fig. 6b shows typical hinge-moment curves obtained from Ref. 21 and the stick force is then obtained from the formula

$$\text{Stick force} = (\tfrac{1}{2}\rho V^2)\,\gamma C_H c_e S_e \quad .. \quad .. \quad (6.5)$$

where

γ = stick gearing in deg/in.

c_e = elevator chord behind hinge

S_e = elevator area behind hinge.

For steady spins this becomes

$$\text{S.F.} = \gamma w c_e S_e \,.\, C_H/C_D$$

and Fig. 6c shows the limiting values of the stick force for the hypothetical cases of infinitely long recovery and instantaneous recovery. The actual value will depend on the time of recovery and the difference between the two limits is quite critical, especially in the later stages.

That the estimation by this method can give reliable indications of the order of forces to be expected is shown by two cases on which detailed estimates have been made. The first was the *Firebrand*. On account of the high forces predicted, the aircraft was fitted with a power-operated elevator, and records of the forces were made during spins. On each occasion forces were measured which were equivalent to push forces of 200 to 250 lb at the stick, which may be compared with Fig. 6.6c. Measurements of stick forces in recovery on the *Prentice* showed them to be about 50 lb, in good agreement with the estimate of 55 lb[20].

CHAPTER VII

Analysis of Scale Effects

7.1. **The Effect of Scale on Spinning.**—The first aim of tests with free-spinning models is to make observations on the spin and recovery behaviour under conditions dynamically similar to those of the full-scale manoeuvre. The next stage is to interpret the observations in relation to the actual full-scale tests. At the outset little was known of the corrections to be applied, and there was some reason to expect that they might be fairly small. In particular, it seems that at least in flat spins the wing is fully stalled, and the forces on a fully stalled wing are less affected by changes in Reynolds number than, for example, is the maximum lift. The change of Reynolds number from model- to full-scale is however a large one, for the aircraft velocity varies with linear scale (n, say) as $n^{1/2}$, to that Reynolds number, $V\bar{c}/\nu = R$, varies as

$$\frac{R_m}{R_a} = \frac{\nu}{\nu_0}\left(\frac{1}{n}\right)^{3/2}$$

where ν_0 is the kinematic viscosity in the tunnel and ν the kinematic viscosity at the 'equivalent altitude'. The equivalent altitude is that corresponding to an air density ρ given by

$$\mu_m = \mu_a$$

where

$\mu_m = W_m/\rho_0 S_m s_m$ = relative density of model

$\mu_a = W_a/\rho S_a s_a$ = relative density of aircraft

therefore $\sigma = \rho/\rho_0 = W_a/n^3 W_m$.

The equivalent altitude is usually 10,000 ft for trainers and light aircraft and 15,000 ft to 30,000 ft for fighters so that ν_0/ν varies from 0·78 to 0·45 according to type. Model-scale varies from 1/12 (rarely) to 1/32 (common) and sometimes to 1/40 of full size so that R_m/R_a varies from 1/32 to 1/115.

An early investigation of the extent of agreement between model- and full-scale data was made by A. V. Stephens in 1932[13] on the *Bristol Fighter*. From his results on that aircraft, the full-scale pro-spin aerodynamic rolling moment appeared to exceed the model value at given α and λ by an amount which lay between 10 and 20 units over a wide range of incidences, whereas the full-scale pro-spin yawing moment exceeded the model value by not more than ten units in the range of α 30 deg to 65 deg.

7.2. **Technique of Model Spinning.**—In the early stages of model work it soon appeared that the primary requisite was satisfied; the dynamic model data were a true first approximation to the full-scale, and all that was needed to bring them into agreement was a minor correction. On this basis, much valuable work was done.

In 1934, Gates and Stephens introduced a technique[22] of applying the required corrections which has remained the basis of all the free-model testing at the R.A.E. It consists of the use of a small light vane carried on a wire outrigger at a distance from the inner wing tip of the model, in such a position that the force on it exerts a pro-spin yawing moment, an anti-spin rolling moment and no appreciable pitching moment. The magnitude of these moments is estimated from the known lift and drag of the vane, the calculated local air speed and its direction and the standard rigging angle of the vane. No attempt has usually been made to simulate the scale effect on rolling moment, on the grounds that this is a secondary correction in its effect on the ability to recover from the spin and merely causes a slight error in the sideslip angle. It is through the yawing moment correction that the vane exerts its major influence. These assumptions are reasonable and appear to be largely confirmed by experience, although of later years the importance of the rolling-moment correction has increased considerably, and it is dealt with later in this Chapter.

This approach to the problem had one notable advantage. It gave an extra variable in addition to the control settings, and so offered the possibility of studying the recovery, making full use of the controls but starting

from any of a large variety of spins from steep to flat. The first effect of applying the pro-spin yawing moment is like that of using more rudder deflection; the spin becomes flatter. We have already seen that this leads to the study of important variables like λ, α and T the recovery time, as functions of the applied yawing moment.

7.3. **Numerical Measure of the Scale Effect.**—From this point of departure it became feasible to study the scale effect directly without making rolling balance tests and without any attempt to analyse the moments. In doing so, however, we change the meaning of the term from something definite, *viz.*, an increment of aerodynamic moment as a function of α, λ and Reynolds number range, to something empirical but with less physical significance.

The meaning given to this new 'scale effect' is as follows. If we gradually vary any parameter in a sense adverse to recovery from the spin, we find that the time of recovery increases, at first gradually, and then rapidly until usually a vertical asymptote is reached. Beyond this no recovery occurs on reversal of the controls. The same applies to full-scale aircraft although data for complete curves are rarely obtained; for example the use of the ballast-tank from which water could be jettisoned was a method of varying the moments of inertia. Reducing the parameter to a non-dimensional coefficient, the results of such experiments could be represented on one graph as in Fig. 7.1. Here the chosen parameter is the 'applied yawing moment'. This is calculated from measurements made during the steady spin, and therefore is strictly relevant only to the initial state before recovery begins. In fact the applied moment must vary during recovery in a manner which does not truly represent the difference between $\overline{n'p}$ for any wing and its model, though it may happen to approximate to that difference. The true variation for the vane can be estimated by reference to the curves in Fig. 7.4 which apply to a vane of area $0{\cdot}01S$ at an arm $1{\cdot}4s$ from the plane of symmetry. From these curves it seems that the steepening of the spin during recovery, especially if accompanied by an increase in rate of rotation, must tend to cause an increase in the applied yawing moment. It would be practicable to measure this larger moment only in cases of non-recovery, and the position of the recovery limit could then be determined by approximation from the right-hand side; there would be no corresponding recovery curve and this new limit would disagree with that of the asymptote reached from the left-hand side, being generally further up the scale of yawing moments. This is brought out in the cases investigated by Gates and Stephens where, for instance, the threshold is at 22 units if approached from the left hand and 30 if approached from the right (Fig. 7.5). The contrast between the moment required for equilibrium and the moment applied with a given vane is expressed in Fig. 7.5 for a particular model; this diagram is based on one given by Gates and Stephens and two transitional curves are drawn showing the variation of moment when two different assumptions are made about the variation of λ in recovery. In practice the recovery will usually follow a different form from the $\lambda - \alpha$ relationship of the steady spin, and λ may be either greater or less; so if recovery is good and λ falls rapidly, the applied moment also falls and recovery is further facilitated, whereas any tendency to accelerate the rotation will increase the applied moment and so further hinder recovery.

The result is usually a very steep recovery curve, if time of recovery is plotted against moments measured at the beginning of the attempt to recover. Another consequence is to deprive the threshold so measured of much of its physical meaning. In particular it would seem to apply weight towards fast spins at steep attitudes against the controls, and perhaps to make this kind of non-recovery appear more common in free-model tests than it should be if it were truly representative of full-scale practice. In spite of these difficulties we adopt as a figure of merit for the model that yawing moment which, measured before recovery, is just sufficient to prevent recovery on control manipulation; this is called the threshold value for the particular model, condition, loading and sense of spin.

7.4. **Model Spinning Standards.**—From these remarks it is a natural deduction that the values of applied moment N (Fig. 7.1) are related to the full-scale recovery characteristics in a manner which can hardly be foreseen, but which may be established empirically. The simplest form which this relationship could take would be that the difference between model and full-scale curves, expressed by Z in Fig. 7.1, should be approximately constant for all types, and then the condition for a finite time of recovery full-scale, *i.e.*, for the full-scale curve to cut the time axis at some point P, is that $N > Z$ where Z has some value unknown at the outset. Then Z would correspond to the largest value of N required to make the model fail, in cases where the full-scale aircraft is known to fail to recover. By comparison with spinning trials in which N was measured as $0{\cdot}007$ it seemed that a reasonable value of Z would be $0{\cdot}010$, especially in view of the *Bristol Fighter* analysis. Accordingly this standard was suggested by Gates and Stephens in 1934[22] as a temporary measure. In a later paper[23] Gates (1937) proposed to raise the standard to $0{\cdot}015$ and this was applied to tests with the pitching moment of inertia of the model 10 per cent above its calculated value to cover possible errors in calculation.

As more full-scale data accumulated, it became necessary to analyse them in more detail and this was attempted by Pringle in 1943[24]. It had become important to ascertain the apparent variability of the 'scale effect' and to decide how much of this was due to genuine aerodynamic difference and how much to failure to simulate the full-scale loading and other experimental conditions relating to the achievement of dynamical similarity. Still more, it was essential to decide whether the scatter due to unknown causes exceeded the difference between model and model, for if so, the model test would lose almost all of its practical value.

7.5. **Factors in the Scale Effect.**—A list of the most important factors determining Z in any practical case will include others besides the truly aerodynamic contributions; and will be somewhat as follows:

(i) Failure to achieve exact similarity of loading
(ii) Difference between right- and left-handed spins
(iii) Accelerations of the tunnel-wind speed
(iv) Simplification of the control procedure on the model
(v) Artificial imposition of anti-spin rolling moment on the model
(vi) Reynolds number effects on the aerodynamic coefficients
(vii) Possibility of misleading full-scale data.

As it is now felt that the available evidence was rather scanty, it is proposed here only to outline the statistical approach used in Ref. 24.

It was clear that if the empirical scale effect followed the normal error law, a mere repetition of the procedure formerly adopted by Gates would eventually lead to an absurdity, since the attempt to set an upper limit would fail and merely demand a progressively higher standard.

In the analysis, the normal error law was assumed, with the various determinations of Z having a mean value X and a probable error Y. The frequency with which any given value of Z occurs among different monoplanes is then as in Fig. 7.2. If a model fails at a threshold value N, the probability that the full-scale aircraft will also fail is determined by the condition that

$$N < Z .$$

This probability of failure may be expressed by a curve of the form shown in Fig. 7.3, which was then fitted by an appropriate choice of X and Y to the data given in Table VII.I (now revised); these values of X and Y appeared to be about 0·015 and 0·010 in Fig. 7.6. The advantage of this procedure lies in that we use both passes and failures, and do not rely only on borderline cases. The percentage of failures in each interval is reckoned by taking borderline cases as $\frac{1}{2}$ and the histogram is so drawn. If we do use the borderline cases only, we find as in Fig. 7.7 that the distribution is broadly consistent with constants of the same order, though X is now seen to have a somewhat higher value. Fig. 7.7 also shows that it is somewhat doubtful whether the large value of Z for the *Wellesely* can be attributed to statistical effects.

TABLE VII.I

Comparison of Model- and Full-scale Recoveries

No.	Type	$\frac{B}{A}$	$\frac{C}{A}$	N^*	N^* ($\delta l = \delta n$)	$Y_A{}^*$	$Y_B{}^*$	Full-scale recovery behaviour
1	Supermarine F7/30	1·36	2·28	35		3	5	Pass
2	*Nighthawk* (i) ..	1·01	1·91	19½		1½	7½	Borderline
	Nighthawk (ii) ..	1·01	1·91	23		1½	7½	Pass
3	*Magister* (i) ..	1·50	2·34	13½		1½	6	Fail
4	*Magister* (ii) ..	1·61	2·43	22		1½	6	P
5	*Hurricane*	1·37	2·24	14½		1	4½	Borderline
6	*Spitfire*	1·29	2·10	15		0	3	P
7	*Defiant*	2·12	2·99	16		0	1	P
	Defiant	2·12	2·99		29	0	1	P
8	Australian Trainer	1·24	2·07	27		1	7	P
9	Miles M18 (i) ..	1·47	2·33	24		5	13½	B
10	Miles M18 (ii) ..	1·47	2·33	31		5	13½	P
11	Miles M20 (i) ..	0·98	1·81	6		3	3	Fail
12	Miles M20 (ii) ..	0·98	1·81	8		3	3	B
13	Miles M20 (iii) ..	0·98	1·81	22		3	3	P
14	*Moth Minor* ..	1·20	2·08	24½		2½	7½	B
	Moth Minor ..	1·20	2·08		23	2½	7½	B
15	Bristol 133	0·75	1·55	25		1	4½	B
16	*Typhoon*	0·67	1·57	22½		3	1½	B
	Typhoon	0·67	1·57		16½	3	1½	B
17	*Wellesley*	0·52	1·37	53		5	12	B
	Wellesley	0·52	1·37		44	5	12	B
18	Percival Trainer ..	0·67	1·54	40		2	15	P
19	*Prentice*	0·95	1·78	27		0	4	B

* The figures are values of $C'_n \times 10^3$.

7.5.1. **Loading of spinning models.**—Errors of loading take different forms. In the first place the equivalent altitude may be in error, because the altitude of full-scale test may itself not be correctly measured. In the earlier model tests a further error might result from the limitations of tunnel speed; for the model speed increases for a given scale of model as the equivalent altitude increases and to keep it below the tunnel maximum the equivalent altitude had sometimes to be restricted to a value lower than the true. This limitation was less serious after the tunnel had been modified although the higher speed has to some extent been overtaken by the upward trend of wing loadings.

It is usually easy to make the model have the correct scaled weight for a known equivalent altitude, neglecting for this purpose the relatively small fluctuations of air density in the laboratory, but it is otherwise with the moments of inertia. The full-scale values are not measured but are arrived at by calculation and are subject to at least a statistical error. This is a fairly serious matter, because it is known that inertia errors exert a measurable influence on recovery. An allowance was therefore made originally in applying the standard of recovery by insisting that the standard should be reached by the model when B had been increased by 10 per cent over its calculated value. This was convenient but was liable to misapplication if it remained in force during any comparison of model and full scale, for it would then result in an apparent lowering of ' scale effects ', and the eventual lowering of the standard would defeat the purpose of the 10 per cent handicap. It is more rational to make all comparisons as near as possible to the true loading, free from systematic errors. Systematic errors in the inertias can be minimised quite simply. The inertias are calculated by entering each item on a sheet with its mass and moments of inertia. There is no reason to expect systematic errors in radii of gyration, so that the moments of inertia will also be free from such errors on condition that the total measured weight is accounted for by the items entered. This is usually easy to check because the aircraft will have been weighed but if there is a small discrepancy it is often convenient to scale the inertias proportionally. Any remaining inertia errors may be assumed to follow a normal error law. Then knowing that the model inertias might be in error by an unknown amount, which should be random in sign if the above procedure has been adopted, and that these errors were significant in recovery, the first problem was to determine whether they were possibly the major constituent of the variance of Z.

The routine model tests have usually included a measurement of the effects of errors in inertia. It is somewhat difficult to make good use of the results, since we are in ignorance of the true variance of the moments of inertia; all we can do for the present is to assume some constant value unless there is more than the usual uncertainty about the full-scale inertias. In Fig. 7.7 the horizontal lines represent the combined effect of probable errors of 15 per cent in both A and B; in Table VII.I. Y_A and Y_B represent the increment and decrement, respectively, in N due to 15 per cent increases in A and B; the errors in A and B are assumed to be uncorrelated and the combined probable error is therefore

$$(Y_A^2 + Y_B^2)^{1/2}.$$

7.5.2. **Effect of inertia errors on variance of Z.**—An attempt has been made to analyse the borderline cases in such a way as to discover the most likely cause of the scatter in Z by finding what numerical assumptions give the ' maximum likelihood ' to the observations. For this purpose it was assumed that the scatter could be divided into two parts, inertia and aerodynamic, both normally distributed, and that the inertias all had the same probable error.

It was concluded that it is not possible to distinguish accurately between the inherent scatter, or aerodynamic variation and that due to the inertia errors without many more determinations of the difference Z. On the basis of the results in Figs. 7.6 and 7.7 it seems fair to adopt a mean empirical ' scale effect ' (X) of 17 units which would appear to have a large combined probable error of at least 7 units, most of which would be due to inherent aerodynamic variation from type to type.

On this set of data it is readily comprehensible that the previous standards have often been substantially correct as well as that they have occasionally lapsed. The policy of insisting on the attainment of some standard with the model overloaded so that B is 10 per cent or 20 per cent in excess is also seen to be reasonable, but to set this standard as low as 15 units is to take a chance on the unknown aerodynamic factors in the scale effect.

The seriousness of the ' scatter ' lies in its being comparable with the range of variation of N from model to model, so that if the tests are to be really significant it is essential to find what are the unknown factors in the aerodynamic scale effect and also to attain the highest possible accuracy in determining the inertias.

It must be pointed out that all but two of the aircraft used in this analysis had values of B/A of 1·5 or less and the above conclusions may well have to be modified as experience is gained with modern aircraft where the trend is towards considerably larger values of B/A.

The next section discusses the remaining factors affecting any model–full-scale comparison, and in the next chapter a further addition to B is proposed when allowance is to be made for the gyroscopic effect of propellers and jet-engine rotors.

7.5.3. **Other constituents of the empirical scale effect :—right-left asymmetry.**—The difference between the two directions of full-scale spinning is probably due to two things. On the one hand, the propeller exerts a gyroscopic effect and the rotating slipstream exerts an asymmetric aerodynamic effect. Even with the propeller stopped or with contra-rotating propellers, however, there would probably remain a residual asymmetry. due to internal and external causes. The internal causes are displacement of the c.g., and deflection of the inertia

axes; the external ones are design asymmetries or minor asymmetries of form allowed by manufacturing tolerances. It is a question for the experimenter to decide whether any or all of these contributions appear in the model test. Certainly the models usually show a marked asymmetry, as may be seen in almost any report on routine model tests. To this, the idling propeller usually contributes, though often in a minor degree. This question is discussed further in the next chapter. The major contributions appear to come from asymmetric loading—which is fortuitous and usually unrelated to the corresponding full-scale quantity—from external mechanisms and from inadvertent asymmetry of model manufacture. It would be somewhat laborious, and has not been attempted, to ensure by adjustment that the only asymmetry was that due to design and the propeller. Furthermore, the propeller is usually not a true dynamic model. Taking these facts into account it seems the most reasonable policy to regard only the mean of left and right spins of the model as significant. This is not, as it stands, the information most relevant to full-scale, for it is in practice the worse direction of spin which will determine the safety of spinning. To allow for this, it seems best to rely for the present on calculated estimates. This question is further elaborated in Chapter VIII.

In assembling the data for Table VII.I, the mean of right and left spins is used where known, so that a standard based on that analysis already contains an implied allowance for the full-scale asymmetry.

7.5.4. **Rolling moment effects.**—One of the difficulties of interpretation of model data obtained by Gates' and Stephens' technique was foreseen by these authors (*loc. cit.*). It is that when the auxiliary vane is set on the model at — 130 deg to wing chord it produces a component anti-spin rolling moment of the same order as the pro-spin yawing moment. It was proposed to neglect the effect for small moments as it would be expected to produce at most a small change of the sideslip angle.

There is a further circumstance that aggravates this source of error, for the available evidence by Pringle[24] (1943) and Seidman and Neihouse[25] (1943) suggests an aerodynamic scale effect on the rolling moment of the opposite sign to that applied by the vane, and of magnitude $\delta l' = 0{\cdot}015$ to $0{\cdot}020$ but larger for small incidences.

We have already seen that a rolling moment l' has an equivalent yawing moment n', given by

$$\frac{n'}{l'} = j = -\frac{\partial n'}{\partial \beta}\Big/\frac{\partial l'}{\partial \beta} = -\frac{n_v + c\lambda^2 \cos\alpha}{l_v + a\lambda^2 \sin\alpha} = -\frac{v_v}{v_v}$$

and that if the aerodynamic derivatives could be neglected

$$\frac{n'}{l'} \simeq -\frac{c}{a}\cot\alpha$$
$$\simeq \left(1 - \frac{B}{A}\right)\cot\alpha .$$

Some support for the idea of equivalence was given by direct free-spinning tests in which further rolling moments were applied by means of a second vane on the outer wing tip set parallel to the wing plane, as shown in Fig. 7.8. Then with various applied yawing and rolling moments we can show that the steady-spin condition is no longer a function of n' alone but of some combination $n' + jl'$ where j may now be determined from the experimental results. This is brought out by Figs. 7.9 and 7.10 for the *Wellesley*, in which case the equivalence ratio, j, is about $0{\cdot}4$. For this model anti-spin rolling moments were used, because pro-spin moments caused the spin to be unsteady. In this case the two vanes were close together on the inner wing-tip, and it is probable that their mutual interference would cause about 10 per cent error in estimating the moments; in addition the fast rotation makes it difficult to estimate the forces correctly, especially if the local incidence falls below about 20 deg at the vane. A somewhat different value of j was obtained from observations of the recovery threshold on this model. Similar data were found for the *Typhoon*, as in Figs. 7.11 to 7.13.

In Table VII.II the values of j measured during recovery for five models are compared with values calculated for the steady spin.

TABLE VII.II

Equivalent Yawing and Rolling Moments

Type	j (Measured for recovery)	j (Calculated for $l_v = -0{\cdot}2$, $n_v = 0$)	$1 - \left(\frac{B}{A}\right)$ in model test
Defiant	−0·32	−0·3	−1·68
Bristol 133	0	0	−0·02
Bristol 133	+0·14	+0·3	+0·49
Moth Minor ..	variable	0·05	0·11
Wellesley	0·25	0·13	0·37
Typhoon	0·19	0·07	0·19

If the scale effect on aerodynamic moments has two principal components $\delta l'$ and $\delta n'$, it is to be expected that the measured threshold will be in error to an extent which can now be calculated, and which will be correlated with $(A - B)$, even if $\delta l'$ and $\delta n'$ are constant.

It is first noted that in the routine tests the applied moments are in a fixed ratio (*see* Fig. 7.8) given by

$$\delta l_1 \simeq \delta n_1 \tan 40 \text{ deg}$$

so that the deviation on a yawing moment scale is given by the equation

$$Z = \delta n' + j\delta l' = \delta n_1 - j\delta n_1 \tan 40 \text{ deg}$$

assuming that j is the same for full-scale as for model, so

$$\delta n_1 = \delta n' + j(\delta l' + \delta n_1 \tan 40 \text{ deg})$$

where the second term represents an error in assessing the scale effect on yawing moment by the routine test. To minimise the resulting 'scatter', an attempt was made to remeasure the threshold for a number of models in which this quantity actually appeared sensitive to applied rolling moments. The new values are quoted for equal rolling and yawing moments, counting for this purpose the total rolling moment applied by both auxiliary vanes, and are used in Fig. 7.6.*

7.5.5. **Misleading full-scale evidence.**—Some consideration was given to the question whether the over-optimistic model results for the Bristol 133, *Wellesley* and *Typhoon*, all borderline cases full-scale, and the pessimistic result for the *Spitfire* by existing standards applied to routine tests, could be connected to the values of $(A - B)$, positive for the first three and negative for the fourth. More recently the model standard proved to be over-optimistic in the case of the *Prentice*, which has $(A - B)$ positive. It thus seemed probable that at least part of the explanation lay in the neglect of scale effect on rolling moments, in the model tests. Ref. 26 confirms this view.

In the case of the *Wellesley*, however, it seems necessary to examine other explanations of the data. This aircraft is placed on the borderline on the evidence of a flight report and a later fatal accident; against the evidence is that it is not the result of systematic spinning trials, but of isolated incidents. The aerodynamic criteria are low and suggest unsatisfactory recovery characteristics. The model tests, with any probable amount of applied rolling moment to simulate scale effect, still show good recovery except, as described in Chapter IV, 4.5, when the elevator is not used fully. There is no independent evidence of failure to use the elevator, but it remains a possibility that the pilot could be mistaken here. He stated that, after trying a stick position just aft of central, he then held the stick forward hard; but the possibility of stretch or even failure of the control circuit should perhaps not be ruled out, for this was also possibly a contributory cause of the initial failure of the *Prentice* in full-scale tests[20].

* A number of other models have been tested with rolling moments applied, since 1947. The results and their implications are discussed by Harper in Ref. 26.

On the whole, however, it seems reasonable to accept the full-scale evidence and to direct further enquiries towards an investigation of the scale effects on aerodynamic moments by direct measurements.

7.5.6. **Model controls.**—A further factor is the simplification of the control manipulation on models. The model controls are moved without restriction through a predetermined range of angular movement, under the action of an escapement mechanism. The full-scale controls are more or less balanced and their use is limited by the pilot according to his discretion and, in some cases, his strength. Hence the optimum use of the controls may remain undiscovered either in the model tests or in full-scale spinning trials of a given aircraft, though this is less likely if the tests are repeated several times.

7.5.7. **Tunnel accelerations and kinetic energy correction.**—Accelerations of the tunnel due to unsteadiness or deliberate accelerations to keep the model in the test sections, may disturb the spin, particularly when the controls have been reversed for recovery and the rate of descent is increasing. Rapid accelerations of the tunnel to prevent the model hitting the bottom net are often observed to speed up recovery, and occasionally to cause recovery where it would not occur if the acceleration were more controlled. In terms of applied yawing moment the effect makes the model result optimistic but is almost invariably small if the tests are performed with the normal amount of care.

In the full-scale spin, the change of density in the air as the aircraft loses height does not occur in the tunnel. Two opposing influences are noted in the effect of changing altitude. The first is a tendency for the rate of descent to be in excess of its equilibrium value for a given C_D; this would only occur at constant incidence, and its order of magnitude can be estimated in the following way.

To a first approximation, if V_H is the true rate of descent at altitude H and if the vertical forces were in equilibrium

$$\sigma V_H^2 = \text{constant}$$

therefore

$$\frac{dV_H}{dH} = -\frac{V_H}{2\sigma}\frac{d\sigma}{dH}.$$

This implies a vertical retardation given by

$$\frac{dV_H}{dt} = \frac{dV_H}{dH}\frac{dH}{dt} = \frac{V_H^2}{2\sigma}\frac{d\sigma}{dH}.$$

In order to produce the extra drag which will cause this retardation, there must be a speed excess, u, say, where

$$\tfrac{1}{2}\rho_0\sigma(V_H + u)^2 C_D = w\left(g - \frac{dV_H}{dt}\right)$$

which gives

$$\frac{2u}{V_H} \simeq -\frac{1}{g}\frac{dV_H}{dt}.$$

If, however, we regard the excess speed as due to an 'altitude error', the aircraft would be as if in uniform descent at a lower air density given by

$$\frac{\sigma + \delta\sigma}{\sigma} = \frac{g - dV_H/dt}{g}$$

$$\frac{\delta\sigma}{\sigma} = -\frac{1}{g}\frac{dV_H}{dt} = \frac{2u}{V_H}$$

$$= -\frac{V_H^2 d\sigma}{2\sigma g\, dH}$$

or

$$\delta H = \frac{V_H^2}{2g},$$

i.e., the height the aircraft would need, if falling *in vacuo*, to acquire the speed V_H. This height correction may be of the order of $15w$ and is comparable with the height lost in one turn of the spin.

The second factor in this correction is more difficult to assess and operates in the contrary sense to the first. Owing to loss of altitude the spin will generally become slightly steeper, but not much is known of the magnitude of the change. The drag coefficient will diminish, and the speed will lag behind this change.

For these two effects to compensate one another we must have

$$\sigma C_D = \text{constant}$$

or

$$\frac{1}{\sigma}\frac{d\sigma}{dH} = -\frac{1}{C_D}\frac{dC_D}{d\alpha}\frac{d\alpha}{dH}$$

or

$$\frac{d\alpha}{dH} = -\frac{C_D}{\sigma}\frac{d\sigma}{dH}\Big/\frac{dC_D}{d\alpha}.$$

For a spin at 45-deg incidence this implies a rate of change of incidence amounting to about $\frac{1}{2}$ deg per 1,000 ft change of altitude. With this rate of change of incidence the true rate of descent would remain sensibly constant. Although few figures are available of sufficient accuracy, the value $\frac{1}{2}$ deg/1,000 ft seems quite reasonable; for the *Hornet* it appeared to be of the order 2 deg/1,000 ft, for the *Meteor* and *Sea Hawk* it is very small. It seems most likely therefore that the kinetic energy correction will be either quite small or will make the aircraft spin like the model, at an altitude slightly below the 'equivalent'.

7.6. **Aerodynamic Factors Bearing on Scale Effect.**—So far we have examined empirical evidence for the existence of a scale effect with a view to ascertaining its probable magnitude, but because of the uncertainties of this procedure it hardly seems practicable to investigate in further detail what factors cause it to vary from type to type. In the previous chapter a case was made for supposing the wing yawing moment to be a function of wing thickness ratio, and this was noted earlier for example by Irving[15]. He remarks that rolling balance tests (*i.e.*, over a wide range of α and λ) indicate a variation of $\overline{n'p}$ from $\pm$ 12 or 13 units for thin wings to $\pm$ 20 units for thick wings.

Owing to the scarcity of monoplane data it is of some value to find from strip-theory calculations what factors may be expected to influence $\overline{n'p}$, and what typical values may be expected from a trapezoidal monoplane. It would then be reasonable to look for the largest effects of Reynolds number in those cases where $\overline{n'p}$ is large, possibly, for example, in thick wings. For this reason the parameter t/c was introduced into Fig. 7.7, so as to exhibit any relationship hitherto unnoticed; but it cannot be said that the relationship is very striking. It is true that there is a wider range of variation amongst the thick wings but that may only be because there are more points in that part of the picture. On the other hand it is inherently probable that the limits of variability should be determined by t/c and the actual position of a point between these limits by α and λ; this would account for the complexity of the data and their apparent inconsistency.

7.6.1. **Strip theory.**—The yawing and rolling moments on an untwisted wing may be most conveniently expressed in terms of the section force coefficients C_x and C^z resolved along and normal to the chord.

Using the same notation as in Chapter V, the local chord is $c_0(\beta + \theta - \beta\theta)$, the local velocity $(1 + \beta^2\lambda^2)^{1/2}V$, and the local incidence $(\alpha \pm \text{arc tan } \beta\lambda)$; we find that

$$\overline{n'p_W} = \frac{1}{1+\theta}\int_0^1 \Delta C_{x(\beta)}\,\beta(\beta + \theta - \beta\theta)(1 + \beta^2\lambda^2)\,d\beta$$

and, if we adopt as a first approximation for wings of constant profile

$$\Delta C_{x(\beta)} = \beta\lambda\frac{\partial C_x}{\partial\alpha},$$

then

$$\overline{n'p_W} = \frac{\left(\frac{1}{2} + \frac{\theta}{6}\right)\lambda + \left(\frac{1}{3} + \frac{\theta}{5}\right)\lambda^3}{2(1+\theta)}\frac{\partial C_x}{\partial\alpha}.$$

A similar expression will hold for $\overline{l'p}$ with $\partial C_z/\partial\alpha$ instead of $\partial C_x/\partial\alpha$. A further factor of $(1 - \beta)$ in the expression for $\overline{n'p_W}$ expressing a diminution of $C_{x(\beta)}$ linearly to zero at the wing tip results in the formula

$$\overline{n'p_W} = \frac{\left(\frac{1}{20} + \frac{\theta}{30}\right)\lambda + \left(\frac{1}{42} + \frac{\theta}{105}\right)\lambda^3}{(1+\theta)}\frac{\partial C_x}{\partial\alpha}.$$

Fig. 7.14 shows how the geometrical factor varies with θ and λ; in particular $\overline{n'p_W}$ would seem to increase with λ, were it not for higher terms in $C_{x(\beta)}$; since measurements indicate a maximum and subsequent decrease, we conclude that such terms are important for larger values of λ, as we should expect. The diagram also suggests a factor of 0·04 for ordinary values of θ and λ (0·2 to 0·4), increasing to 0·1 for those aircraft that spin fast (*e.g.*, *Prentice*) or even to 0·2 for abnormal aircraft (*e.g.*, *Wellesley*). The diagram also brings out that profile gradation is probably more important than taper ratio

in determining the yawing moment; the tip sections are heavily ' weighted ', and we recall the analogous effect of tip profile on stalling characteristics.

Can we, on this basis, account for the variation of 20 units in Fig. 6.1 due purely to variation of t/c? This would evidently demand that $\partial C_x/\partial\alpha$ should vary by an amount between 0·4 and 0·2 in going from thin aerofoils to thick.

7.6.2. **Values of the chordwise force coefficients.**—From the present aspect, the data usually obtained from wind-tunnel tests on aerofoils are deficient in not including high enough incidences. The available data, however, are of interest. For example, we have lift and drag data up to 90-deg incidence for the RAF 6 monoplane wing, measured by Bradfield and Coombes[27] (1925), presented in a polar diagram in Fig. 7.15. This shows that the chordwise component is practically negligible at and above 30 deg. Fig. 7.16 shows data abstracted from American sources[28] (1933) for 25-deg and 30-deg incidence and a variety of different aerofoils. The symmetrical aerofoils show that C_x becomes appreciable at this Reynolds number for thickness ratios just below 0.10, after which there is a rapid increase to a maximum at about 0·17; here in the short range of α, $\partial C_x/\partial\alpha \simeq 1{\cdot}4$ whereas with cambered aerofoils the maximum is at 0·09 thickness ratio and reaches about 2·0. Thus for at least some conventional aerofoils there is every reason to expect large values of $\overline{n'p_w}$ even if this large α-gradient is not maintained over a wider range of incidences.

7.6.3. **Forces on an elliptic cylinder.**—A potential-flow calculation relevant here is that of forces acting on an elliptic cylinder at various incidences. To avoid the trivial result of zero chordwise force, we consider the forces acting on each half separately (but basing the coefficients on the whole major axis as chord). If the forces in which we are interested originate chiefly in the aerofoil nose, they may bear some general relationship to these values for inviscid flow without circulation. It is therefore surprising that the ' negative drag ' coefficient $-C_x$ varies little in the range of t/c from 0 to 0·2, in Fig. 7.17. It therefore appears probable that the great sensitivity noted in the measurements at Reynolds number $= 3 \times 10^6$ is due to variation of breakaway and circulation. The actual values in Fig. 7.17 are of the same order as the measured coefficients at 25 deg and 30 deg incidence.

7.6.4. **Pressure-plotting at high incidence.**—These considerations lead to the supposition that thick wings may not only display quite large values of $\overline{n'p}$ but that these values may prove very sensitive to Reynolds number. In the absence of any means of measuring $\overline{n'p}$ it was decided to pressure-plot a thick aerofoil up to the highest possible incidence over a range of Reynolds number. For this purpose a modified RAF 48 aerofoil was used. Two models were made, one of 3·1-ft chord for use in the R.A.E. 24-ft Tunnel, the other of 0·64-ft chord for the 5-ft Tunnel. In this way the range of Reynolds number was extended from about 3×10^6, close to full-scale values obtained in the spin, down to $0{\cdot}8 \times 10^5$, which is almost within the range appropriate to free-model tests.

The pressure measurements showed qualitatively a marked scale effect and the measurements, hitherto unpublished, are reduced to chordwise and normal-force coefficients in Fig. 7.18, C_x and C_z being given as functions of Reynolds number and α. These values are, of course, only the contribution analogous to form drag, and skin friction is a separate contribution.

From these curves we see at once that the whole interval of Reynolds number between model- and full-scale values is a region of critical changes. For each incidence there is at some narrow range of Reynolds number a rapid increase in C_x analogous to the increase in $C_{L\,\max}$ but with the important addition that the critical Reynolds number is different for each incidence, changing by a factor of 25 between incidences of 20 deg and 60 deg. The biggest critical change is for the lowest of the incidences studied. It follows from the results that no practicable increase of model scale will give complete freedom from wing-scale effect.

Perhaps the simplest way of considering the results is by analogy with the critical flow change about a circular cylinder, which occurs, for some Reynolds number of the order of 10^5 depending on the turbulence of the wind stream and the surface condition. Here we have, as it were, the critical flow change about a body of variable effective diameter, as the incidence increases, the most important flow changes take place nearer to the nose of the aerofoil, *i.e.*, at smaller radii of curvature. Hence the critical Reynolds number based on the aerofoil chord will increase, as the chord becomes larger and larger in relation to the ' effective ' diameter of the equivalent cylinder. For this particular aerofoil the nose radius is about 0·035 times the chord so that the large range of variation of critical Reynolds number is to be expected if we accept the analogy. It may also be expected that the whole phenomenon will be to some extent conditioned by the turbulence and surface condition, for it is highly probable that the basic physical cause is the transition from laminar to turbulent flow in the boundary layer.

Applying these data to the formulae of section 7.6.1 we find that a typical wing moment will vary considerably with scale; to make the calculation more realistic, the measured forces are taken to apply only at the root, and C_x is assumed to vary linearly to zero at the tip of a wing with plan-form taper 2. (Variations of Reynolds number along the span are neglected.) Fig. 7.19 shows the result for $\overline{n'p}$ at 40-deg and 60-deg incidence; this is for ' thin ' tips. Constant profile along the whole span gives the much larger values for ' thick ' tips in Fig. 7.20. The calculations for 60-deg incidence were made on the assumption that C_x is constant above 60 deg where we have no measurements.

These tentative calculations need of course a full investigation by experiments on a rolling balance to give them a really sound basis, but meanwhile we may conclude with some confidence that a scale effect between 5 and 30 units may be expected; that it will prove to be a complicated function of α and λ but generally will be greatest for faster spins, and that the effects will be most marked in a range of λ which makes the local incidence of the 'rising' tip 30 deg or less; and further that the thickness ratio of the profile at the tip will be a major factor and plan-form taper a minor one. The eventual verification of fairly large effects, such as we have already seen to be probable by inference (Figs. 7.6 and 7.7), seems now more definitely foreshadowed.

CHAPTER VIII

The Effects of Propellers and Engines on the Spin and Recovery

8.1. **Introduction.**—The effects of the propellers in the spin have been discussed by Gates and Bryant[3] (1926), and it is now a question of applying similar considerations to modern aircraft. This was attempted by Pringle in 1944[29] and work has also been continued in the experimental field since then. Owing to the large moments of inertia of modern propellers, and to the high rotational speeds of jet-engine rotors, appreciable gyroscopic effects are to be expected, leading to a steepening of spins 'with' the direction of rotation and flattening those 'against'. This has been demonstrated quantitatively in the vertical tunnel.

The direct aerodynamic effect of propellers has also been recalculated, and appears to be mainly due to their 'lift' or 'fin' effect; in spins 'with' the propeller direction the gyroscopic moment is likely to dominate and the propeller will probably assist recovery. In the case of jet propulsion, the only direct aerodynamic effect considered is a damping in yaw proportional to the mass flow and usually favourable to recovery from the spin.

The indirect effect of propellers in altering the airflow about the rest of the aircraft is the component about which least is known, and calculation is impracticable. Some model tests have been made, however, with small electric motors installed in the model, and the effect investigated experimentally.

8.2. **Definition of Symmetry.**—Owing to the directional property of propellers, it becomes necessary to distinguish between effects which are the same for both directions of spin and those which upset the mirror image likeness of right- and left-handed spins. Gates and Bryant pointed out that departure from symmetry in this sense must be accounted for by

(i) Components of lift, drag and pitching couple which depend on the sense of spin.

(ii) Components of lateral force and asymmetric couple which are independent of the sense of the spin.

They also concluded that the propeller effects were large enough to account qualitatively for the observed differences between spins in opposite directions; but it seems desirable to consider again all the factors which could operate here.

For the purposes of this discussion, it is convenient to drop the usual definition of symmetric (pitching) and asymmetric (rolling and yawing) couples, and to re-define symmetry relative to the spin direction rather than the aircraft's plane of symmetry. Then both categories (i) and (ii) are anti-symmetric. If we use right-hand axes for right-hand spins and left-hand axes for left-handed spins, then anti-symmetric terms are characterised by $\pm$ signs in the equations of motion.

It is also convenient to define 'favourable' couples as those favourable to recovery, not the maintenance of spinning, *e.g.*, negative pitching and yawing moments are favourable.

8.3. **Components of the Gyroscopic Couple.**—In accordance with our definition, the sign of moments is taken to be positive if pro-spin; this agrees with normal conventions for the right-hand spin. The sign of propeller rotation and angular momentum is also positive if it agrees with the direction of spin. The gyroscopic effects are wholly anti-symmetric except in the hypothetical case of opposite-handed propellers running at different speeds.

The tendency of gyroscopic effects to be masked by aerodynamic effects is less likely in jet-propelled types and the effects in this case may be expected to agree with calculation.

Qualitatively the largest effect is the pitching moment, favourable to recovery when the spin and rotor directions agree, and adverse in the other case. The direct yawing component has, however, the opposite sign for inwardly tilted wings, so that a partial compensation occurs, whereas with outward tilt the two components reinforce one another. This is a practical case because outward tilt often precedes recovery after control reversal. Fortunately a probable answer can be given to the question of the relative dominance of the two components by the methods of sections 8.4 and 8.8.

To calculate the moments we may suppose the rotary parts to rotate about an axis parallel to the aeroplane x-axis; the angle between this and the thrust axis being neglected. The polar moment of inertia is denoted by

A' and the angular velocity by ω. The rate of spin Ω has components p', q', r' in body axes where approximately, in the steady spin

$$p' = \Omega \cos \alpha$$
$$q' = \Omega\theta_y \ (\theta_y = \text{angle of tilt of outer wing tip above the horizontal})$$
$$r' = \Omega \sin \alpha .$$

The gyroscopic moments are

$$L' = 0$$
$$M' = -A'\omega r' = -A'\omega\Omega \sin \alpha$$
$$N' = A'\omega q' = A'\omega\Omega\theta_y .$$

Hence the pitching moment increases with incidence as $\sin \alpha$ and all the more so as Ω usually increases also with α, but the yawing moment changes chiefly through the wing tilt.

Table VIII.I shows the order of magnitude for three cases:

(*a*) modern fighter with a propeller of 4 blades, 14 ft in diameter

(*b*) modern fighter with jet engine, the rotor having polar moment of inertia of 3·25 slug ft^2

(*c*) *Bristol Fighter* with a propeller of 4 blades, 9 ft in diameter.

This Table shows that there has been a significant increase in the moment coefficients, even allowing for increased linear velocities, partly due to the large rates of spinning assumed in the calculation but mainly due to the large angular momentum of the rotating parts.

TABLE VIII.I

Gyroscopic Moments in Spinning

$S = 300$ ft^2, $s = 20$ ft, $V = 200$ ft/sec } for (*a*) and (*b*)

$S = 400$ ft^2, $s = 20$ ft, $V = 100$ ft/sec } for (*c*)

Data below relate to 15,000 ft altitude
Direction of spin the same as that of the rotor

	Fighter with		*Bristol Fighter:* (*c*) with 9ft propeller
	(*a*) 14-ft propeller	(*b*) with jet engine	
A'	89 slug ft^2	3·25 slug ft^2	6 slug ft^2
Maximum speed (r.p.m.)	1,000	10,500	1,000
Minimum speed (r.p.m.)	500	4,900	500
α, Ω	45-deg incidence, 3 radn/sec, no tilt		45-deg incidence, 2 radn/sec
$C_{m\,(max)}$	−0·055	−0·021	−0·0074
$C_{m\,(min)}$	−0·0275	−0·010	−0·0037
α, Ω, θ_y	30-deg incidence, 3·5 radn/sec, −15-deg tilt		30-deg incidence, 2·5 radn/sec, −15-deg tilt
$C_{m\,(max)}$	−0·045	−0·017	−0·0065
$C'_{n\,(max)}$	−0·025	−0·009	−0·0034

8.4. **Effect of the Gyroscopic Couple on the Steady Spin.**—In all cases where a displacement of spinning equilibrium consists of more than one component, there is a difficult problem to decide the total resultant effect on the spin, and still more on the recovery. For example, the application of infinitesimal pitching and yawing couples will change the incidence by

$$\delta\alpha = \frac{\partial\alpha}{\partial m}\,\delta m + \frac{\partial\alpha}{\partial n}\,\delta n$$

but the evaluation of the derivatives demands a knowledge of the aerodynamic coefficients. So in a practical case we can only make 'specimen' calculations with

assumed coefficients. If the applied couple is finite, the usual procedure is to follow through the calculation of the unbalanced yawing moment as a function of α by means of the simple spinning equations. When this is done for the gyroscopic case, the $\lambda - \alpha$ relationship required by the balance of pitching moments is displaced. The sideslip condition is however, practically unaffected. We therefore find in the yawing equation, not only the direct term, $\overline{n'g}$ say, but indirect contributions due to the effect of varying λ on $\overline{n'p}$ and also on $\overline{n'i}$. A specimen calculation of this kind was made with the following terms inserted in the moment equations, so as to compare with the case in the absence of gyroscopic terms :—

$$\overline{mg} = -a'\lambda'\lambda \sin\alpha$$
$$\overline{n'g} = a'\lambda'\lambda\theta_y$$

where $a' = A'/\rho Ss^3$

$\lambda' =$ non-dimensional rotor speed

$= \omega s/V$.

This type of calculation enables us to see in any given case whether the change of unbalanced moments is favourable or not, and to assess the change quantatively in its effect on recovery. The qualitative effect is hardly in doubt, for the direct and indirect contributions to the yawing equation are of the same sign except for inward tilt angle, so that only with extreme amounts of inward tilt would the gyroscopic couple be adverse on the whole, if the rotor is ' with ' the spin direction.

8.5. **Simulation of the gyroscopic effects.**—Although there is usually no short cut to the estimation of a complex effect, there is some reason to think that the gyroscopic effect in particular can be simulated by redistribution of aircraft mass, keeping the total mass constant, so that tunnel tests can easily be performed.

The inertial moments are given by Euler's equations

$$L = (B - C)q'r'$$
$$M = (C - A)r'p'$$
$$N = (A - B)p'q'$$

and we have just seen that the gyroscopic moments are

$$L' = 0$$
$$M' = -A'\omega r'$$
$$N' = A'\omega q'.$$

In order to simulate the gyroscopic moments we should have to change B and C in such a way that

$$-A'\omega = \delta(C - A)p'$$

and

$$A'\omega = \delta(A - B)p';$$

these conditions happen to be compatible and can be satisfied by a definite redistribution of mass along the x-axis, increasing B and C equally to the extent

$$\delta B = \delta C = -A'\omega/p'$$
$$\delta A = 0.$$

The representation holds only for a particular incidence, direction and rate of spin. Figs. 8.1 to 8.3 show in more detail how the representation applies in the neighbourhood of a selected incidence of 60 deg, keeping the fuselage loading at its new value. The agreement at neighbouring incidences is inexact because an inertial term varying as $\sin 2\alpha$ cannot correctly represent a gyroscopic term varying as $\sin\alpha$; there is also a further discrepancy resulting from the different variations of λ and λ'. This becomes more serious as the spin less resembles the steady spin at the incidence already selected.

There is thus no strong reason for expecting the equivalence to hold in recovery tests, and accordingly an experiment was arranged to test this point for a particular aircraft.

8.6. **Tunnel Tests of Meteor Model.**—For dynamic similarity in a spinning model, the approximate constants are scaled in the following ratios :—

	Model/full-scale values
Linear dimensions	n^{-1}
Linear velocities	$n^{-1/2}$
Angular velocities	$n^{1/2}$
Moments of inertia	$\sigma^{-1}n^{-5}$
Angular momenta	$\sigma^{-1}n^{-4\cdot5}$

where σ is the relative air density at the altitude of the full-scale spin.

It is clear that for gyroscopic apparatus the separate scale relations for angular velocity and moment of inertia, need not be fulfilled so long as their product is correctly represented. Otherwise, the model of a gyrone rotor would have an impractically high angular velocity and low moment of inertia, and a separate flywheel would be required for each model scale. Instead, a model flywheel of higher moment of inertia has been used, and the angular velocity calculated for each case. Fig. 8.4 is a diagram of the apparatus, showing the flywheel and the manner of accelerating it *in situ* by means of a motor-driven wheel of larger diameter.

The following measurements were made:

(i) The speed of the driving wheel (1 to 2,000 r.p.m.) was measured by visual stroboscope; the ratio of diameters then gives the flywheel speed approximately

(ii) The polar moment of inertia of the flywheel was computed from drawings

(iii) The total weight of the flywheel unit. The initial rate of precession was also timed for the flywheel unit freely suspended from each of two attachment lugs in turn. This gave a check of the angular momentum which in fact agreed closely enough with the product $A'\omega$.

The actual polar moment of inertia is 3·5 gm in^2. For an aeroplane with two jet engines each having a rotor moment of inertia of 3 slug ft^2 and a maximum r.p.m. of 10,550, the angular speed for the 1/32 scale model should be approximately the same as full-scale, 10,250 r.p.m. for dynamic similarity at 15,000 ft. The actual initial speed was 17,700 r.p.m. decreasing to zero

in about two minutes. The speed after about 20 sec from starting is approximately 15,000 r.p.m. and this is the time taken to launch the model, allow the spin to develop, and finally release the controls. The speed was purposely kept high so as to make the measurements easier.

The direction of rotation of the flywheel was left-handed, and this made the left-handed spin steeper than with the flywheel at rest, whereas the right-handed spin was noticeably flatter. The recovery curves are plotted in Fig. 8.5 in the usual way as functions of applied yawing moment. The equivalent effect of the gyroscopic moments is -6 units of applied yawing moment for right-handed spins and $+4\frac{1}{2}$ units for left; the mean scaled down linearly to the correct r.p.m. is $\pm 3{\cdot}6$ units, and this is the magnitude of the effect to be expected in full-scale with full engine speed. With idling engine speed the effect will be approximately halved at 15,000 ft to $\pm 1{\cdot}8$ units. The advantage to be gained by opening the throttle in a left-hand spin, supposing that the strength limitations do not prevent it, would therefore not be large, but might be appreciable, especially in an emergency.

Fig. 8.5 also gives an approximate estimate of the effect of the gyroscopic moments on the incidence of the steady spin.

The continuation of the tests to cover the mass-redistribution was limited on the *Meteor* model by the difficulty of lightening the fuselage, and they were only made with the increased loading required to represent right-handed spins. Fig. 8.5 shows that the recovery curve agrees surprisingly well with the corresponding gyroscopic case.

The correct loading of the body to represent the right-hand spin at 60-deg incidence with the gyroscope running is with $b = 4{\cdot}11$ instead of $b = 2{\cdot}81$. This is achieved with B at 173 per cent of its normal value; the actual value in the tests was 180 per cent. Scaling down in the ratio of these values we find the equivalent effect to be $6{\cdot}3$ units, agreeing with the measured gyroscopic effect of 6 units, within the accuracy of the experiment.

Further experiments on different types would be of value. In view of what has been said about the principle of representation involved here, it would seem a natural deduction that the initial phase of the spin is what determines the recovery of the *Meteor*. This should not be taken as an assertion of a general principle.

8.7. **Gyroscopic Moments in Turns.**—A brief calculation has been made of the gyroscopic couples that would be experienced in a typical case of stalling in turns at various speeds, for comparison with the spinning case. Fig. 8.6 gives the results of this calculation for the *Tempest*; Ref. 29 gives the method in full.

Each coefficient passes through a maximum; the pitching-moment maximum occurs just above stalling speed, but the yawing moment maximum, amounting to $1{\cdot}8$ units, occurs at $2\frac{1}{2}g$ and with 60 deg of bank. Compared with the spinning case the coefficients are smaller but not insignificant.

8.8. **Propeller Moments.**—A more detailed examination of the propeller moments than that given in section 8.3 was made in Ref. 29, by taking into account the direct aerodynamic effects of the propeller. It is only proposed here to outline the conclusions reached for each of the three main kinds of propeller installation.

The case considered for the first two was that appropriate to the *Tempest*, and the third was based on the same aircraft but with the wing dimensions increased by $\sqrt{2}$. The conclusions are generally applicable. It is assumed that moments of a given magnitude are important in the order—yawing, pitching, rolling.

8.8.1. **Single engine ; single-rotating propeller.**—The symmetric pitching moment (due to 'lift' effect) tends to be of opposite sign to the symmetric yawing moment (due to 'fin' effect) but larger, so that it is difficult to decide which dominates. However, as the anti-symmetric pitching moment, mainly on account of the gyroscopic term, is large it appears certain that the spin will be better in the same direction as the propeller rotation, and that increase of propeller speed favours recovery.

In spinning against the propeller, a large adverse pitching moment is combined with a favourable yawing moment, and in this case the overall effect cannot be foreseen, but with outward tilt the yawing moment may become positive and the overall effect is then adverse.

The pitching moments involved are of the same order as are obtained with the usual size of anti-spin parachute. Their effectiveness in recovery is in general agreement with full-scale experience, although the evidence is incomplete. The *Typhoon*[30] (1943) with a left-hand propeller recovers more rapidly from left-hand spins when the throttle is opened. The *Firefly* has been reported to recover automatically from spins 'with' the propeller rotation when the throttle is opened. Again, the *Mustang* has an asymmetric spin, engine on. It has a right-handed propeller and spins flat to the left, oscillating about an almost horizontal attitude instead of at an incidence of 30 deg to 50 deg as in the power-off spin, the angles being from pilots' impressions. For this aeroplane evidently the anti-symmetric pitching moment predominates and use of the propeller is advised against. In the very flat spin it seems unlikely that the slipstream effect on the tail can be important, but all comparisons are subject to uncertainty about slipstream effects which might be of either sign.

8.8.2. **Single engine ; contra-rotating propeller.**—In this case, as would be expected, the anti-symmetric moments are negligible. There are however, a positive pitching moment, and a smaller yawing moment depending on the tilt and negative for inward sideslip. It is thus practically impossible to give any rule for the effect of using the propeller, as so much depends on the sideslip angle.

8.8.3. **Twin engine ; single rotating propellers.**—The well known use of the inner engine to provide an anti-spin yawing moment proves to be the dominant case. In

spins ' with ' the propeller rotation the anti-symmetric pitching moment is also large, and doubling it by using the outer engine as well provides some compensation for the loss of yawing moment. In spins ' against ' the propellers, only the inner engine should be used.

8.9. **Forces Due to Internal Gas Flow in Spinning.**—The gyroscopic moments do not complete the list of spinning effects due to jet engines. Different amounts of air intake as the throttle is varied will affect the external airflow, thus indirectly affecting the aerodynamic coefficients. No attempt is made here to estimate this effect. In addition, there will be a kinetic reaction of the longitudinal gas flow as it is deflected sideways by the spinning rotation (the so-called Coriolis forces). Calculation shows that these forces give a lateral resultant and also a damping moment of the type $r \,.\, n_r$ assisting the damping in yaw. The magnitude of the moment can be appreciable for some designs in a spin at full throttle but will be negligible with the engine throttled.

For the calculation we may assume a continuous mass flow m_1 from entry to exit through the fuselage or nacelle. As the gases recede from the spin axis each element exerts on its surroundings a force given in terms of its relative velocity v_1 by the vector equation for the virtual acceleration:

$$-2\bar{\Omega}\dot{x}\bar{v_1} = 2r'v_1 j$$

where j is the unit vector along the y-axis.

The gas enclosed between planes of cross-sectional area K and separated by a longitudinal distance dx will therefore exert a force laterally equal to

$$2r'v_1\rho_1 K\,dx \ (\rho_1 = \text{gas density})$$

but $\rho_1 K v_1 = m_1$ the mass flow.

Therefore side force due to each element $= 2r'm_1\,dx$.

If the origin of x is taken at the c.g. and x_1, x_2 are the abscissae of the entry and exit planes

$$\text{Total side force } Y = 2r'm_1(x_1 - x_2)$$
$$= 2r'm_1 d'$$

where d' = length of fuselage or nacelle.

$$\text{Moment of side forces } N = r'm_1({x_1}^2 - {x_2}^2)$$
$$= \Omega m_1({x_1}^2 - {x_2}^2)\sin\alpha$$
$$= Yd''$$

where d'' = distance of c.p. from c.g. the centre of pressure being approximately at the mid-point $\frac{1}{2}(x_1 + x_2)$.

In all probability the resultant side force is unimportant but the moment, being negative, will assist the damping in yaw. Typical values of the moment coefficient are 3 units with maximum engine speed and about $\frac{1}{2}$ unit at engine idling.

Tunnel tests are incapable of showing the yawing moment due to gas flow by free-spinning tests. It is also noted that the models have blocked air intakes and so simulate the throttled condition more closely than the engine-on condition. The improvement of the entry flow with engine on may cause indirect external effects more important than the more easily calculated internal effects.

8.10. **Conclusions Regarding Full-scale Practice.**—General conclusions are difficult to make in detail because so much depends on unforeseen characteristics of the individual type of aeroplane. It is most probable, however, that there will always be some advantage in recovering from spins ' with ' the rotor or propeller, due to gyroscopic forces. In recovering from spins ' against ' the rotor, jet engines are likely to be unfavourable, and the same is true of propellers in spite of the symmetric yawing moment, because any tendency to sideslip outwards brings the propeller ' fin ' effect into action.

8.11. **Differences Between Left and Right Spins of Models.**—It has been noted in Chapter VII that the asymmetry of left and right spins of a model contains other factors besides those listed amongst propeller effects, and that its magnitude cannot rationally be linked with its full-scale counterpart. The chief contributions seems to be these:

(*a*) Propeller effects
(*b*) Asymmetric loading
(*c*) External rigging
(*d*) Inadvertent asymmetries of model making.

Very often the whole asymmetry is small and it has become the practice to use the mean of the two directions for most purposes. In some few cases, the asymmetry has been large and has appeared to need further investigation. On the *Sea Fury*, the difference between right and left spins originally amounted to 11 units of yawing moment, the mean threshold being only $10\frac{1}{2}$ units. It was mentioned in Chapter VII that the propeller of this model had only a small effect on the balance of pitching moments; it was also necessary to assess its contribution to the yawing moments.

It is not easy to make measurements of model threshold accurate to $\frac{1}{2}$ unit or sufficiently consistent to measure very small changes. However, a reasonable set of values was obtained as shown in Fig. 8.7, and these data are analysed in Table VIII.II overleaf.

These tests are not quite consistent as to the symmetric effect of the idling propeller; this varies between $-\frac{1}{2}$ (unfavourable) and $+1\frac{1}{2}$ (favourable). There seems no substantial doubt that the asymmetric effect is of the order of 5 units.

We can also deduce that the model has an inherent asymmetry of $2\frac{3}{4}$ units in favour of left-hand spins, and it was the coincidence of this with the left-hand propeller and mechanism left which produced the very large original total of 11.

A brief test was made to examine whether this inherent asymmetry was due to the fin, as it seemed to have a slightly asymmetric stall from opposite sides. A small movable flap was fitted in the fin leading edge and deflected each way in turn through 30 deg. This had remarkably little effect on the recovery (about one unit between the extremes). It therefore seemed probable that the inherent asymmetry was due mainly to the wings and body.

TABLE VIII.II

Asymmetry of Model Recovery—Sea Fury

Model condition	Model Threshold $10^3\ C_n'$			Asymmetry
	Left	Right	Difference	
Left-hand propeller, mechanism left	16	5	11	5 units due to propeller; $3\frac{1}{4}$ units due to mechanism; 2 units due to mass of mechanism
Propeller removed and replaced by mass ..	14	8	6	
Mechanism changed to right-hand side	$10\frac{1}{2}$	11	$-\frac{1}{2}$	
Mechanism mass counterpoised	12	$10\frac{1}{2}$	$1\frac{1}{2}$	
Oil cooler removed	$10\frac{1}{2}$	9	$1\frac{1}{2}$	No effect of oil cooler
No propeller	10	$7\frac{1}{2}$	$2\frac{1}{2}$	5 units due to propeller
Left-hand propeller	14	$6\frac{1}{2}$	$7\frac{1}{2}$	
Right-hand propeller	$8\frac{1}{2}$	$11\frac{1}{2}$	-3	$5\frac{1}{2}$ units due to propeller

8.12. **Propeller Effects on a Model of a Twin-Engined Aircraft.**—On twin-engined aircraft there are more possibilities than on single-engined, because of the combinations of ' handed ' propellers. The *Hornet* was a case of practical interest and all four possibilities were tried on the model in turn, with the results tabulated below. These tests were unusually difficult because the *Hornet* model is unusually sensitive to tunnel accelerations.

TABLE VIII.III

Effect of Propeller Rotation on Recovery of Hornet Model

Model Condition	Model Threshold, $10^3 C_n'$				Asymmetry
	Mean	Left	Right	Difference	
No propellers	23	22	24	2	Mean of four units due to propellers
Right-handed propellers	$23\frac{1}{4}$	20	$26\frac{1}{2}$	$6\frac{1}{2}$	
Left-handed propellers	$23\frac{3}{4}$	$24\frac{1}{2}$	23	$-1\frac{1}{2}$	
Propellers ' handed ' ↙ ↘	24	$22\frac{1}{2}$	$25\frac{1}{2}$	3	Mean improvement small
Propellers ' handed ' ↖ ↗	24	$21\frac{1}{2}$	$26\frac{1}{2}$	5	

From these figures it seems that there is an easily detectable asymmetry due to similar propellers, of the same order as on the *Sea Fury* model. If we dismiss the increase of asymmetry over the no-propeller case when opposite-handed propellers are fitted as due to experimental errors, we are left with only a very minor symmetric effect hardly appreciable by experiments of this limited accuracy.

In connection with oppositely handed propellers, it is to be noted that the arrangement ↖ ↗ may be somewhat better than ↙ ↘ if it is a question of using the inner engine to assist recovery, because in the former case the gyroscopic pitching moment will give further assistance.

8.13. **Note on the Nature of Asymmetry.**—The fact that models recover less easily from spins in one direction

finds a convenient expression in the difference of the threshold yawing moments measured in the steady spin. These yawing moments have also a slightly deeper significance, for it seems that at least in some cases those moments which correspond in their effect on time of recovery also bring the steady spin into agreement. This is brought out by some measurements on the *Hornet*, the results of which are given in Fig. 8.8. From this diagram it is seen that the threshold of recovery occurs when the steady left-hand spin is at $62\frac{1}{2}$ deg and when the steady right spin is at 64 deg, agreeing within the probable accuracy of the measurements; the values of λ also agree fairly closely. If, on the other hand, we compare incidences when the same yawing moment is applied for both spins, we find a difference of about 8 deg, and a correspondingly large difference in λ. It seems therefore that the application of an extra yawing moment of 7 units in the right-hand spin does quite well compensate for some aerodynamic yawing moment deficiency peculiar to this condition of the model.

8.14. **Experiments with Powered Models.**—The spinning requirements for fighters allow for the possibility of recovery with the use of the engines, and it seems probable that the use of the propeller slipstream can be of value, at least in some cases. Hitherto we have been obliged to admit that an important part of the propeller effect is not amenable to calculation, because the influence of the slipstream on the wing and empennage is highly complex. It seemed all the more important to attempt model tests if the technical difficulties could be overcome. The matter was to some extent precipitated by the results of model tests of the Fighter B. On this model the recovery characteristics were not expected to be satisfactory even from an inspection of the design. The usual type of modification of the empennage also seemed rather ineffectual, perhaps because of the tendency of forward-placed fins to be shielded by the wing. On the other hand, the propellers are contra-rotating and if used with engine on would introduce no troublesome asymmetry; but the only calculable effect of appreciable magnitude is the adverse pitching moment. If it could be shown that the slipstream 'cleans up' the flow round the empennage in a spin, a useful step forward would have been taken.

To simulate a full-scale power in the model we require to observe the following scale relationships:

	Model/full-scale values
Linear dimensions	n^{-1}
Angular velocities	$n^{1/2}$
Power	$\sigma^{-1}n^{-3\cdot5}$

To represent a full-scale thrust power of 3,000 horse power at 15,000 ft, *i.e.*, about 3,500 brake horse power with a propeller speed of 1,200 r.p.m. in a 1/32 scale model we therefore require a thrust output of $19\frac{1}{2}$ watts and a model propeller speed of 6,800 r.p.m.

The first step was unsuccessful, as it seemed that the motor installed in the model was not yet sufficiently powerful. It was, however, useful in providing laboratory experience, and all that remained was to obtain a motor of adequate power.

The motors actually used were small electric permanent-magnet motors of German origin, each giving a maximum power of $2\frac{1}{2}$ watts at 12 volts. By using two of these with opposite rotation undesired gyroscopic effects of the armatures were eliminated. The motor and propeller unit is shown in Fig. 8.9. The efficiency of the gearing shown there was approximately 65 per cent, so that with a propeller efficiency of 70 per cent a thrust power of 2·3 watts was expected, equivalent to about 360 t.h.p. at 15,000 ft.

The propellers were not scale models of the full-scale, but in accordance with usual model practice had a higher solidity to allow for scale effects, and were computed so as to give a definite power at the correct scaled speed of rotation. The higher solidity was also of advantage in making the blades stronger.

Some difficulty was expected in spinning the model with sufficient freedom with wires attached for the power supply. This proved less serious in practice and the wires, of 36 S.W.G. enamelled copper covered with one layer of silk, were sufficiently flexible and had a low enough resistance. The wires were suspended from a point just below the tunnel fan, and hung down the centre of the tunnel, being long enough to allow the model to descend to within 2 to 3 ft of the bottom catch net without the wires becoming taut. It was found advantageous to give the wires an initial twist against the spin, so that the total number of turns was as large as possible before the final twist became too great. The wires were prevented by the air stream from fouling the model and came out of the model above the c.g. so that the drag of the wires would only impose a negligible drag force on the model, and no moment. A brief test on another model showed that this arrangement had no measurable effect on the model behaviour; the wires were arranged to become disconnected easily if they became taut.

With this arrangement, the model could be given bursts of power after it had failed to recover in the ordinary way with power off, simply by moving a rheostat control. It was soon found that with the original power unit, bursts of power up to the maximum using about 30 volts equivalent to $\sim$800 b.h.p., were unavailing. The reason was clear on examining the propeller slipstream by means of smoke while the model was held fixed at high incidence in the tunnel. The slipstream was seen to be quickly deflected upwards and did not reach the tail unit, so no major improvement of the flow over the tail could be expected.

The second attempt, however, gave better results. A single motor of much higher power, $13\frac{1}{2}$ watts maximum at 36 volts, was used with a redesigned gearbox and propellers of higher solidity to absorb the extra power. The motor and propeller unit is shown in Fig. 8.10.

With this unit the model loadings were only slightly above the correct scale values, the weight being 10 per cent and the pitching moment of inertia 15 per cent in excess. The threshold was first measured for both directions of spin under conditions of no power, and then

the following procedure was adopted. A vane was selected which was just large enough to prevent recovery by the normal method, and the model launched into the tunnel with the controls pro-spin and with the wires connected. The current was then switched on with the rheostat fully in circuit; this corresponded to a very small amount of power, full-scale. When the controls were reversed and it was seen that recovery was not taking place, the variable resistance was reduced quickly to zero, giving full model power which corresponded to about 2,000 b.h.p. full-scale. This was left for not more than one second and then the resistance was increased again to its full amount. This simulated a burst of power of about 5 seconds duration full-scale. The bursts were repeated until the model either recovered or it became apparent that recovery would still not take place, according to the size of the vane. In this way the threshold value of the applied yawing moment was again determined, although a recovery curve in the ordinary sense could not be obtained. The threshold was measured in both directions of spin to avoid complications arising from the gyroscopic effect of the motor armature, and a mean improvement of $1\frac{1}{2}$ units was measured; with the full power of about 3,700 b.h.p. represented this would correspond to about $2\frac{1}{2}$ units improvement, and is thus appreciable though not decisive.

CHAPTER IX

Tailless Aircraft

9.1. **General Discussion.**—The function of providing a controllable pitching moment to ensure longitudinal stability and control devolves, in the absence of a tail, on the wing itself, and this leads naturally to the application of controls built into the trailing edge of a swept-back wing. The same controls function as 'ailerons' and 'elevators' and are conveniently designated 'elevons' but it is sometimes briefer to refer to them by the alternative names in speaking of the transverse and longitudinal stick movements. In discussing the balance of pitching moments in the spin we have to allow for two aspects of the forces called into play by the elevons; *i.e.*, the magnitude and the centre of pressure, and if we are thinking of the normal force on the corresponding wing section as a whole, we may regard this as a localised vector moving to and fro along the wing chord as its magnitude changes with elevon deflection. On conventional aircraft the corresponding movements of centre of pressure on the tail unit with elevator movement would be quite unimportant because the tail arm is relatively so much larger, but here the chord and sweepback are of similar magnitudes and no such simplification is permissible. This is not the only fundamental difference between the two types of control. In the spin, different parts of the wing are at different distances from the axis of spin and therefore in regions of different relative airspeed (this, of course, is true of both types) and this gives rise to pitching-moment terms which are quadratic in λ. These counteract the familiar centrifugal pitching moment which is also quadratic in λ. If b is particularly small, as it tends to be for tailless types, we find that the centrifugal moment is in large part balanced by this new aerodynamic term, to such an extent that the relation between incidence and rate of rotation is materially altered. Not only is the magnitude of λ thereby very much changed, but the tendency for a minimum rate of rotation near 45-deg incidence may quite disappear. Measurements on a model show this in Fig. 9.1. In the particular case about to be considered, the balance of moments would occur for a markedly low value of λ but for the aerodynamic quadratic term, as it is, the values turn out much nearer the usual order of λ for conventional aircraft. The form of variation of Ω with α however is mainly determined by elevon pitching moments.

9.2. **Normal-force Coefficients.**—In applying these arguments to actual cases most of the data are unknown, and guidance can therefore at the moment only be sought by applying simplifying assumptions. The following are a set of such assumptions:

(i) That the calculations of strip theory apply

(ii) That the local velocity may be taken as the relative velocity of the quarter-chord point

(iii) That the local normal-force coefficients are linear in local incidence apart from a discontinuity at the inner end of the elevon, depending on its deflection. The centre-of-pressure coefficient has a corresponding form

(iv) That the section-drag coefficient is linear in local incidence and unaffected by elevon deflection; the aircraft drag is due solely to the wing. On these assumptions, the aircraft drag coefficient and pitching-moment coefficient are determined as definite integrals with respect to the parameter $\beta(= y/s)$.

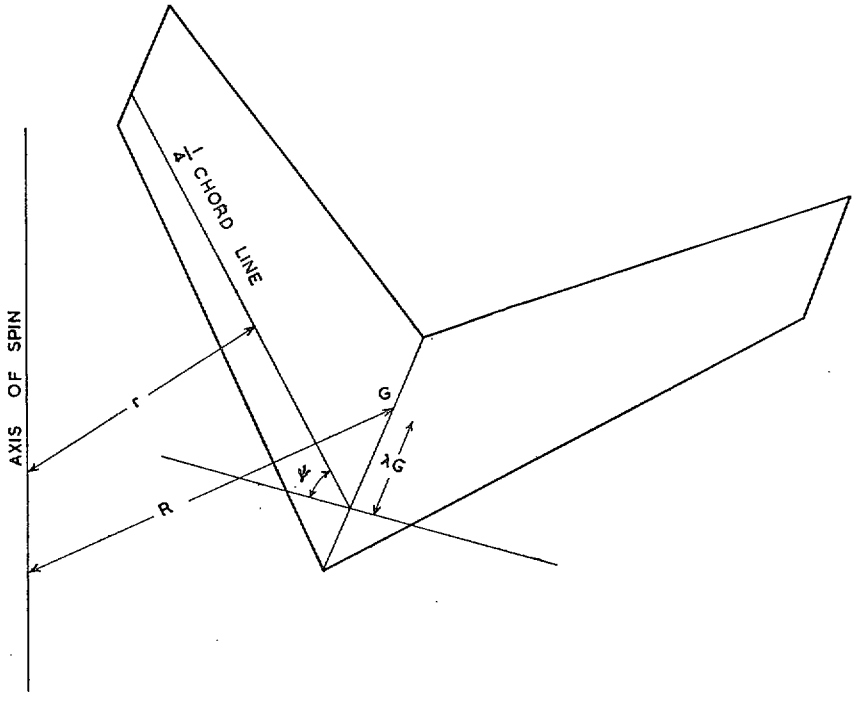

FIG. 9.2. Geometry of trapezoidal swept-back wing for strip-theory calculations.

The radius r, Fig. 9.2, is given by the equation

$$r^2 = \{R + (y \tan \psi - h'c_1) \sin \alpha\}^2 + y^2$$

provided that we neglect both dihedral of the wing and tilt of the aircraft. From this we can show that

$$\frac{V^2}{V_H^2} = v_0 + v_1\beta + v_2\beta^2$$

where the functions v_0, v_1 and v_2 have the following values

$$v_0 = \sec^2\gamma - \frac{h'c_1}{\mu s} C_D^x \cos\alpha + \lambda^2 \frac{h'^2 c_1^2}{s^2} \sin^2\alpha$$

$$v_1 = \frac{C_D^x}{\mu} \cos\alpha \tan\psi - 2\frac{h'c_1}{s}\lambda^2 \tan\psi \sin^2\alpha$$

$$v_2 = \lambda^2(1 + \tan^2\psi \sin^2\alpha)$$

but these expressions are not immediately applicable because they contain C_D^x, the dynamic drag; this is in turn expressible as an integral which, in the special case of central elevons is as follows for a simple trapezoidal wing:

$$\frac{C_Z'^x}{C_Z'} = \frac{C_D^x}{C_D} = \frac{2}{1+\theta}\int_0^1 (v_0 + v_1\beta + v_2\beta^2)(\theta + \theta'\beta)\, d\beta = I_2 \text{ say}$$

in which

$$\theta = \text{root chord/tip chord} = \frac{c_1}{c_0}$$

$$\theta' = 1 - \theta .$$

On performing the integration we find that

$$I_2 = v_0 + \frac{2+\theta}{3(1+\theta)} v_1 + \frac{3+\theta}{6(1+\theta)} v_2$$

so that finally

$$I_2 = \left[\sec^2\gamma + \lambda^2\left\{\frac{h'^2c_1^2}{s^2}\sin^2\alpha - \frac{2(2+\theta)}{3(1+\theta)}\frac{h'c_1}{s}\cdot \tan\psi \sin^2\alpha + \frac{3+\theta}{6(1+\theta)}(1 + \tan^2\psi \sin^2\alpha)\right\}\right] \Big/ \left[1 + \frac{h'c_1}{\mu s}\cos\alpha\, C_D - \frac{2+\theta}{3(1+\theta)}\frac{C_D}{\mu}\cos\alpha \tan\psi\right]$$

$$= i_2 + j_2\lambda^2 \text{ say, (defining } i_2 \text{ and } j_2).$$

By a similar process of integration

$$C_m = \frac{C_Z'}{1+\theta}\int_0^1 (v_0 + v_1\beta + v_2\beta^2)(\varphi_0 + \varphi_1\beta)(\theta + \theta'\beta)\, d\beta = \frac{C_Z'}{1+\theta} I_1$$

where

$$\varphi_0 = h_1 c_0 \theta/s; \quad \varphi_1 = \tan\psi + h_1 c_0 \theta'/s .$$

If we also neglect the small variation of h_1 with local incidence,

$$I_2 = v_0\varphi_0 \frac{1+\theta}{2} + (v_0\varphi_1 + v_1\varphi_0)\left(\frac{1}{3} + \frac{\theta}{6}\right) + (v_2\varphi_0 + v_1\varphi_1)\left(\frac{1}{4} + \frac{\theta}{12}\right) + v_2\varphi_1\left(\frac{1}{5} + \frac{\theta}{20}\right)$$

$$= i_1 + j_1\lambda^2 \text{ say (defining } i_1 \text{ and } j_1).$$

The equation of pitching moments now takes the form

$$\tfrac{1}{2}b\lambda^2 \sin 2\alpha = \frac{C_z'}{1+\theta}(i_1 + j_1\lambda^2) - \frac{h'c_1 C_z'}{2s}(i_2 + j_2\lambda^2)$$

in which the aerodynamic quadratic terms are evident on the right-hand side. Finally the expression for λ is

$$\lambda^2 = \frac{C_z'\left(\dfrac{i_1}{1+\theta} - \dfrac{i_2 h' c_1}{2s}\right)}{\tfrac{1}{2}b \sin 2\alpha + C_z'\left(\dfrac{j_2 h' c_1}{2s} - \dfrac{j_1}{1+\theta}\right)}.$$

To apply this to an actual case, the General Aircraft glider, it was assumed that λ would be unaffected in its dependence on α by differential use of the elevons. The static drag was assumed to be as measured for the model (Fig. 9.3), and C_z' was assumed to vary as in Curve I, Fig. 9.4. h_1 was assumed to vary with aircraft incidence as for conventional aircraft, taking the same data as in Chapter V, but for elevons deflected upwards it was assumed to approach the quarter-chord line, reaching it when the normal-force coefficient over the outer part of the wing, C_z'', reached $\frac{1}{2}C_z'$. C_z'' was then chosen to fit the measured rates of rotation (Fig. 9.1), giving the values plotted as Curve II, Fig. 9.4. It is seen that these values are quite reasonable and that we are not obliged at the moment to introduce a more refined theory, although further consideration might prove such a refinement to be necessary.

9.3. **Balance of Asymmetric Moments.**—It is to be expected that tailless aircraft wings will show similar characteristics in many respects to wings of conventional aircraft. The important differences will arise from the absence of a rear fuselage and empennage on the one hand, and from the use of elevons on the other. A third point of contrast will also occur if there are rudders placed either at the wing-tips or on the rudimentary body.

In considering the rolling moments we have to reckon with the use of ' aileron ' as a more probable and fundamental contribution to the spin, whereas on conventional types it was only a variant from the normal spin without use of ailerons. The main contributions are

$$\overline{l'pv} + \overline{l'\xi} + \overline{l'i}$$

and these must balance out for steady spins.

With the aid of data such as that of Fig. 9.4 it is possible to make a rough estimate of the rolling moment $\overline{l'\xi}$ to be expected. This appears to be large and of the order of 70 units; in addition there might be the term $\overline{l'p}$ of order 10 units if the spin qualitatively resembles that of a conventional aircraft. These couples are ' controlled' by the total sideslip derivative $(l_v + a\lambda^2 \sin\alpha)$ which would not be expected to have any but normal values, say $-0{\cdot}25$; consequently the sideslip angle should be of order $\frac{1}{3}$ radian. Values of this order have been observed in model spins at moderate incidences (unpublished results).

If this value of sideslip is reasonable and typical, it upsets the validity of some of our simplifying assumptions. Thus it might imply that the mean air stream meets one wing at 45 deg if the sweepback has the fairly low value of 30 deg; the conditions for this wing would resemble those for a highly swept wing without sideslip, *i.e.*, there would be a marked reduction in the aerodynamic forces, the other wing acting like a conventional wing. The result would be a marked contribution to the values of l_v and n_v tending to oppose the sideslipping motion. The former will help to keep the sideslip lower than our rough estimate, the latter will generate a yawing moment which will be of importance in the recovery. In these circumstances the analysis of Chapter VII, section 7.6.1 will no longer apply without modification. We may note, however, that the direction of this increased contribution will not necessarily be consistent but will probably depend on λ, α and Reynolds number in a manner as complicated as for $\overline{n'p}$. Qualitatively we may conclude that if $\overline{n'p}$ is large and pro-spin as a result of a strong suction peak on the leading wing, the further contribution due to $\overline{n'v}$ will be pro-spin for anti-spin ' aileron ' deflection, and *vice versa*. This term therefore cannot be left out of account in considering the effectiveness of the controls and the ease of recovery.

9.4. **Centrifugal Yawing Moments.**—The centrifugal yawing moment is a more or less definite function of sweepback angle, ψ, since the moments of inertia A and B can be expressed approximately by

$$A \simeq A_0 \cos^2\psi$$
$$B \simeq A_0 \sin^2\psi$$
$$A - B \simeq A_0 \cos 2\psi .$$

This would tend to result in a zero or low value near 45-deg sweepback, irrespective of the rate of rotation.

The importance of sweepback probably shows itself more definitely in the aerodynamic moments, of which detailed measurements on a rolling balance are required for a full discussion. At the moment, placing the emphasis rather on considerations of inertia we may merely observe that the arguments of Chapter IV will apply here, at least in a modified form. The essential point would be that rolling moments, such as those due to ' aileron ' deflection, should produce tilt changes of the same sign (*i.e.*, outward tilt for anti-spin ' aileron ' deflection) and that the consequent inertial moment in yaw should reinforce the ' aileron ' effectiveness in recovery. Model tests certainly show the rolling action of the ' ailerons ' to be positive, although in certain circumstances a powerful direct yawing moment due to the ailerons, $\overline{n'\xi}$, appears to be set up and somewhat confuses the issue; this is further discussed in the next section. The model tests also show on the whole a wider variation in tilt angle, both positive and negative, than conventional aircraft; tilt tends to be positive when associated with pro-spin ' aileron ' deflection, but depends also on incidence to a large extent.

9.5. **Control Movements for Recovery.**—This is a subject on which the study of the model behaviour is yet very incomplete, and still more so is the knowledge of full-scale data with which to compare it. We have therefore

confined these studies mostly to a comparison with conventional models. The most detailed investigation was made on the General Aircraft glider of 28·4-deg sweepback; some definite conclusions could be drawn about the effectiveness of control. The most natural question to ask first is whether the standard method of recovery is to be recommended and whether it can be improved.

The model tests showed that the two main controls, rudder and 'elevator', are similar in their relative effectiveness to those on a more conventional aircraft which has $(A - B)$ large and positive, *e.g.*, the *Wellesley*. So we find that, although loss of fin and rudder area are seriously detrimental to recovery, the important control is the 'elevator' and full downward movement appears to be essential to good recovery. The timing of this movement is also important, for if the 'elevator' is moved down before the rudder is reversed, we find, as we have seen may happen with conventional aircraft, that the spin becomes faster and flatter, and since the 'elevator' is well down, recovery has to be by rudder reversal alone and becomes most unlikely. This state of affairs may well occur, for the 'elevator' tends to be held well down at the stall, on account of the strong self-stalling characteristics of these aircraft; this of itself makes a spin more likely and the resulting spin with the 'elevator' down will be fast and flat. However the model tests indicate a solution to the problem, for if the stick is moved fully back the spin reverts to its normal condition at a steeper attitude, and normal recovery action may then be preceded with, taking care that the reversal of the rudder takes full effect before the 'elevator' is reversed.

Whether normal recovery action will then ensure recovery appears to depend as usual on the amount of unshielded fin and rudder area. Reducing this on the G.A. glider made the model threshold of recovery lower—here the fins were mounted at the wing tips—and the recovery of the D.H.108 model[31] was poor, chiefly, it is thought, because the fin and rudder were mounted in the plane of summetry and were obviously in the wing wake.

A study of the results, both published and unpublished, of tests with 'aileron' deflections for recovery for these two models yields the interesting information[26] that the effect of 'aileron' deflection depends critically on the amount of down 'elevator' deflection on which it is superimposed. Thus if the 'elevator' movement for recovery is limited to centralising it and the 'aileron' deflections are then made, the direct yawing moment is negligible and the rolling-moment effect is then what we should expect, *i.e.*, for an anti-spin deflection, the rolling moment is anti-spin and induces an anti-spin yawing moment, as we have seen, helping recovery. If, however, the 'elevator' position for recovery is a downward angle of the same order as the 'aileron' deflection, then one elevon is practically undeflected and the other has a large downward deflection. Although this still gives a rolling moment, it also gives a large yawing moment in the opposite sense, and this dominates, so that we now have pro-spin 'ailerons' promoting recovery through their direct anti-spin yawing moment, although at some large value of $(A - B)$ the indirect yawing moment might again assert itself.

The balance between the amount of downward 'elevator' deflection and the use of pro- or anti-spin 'aileron' deflections can only be struck at present by examining each particular case individually, for it depends on many variables such as $(A - B)$, size of elevons, angles in the 'elevator' and 'aileron' senses, limitations of these angles by mechanical considerations, etc.

CHAPTER X

Safety Devices

10.1. **The Purpose of Safety Devices.**—Use of safety devices in spinning occupies a position midway between the use of ordinary controls for recovery, and the last resort of abandoning the aircraft in a dangerous spin. The use of landing flaps or brake flaps or the lowering of the undercarriage, in cases where this may be of assistance, is not classified under the present heading, which implies rather the use of gear specially fitted to ensure recovery.

10.2. **Possible Forms of Safety Device.**—To recover in an emergency from a bad spin, it is necessary to upset the balance of moments as completely as possible, and this may be attempted by the application of large yawing and/or pitching moments. It would seem a natural approach to the problem to break, as it were, the main-spring of the spin by so spoiling the airflow over the wings that they no longer apply a pro-spin yawing moment. Another way of achieving the same end would be to increase the body damping moment artificially by means of suitably placed fin or keel area. To upset the pitching equilibrium, the most practicable suggestion, and that actually adopted, is the anti-spin tail parachute.

10.3. **Slats, Spoilers, Keels and Fins.**—We have already seen that the closing of the outer slot on a wing fitted with movable slats would prove, so far as small-scale tests can indicate what to expect, an effective means of promoting recovery. However, this could at most be of extremely limited application on modern aircraft, as slats are not often fitted on aerobatic designs,

and in any case the mechanical complications would probably be prohibitive. Since the trend of design may lead back to the use of slats, the matter is briefly considered by referring to the effects of slots as observed during model tests on the D.H.108[31]. On this model a number of combinations of slots were tested and the results indicated that there was only a small effect on recovery if both slots were open. If the outer was shut and the inner open, improvements in recovery threshold of about 1.5 units were obtained, and the opposite arrangement of slots made recovery correspondingly worse.

There is some evidence of the effectiveness of special fins attached to the body for the purpose of increasing the damping moment, and model tests by Francis[32] (1935) showed that they would, in theory, be of value. However, to be effective, the fin area would have to be quite large and the practical difficulties of supplying it in a sufficiently strong form, completely retracted in normal flight, and without undue aerodynamic, structural or load sacrifice are too obvious to need emphasis. One recent practical suggestion has been to attach a rigid, or else a roller-blind, fin to the existing sting-hook of a deck-landing aircraft, but here the difficulty is to achieve effectiveness, because the size of fin is limited by the available space and the objective would be thereby limited to a slight improvement of the spinning characteristics rather than a true safety device.

On the subject of wing spoilers, two main types may be mentioned:

(*a*) Small spoilers on the upper surface. These may be compared with brake flaps for instance on the *Meteor* (Chapter III, section 3.9), and are likely to have barely detectable effects on recovery since they are in a region of completely stalled air.

(*b*) Flaps on the leading edge of the wings. We have already seen in Chapter III that these flaps affect the maximum lift considerably, and model tests of their effects on recovery show that these are large under certain circumstances. In fact leading-edge flaps are akin to slats in their effects on recovery, and we have, for the D.H.108 for instance that flaps open on both wings gave a small improvement and if the flap was open on the inner wing only then an improvement varying from $8\frac{1}{2}$ to 23 units, depending on the flap size, was obtained, Here again, installation problems probably prohibit consideration of such a safety device, except in extreme cases, but it is evidently extremely effective.

10.4. **Anti-spin Parachutes.**—A device which has proved of great practical value and is fitted for all official spinning trials, is the tail parachute. Model tests by Francis[32] showed that the spin could be arrested by streaming a single parachute from the aircraft with a tow cable attached to a suitable point at the tail. It was not possible to give a detailed theoretical treatment of the matter at the outset because it was not known where in the turbulent wake of a spinning aircraft the canopy of a parachute would ride. Hence it was not known whether the moment applied is chiefly about the pitching axis or not, and if not, how important is the yawing component. Whilst it cannot be said that all is now known about tail parachute action, some of the problems have been recognised and solved, particularly those with a direct bearing on practice.

Tunnel tests have now shown that the tendency is for the parachute, if attached by a relatively long bridle, to ride down or near the axis of spin, as shown in Fig. 10.1, and in such a case, apart from a contribution due to bridle drag, the moment is largely in pitching.

In this event, the optimum length of bridle will combine a reasonable distance downstream, to avoid shielding by the aircraft, with a fairly large tow-cable angle ε, Some brief tunnel tests seemed to indicate that effectiveness increases at least to cable length $= 2l$, where $l =$ distance from c.g. to attachment point. The increase of length diminishes ε, for

$$\varepsilon \simeq \alpha\left(1+\frac{1}{m}\right)$$

if α is small, so that in the moment, $C_P S_P \cdot \frac{1}{2}\rho V^2 l \sin\varepsilon$, the term V increases as ε diminishes and a maximum may therefore be expected. It is found that with short bridles, and especially if the spin is flat, the tendency is for the parachute to ride away from the spin axis. In such an event, the parachute exerts a pull with a smaller pitching moment, but the yawing moment may be considerable. It must therefore be emphasized that the justification of design based on pitching-moment assumptions is in their effectiveness in tests and full-scale trials rather than in fulfilling a model theoretical programme. The order of pitching-moment coefficient with the customary size, $D = (0{\cdot}064Ss/l)^{1/2}$, of parachute will be (if $V \sim$ free-stream velocity and $\varepsilon \sim 90$ deg) 0·025, which is of the same order as provided by the elevators, and will therefore as a rule be adequate unless the aircraft is both a bad spinner and the elevators lock upwards. The moment has the advantage of being impulsive.

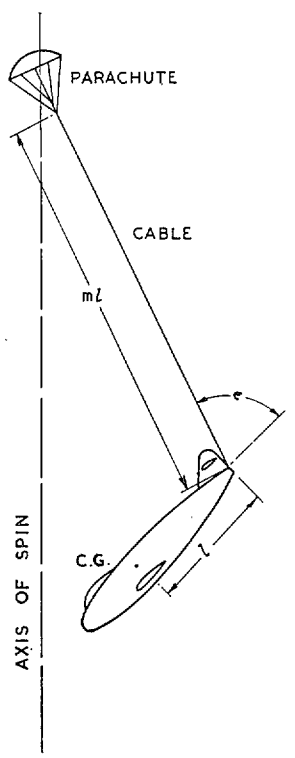

FIG. 10.1. Tail parachute geometry.

10.5. **Problems Arising from the Use of Anti-spin Parachutes.**—The problems to be solved may be roughly classified as follows:

10.5.1. **Aerodynamic.**—The parachute must leave its housing without fouling the aircraft and must exert the forces necessary to cause rapid recovery. The motion of the aircraft in the spin must be foreseen with sufficient accuracy to allow calculations on the aircraft strength with parachute attached.

10.5.2. **Strength.**—The parachute must be strong enough to withstand the forces it experiences on opening. The cable and attachment must be capable of transmitting both the steady pull of the parachute and any shock loads incidental to opening. An attachment point must be found or provided on the aircraft sufficiently strong to hold the concentrated load and transmit it to the aircraft.

Owing to the diminution of aircraft incidence, recovery is always accompanied by an increase of speed, and this must obviously exceed the stalling speed, with something in hand to cover increases in virtual acceleration during the pull out, before recovery can be considered complete. Consequently the parachute drag can vary from its relatively small initial value to something large enough either to burst it, or to break the cable, or to damage the aircraft. To make the order of events definite, it is usual to fit a safety link or some overriding device which will automatically jettison the cable and parachute at a load too small to allow anything untoward to happen.

10.5.3. **Installation.**—Practical problems of installation are connected with the provision of a suitable box in a position from which ejection, aided by springs if necessary can cause a smooth deployment into the towed position. In addition, there must be provided controls which will stream and jettison the parachute, in that order only, and such that accidental streaming cannot occur. Recommendations for giving effect to the official requirements are found in the appropriate part of A.P. 970.

10.6. **Speed Variations in Recovery.**—Strength calculations for the flat-spin case were made on the assumption of a steady rate of descent with drag coefficient 1·0. However, it has been realised that though the dangerous spin against which we are trying to guard may itself be flat, the resulting spin during the attempt to recover with anti-spin controls may be either flat or steep. In the latter case, a drag coefficient of 0·5 would be quite probable. To evaluate precisely how the speed will vary under the influence of changing incidence is obviously a most complex problem, which for practical purposes it is unnecessary to solve, as an upper limit can more easily be set.

It can readily be shown that the equation governing the vertical motion of the aircraft, if C_D is assumed to be unaffected by the rotation, is

$$\frac{1}{C_D}\frac{d}{d\tau}(vC_D^{1/2}) + v^2 - 1 = 0$$

where $\tau = gt(\rho/2w)^{1/2}$

t is the time

ρ is the air density

w is the wing loading

$$v = \frac{\text{equilibrium speed at the same } C_D}{\text{actual speed}}.$$

Particular examples can be followed by solving the equation for a given variation of C_D with τ. In the worst case, with α changing at the beginning of the motion discontinuously when the parachute is deployed, the drag coefficient changing from C_{D1} to C_D,

$$gt = \frac{V_1 C_{D1}^{1/2}}{2C_D^{1/2}} \log_e \frac{V_1 C_{D1}^{1/2} + VC_D^{1/2}}{V_1 C_{D1}^{1/2} - VC_D^{1/2}} \frac{C_{D1}^{1/2} - C_D}{C_{D1} + C_D}.$$

Fig. 10.2 shows the type of speed variation which results in this case and also when the incidence varies linearly with time; the discontinuous case leads to higher speed as the figure shows; it is in fact the worst case.

10.7. **Design of Parachutes.**—The first anti-spin parachute installations were made with little knowledge of parachute stability and of the shock loads experienced in the canopy, lines and cable. During the war, a good deal was learned about these things in the development of brake parachutes, knowledge which was useful in the design of anti-spin parachute installations. In many of these there is little to spare in the strength of the aircraft and it is of importance not to make the loads more severe than they need to be to fulfil their aerodynamic function. Let V_1 be the speed at opening, and V_2 the highest speed during the subsequent manoeuvre before the parachute is jettisoned. Then the opening case will be the worst, other things being equal, if the ' shock-load factor ' exceeds $(V_2/V_1)^2$; which this factor accordingly may not exceed, or even equal.

The designs now customary are based on the following data:

C_D = drag coefficient of parachute based on mouth diameter	1·07
Most probable shock factor $\left(= \frac{\text{instantaneous maximum drag on opening}}{\text{steady drag at same speed}}\right)$	$\sim$ 1·2
Safety link strength/opening pull	1·1 to 1·2
Factor of safety (not less than maximum probable shock factor)	1·5
Velocity at which safety link should fail/ design speed at opening	$(1{\cdot}5 \times 1{\cdot}15)^{1/2} = 1{\cdot}3$

For our present comment the most significant item is that expressing the ' shock factor '. Without the achievement of practical designs of parachute with factors below 1·5 the anti-spin parachute installation would have had to be ruled out from some spinning trials; this is understandable when we reflect that some of the older types of parachute gave shock factors on opening of the order of 5. The low values near unity are achieved with the aid of material having high porosity and of the ' snatch bag '* technique of deploying the parachute. The canopy is packed in a light bag from which it is released into the open position by a ripping action brought about by the tensioning of the cable. This successfully prevents cable snatch. The porous parachute, properly designed, has the added advantage of flying stability and therefore

* Since developed into the ' roll pack ' technique, which has the same principle.

in 'clean' airflow it can be relied upon to remain in position and exert a fairly steady pull in a constant direction. A potential drawback is the possibility of lower 'squidding' speeds than would be observed for less porous parachutes. This is therefore a point which must be carefully considered in design. The question has been studied in some detail in relation to anti-spin wing parachutes for tailless aircraft.

10.8. **Anti-spin Wing Parachutes.**—The renewed interest in tailless aircraft set a problem in the requirement for an anti-spin device for use in spinning trials or in prototype testing. A possible solution, apart from the use of slats or flaps, was already to hand in the application of some older flight observations by Alston[33]. These showed that the characteristics of the spin could be materially influenced by quite a small parachute towed from the wing-tip of a biplane. To apply this information to tailless monoplanes for use in a safety device it seemed best to use fairly long cables and to stream parachutes from both tips simultaneously. Model tests were made on the General Aircraft glider and showed an adequate improvement in recovery, of the order of 15 units of yawing moment with parachutes of 30-in. diameter full-scale attached at the tips. This led to the adoption of the formula :—

$$D = 0{\cdot}14S^{1/2}$$

for parachutes attached at the tips, which should ensure a reasonably constant active moment for different types at a given value of λ, increasing with λ. For, if the parachutes ride at an angle $\tan^{-1}\lambda$ to the vertical, the moment coefficient about the spin axis is roughly $\lambda C_p S_p/S$, which with the given parachute diameter is proportional to λC_p, and is of the order of 10 units. There can be no doubt that in this case it is the moment about the spin axis which is the active component, though it is reasonable to suppose that the nose-down pitching moment also helps recovery, for the rolling component, which is anti-spin, will assist the yawing component in body axes in the usual way if $A > B$, as is usual for tailless types.

10.9.—**Wake Effects on Wing Parachute Installations.**—For wing parachute installations bridle length is undoubtedly a critical variable. An analysis of some experimental and flight evidence bearing on this was made early in 1947[34]. Though this work was only a preliminary exploration of the matter, it showed beyond doubt the existence of important wake phenomena. We have to recognise the known fact that a given parachute has a fairly definite 'opening speed' and a higher 'closing speed', each depending, though not necessarily in the same way, on design parameters such as number and closeness of rigging lines, length of lines, porosity, etc. A basic theory of value for visualising the mechanism determining these critical speeds was developed by Prof. Duncan[35] (1943). In the light of this theory it is to be expected that a marked effect will be felt if any situation influences the local incidence of airflow on the parachute lip. Such an influence is to be found in the convergent airflow behind an obstacle, and we have also to reckon with the strong turbulence of the wake flow, and the fact that the mean speed differs from that in the main stream. The two main parameters are the distance x of the parachute downstream from the wing, and the ratio D/d of parachute diameter D to projected wing chord d, and all these variables are interdependent.

Broadly speaking the experimental results fit into the general concept of Fig. 10.3. We here picture the wake effects to be chiefly in two parts :

(i) Owing to the difference between the wake velocity and free-stream velocity, the critical speeds measured as aircraft speeds differ from the free-air values.

(ii) The chief influence of turbulence and convergence in on the closing speed (upper curve). As x decreases we reach a point where the curves would appear to be about to intersect. The result is that the opening speed is depressed towards lower speeds, leaving only a very narrow band of speeds between the opening and closing speeds in which the parachute is unstable, oscillating between open and closed. In practice, the speed at which it is proposed to use the parachute must be less than the opening speed, and the closing speed must be greater than the speed reached during the recovery motion. The lowering of the opening speed is thus extremely serious. This régime begins at a distance we have proposed to define as the critical distance $\overline{X}$ downstream. We have not analysed in detail how $\overline{X}$ varies with the possible parameters, though this would be a condition for a full understanding of the problem. It seems highly probable that increasing wing incidence will promote the closing action. Since, however, the tunnel investigation was limited to about 45-deg incidence, more information is required before more detailed analysis may be made.

On the basis of the information collected, a long bridle of about one span length was recommended. A further model experiment bears on this matter. Since the tunnel tests referred to above were static, it was desired to find whether the position was substantially affected by rotation. A simple experiment clearly indicated that centrifugal forces were playing a real part. A model was held static in the vertical tunnel with model parachutes attached at the wing tips while the incidence was gradually increased. On this scale it was of course impracticable to demonstrate the critical speeds, but as the incidence increased substantially above 45 deg a stage was reached where the 'parachutes', themselves inherently stable, ceased to ride aft and eddied to and fro, snatching at the 'cables'; eventually the parachutes settled on the wing, and thus directly downstream from the tips the gross turbulence was sufficient to overwhelm them. However, in a free spin at the same incidence this did not occur with parachutes of roughly dynamically correct mass, and it was obvious that they now rode somewhat further from

the axis than in the static test. It has been suggested that this centrifugal effect could if necessary be increased by using heavier cables or loaded parachutes.

10.10. **Other Aspects of Safety in Spinning.**—10.10.1. **Pilots' experience.**—This is of course a most important factor. Some attention has been given, especially in other countries, to the dangers inherent in the spin by reason of the unfamiliarity of the sensations and by disturbances of judgment in flying either by visual reference or by instruments. In this country emphasis is given chiefly to the necessity of familiarising pilots with the spin as the best means of correcting the possible errors in judgment, as the element of surprise is thereby minimised. For this reason the demand has been for good spinning characteristics in a wide range of aircraft types, although recently the requirements for fighters have been relaxed owing to the increased difficulty in meeting the requirements with present-day designs; practice spinning in fighters is now no longer permitted, but this throws the burden still more on to trainers, and emphasis needs to be placed on their having good characteristics of spin and recovery.

10.10.2. **Control forces.**—It is of some interest whether control forces can be so large in the spin that the pilot's strength is itself a limitation. We have given, in Chapter VI, section 8, a method of estimating the elevator forces, which appear to be the most serious problem, and this indicates that large forces may be attained on large and heavy aircraft. Such forces have rarely been reported in test flights, though in some tests of a *Typhoon* spinning at nearly 30,000 ft the pilot reported elevators apparently locked up, and an accident was narrowly averted. Another case, cited in Chapter VI, was that of the *Firebrand*, where large forces were anticipated and a power-assisted elevator was used for spinning tests. Forces which would have been beyond the pilot's strength without this assistance were measured.

There are serious objections to safety devices, such as the centrifugally-operated mechanism introduced by A. V. Stephens for spinning trials of the *Pterodactyl*[36] (1932), which can take the control out of the pilot's hands, and the ideal solution on large aircraft seems to be the installation of some form of power assistance.

CHAPTER XI

The Design of Vertical Tunnels

11.1. **The R.A.E. Vertical Tunnel.**—This was erected in 1933, and modified, with an increase in motor power, in 1935. It is of a very simple design which has proved of great practical value, whilst having also some notable defects. Fig. 11.1 shows the general outline of the design; the straight working-section, slightly flared entry, simple honeycomb, and conical diffuser. With this arrangement, we achieve an easily controllable air stream with speeds up to about 50 ft/sec, by using a steady power of 130 h.p. It is of course fundamental in vertical tunnel procedure to require a considerable overload for rapid acceleration.

To judge the performance we have to consider chiefly the speed, turbulence, velocity distribution and quickness of response to the controls. Fig. 11.2 shows the results of an attempt to estimate the critical Reynolds number for cylinder drag; this Reynolds number appeared to be about 10^5 at the working-section. It has often been observed, however, that a model allowed to sink rather low in the tunnel will change its spin behaviour; in all probability this is due to a gross turbulence or buffeting originating in the honeycomb.

11.2. **The Velocity Distribution.**—Figs. 11.3 and 11.4 give a general idea of the velocity distribution and it is now known both by particular experiment and by many day-to-day difficulties of operation that this falls far short of the ideal. The velocity across the jet is reasonably constant but inevitably falls off close to the wall, all the more so as the safety net itself must exert some drag and so tend to thicken the boundary layer. Experimental evidence obtained both in Canada and in this country suggests that a slightly 'dished' velocity distribution, with the maximum velocity as close to the sides as possible, is favourable to lateral stability. The importance of this factor in saving time cannot be overstated. Secondly, the vertical velocity gradient is of the wrong sign for stability, as a brief consideration shows that the velocity should preferably slightly diminish upwards, contrary to the natural trend caused by the blocking effect of the thickening boundary layer.

11.3. **Another Aspect of Stability.**—A further desirable quality of a good tunnel is a steady flow free from random changes of calibration. The R.A.E. Vertical Tunnel only satisfies this condition very roughly, in that calibrations on different occasions give an unexpected variation of $\pm$ 3 per cent in speed. This is probably determined by the flow conditions in the diffuser, where there is general breakaway of flow from the conical walls. These speed variations occur spontaneously and contribute to the difficulty of accurate measurement.

11.4. **The Reynolds Number of Model Tests.**—In free spinning, we may not seek to obtain maximum Reynolds number by using the maximum speed and scale since the requirement of dynamical similarity imposes a relation on these quantities. In fact we have the following ratios:

Parameter	*Model/Full-Scale Values*
Length	n^{-1}
Velocity	$n^{-1/2}$
Time	$n^{-1/2}$
Angular velocity	$n^{1/2}$
Kinematic viscosity	ν_G/ν_H
Reynolds number	$\frac{\nu_H}{\nu_G} n^{3/2} = \frac{\sigma'}{0{\cdot}7} n^{3/2}$ at 15,000 ft

where ν_G and ν_H are the kinematic viscosities in the tunnel and at altitude respectively, and σ' is the pressure ratio of the tunnel, if it is pressurised.

The first factor in a close approach to full-scale Reynolds number is therefore a reasonably large model scale. In Fig. 11.5 are shown the Reynolds number as a function of scale and tunnel input power (per unit power factor). This diagram shows that Reynolds number can be increased to 1/60 of full-scale by using a 1/20 scale model and a 15-ft tunnel, or to 1/15 if an absolute pressure of 4 atmospheres were available. A pressurised tunnel has a clear advantage over a larger atmospheric tunnel having similar power. The power required to drive the tunnel varies as $\sigma'\sigma^{3/2}$ where σ' is the pressure ratio of the tunnel and σ is the relative density at altitude; this is approximately the same for $\sigma' = 4$ and altitude 15,000 ft as for $\sigma' = 1$ and altitude 40,000 ft so that, by using the same model suitably loaded, a change of altitude can be simulated without using a higher power, but with some sacrifice in Reynolds number ratio.

11.5. **Rolling Balance Tests.**—From the outset it has been an aim to provide equipment not only for free-spinning work but also for rolling-balance tests. Because of its rather long working-section, a vertical tunnel is quite suitable for such tests. On the other hand it is desirable that they should take place in an air stream without the stabilising velocity gradients. It should be easy to arrange for the two types of air stream by the use of suitable removable liners.

At present there is no rolling-balance at the R.A.E. The design of an adequate one will require much consideration, but it seems worthwhile to do this as measurements which can best be made with a rolling-balance are often required at incidences below the stall, as well as for spinning research.

REFERENCES

No.	*Author*	*Title, etc.*
1.	K. V. Wright	The virtual mass correction to the measured moments of inertia of a *Bristol Fighter*. R.A.E. Report B.A.888. October, 1930. (Unpublished.)
2.	W. Gracey	The additional mass effect of plates as determined by experiments. N.A.C.A. Report 707. 1941.
3.	S. B. Gates and L. W. Bryant ..	The spinning of aeroplanes. R. & M. 1001. October, 1926.
4.	E. Finn and W. H. Stephens ..	Note on the differential operation of wing flaps in spinning. Model tests on *Hurricane*. R.A.E. B.A. Departmental Note Full Scale 57. December, 1936. (Unpublished.)
5.	H. Lamb	*Higher Mechanics*, p. 5. Oxford University Press, 1929.
6.	L. W. Bryant and I. M. W. Jones	Notes on recovery from a spin. R. & M. 1426. March, 1932.
7.	F. B. Bradfield, G. F. Midwood and A. V. Stephens.	Tests of floating ailerons on a *Bristol Fighter* aeroplane. R. & M. 1501. January, 1932.
8.	H. B. Irving and A. S. Batson ..	Spinning calculations on some typical cases. R. & M. 1498. February, 1932.
9.	A. I. Neihouse	A mass distribution criterion for predicting the effect of control manipulation on the recovery from a spin. N.A.C.A. Advance Restricted Report. Wartime Report L.168. A.R.C. 6282. August, 1942.
10.	G. E. Pringle and V. G. Warren..	Further model spinning tests of the *Typhoon*. R.A.E. Report Aero. 1819. A.R.C. 7009. May, 1945. (Unpublished.)
11.	G. E. Pringle	Note on rates of turning in the spin of twin-engined types. R.A.E. Tech. Note Aero. 1317. November, 1943. (Unpublished.)
12.	G. E. Pringle	Model spinning data affecting strength requirements. R.A.E. Tech. Note Aero. 1576. A.R.C. 8547. January, 1945. (Unpublished.)

REFERENCES—*continued*

No.	*Author*	*Title, etc.*
13.	A. V. Stephens	Spinning of a *Bristol Fighter*. R. & M. 1515. July, 1932.
14.	M. J. Bamber and C. H. Zimmerman.	Effect of stabiliser location upon pitching and yawing moments in spins as shown by tests with the spinning balance. N.A.C.A. Tech. Note 474. November, 1933.
15.	H. B. Irving	A simplified presentation of the subject of spinning of aeroplanes. R. & M. 1535. March, 1933.
16.	H. B. Irving, A. S. Batson and J. H. Warsap	The contribution of the body and tail of an aeroplane to the yawing moment in a spin. R. & M. 1689. November, 1935.
17.	E. Finn	Analysis of routine tests of monoplanes in the R.A.E. free-spinning tunnel. R. & M. 1810. July, 1937.
18.	R. H. Francis	Interim report on systematic model research in free spins: low-wing monoplanes. R. & M. 1714. January, 1936.
19.	W. Tye and S. V. Fagg	Spinning criteria for monoplanes. R.A.E. Report A.D. 3141. A.R.C. 4653. May, 1940. (Unpublished.)
20.	D. J. Harper	Comparison of model and full-scale spinning tests on a basic trainer (Percival *Prentice*). R.A.E. Report Aero. 2298. A.R.C. 12,142. November, 1948. (Unpublished.)
21.	R. I. Sears and H. P. Hoggard, Jr.	Characteristics of plain and balanced elevators on a typical pursuit fuselage at attitudes simulating normal flight and spin conditions. N.A.C.A. Advanced Restricted Report. Wartime Report L.379. A.R.C. 5971. March, 1942.
22.	S. B. Gates and A. V. Stephens..	A method of providing for scale effects in model spinning tests. R.A.E. Report B.A. 1154. September, 1934. (Unpublished.)
23.	S. B. Gates	Note on model spinning standards. R.A.E. Report B.A. 1436. A.R.C. 3240. October, 1937. (Unpublished.)
24.	G. E. Pringle	The difference between the spinning of model and full-scale aircraft. R. & M. 1967. May, 1943.
25.	O. Seidman and A. I. Neihouse ..	Comparisons of free-spinning wind-tunnel results with corresponding full-scale spin results. N.A.C.A. Wartime Report L.737. December, 1938. A.R.C. 6958. August, 1943.
26.	D. J. Harper	The influence of rolling moments on spin recovery as observed in model spinning tests. R. & M. 2831. April, 1950.
27.	F. B. Bradfield and L. P. Coombes	Auto-rotation measurements on a model aeroplane with zero stagger. R. & M. 975. April, 1925.
28.	E. N. Jacobs, K. E. Ward and R. M. Pinkerton.	The characteristics of 78 related aerofoils sections from tests in the variable density wind tunnel. N.A.C.A. Report 460. 1933.
29.	G. E. Pringle	Factors affecting the symmetry of right- and left-handed spins. R.A.E. Report Aero. 1915. A.R.C. 7967. June, 1944. (Unpublished.)
30.	Staff of A. & A.E.E.	*Typhoon* 1B, R.7673 (Sabre II). Brief spinning trials. 24th part of A. & A.E.E. Report 761a. January, 1943. (Unpublished.)
31.	D. J. Harper	Model spinning tests on an experiment tailless aircraft. R.A.E. Report Aero. 2305. December, 1948. (Unpublished.)
32.	R. H. Francis	Safety devices for full-scale spinning trials. R.A.E. Report B.A. 1195. April, 1935.
33.	R. P. Alston	Note on the use of a wing-tip parachute in recovering from spins. R.A.E. Report B.A. 1014. A.R.C. 586. March, 1933. (Unpublished.)
34.	D. J. Harper, J. R. Mitchell, J. Picken and G. E. Pringle.	Wing parachutes for recovery from the spin: Part II—Wake phenomena. R. & M. 2543. March, 1947.
35.	W. J. Duncan	The cause of the spontaneous opening and closing of parachutes (the phenomena of squidding). R. & M. 2119. December, 1943.
36.	A. V. Stephens and J. Cohen ..	Spinning of *Pterodactyl* Mark IV. R. & M. 1576. July, 1932.

LIST OF SYMBOLS

Note.—The usual notation for the moment coefficients in spinning work is as follows. Examples are: $\overline{lv}$, $\overline{mq}$, $\overline{n'\xi}$, etc. The first letter indicates the axis, *l* rolling, *m* pitching and *n* yawing. The second letter or symbol denotes to what the moment is due, the definition of the letter or symbol being given in the list below with the following exceptions: $\overline{li}$, $\overline{mi}$, $\overline{ni}$ are moments due to inertia: $\overline{m\alpha_P}$, $\overline{mg}$ are aerodynamic and gyroscopic pitching moments due to the propeller: $\overline{n'p_B}$, $\overline{n'p_W}$ are body and wing contributions to yawing moments. A primed first letter indicates that body axes, not wind axes are referred to, except in Chapter IV where the primes are omitted. All the moments are divided by $\rho V^2 Ss$ to obtain the coefficients; $\bar{c}$ is not used for the pitching moments as it usually is.

A Rolling moment of inertia of model or aircraft

ΔA Virtual rolling moment of inertia of model

A_1 Wing aspect ratio

A' Polar moment of inertia of propeller or engine

A_R Unshielded rudder area

B Pitching moment of inertia of model or aircraft

ΔB Virtual pitching moment of inertia of model

C Yawing moment of inertia of model or aircraft

ΔC Virtual yawing moment of inertia of model

Coefficients

C_D Drag

C_H Elevator hinge moment

C_L Lift

C_l' Applied rolling moment

C_m Aerodynamic pitching moment

C_n' Applied yawing moment

C_P Drag coefficient of anti-spin parachute

C_R Resultant force—wing

C_X Chordwise force—wing

C_Y Side force

C_Z Normal force—wing

C_Z' Normal force—tailplane

C_Z'' Normal force—outer wing of tailless aircraft

D Diameter of mouth of inflated parachute

H Altitude

K Cross-sectional area of duct

$K_1 = S(k_O^2 - k_A^2)/2gS'x'$

$K_2 = x'^2 C'_z/2g\mu S$

$K_3 = h_1/\overline{V}$

} constants in equation (5.6)

L Rolling moment in body axes

M Pitching moment in body axes

N Chapter IV, VIII, yawing moment in body axes
Chapter VII, threshold value of applied yawing moment

R Chapter III, V, IX, radius of spin
Chapter II, VII, Reynolds number

S Wing area

S' Gross area of tailplane and elevator

S_e Area of elevator aft of hinge-line

S_P Area of mouth of inflated parachute

T		Chapter II, period of oscillation of model swinging as a compound pendulum Other Chapters, time of recovery
V		Velocity
V_G		Velocity of centre of gravity
V_H		Rate of loss of height
$\overline{V}$		Tail volume coefficient, $= S'x'/S\bar{c}$
W		Aircraft weight
X		Mean value of yawing-moment difference between model- and full-scale for a number of comparisons
$\overline{X}$		Critical distance of anti-spin parachute downstream from wing
Y		Probable error in the determination of X
Y_A, Y_B		Effect on recovery in terms of applied yawing moment of changes of 15 per cent in the model loadings A and B
Z		Typical determination of the difference between model- and full-scale recoveries
a	=	$(B - C)/\rho Ss^3$, rolling inertia difference coefficient
a'	=	$A'/\rho Ss^3$
b	=	$(C - A)\rho Ss^3$, pitching inertia difference coefficient
c	=	$(A - B)\rho Ss^3$, yawing inertia difference coefficient
$\bar{c}$		Wing mean chord
c_0		Tip chord
c_1		Root chord
c_e		Elevator chord aft of hinge
d		Projected chord of wing at right-angles to wind direction, $= \bar{c} \sin \alpha$
d'		Length of fuselage or nacelle duct, $= (x_1 - x_2)$
d''		Distance of centre of pressure of duct from centre of gravity $= \frac{1}{2}(x_1 + x_2)$
g		Acceleration due to gravity
h		Chapter V, centre of gravity coefficient in terms of $\bar{c}$ Chapter VI, body depth in side view
h_1		Chapter V, wing centre-of-pressure coefficient relative to c.g. Chapter IX, wing centre-of-pressure coefficient relative to quarter-chord
h_1'		Wing centre-of-pressure coefficient, $= h + h_1$
$h'c_1$		Distance between c.g. and quarter-chord at root of wing
i_A, i_B, i_C		Inertia coefficients, $= A/Ws^2$, *etc.*
j		Chapter VIII, unit vector along y-axis Other chapters, ratio of equivalent yawing and rolling moments, $= -\nu_v/\lambda_v$
k_A, k_B, k_C		Radii of gyration about x, y and z-axes
l		Chapter X, distance between c.g. and point of attachment of parachute cable Other chapters, applied rolling moment
l_E, l_R		Distances between nose of aircraft and elevator and rudder hinges respectively
l''		Distance from c.g. to mean quarter-chord point of fin and rudder
$\overline{lpv}$, etc.		Rolling-moment coefficients, *see* note at beginning of list of symbols
l_v		Sideslip derivative of rolling moment $= \partial \overline{lv}/\partial \beta$
m		Element of mass
ml		Length of parachute cable
m_1		Mass flow of gas
$\overline{m\alpha}$, etc.		Pitching-moment coefficients, *see* note at beginning of list of symbols
m_v		Sideslip derivative of pitching moment
n		Applied yawing moment where appropriate Chapter II, VII, VIII, XI, scale of models, ratio of full-scale/model length Chapter VI, weight factor in evaluation of damping coefficient

$\overline{n\zeta}$, etc.	Yawing-moment coefficients, *see* note at beginning of list of symbols
n_r	Yawing derivative of yawing moment
n_v	Sideslip derivative of yawing moment
p	Rolling
q	Pitching
r	Yawing
	components of rotation about x, y, z wind axes. Primed letters indicate body axes not wind axes, except in Chapter IV
	Chapter V, IX, radius of chord element of wing
s	Wing semi-span
t	Time
t/c	Wing thickness/chord ratio
u	Chapter VII, excess of speed required to produce retardation of rate of descent, V_H
	Other Chapters, linear velocity along Ox, wind axis
v	Chapter X, equilibrium speed at same C_D/actual speed
	Other chapters, linear velocity along Oy, sideslip velocity
w	Wing loading, $= W/S$
x	Fore-and-aft distance
	Chapter VI, distance between element of side area and c.g.
	Chapter X, distance of parachute downstream from wing
x'	Distance from c.g. to mean quarter-chord point of tailplane and elevator
x_1, x_2	Abscissae of entry and exit planes of duct
y	Spanwise distance
z	Vertical distance
α	Wing incidence
α' α''	Geometrical incidences at ' rising ' and ' falling ' wing tips
α^x	Angle between wing chord and principal axis of inertia in the fuselage
β	Chapter III and where obviously appropriate, sideslip angle
	Other chapters, non-dimensional spanwise distance $= y/s$
γ	Chapter VI, stick gearing—ratio of elevator/stick movements
	Other chapters, inclination of flight path to vertical, $= \frac{\pi}{2} - \theta_1$
ε	Chapter III, inclination of resultant force to plane of symmetry
	Chapter VI, weight factor for fuselage section, in evaluation of $\overline{n'p_B}$
	Chapter X, angle between aircraft x-axis and parachute cable
ζ	Rudder angle
η	Elevator angle
θ	Chapter III, pitch of wind axes
	Other chapters, taper ratio $= c_1/c_0$
θ' =	$(1 - \theta) = (1 - c_1/c_0)$
θ_1	Inclination of path of c.g. below the horizon—helical pitch
θ_y	Inclination of ' outer ' span above horizon—tilt angle
θ_z	Inclination of lift axis to horizon
λ	Spin parameter $= \Omega s/V$
λ'	Non-dimensional rate of rotation of propeller or engine $= \omega s/V$
λ_v	Total sideslip derivative of rolling moments, including inertia term
μ	Relative density of aircraft or model $= W/\rho Ss$

ν	Kinematic viscosity
ν_v	Total sideslip derivative of yawing moments, including inertia term
ξ	Aileron angle
ρ	Density of atmosphere
σ	Relative density of atmosphere at altitude
σ'	Pressure ratio of pressurised tunnel
τ	Chapter IV, period of rotation in steady spin
	Chapter X, a form of aerodynamic time $= gt(\rho/2w)^{1/2}$
φ	Chapter III, bank of wind axes
	Chapter VII, inherent scatter in Z due to causes other than inertia errors
ψ	Sweepback angle at quarter-chord line
Ω	Resultant angular velocity
ω	Angular velocity of propeller or engine

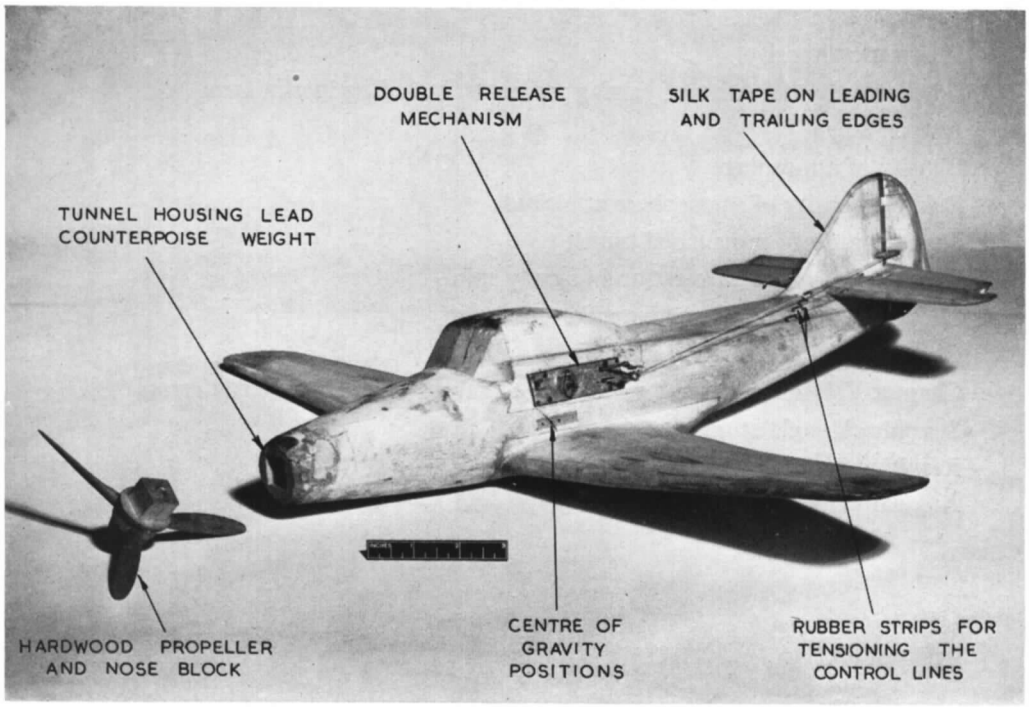

FIG. 2.1a. Three-quarter front view.

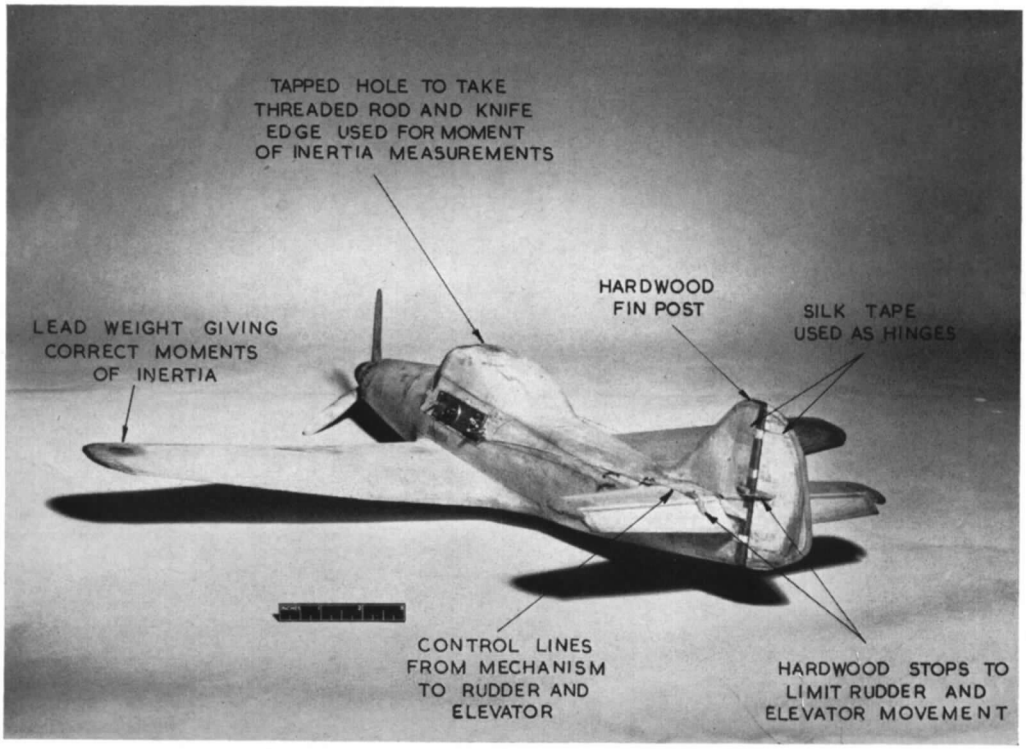

FIG. 2.1b. Three-quarter rear view.

FIG. 2.1. Constructional features of a typical dynamic model for spinning tests.

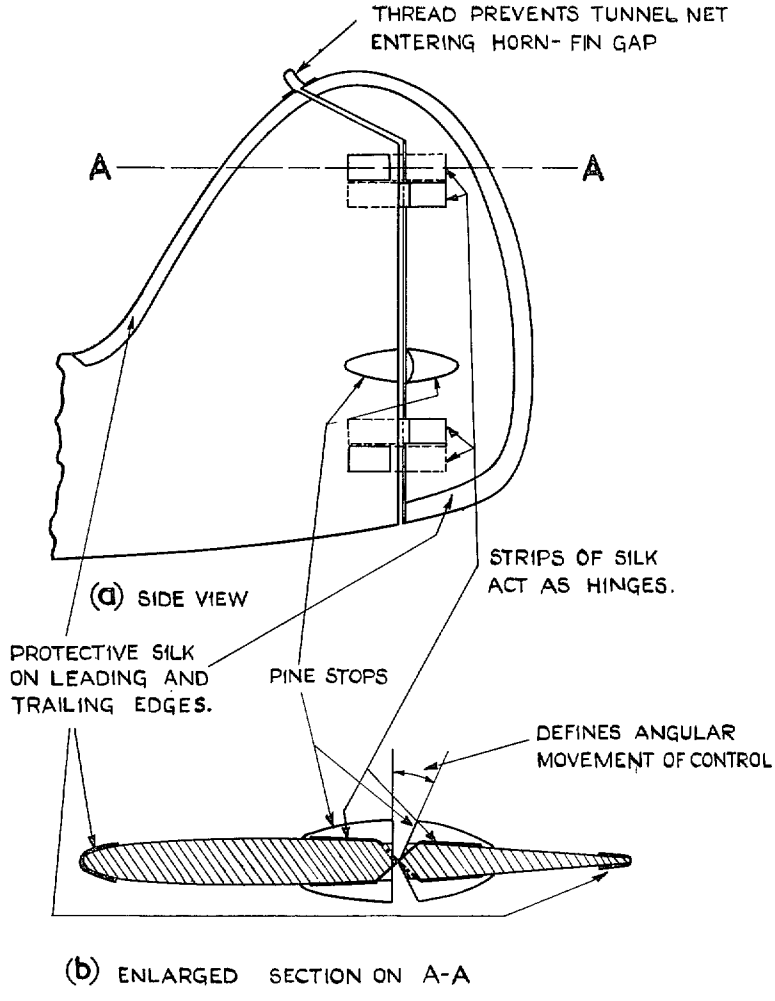

FIG. 2.2. Method of mounting movable controls.

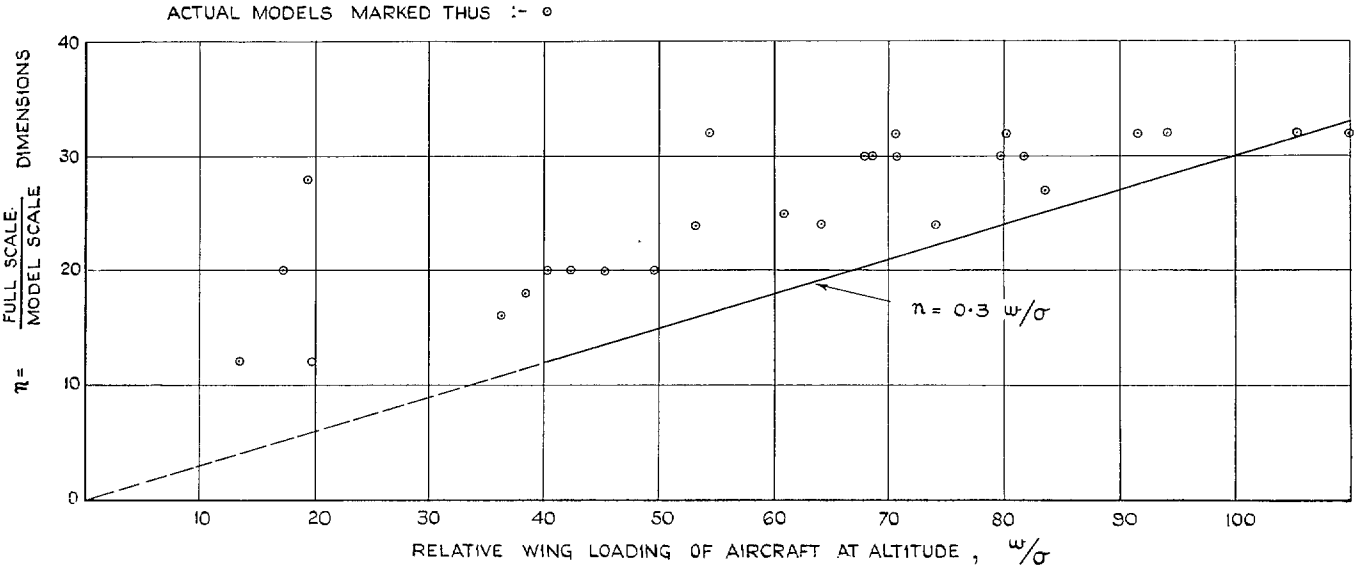

FIG. 2.3. Scale of dynamic models in the R.A.E. Vertical Tunnel.

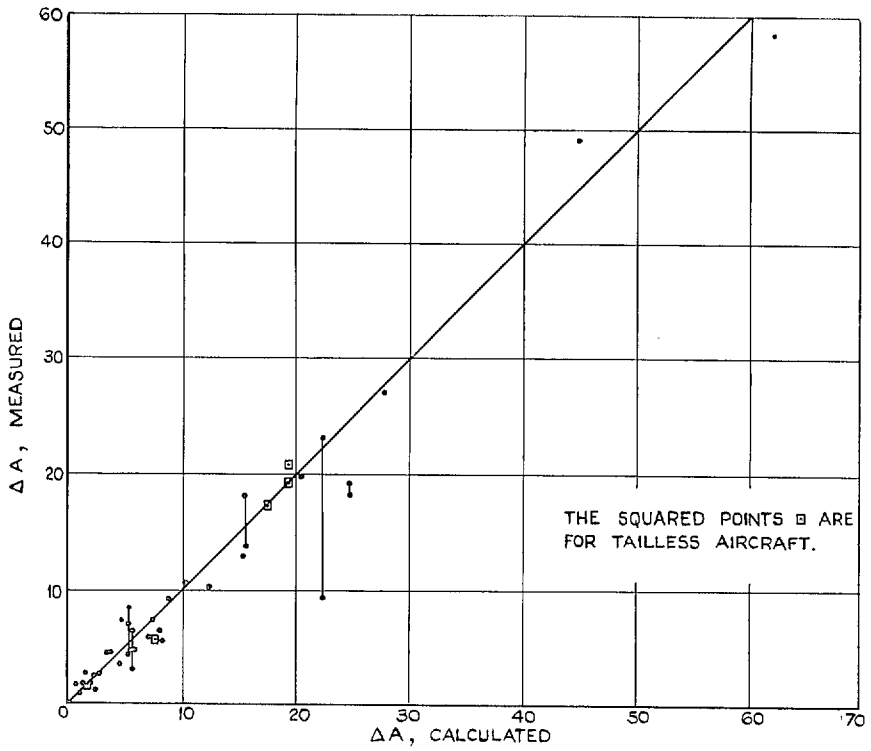

FIG. 2.4. Virtual rolling moment of inertia, ΔA, for various models.

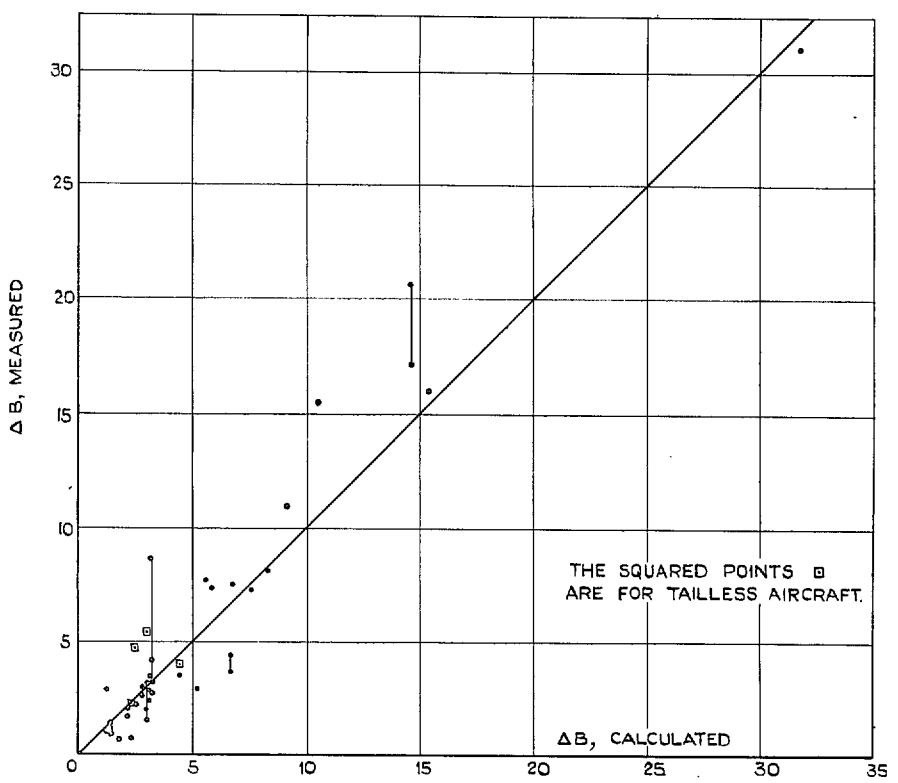

FIG. 2.5. Virtual pitching moment of inertia, ΔB, for various models.

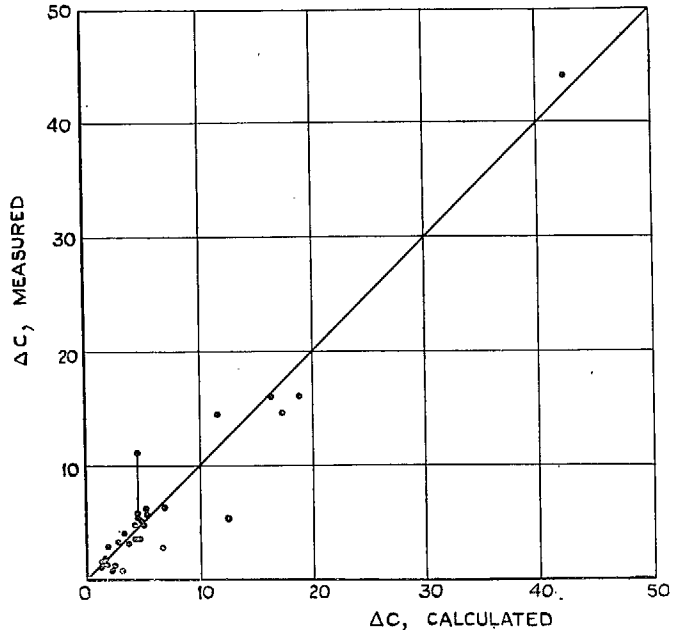

FIG. 2.6. Virtual yawing moment of inertia, ΔC, for various models.

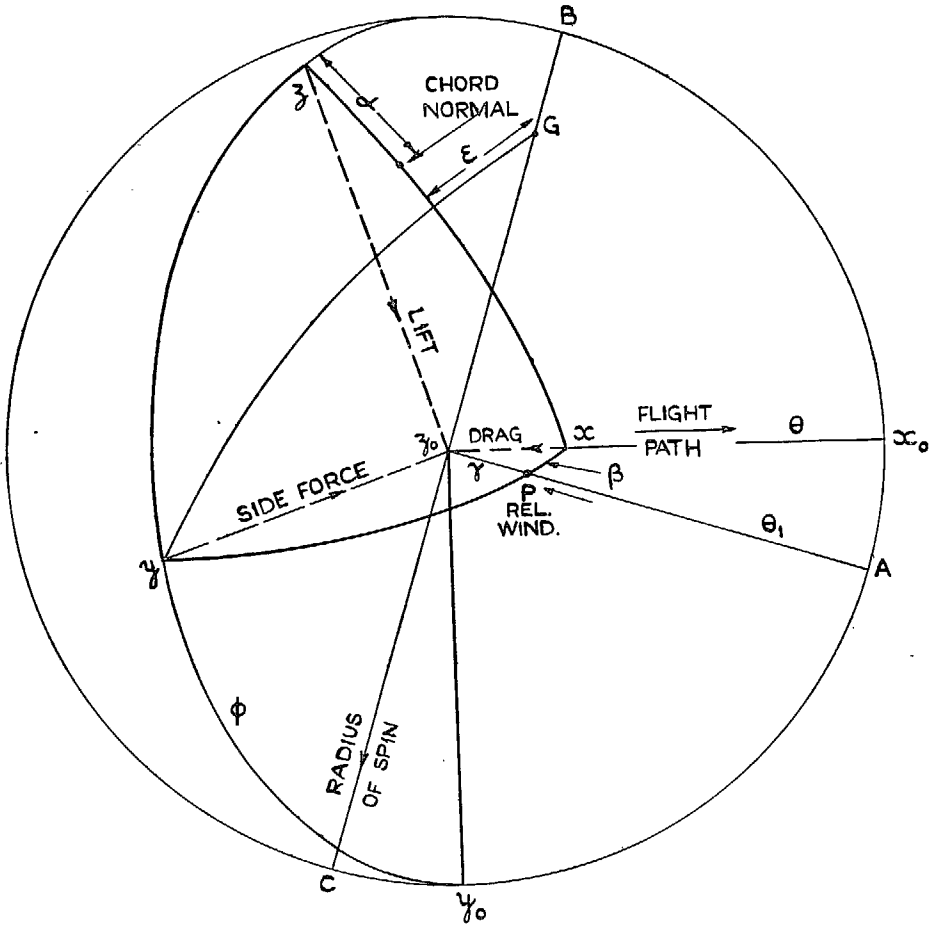

FIG. 3.1. The geometry of a spin.

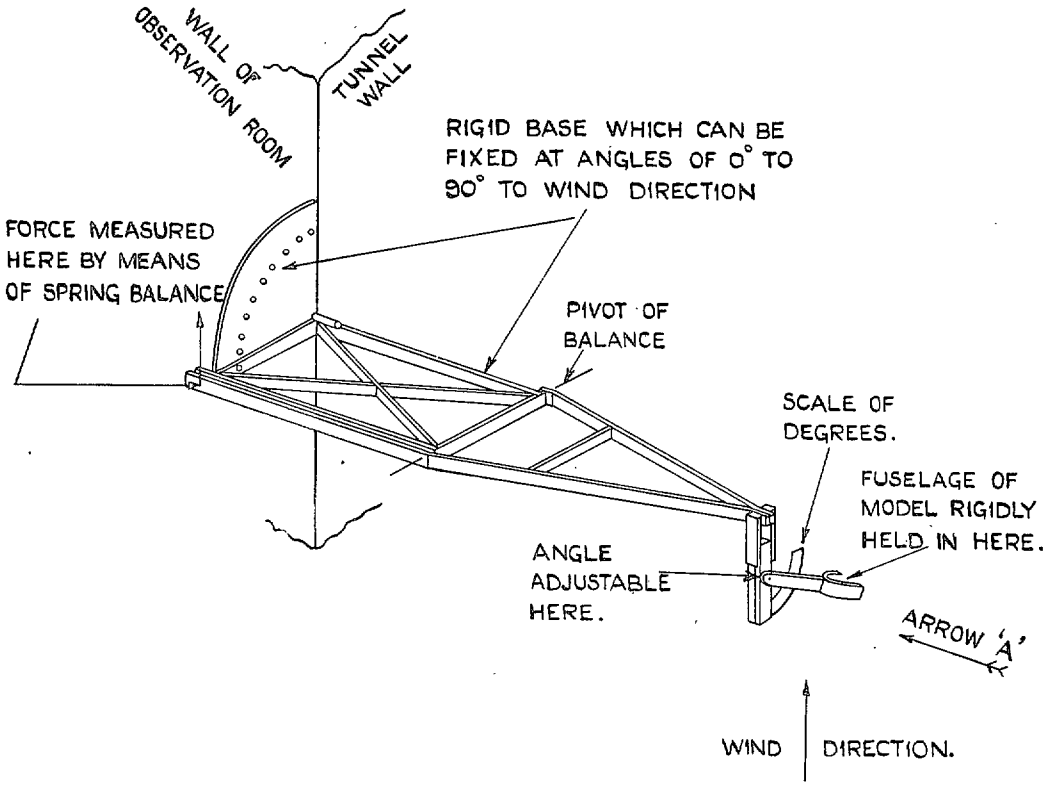

SKETCH OF BALANCE MOUNTED IN VERTICAL TUNNEL

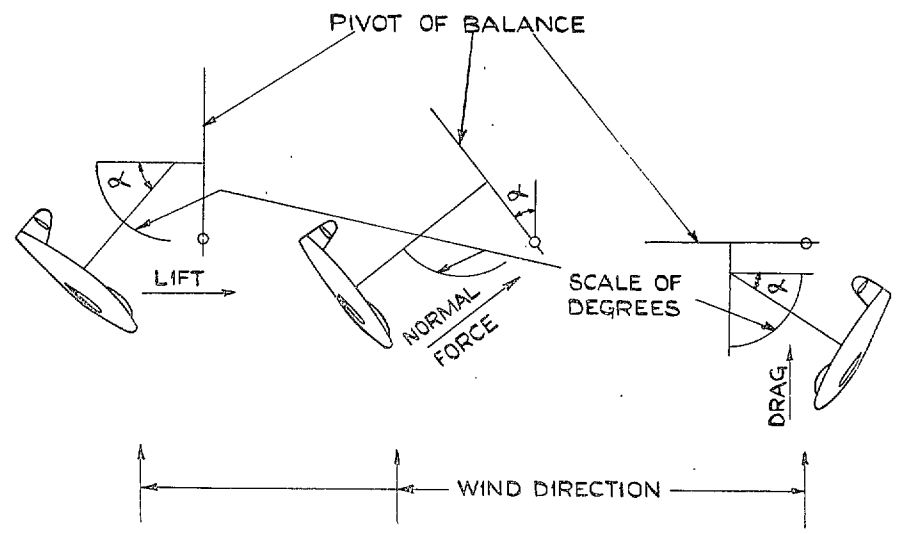

LINE VIEWS IN DIRECTION OF ARROW 'A' SHOWING ARRANGEMENT OF MODEL AND BALANCE FOR MEASUREMENT OF LIFT, NORMAL AND DRAG FORCES.

FIG. 3.2. Diagrammatic representation of static-force balance in vertical tunnel.

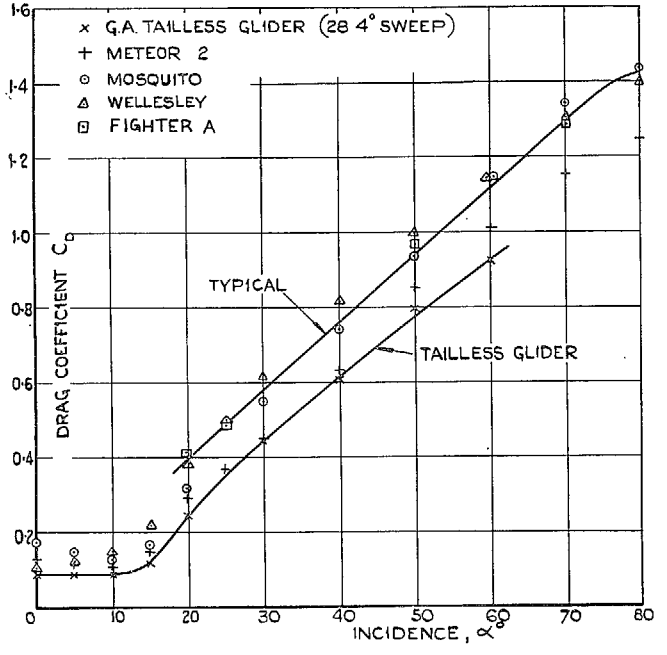

FIG. 3.3. Static drag of spinning models.

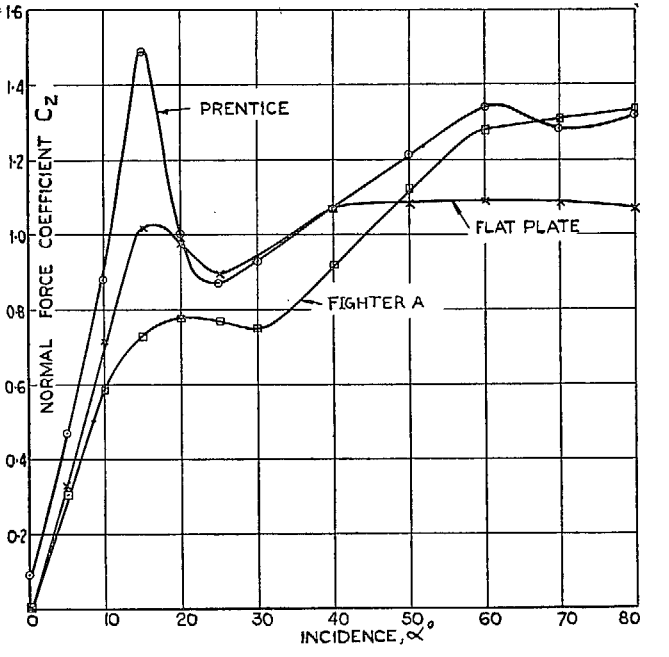

FIG. 3.5. Static normal-force of spinning models.

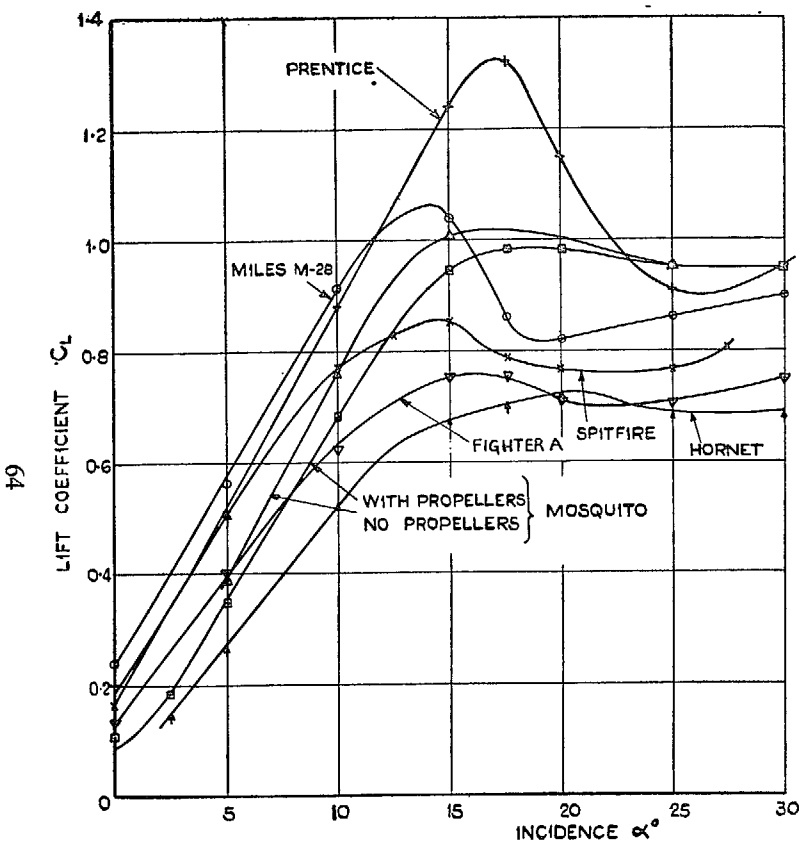

FIG. 3.6. Static maximum lift coefficients of spinning models. Reynolds number ~ 50,000.

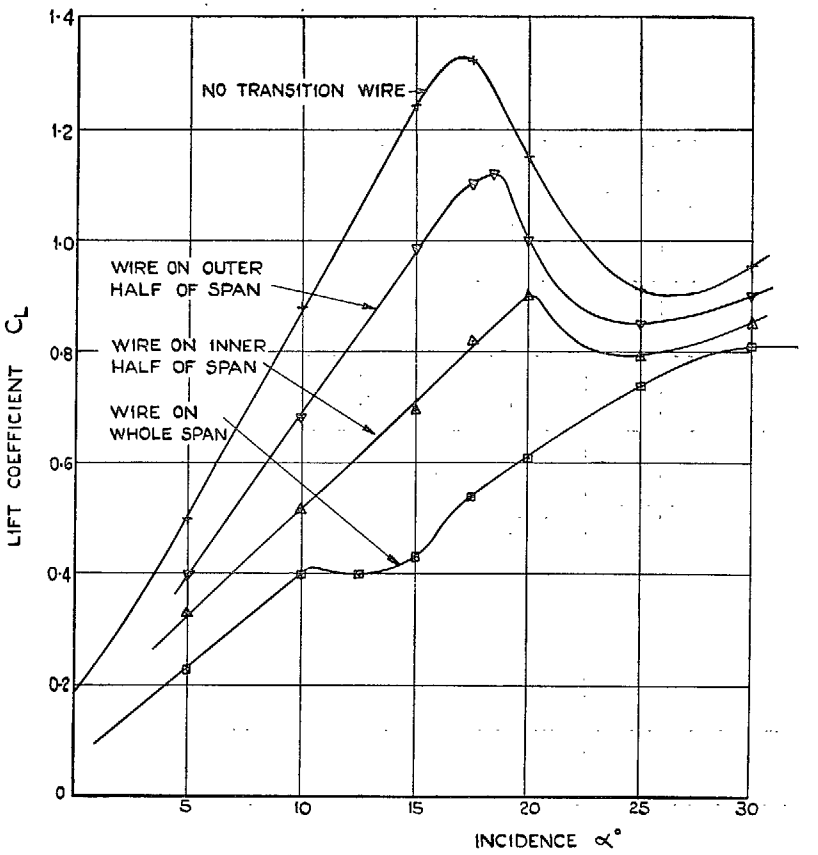

FIG. 3.7. Effect of transition wire at 10 per cent chord on $C_{L\,max}$ of *Prentice*. Reynolds number ~ 50,000.

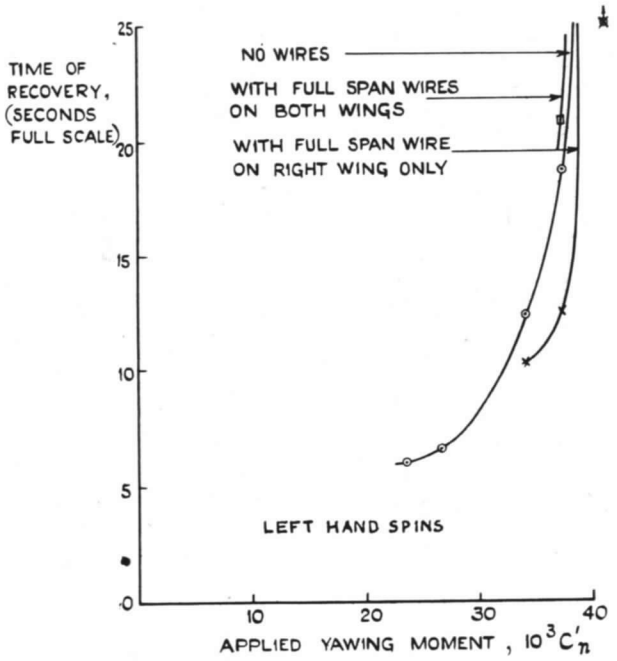

FIG. 3.8. Recovery of *Prentice* model with various transition wires in place.

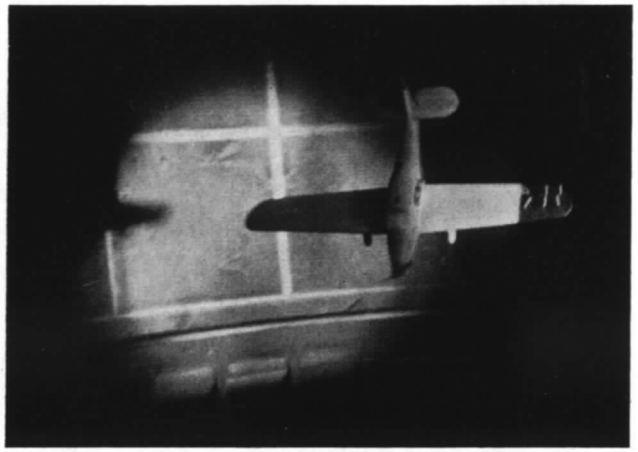

FIG. 3.9a. Steep spin, no applied yawing moment.
$\alpha = 40$ deg; $\lambda = 0{\cdot}46$; $\alpha' = 15$ deg.

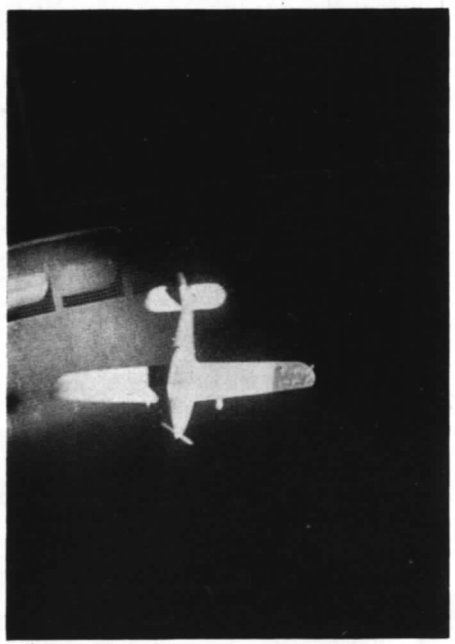

FIG. 3.9b. Flatter spin ~ 15 units applied yawing moment.
$\alpha = 49$ deg; $\lambda = 0{\cdot}51$; $\alpha' = 22$ deg.

FIG. 3.9. Stalling of ' rising ' wing tip—*Prentice*.

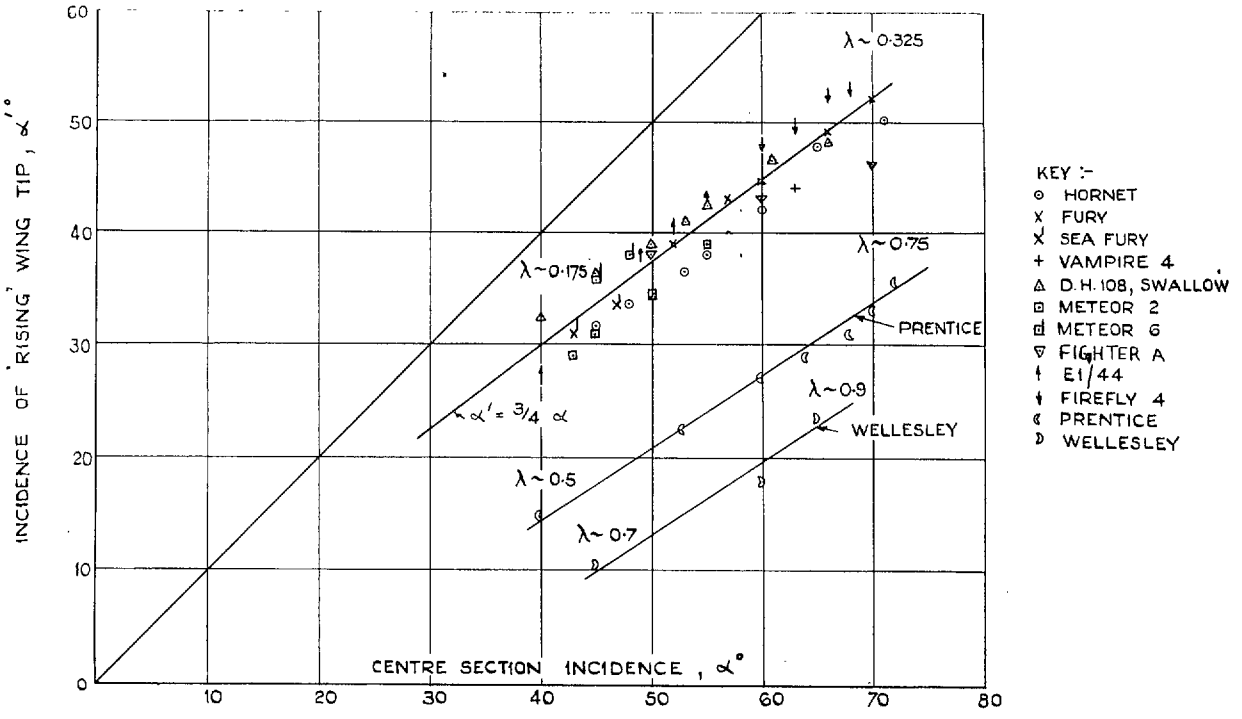

FIG. 3.10. Variation of incidence of ' rising ' wing tip with centre-section incidence.

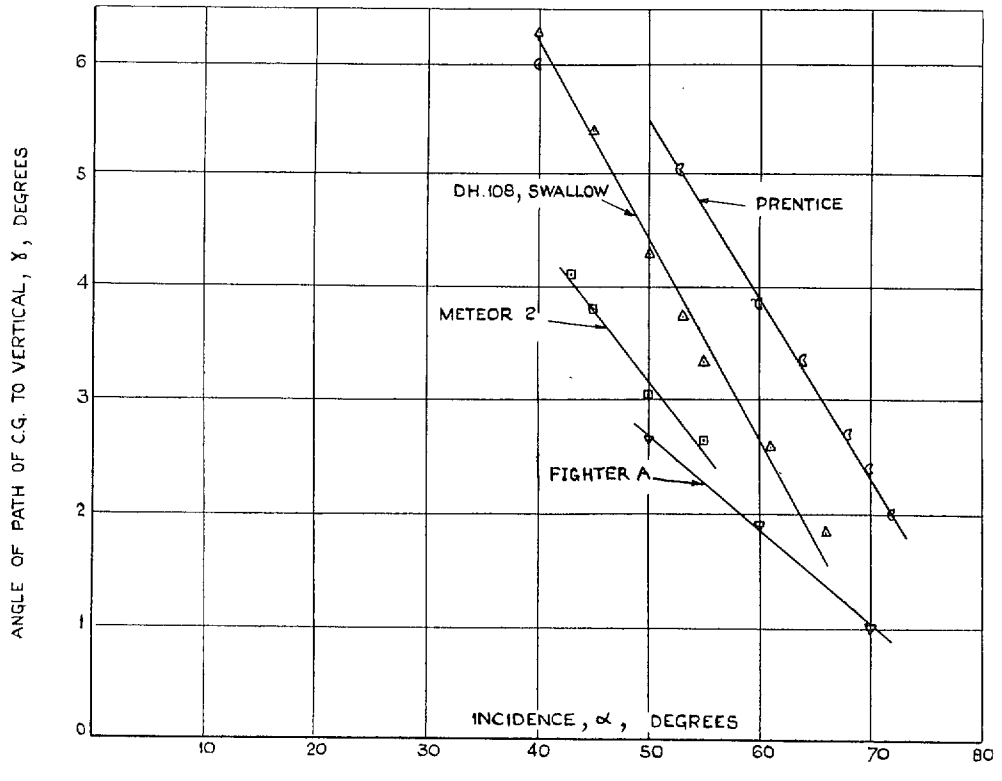

FIG. 3.11. Variation of spiral path with incidence.

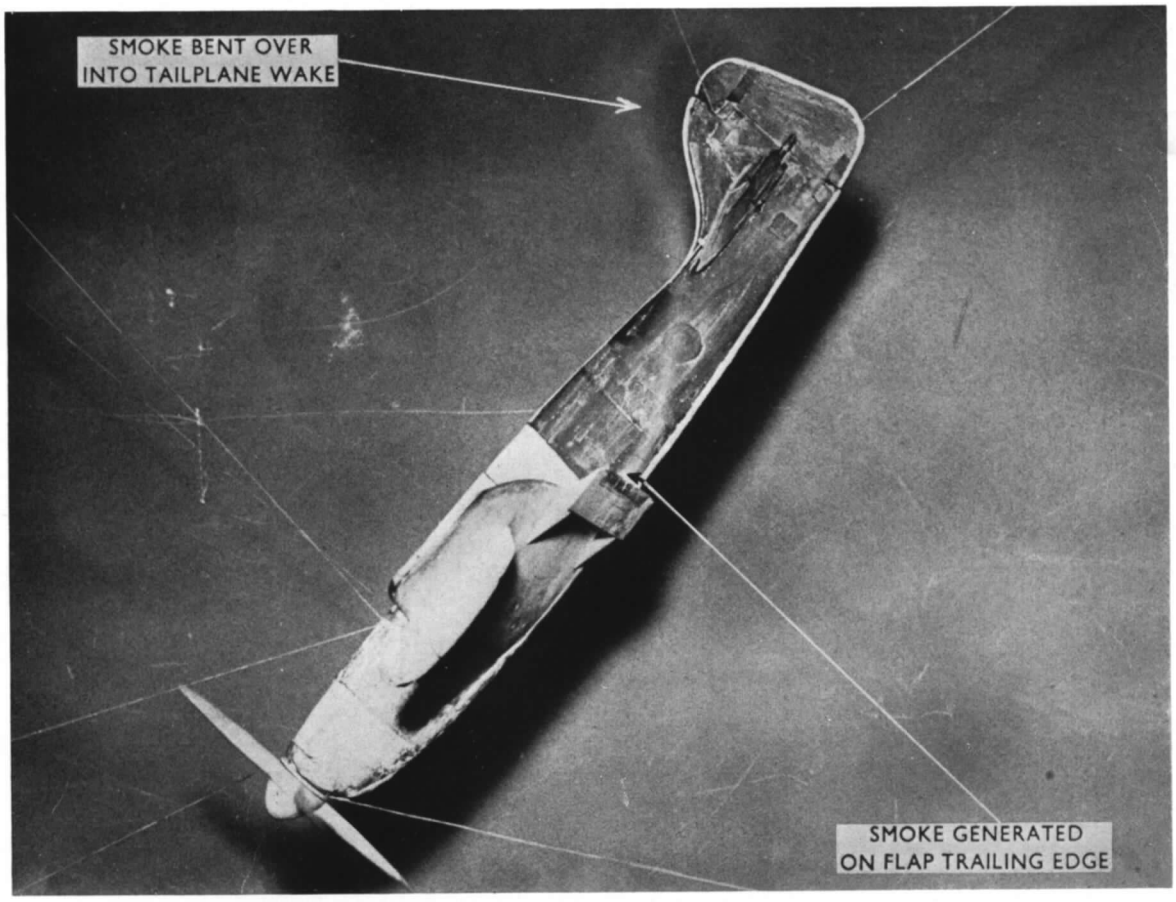

FIG. 3.12. Visualisation of wake from flaps—*Firefly* 4. Incidence, 45 deg; no rotation; flaps in cruising position.

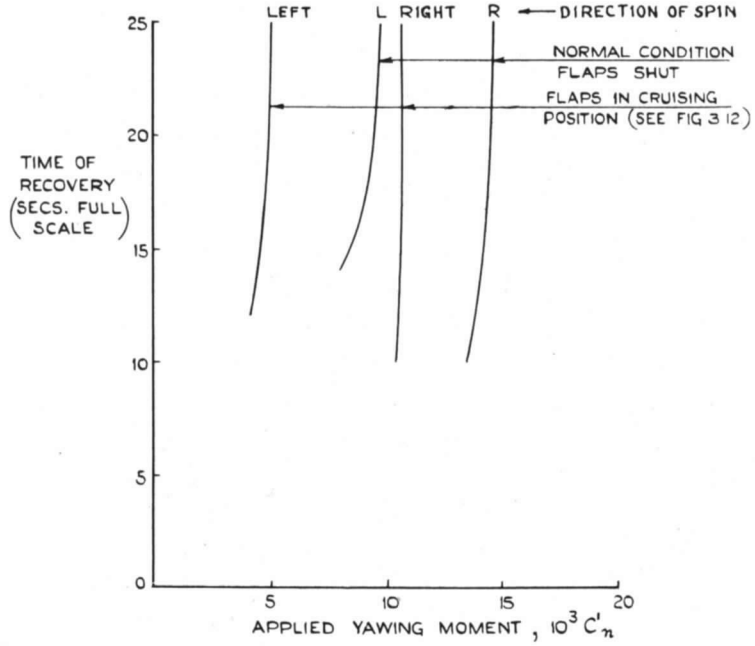

FIG. 3.13. Effect of flaps on recovery—*Firefly* 4.

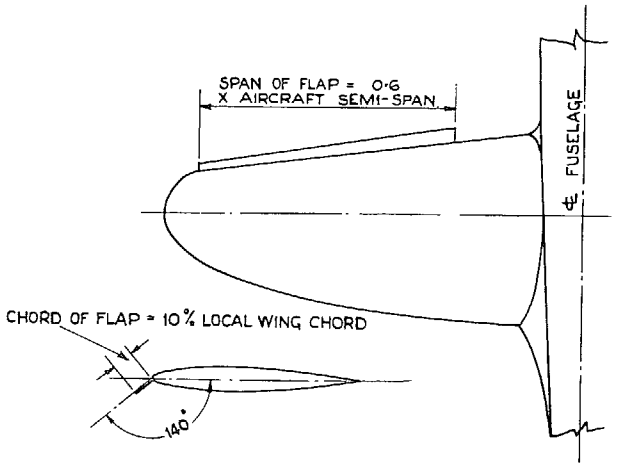

FIG. 3.14a. Arrangement of wing leading-edge flaps.

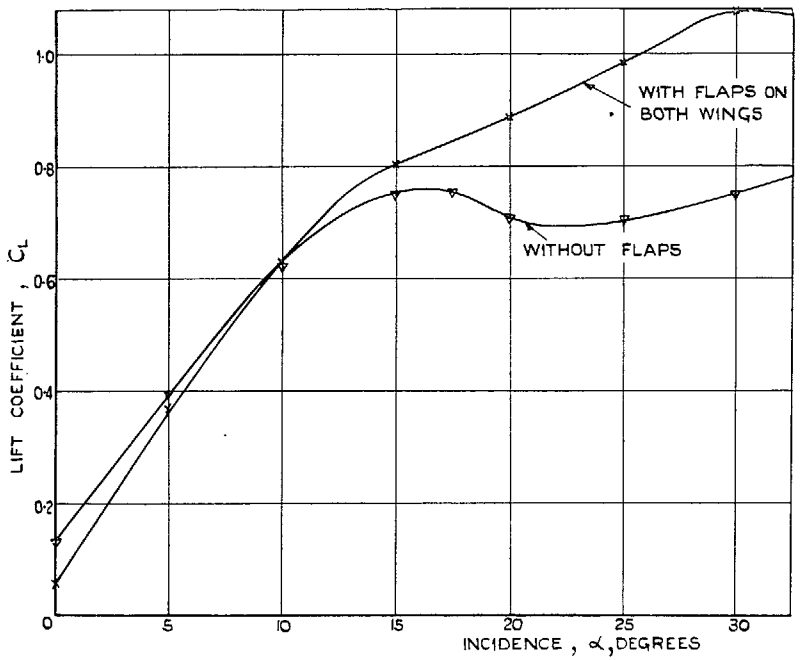

FIG. 3.14b. Effect of flaps on lift.

FIG. 3.14. Wing leading-edge flaps on Fighter A.

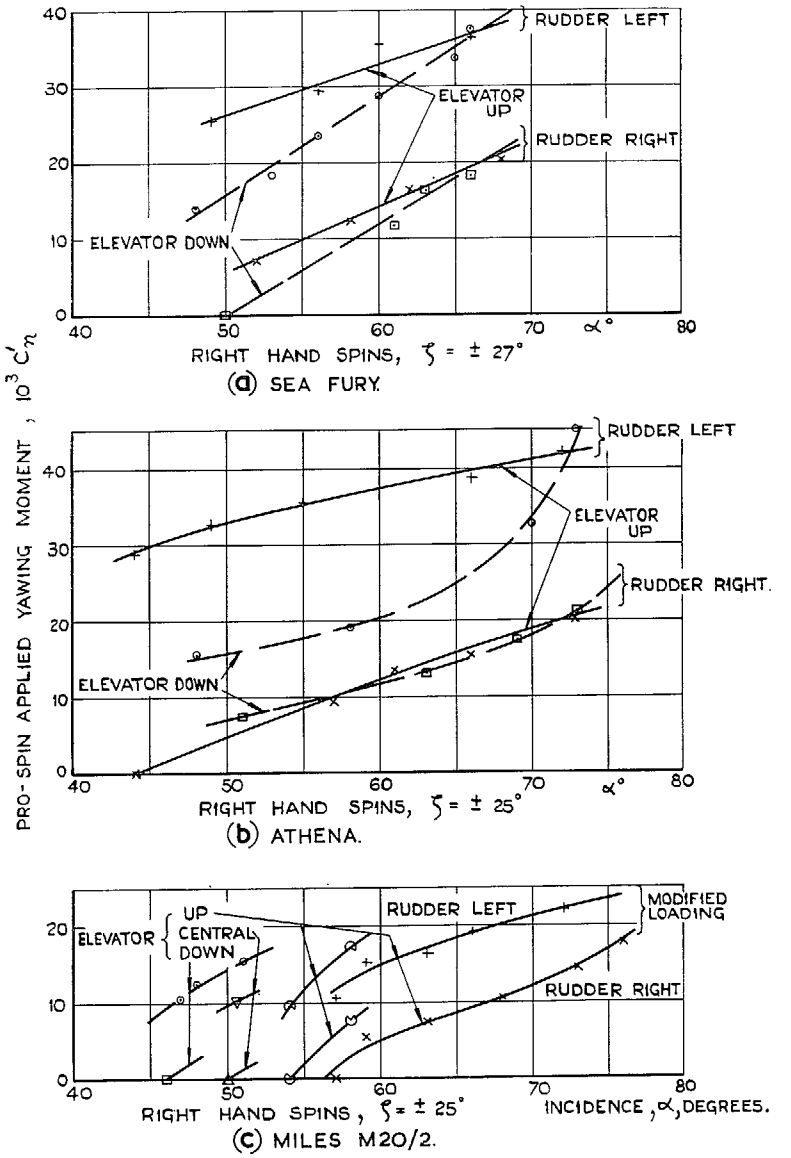

FIG. 3.15. Rudder yawing moments in the spin.

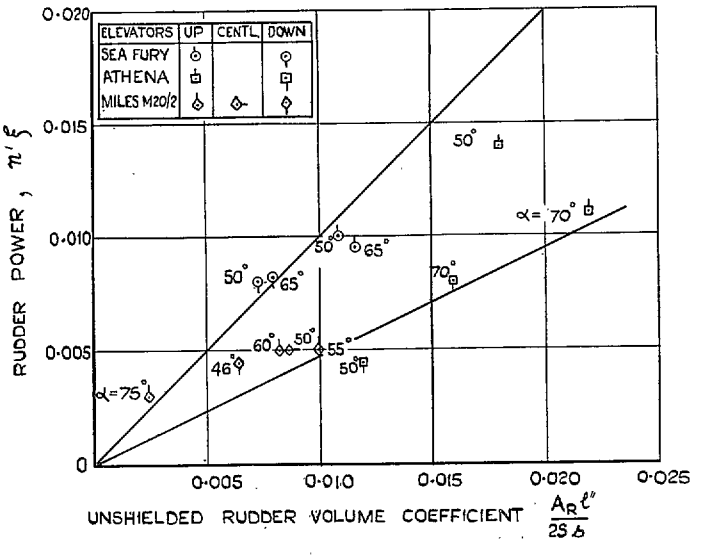

FIG. 3.16. Rudder power in free model spins.

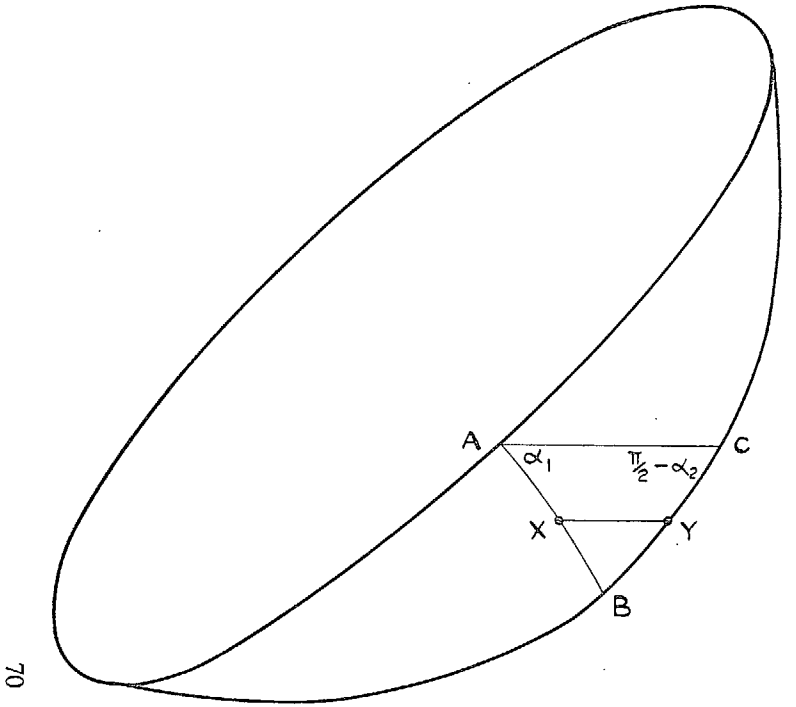

FIG. 4.1. Combination of successive rotations.

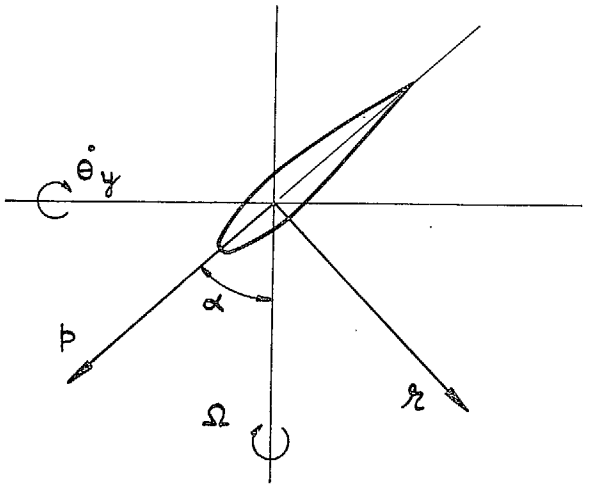

FIG. 4.2. Components of angular velocity in the plane of symmetry.

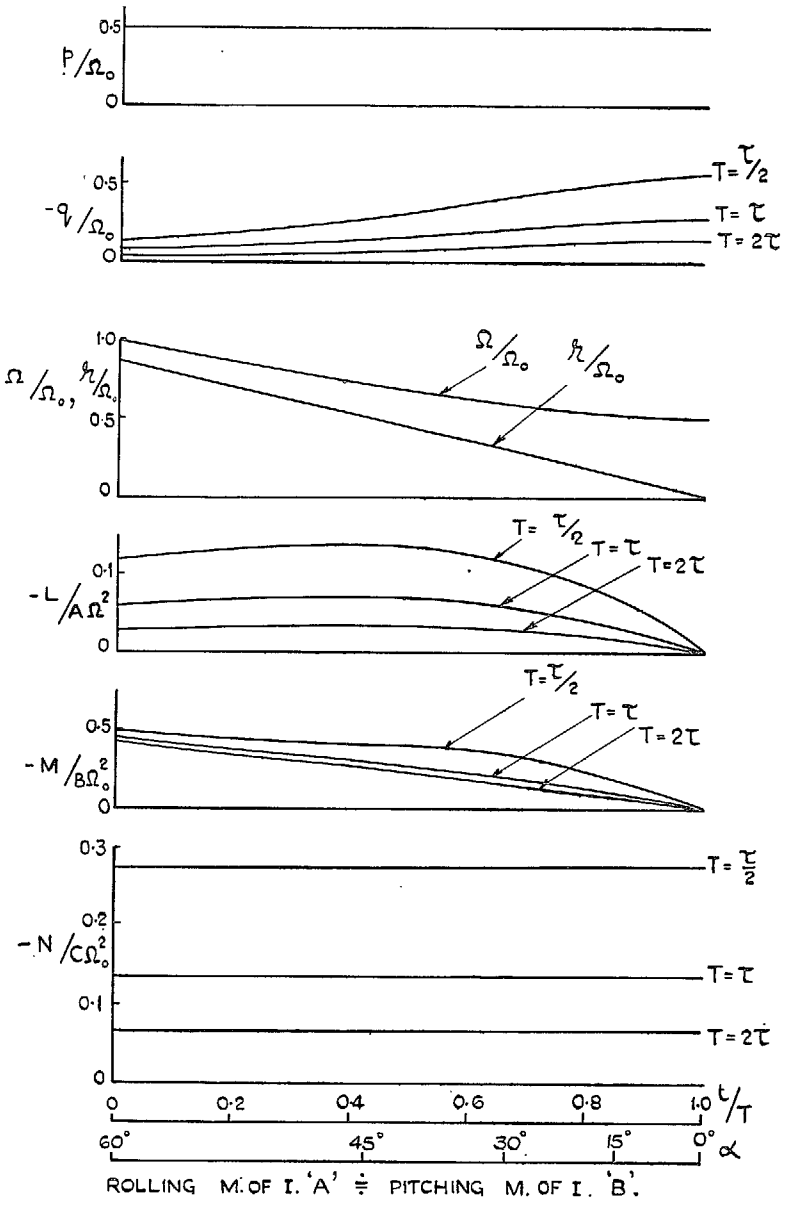

FIG. 4.3. Kinetics of recovery from 60-deg spin, with wings level, Case I : p constant, r varies linearly.

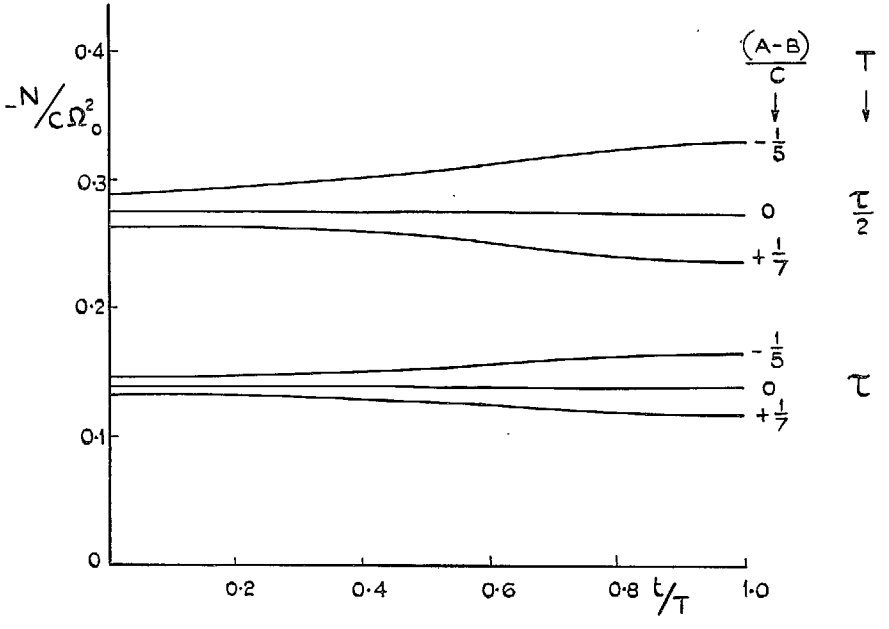

FIG. 4.4. Effect of mass distribution on kinetics of recovery with wings level, Case I.

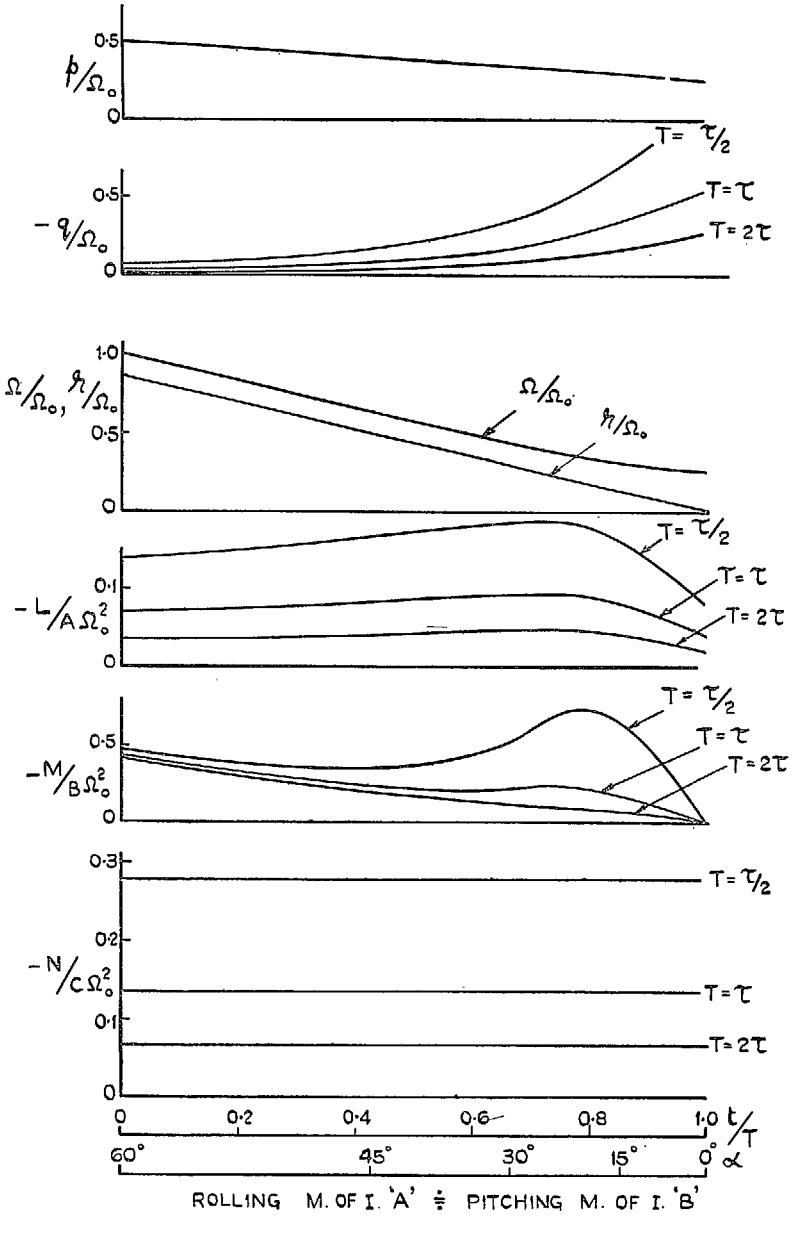

FIG. 4.5. Kinetics of recovery from 60-deg spin, with wings level, Case II : p and r both vary linearly.

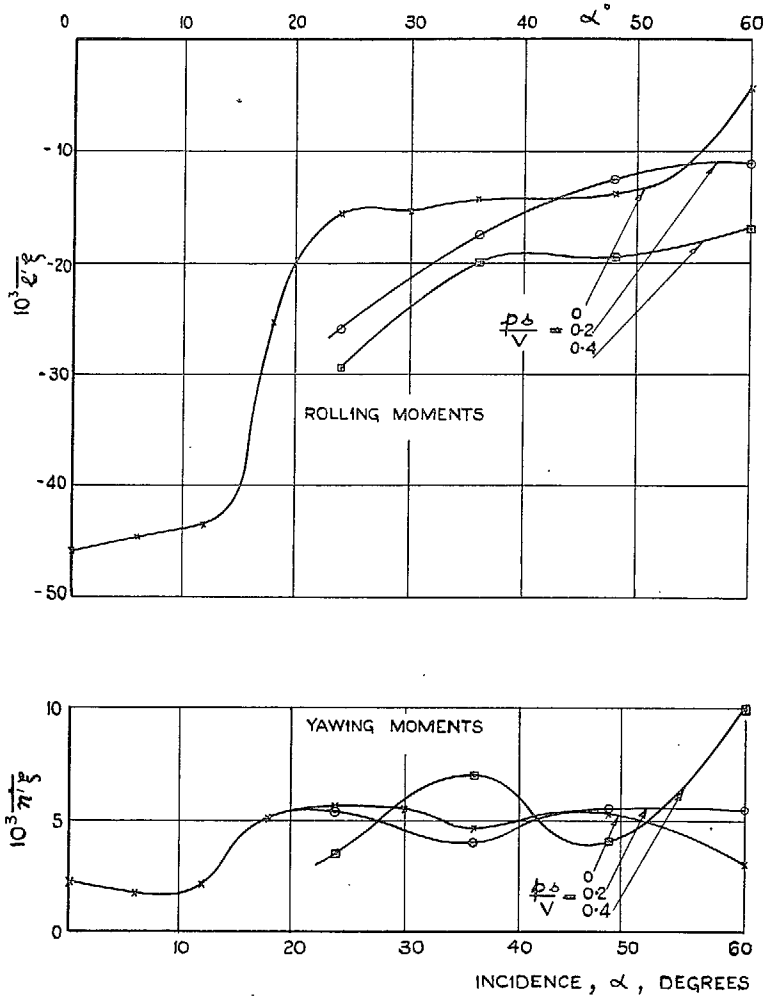

FIG. 4.6. Rolling and yawing moments about chord axes due to ailerons. Extracted from R. & M. 1501. Aileron angle ±10 deg, port aileron up.

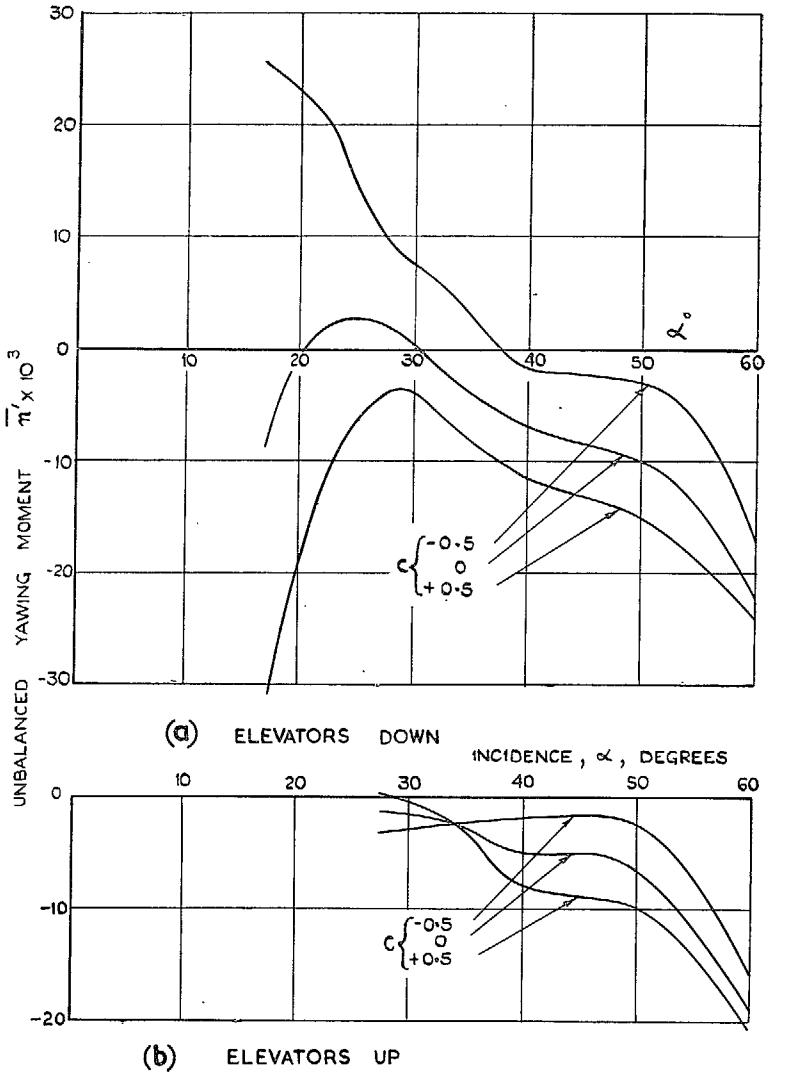

FIGS. 4.7a and 4.7b. Balance of yawing moments (rudder central).

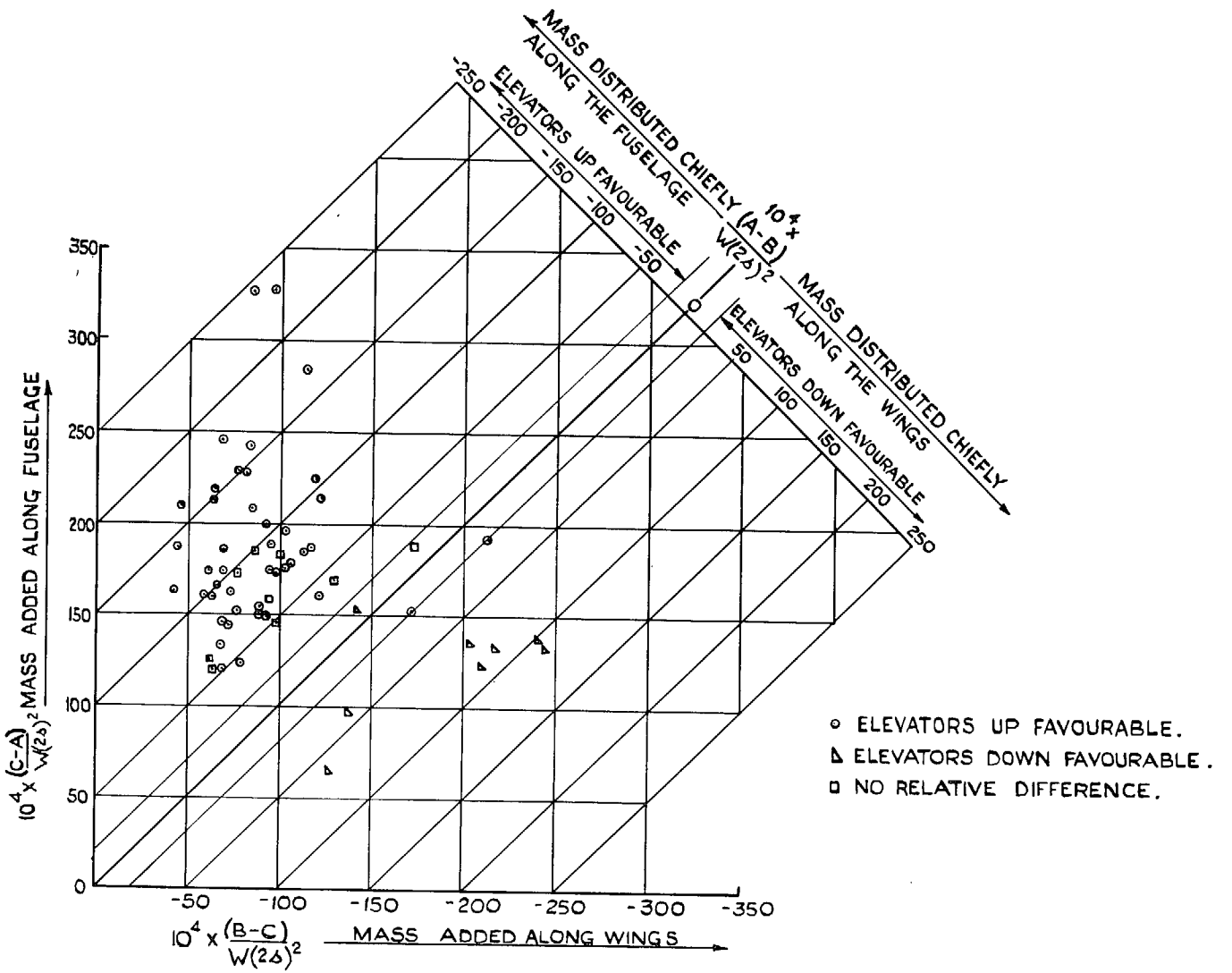

FIG. 4.8. Prediction of elevator effect during recovery by use of mass parameter. (From Ref. 9.)

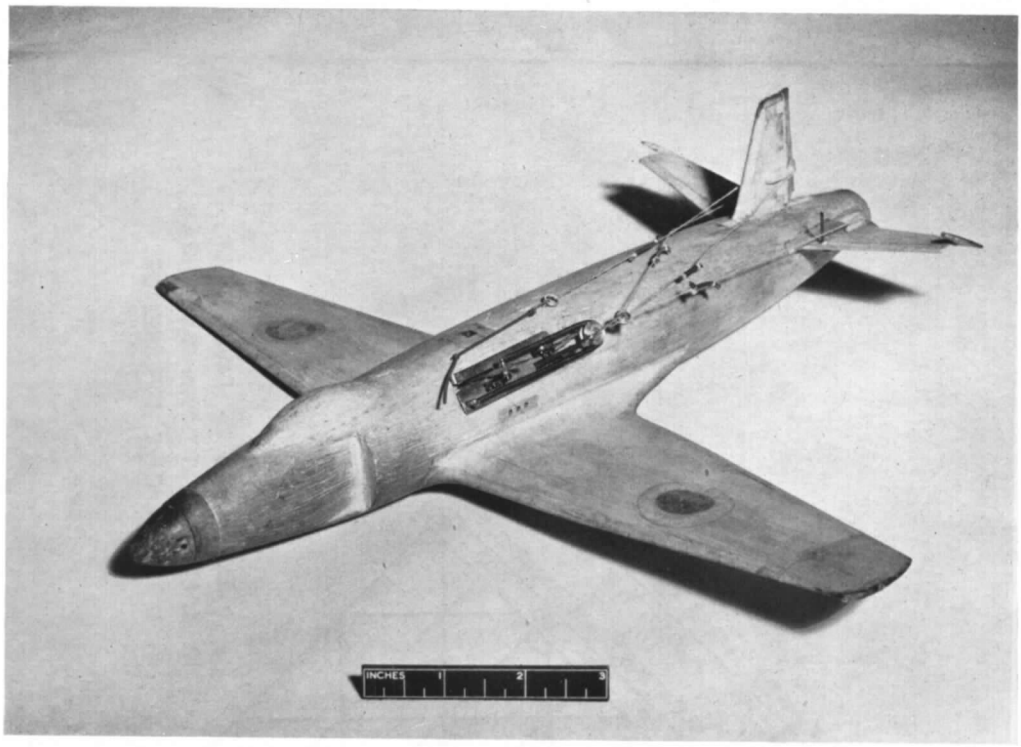

FIG. 4.9a. Model with single release mechanism.

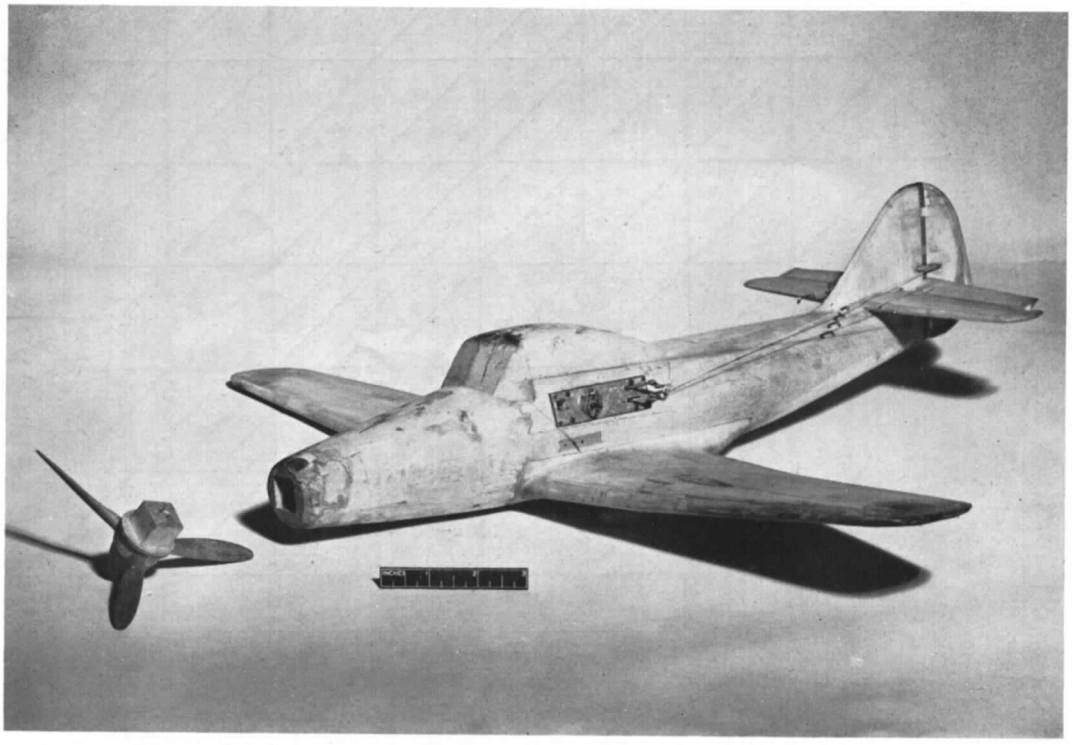

FIG. 4.9b. Model with double release mechanism.

FIG. 4.9. Delay mechanisms for operating the controls on spinning models.

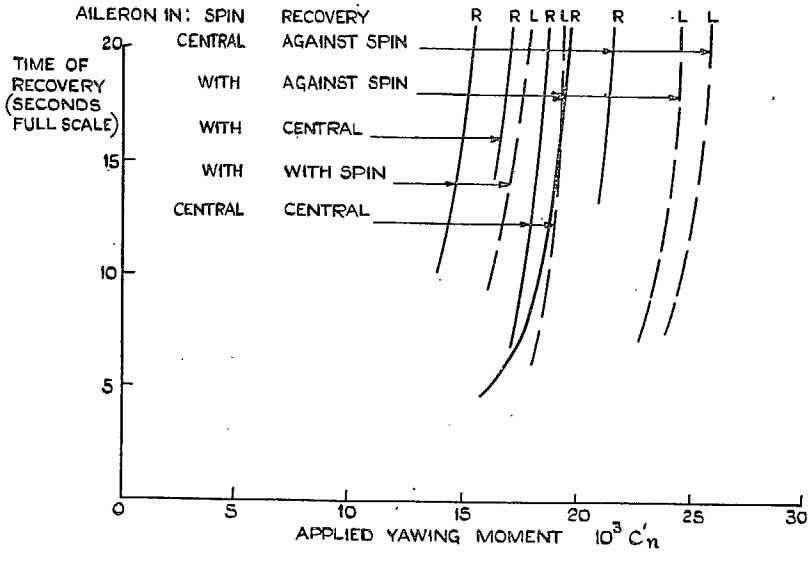

FIG. 4.10. Effect of using ailerons: *Typhoon.*

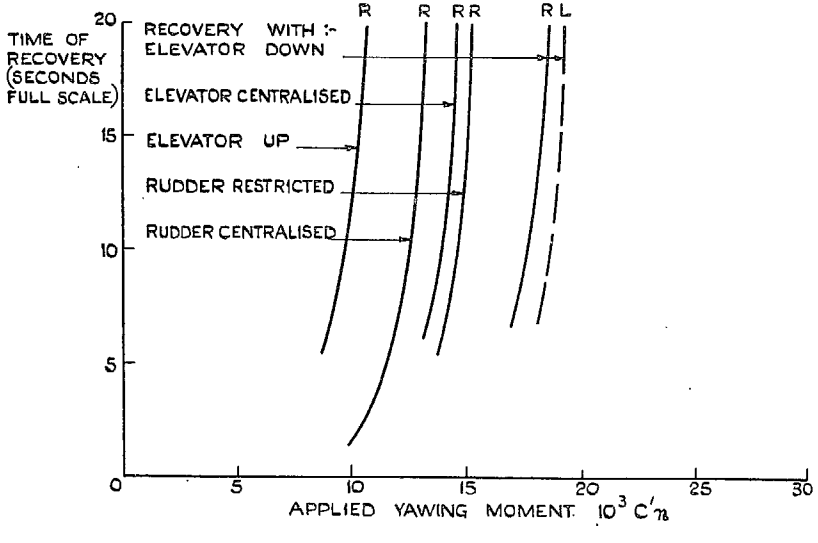

FIG. 4.11. Effect of different use of rudder and elevator: *Typhoon.*

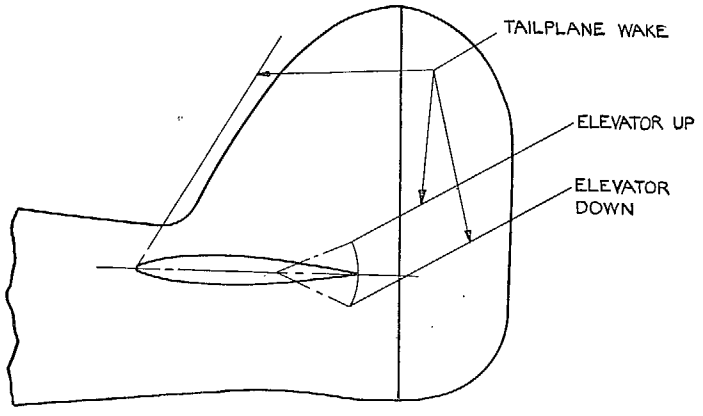

FIG. 4.12a. *Typhoon.*

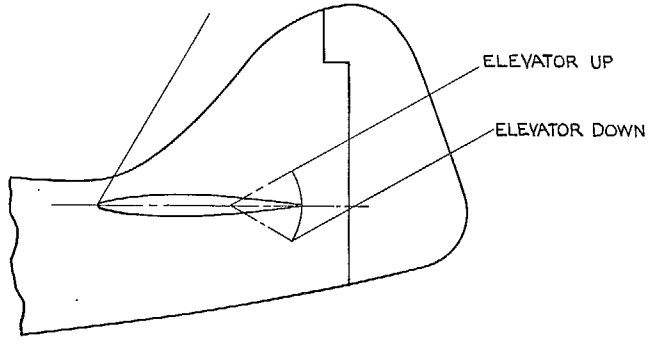

FIG. 4.12b. *Firefly.*

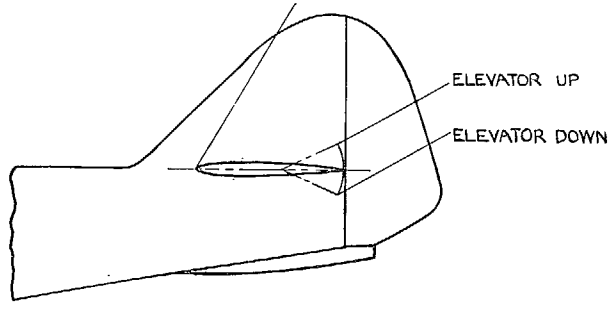

FIG. 4.12c. *Athena.*

FIGS. 4.12a, 4.12b and 4.12c. Shielding effects of elevators.

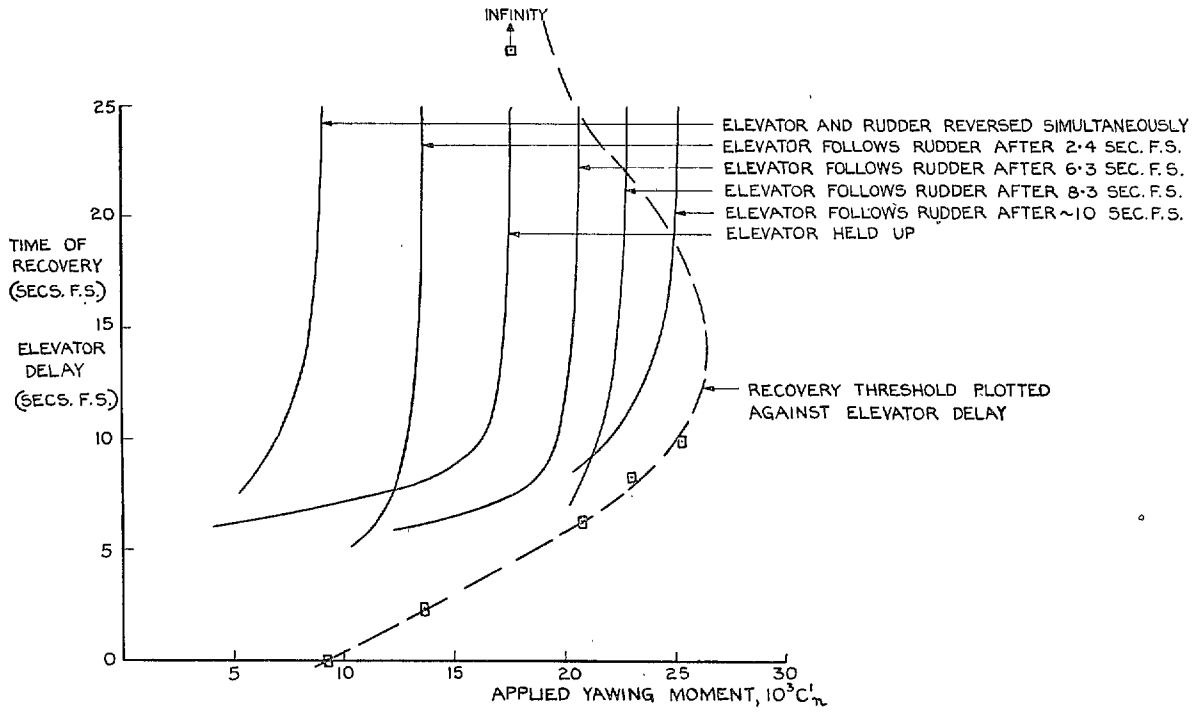

FIG. 4.13. Effect on recovery of delaying elevator reversal: *Firefly*.

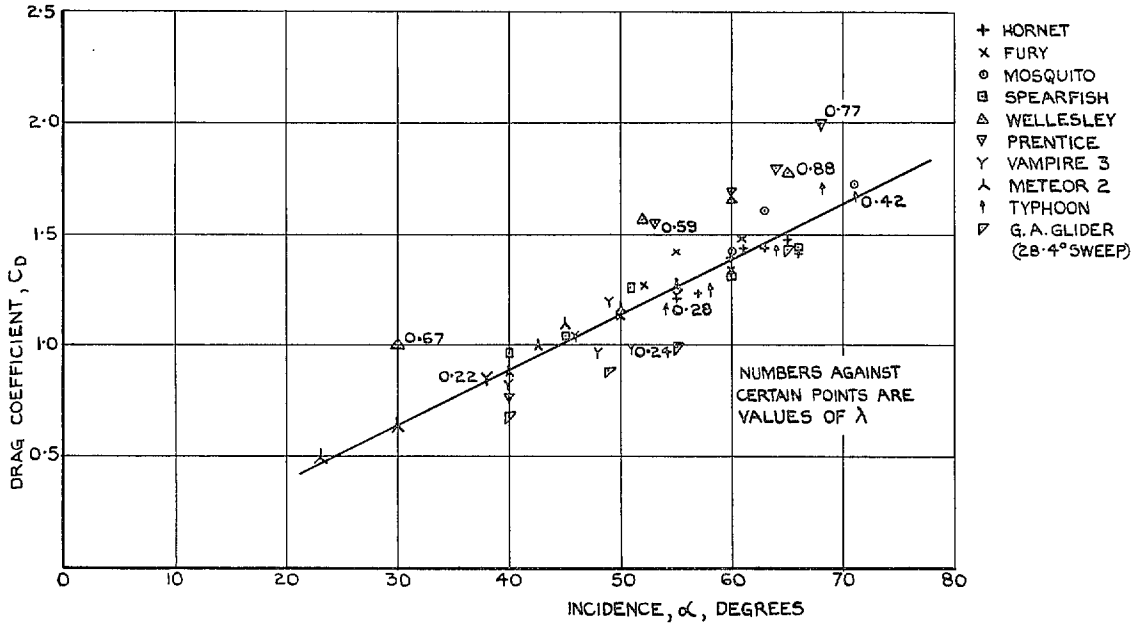

FIG. 5.1. Variation of measured drag coefficients on spinning models.

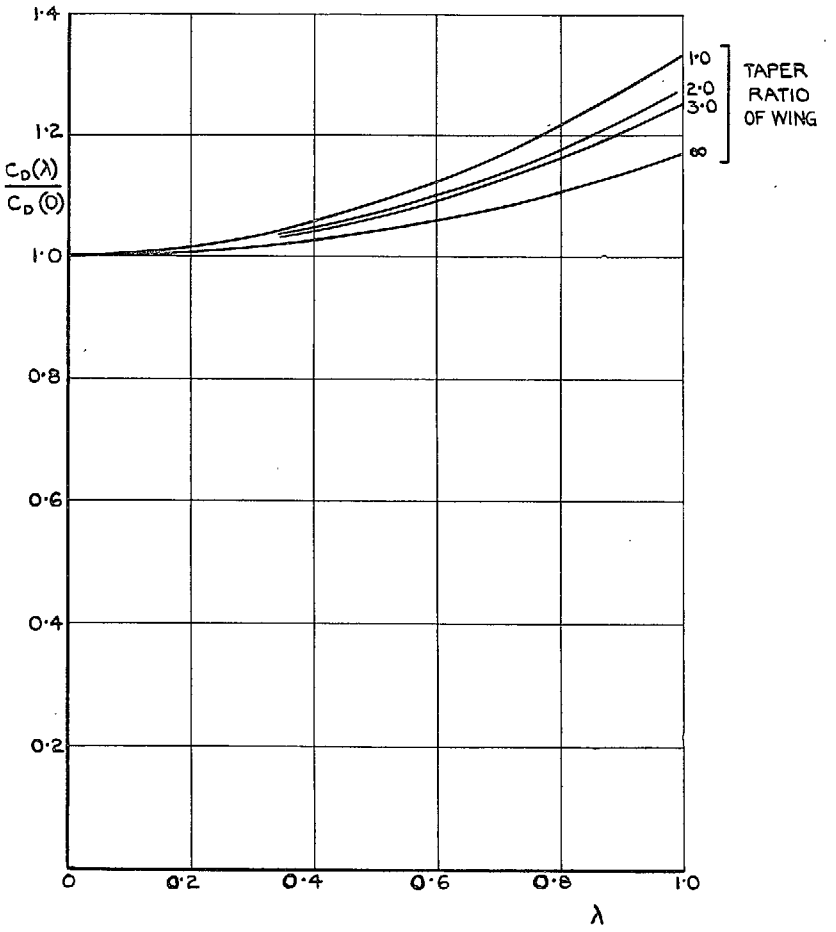

FIG. 5.3. Calculation from strip theory of drag of wings as affected by rotation.

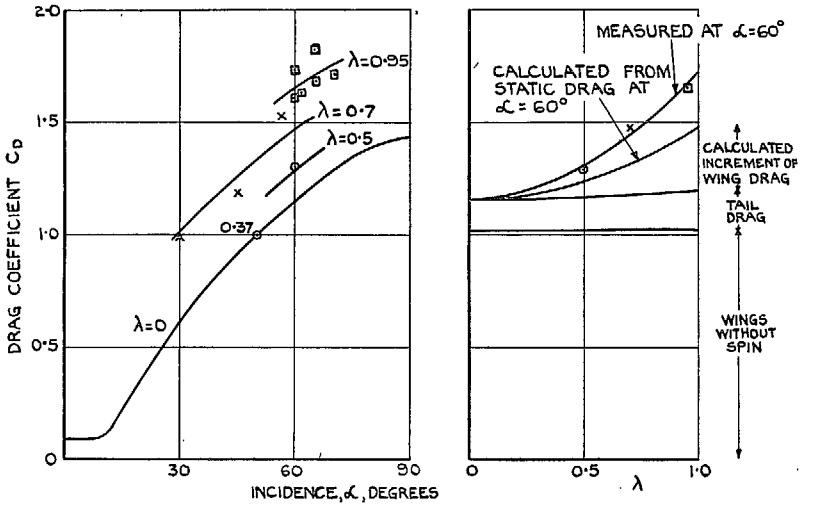

FIG. 5.4. Drag of *Wellesley* model as affected by rotation.

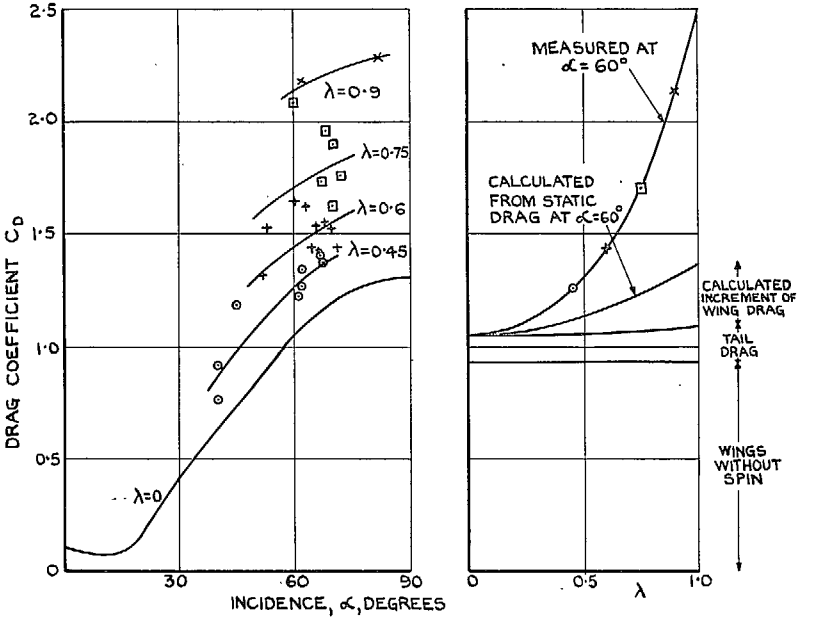

FIG. 5.5. Drag of *Prentice* model as affected by rotation.

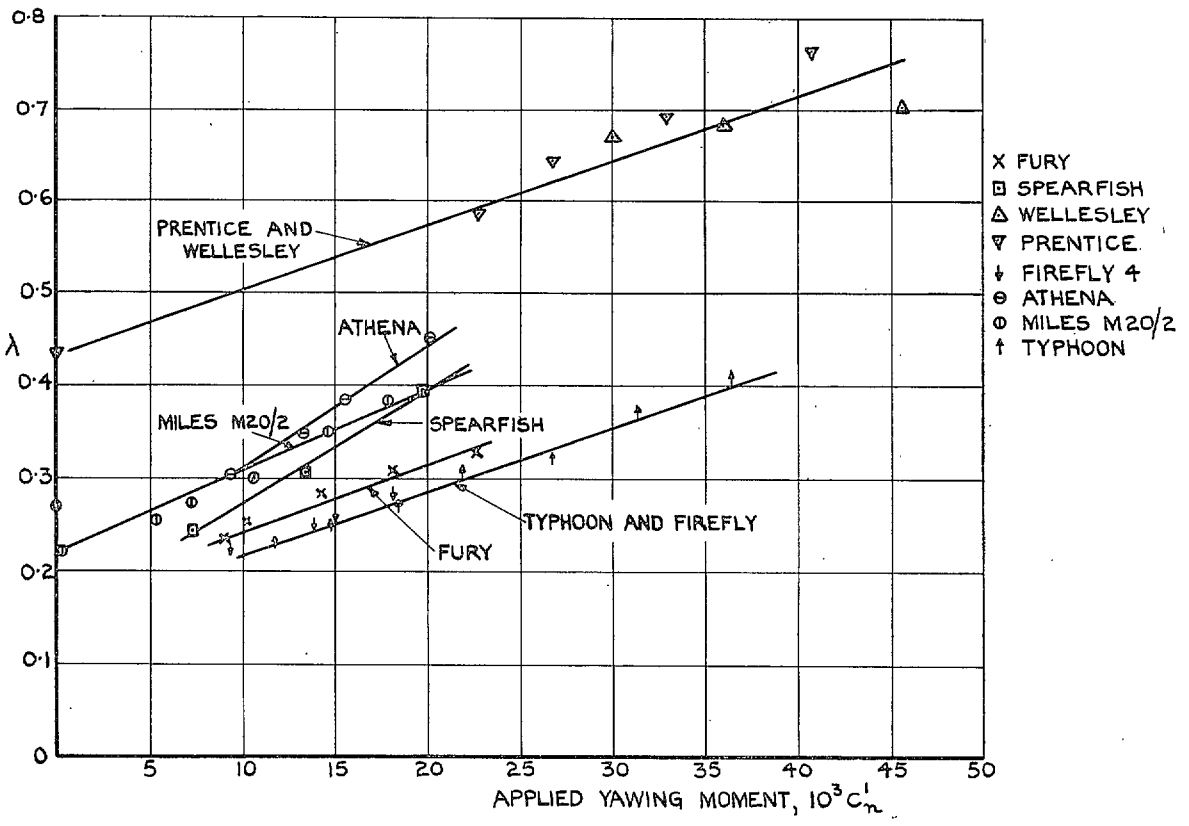

FIG. 5.6. Variation of $\lambda = \Omega s/V$ with applied yawing moment: single-engined models.

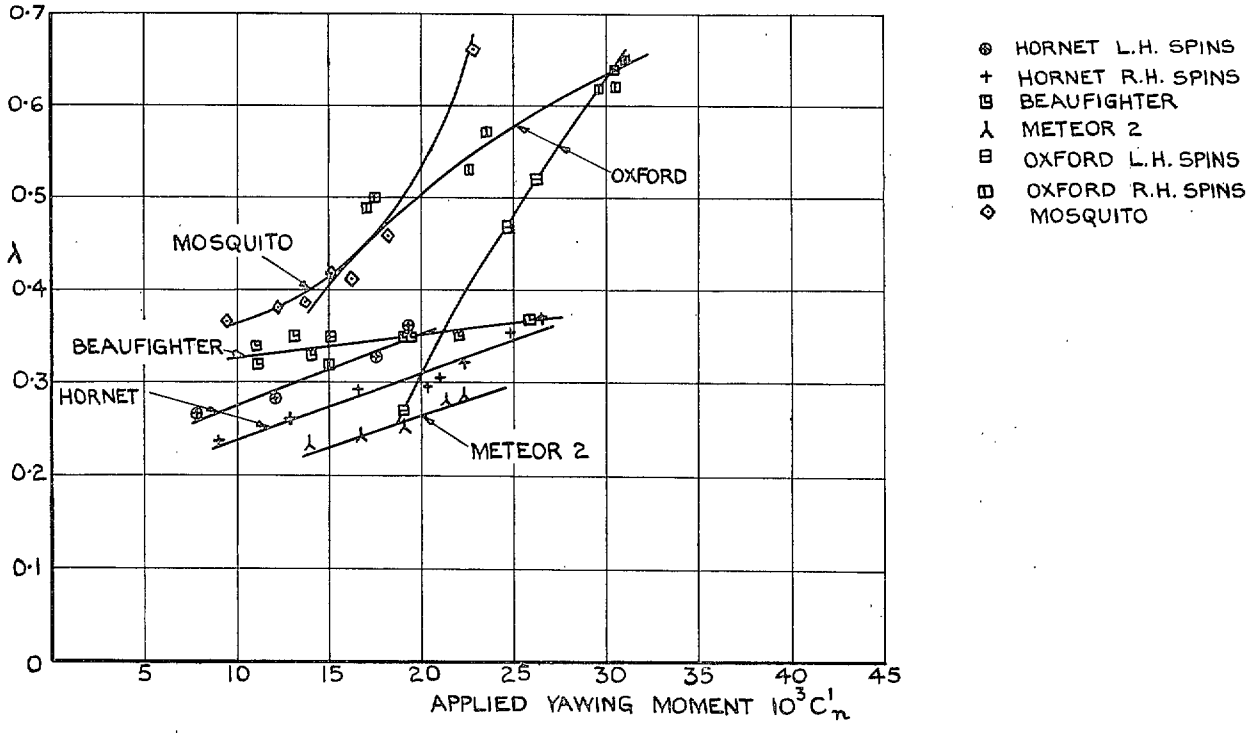

FIG. 5.7. Variation of $\lambda = \Omega s/V$ with applied yawing moment: twin-engined models.

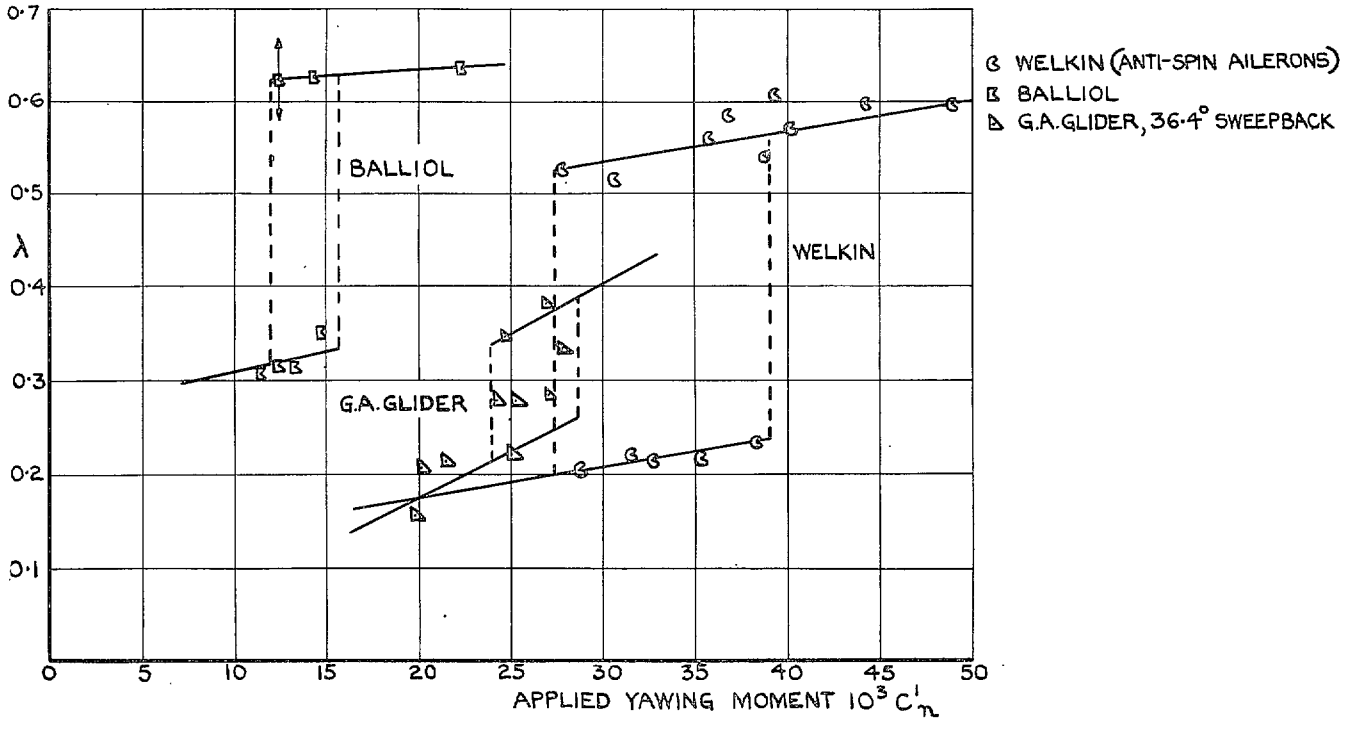

FIG. 5.8. Variation of $\lambda = \Omega s/V$ with applied yawing moment: some discontinuous results.

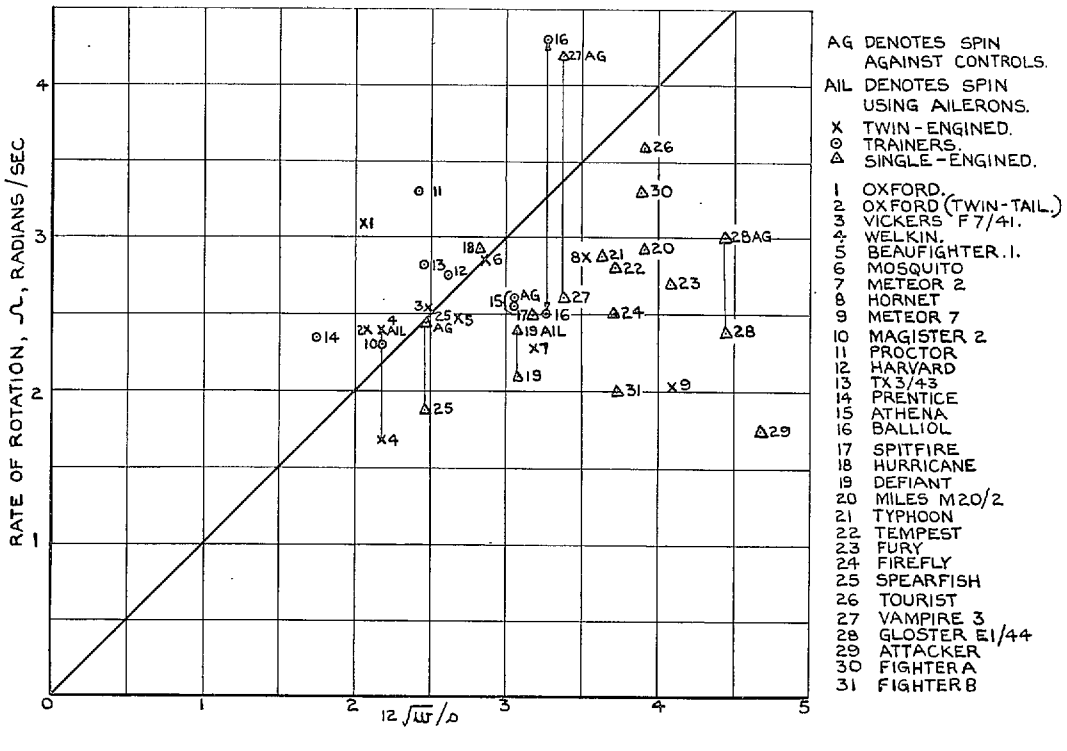

FIG. 5.9. Variation of rate of rotation with wing loading and span.

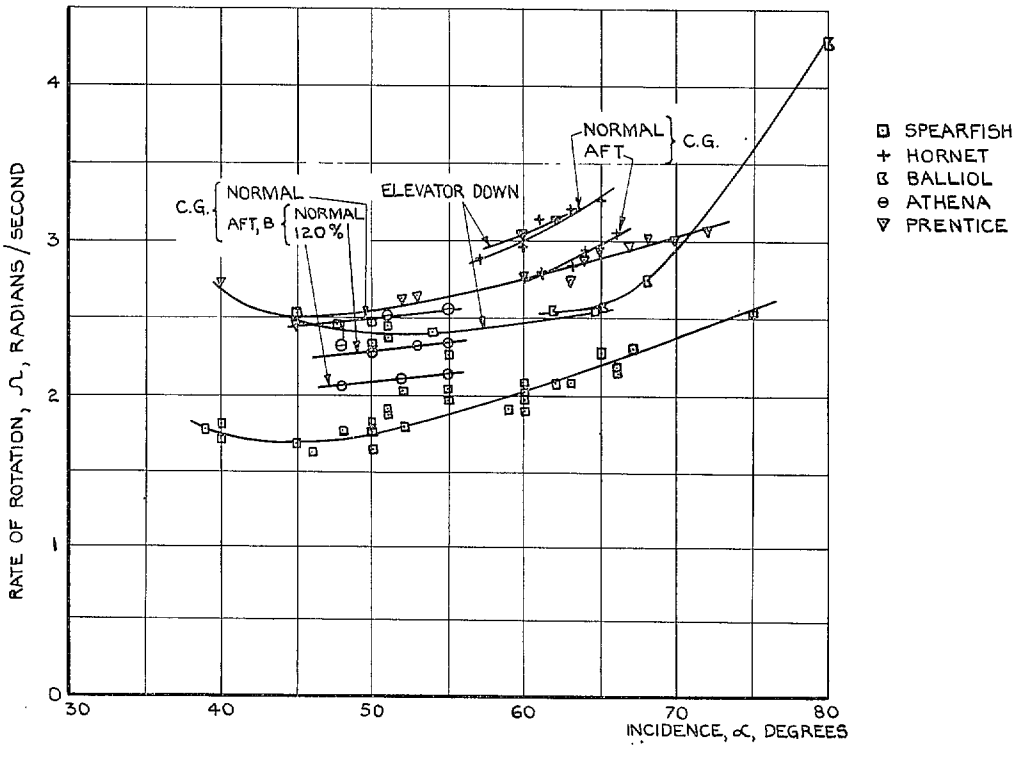

FIG. 5.10. Variation of rate of rotation with incidence.

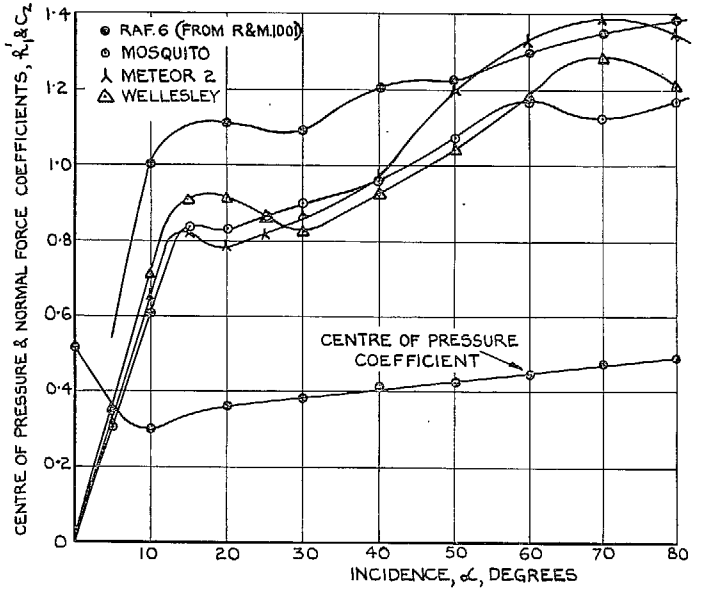

FIG. 5.11. Centre of pressure and normal-force coefficients on models without rotation.

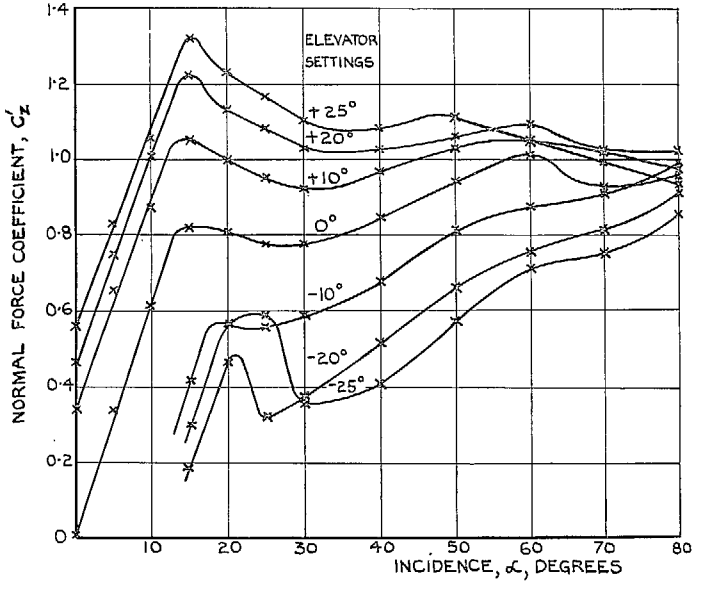

FIG. 5.12. Normal-force coefficients of tailplane: no fuselage.

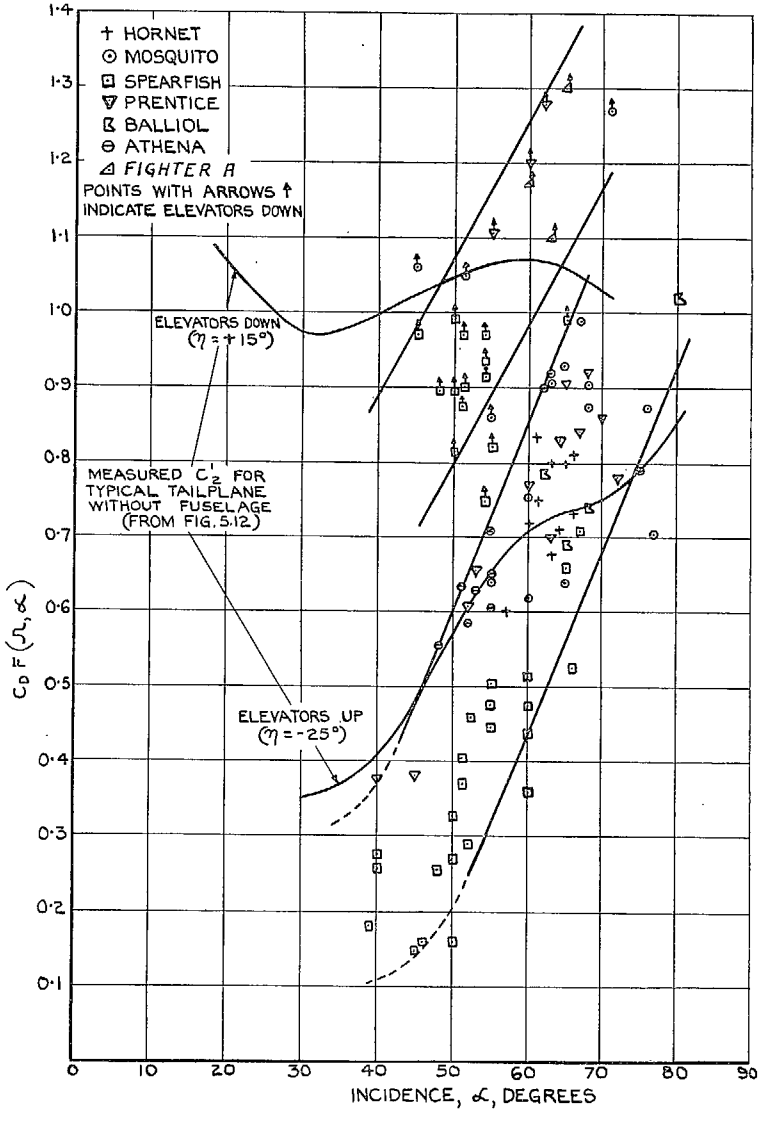

FIG. 5.13. Tailplane normal-force coefficients as estimated from measurements on free model spins.

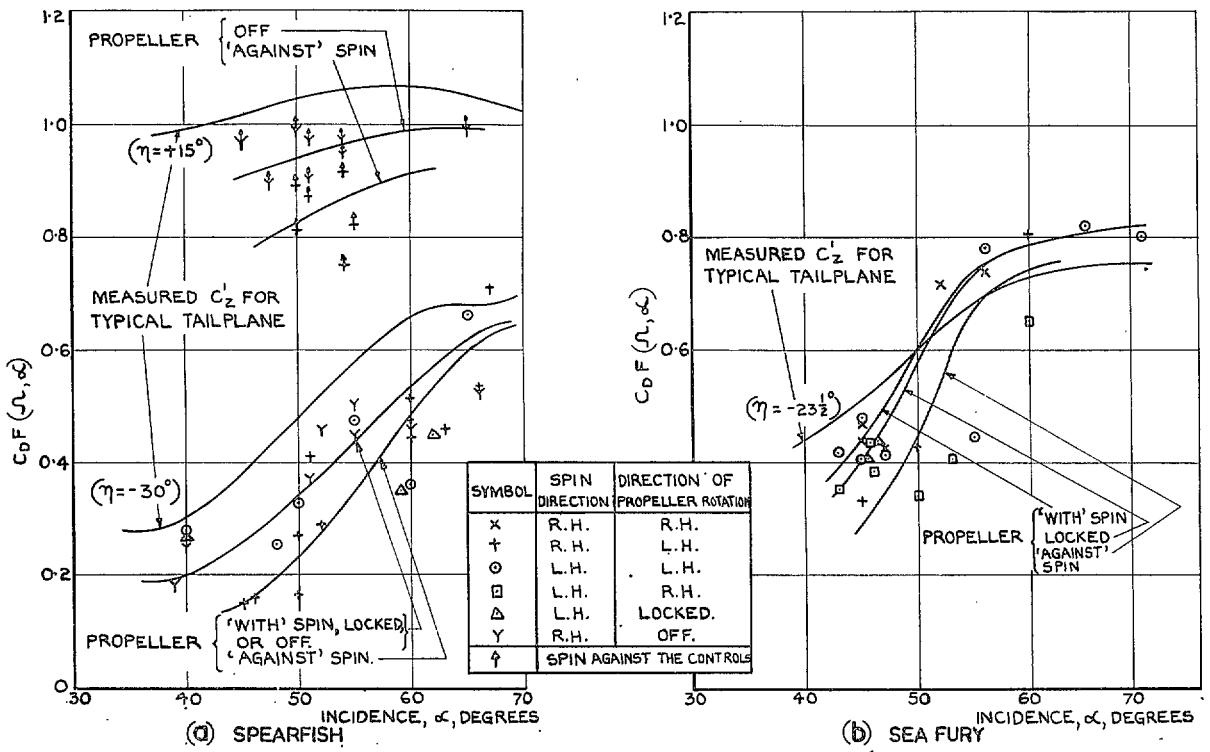

FIG. 5.14. Effect of propellers on estimation of tailplane normal-force coefficients.

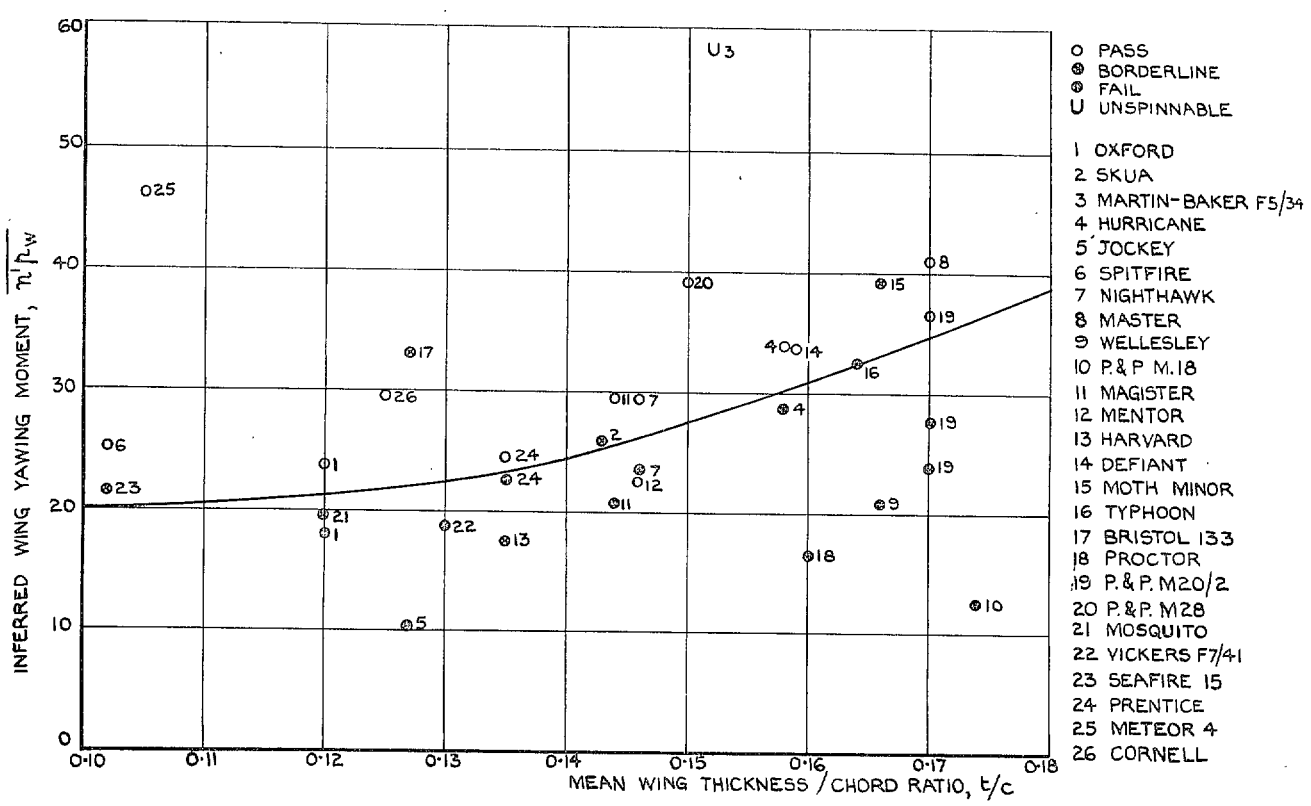

FIG. 6.1. Suggested criterion for recovery, based on wing characteristics.

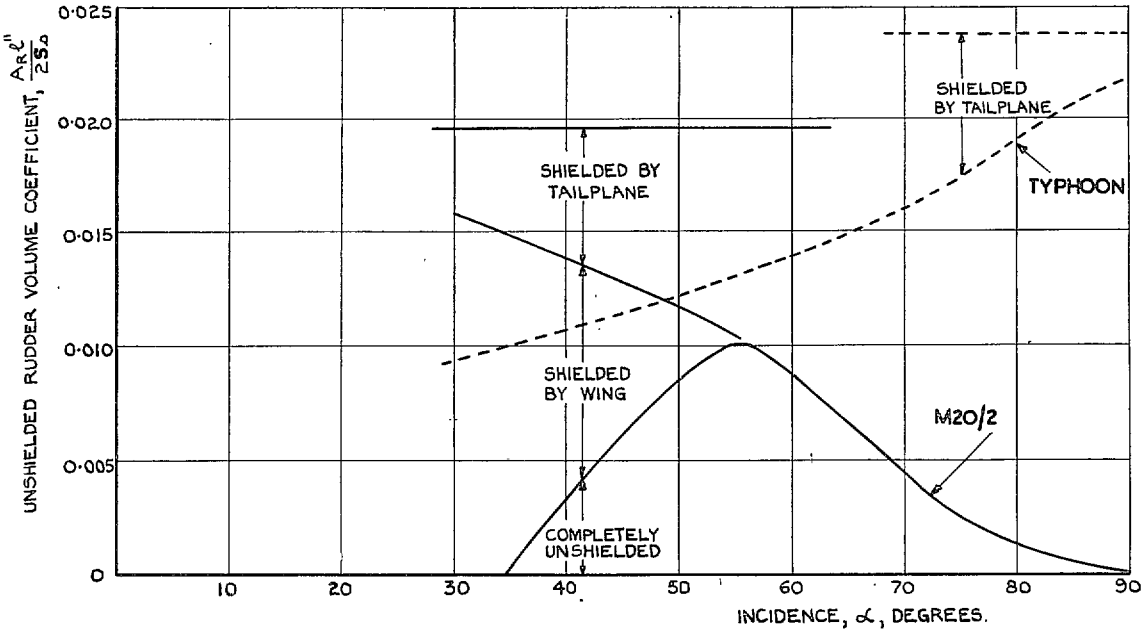

FIG. 6.2. Shielding effects of wings and tailplane on rudder.

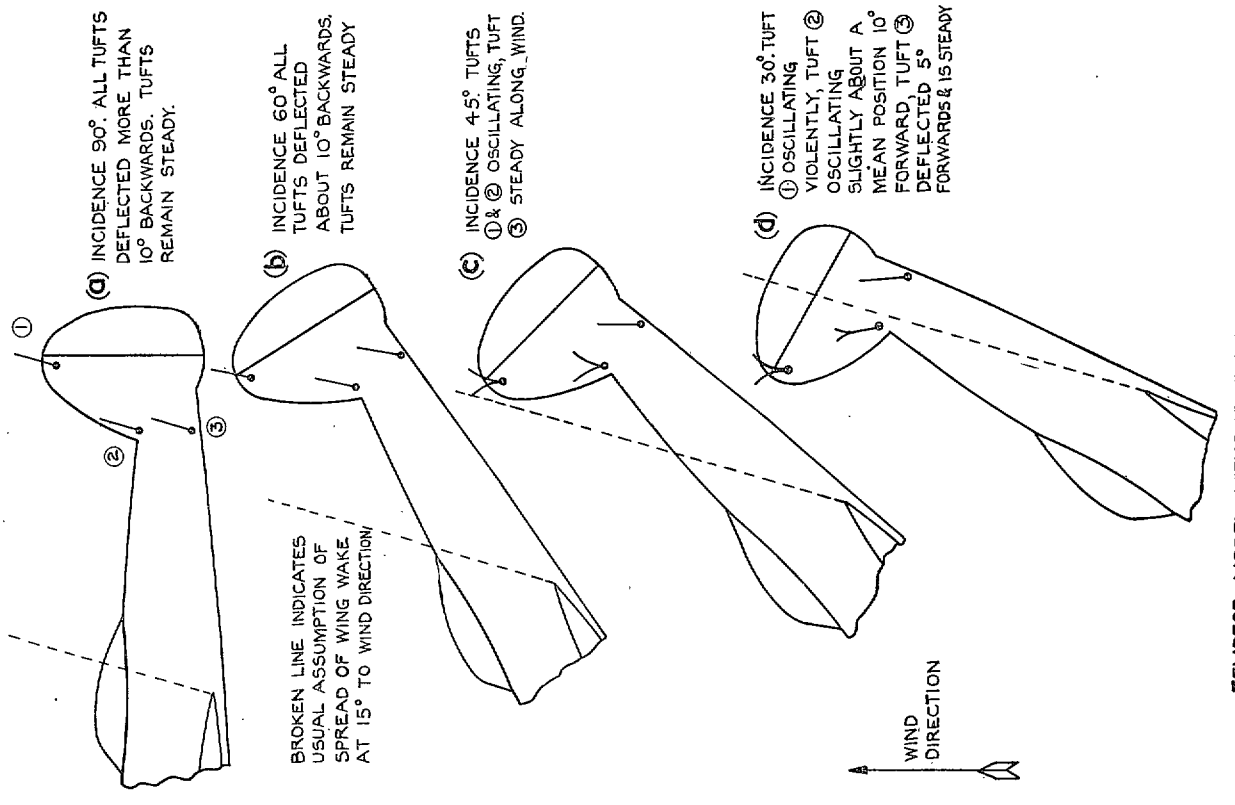

FIG. 6.3. Influence of wing wake on direction of flow over tail unit.

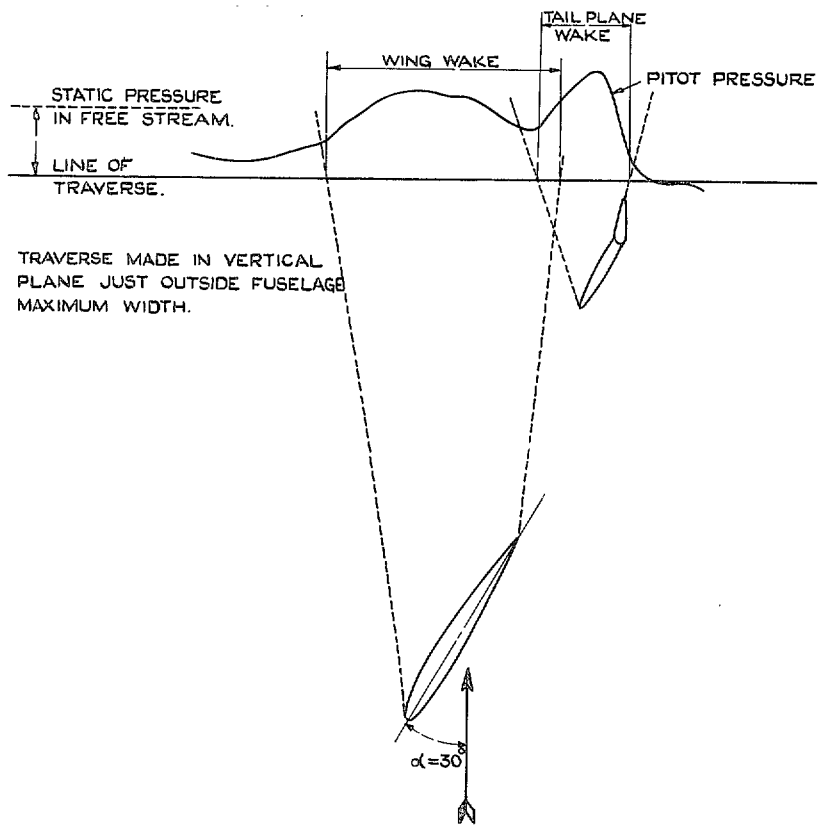

FIG. 6.4. Pitot traverse across wake: Fighter A.

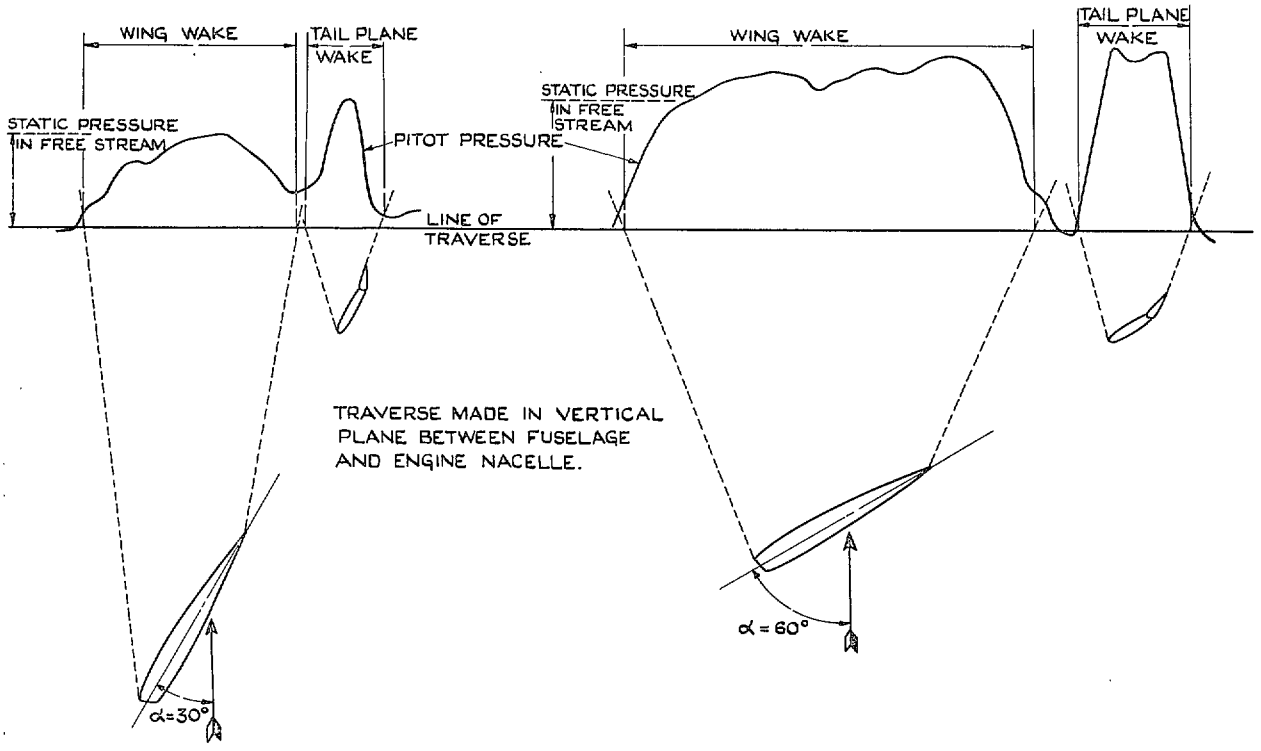

FIG. 6.5. Pitot traverses across wake: *Mosquito*.

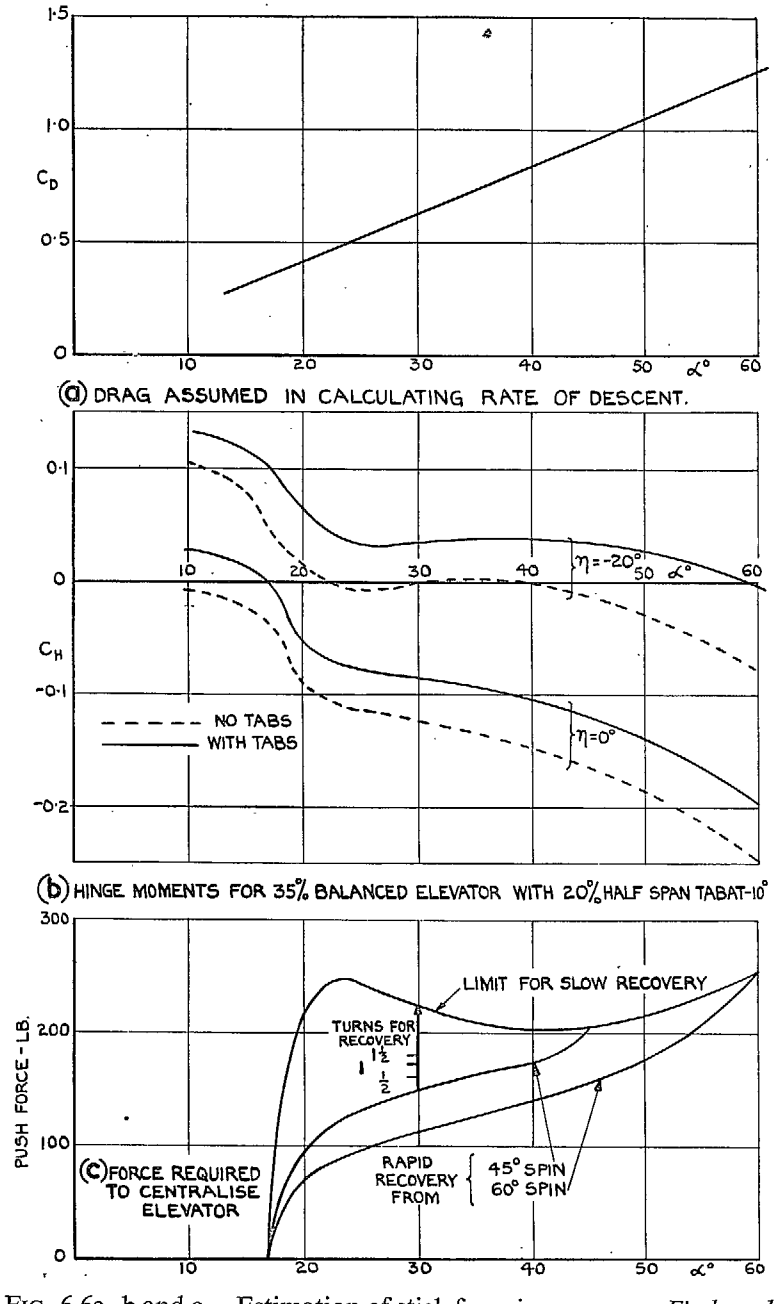

FIG. 6.6a, b and c. Estimation of stick force in recovery : *Firebrand.*

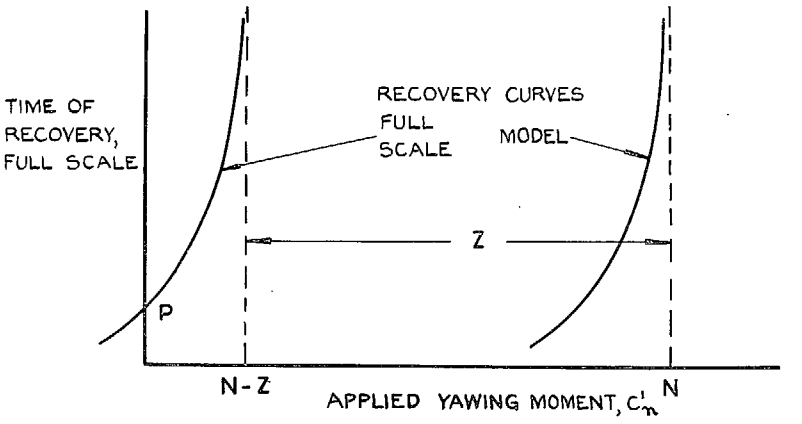

FIG. 7.1. Sketch showing relative position of model- and full-scale recovery curves.

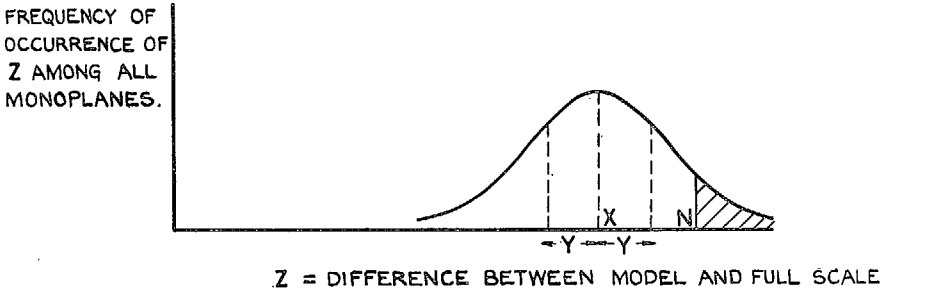

FIG. 7.2. Distribution of various values of Z among different types (theoretical).

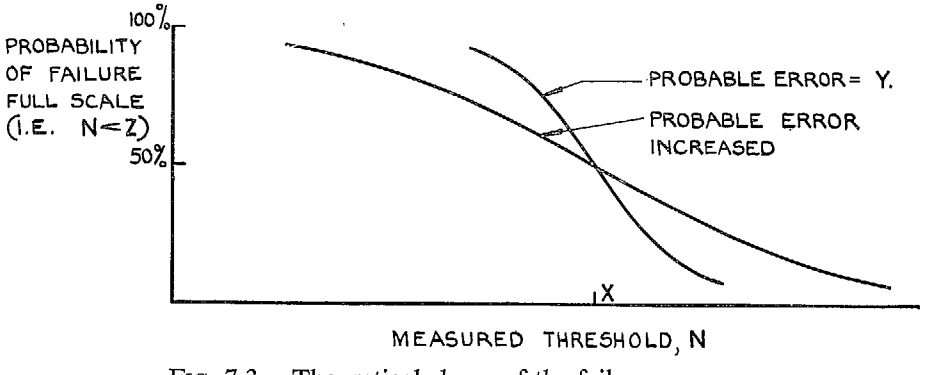

FIG. 7.3. Theoretical shape of the failure curve.

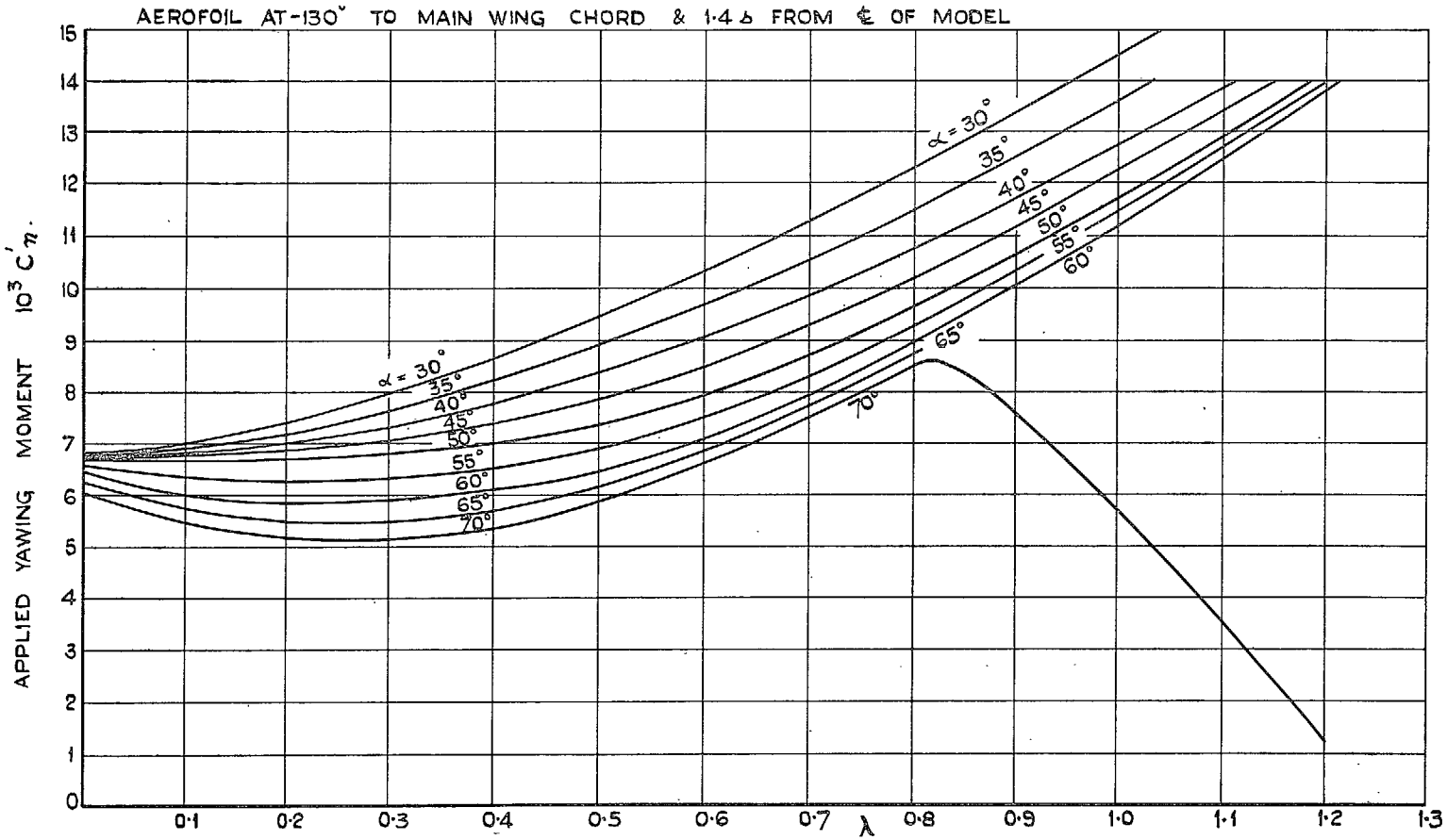

FIG. 7.4. Yawing moment applied by vane of area 0·01 × model wing area.

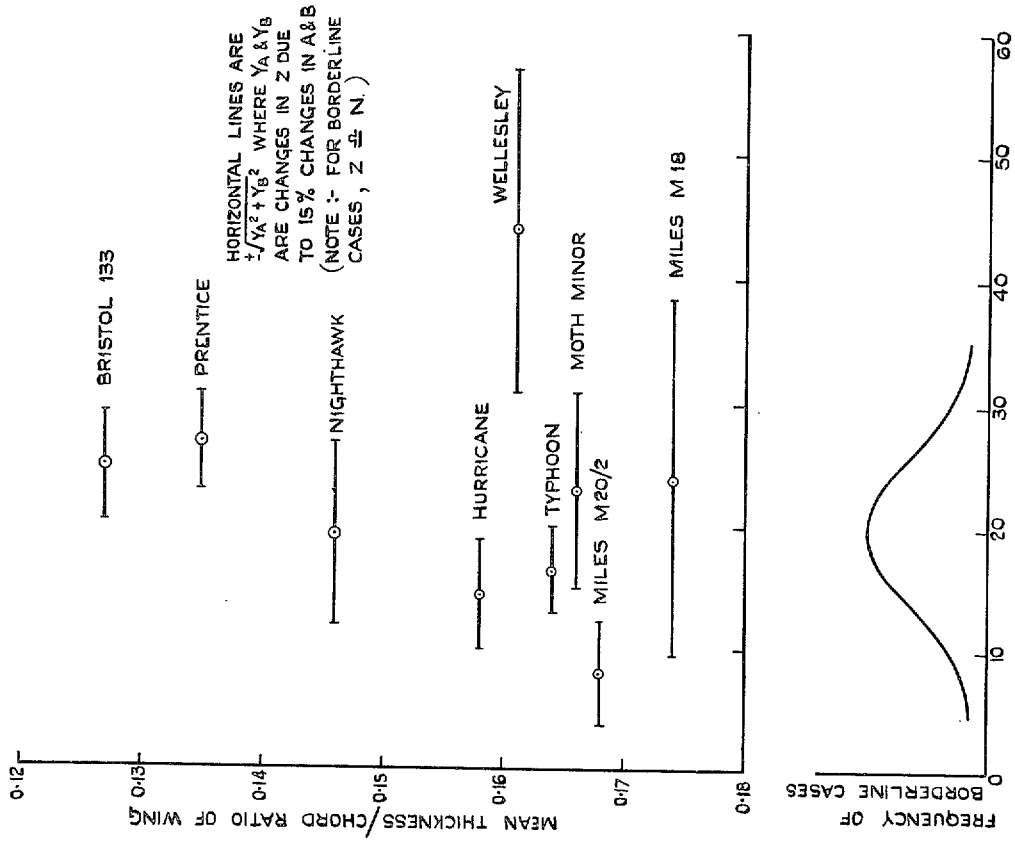

FIG. 7.7. Distribution of borderline cases showing effects of inertia errors.

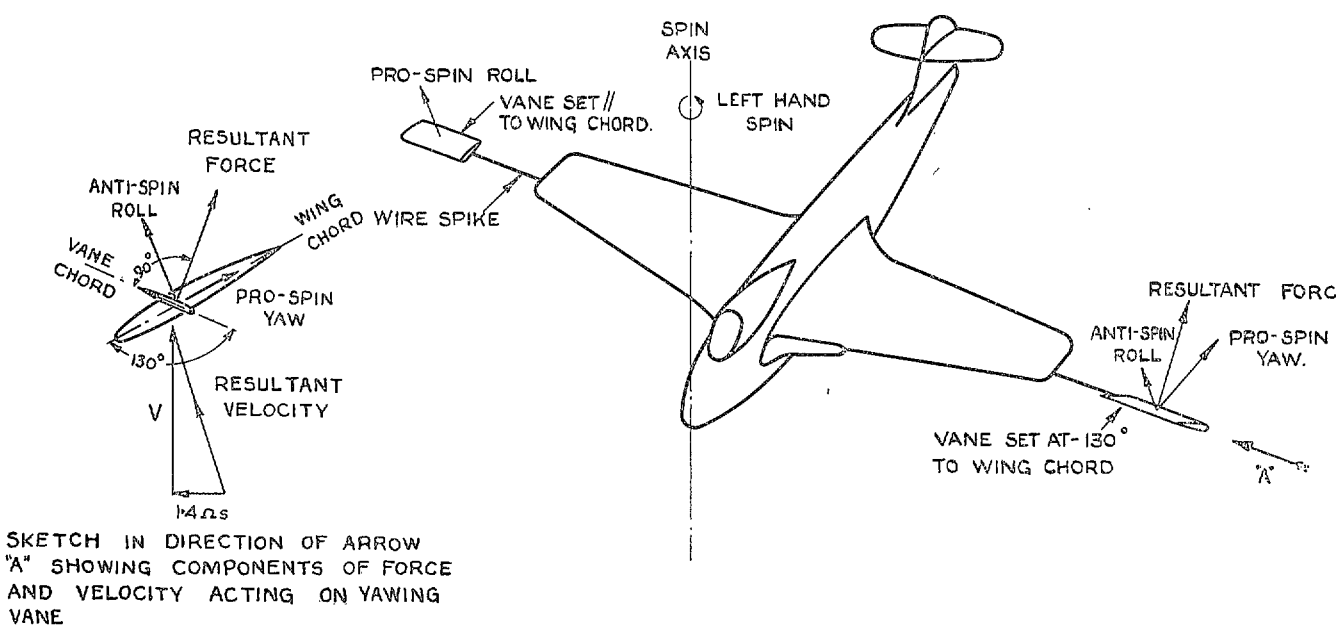

SKETCH IN DIRECTION OF ARROW "A" SHOWING COMPONENTS OF FORCE AND VELOCITY ACTING ON YAWING VANE

FIG. 7.8. Method of applying moments to spinning model.

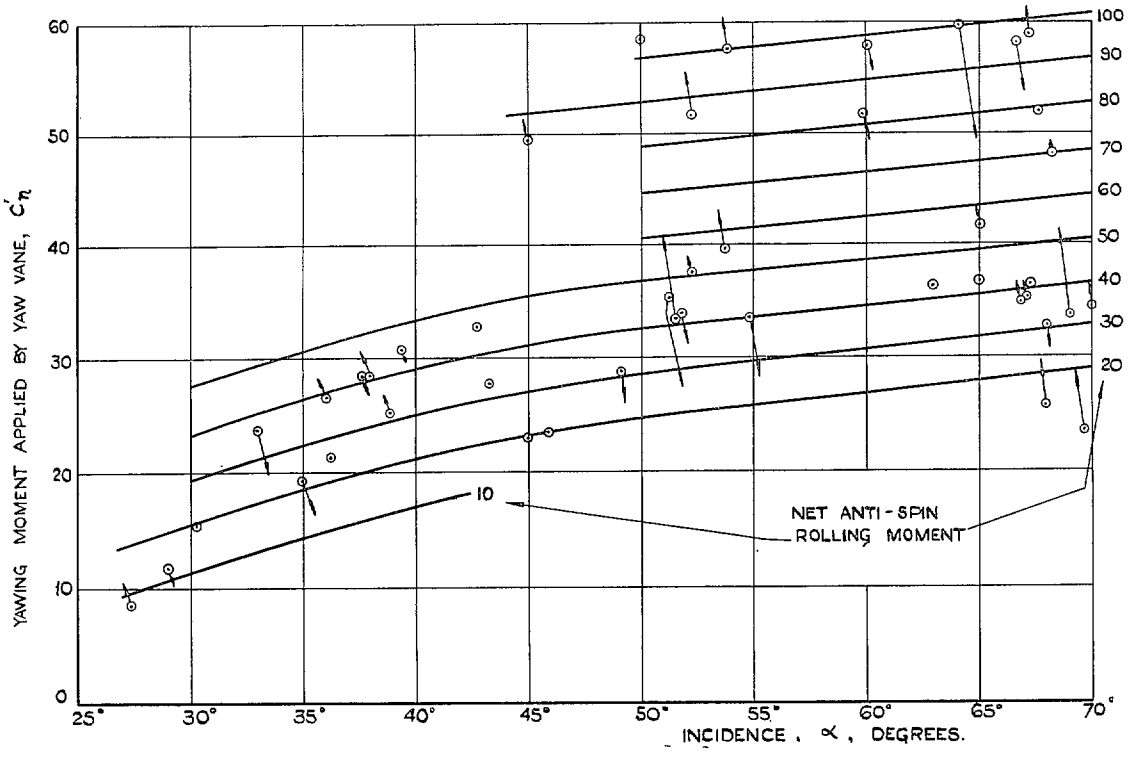

FIG. 7.9. Effect of applied rolling moment on steady free spins : *Wellesley.*

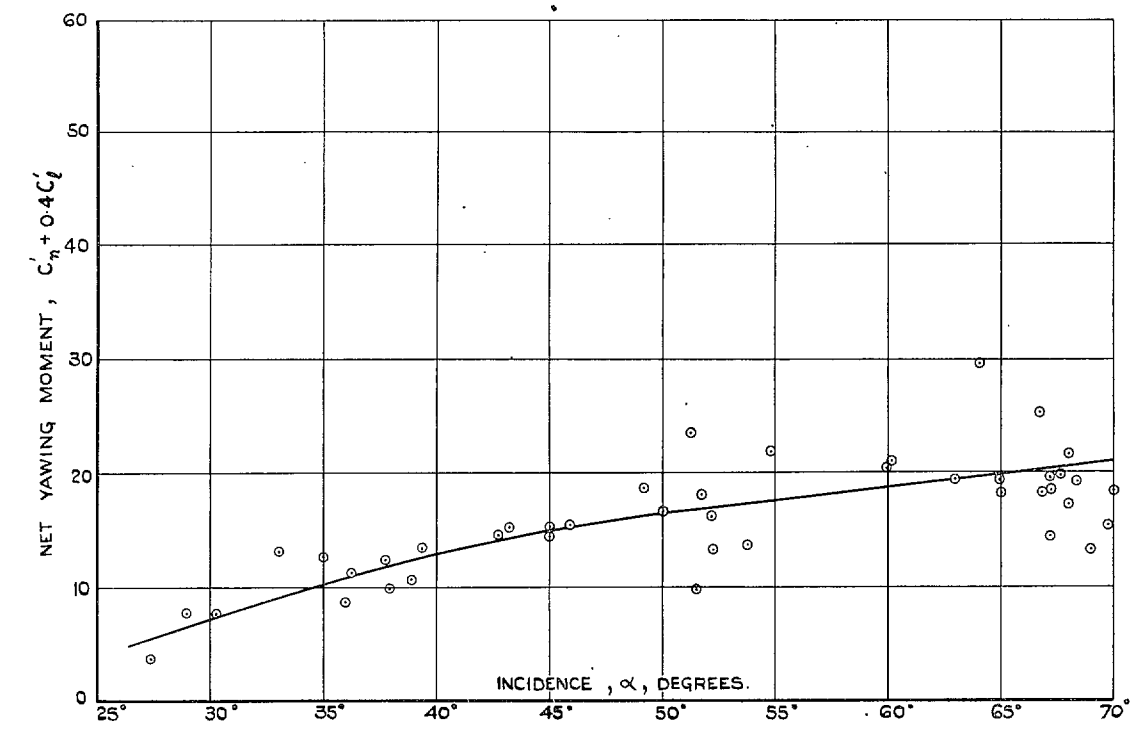

FIG. 7.10. Yawing-moment equivalent of rolling moment in free spins (*cf.* Fig. 7.9.) : *Wellesley.*

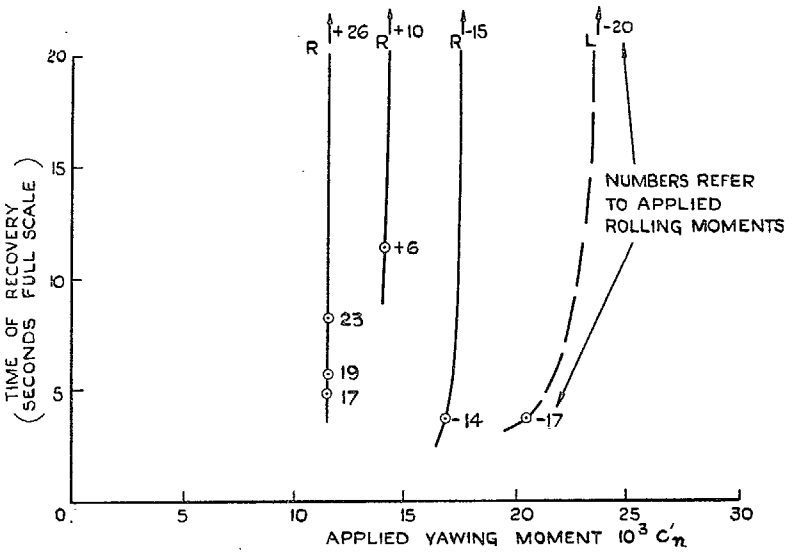

FIG. 7.11. Effect of applied rolling moments on threshold of recovery : *Typhoon.*

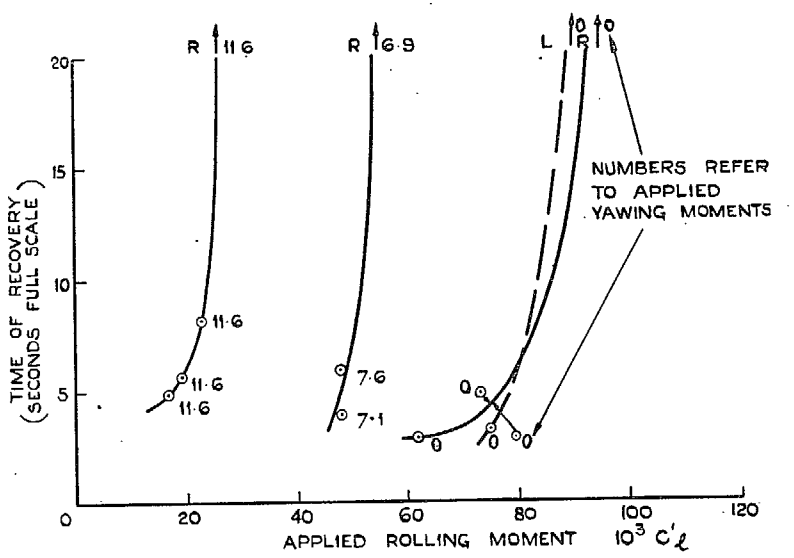

FIG. 7.12. Threshold of recovery in terms of applied rolling moments : *Typhoon.*

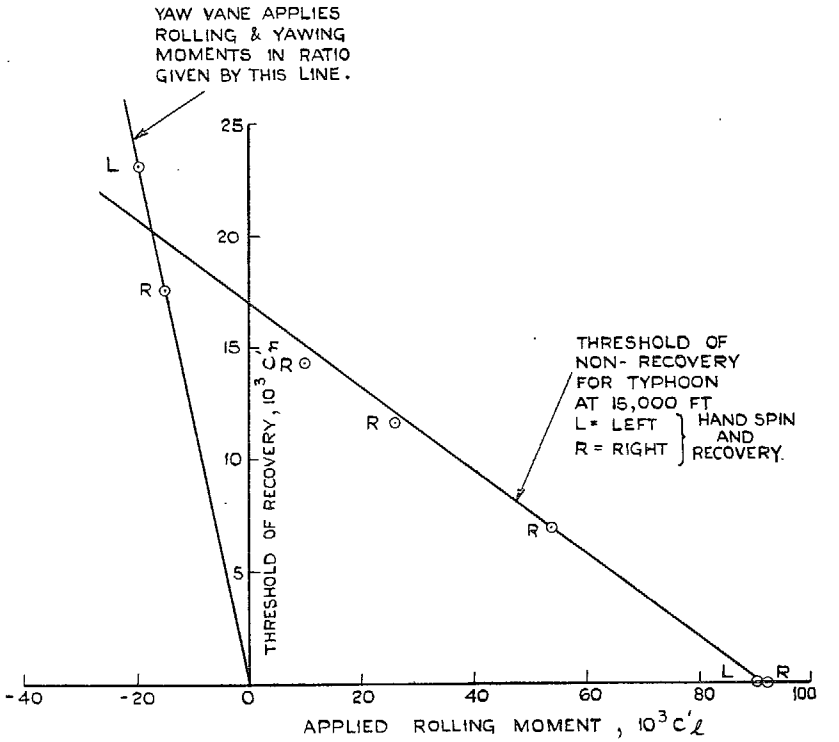

FIG. 7.13. Relation between yawing and rolling moments required to cause non-recovery of the *Typhoon.*

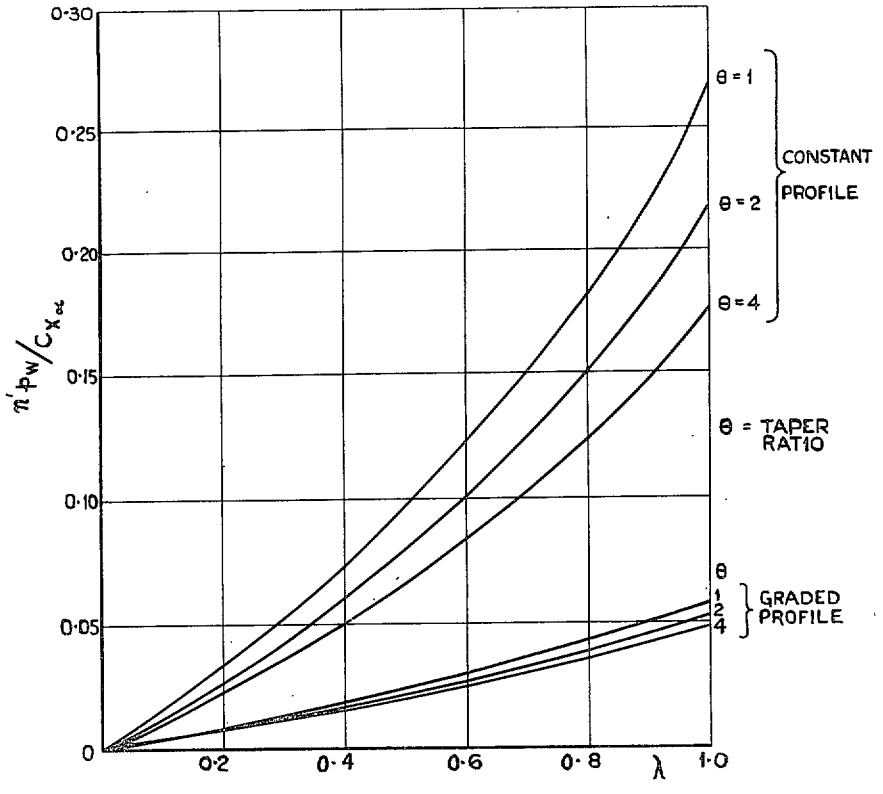

FIG. 7.14. Effect on wing yawing moments of changes of profile and plan-form.

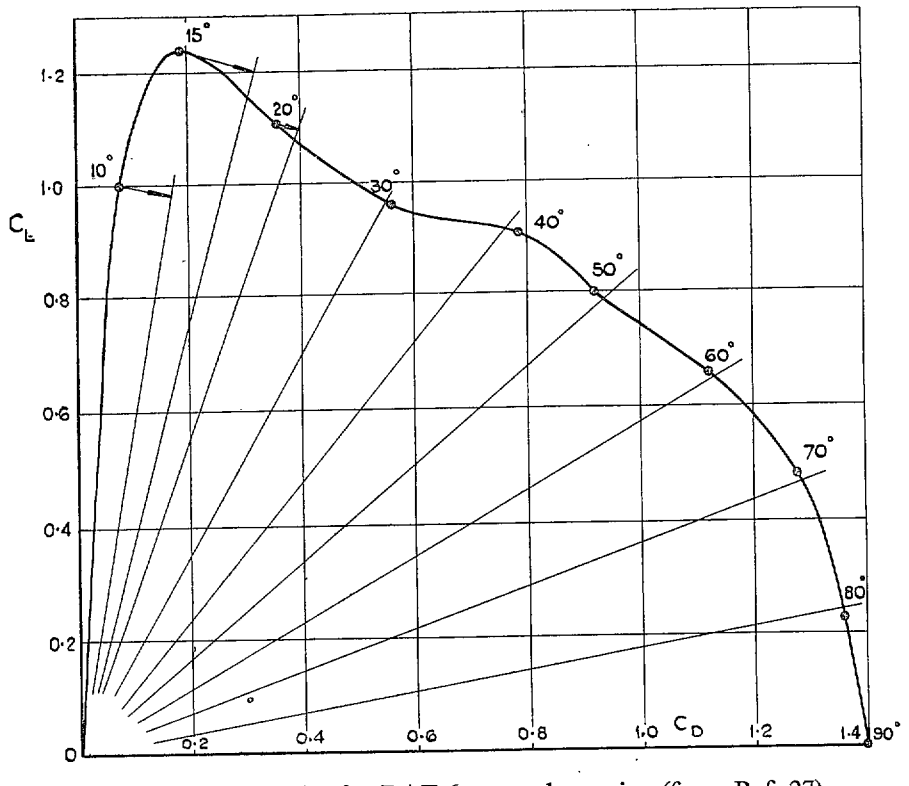

FIG. 7.15. Lift-drag polar for RAF 6 monoplane wing (from Ref. 27).

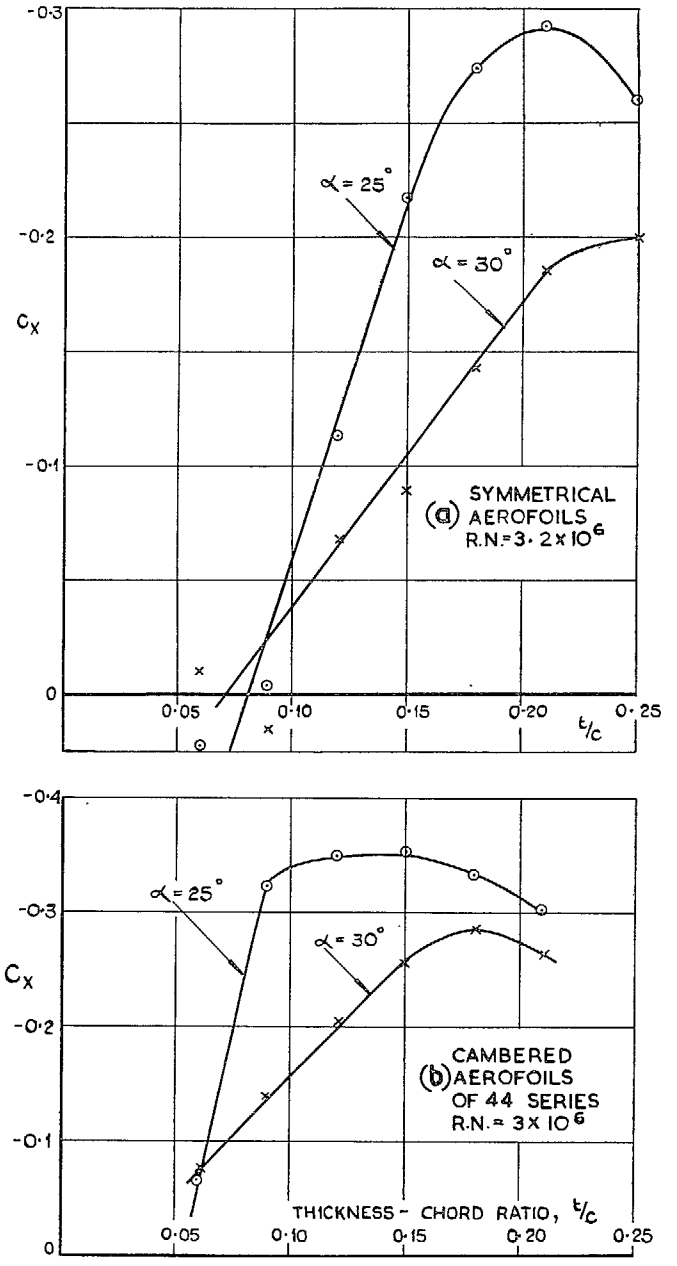

FIG. 7.16. Variation of chordwise force with thickness ratio and incidence (from Ref. 28).

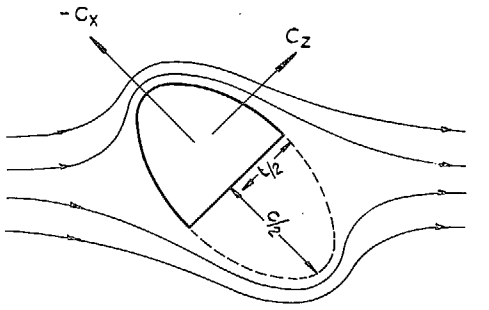

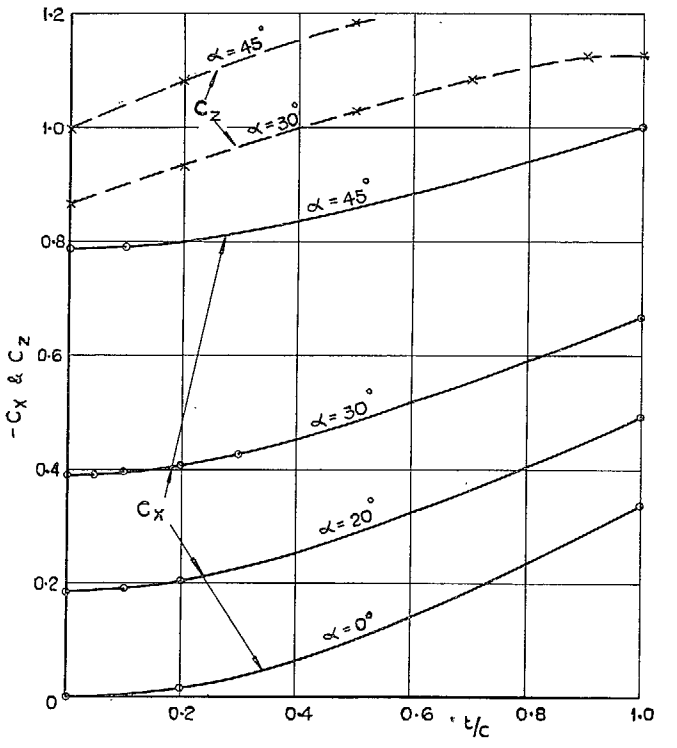

FIG. 7.17. Forces acting on semi-ellipses in potential flow.

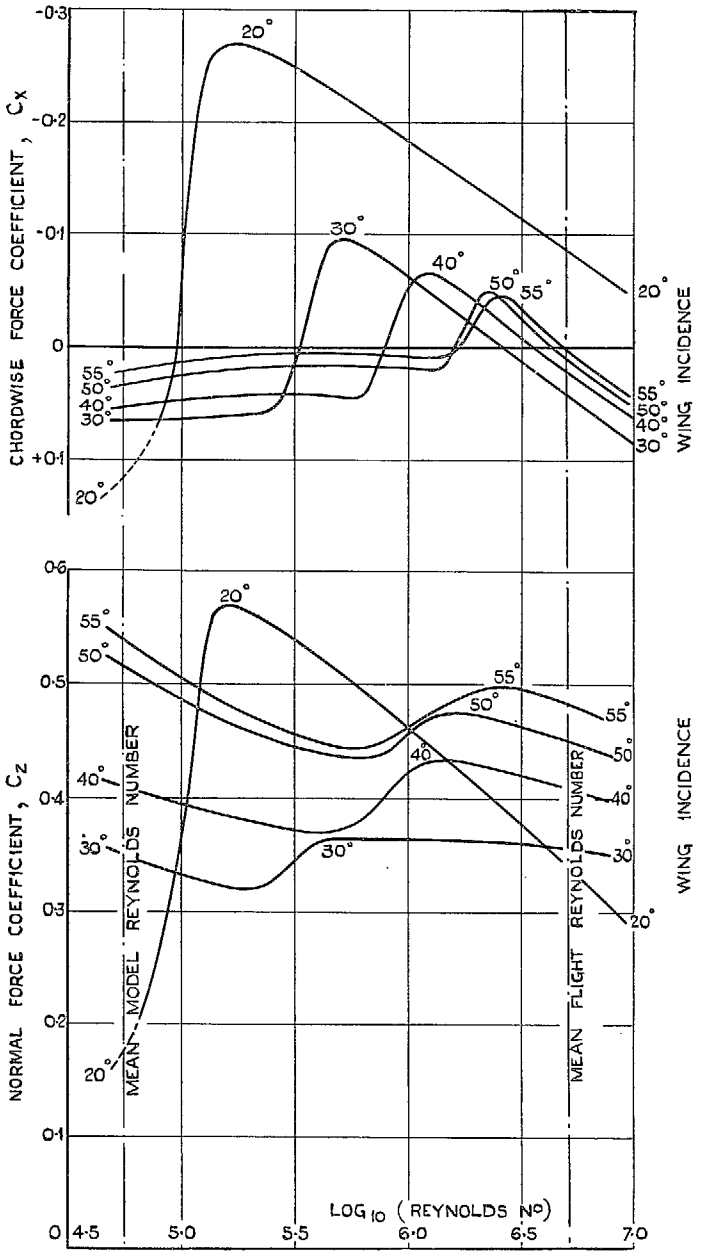

FIG. 7.18. Variation of chordwise and normal forces on a 21 per cent. thick wing.

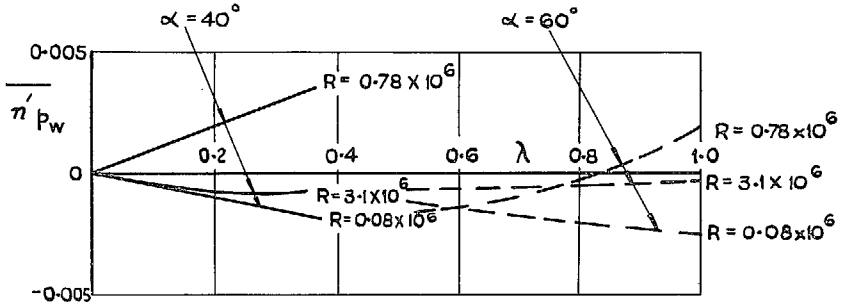

FIG. 7.19. Calculated wing yawing moments for graded profile. (Taper ratio = 2; C_x at tips = 0.)

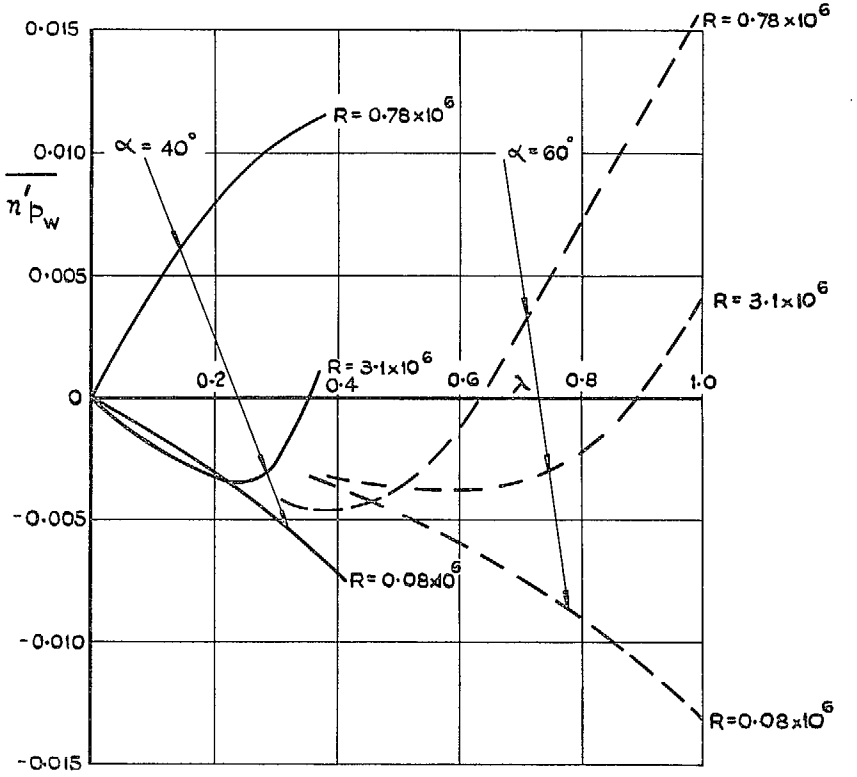

FIG. 7.20. Calculated wing yawing moments for constant profile. (Taper ratio = 2.)

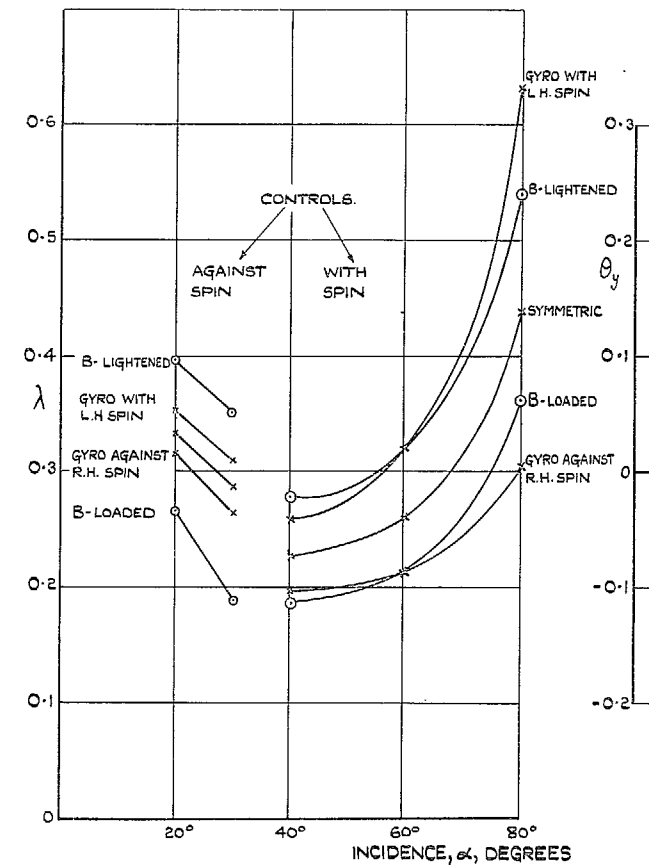

FIG. 8.1. Spin parameter as a function of α with and without gyroscopic moments.

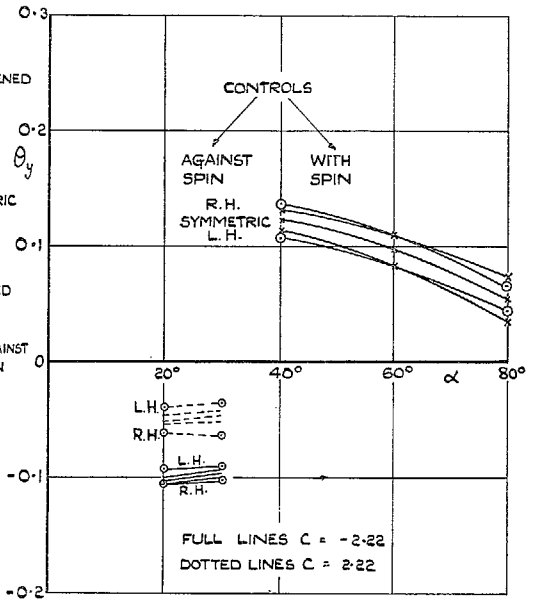

FIG. 8.2. Tilt angle against incidence.

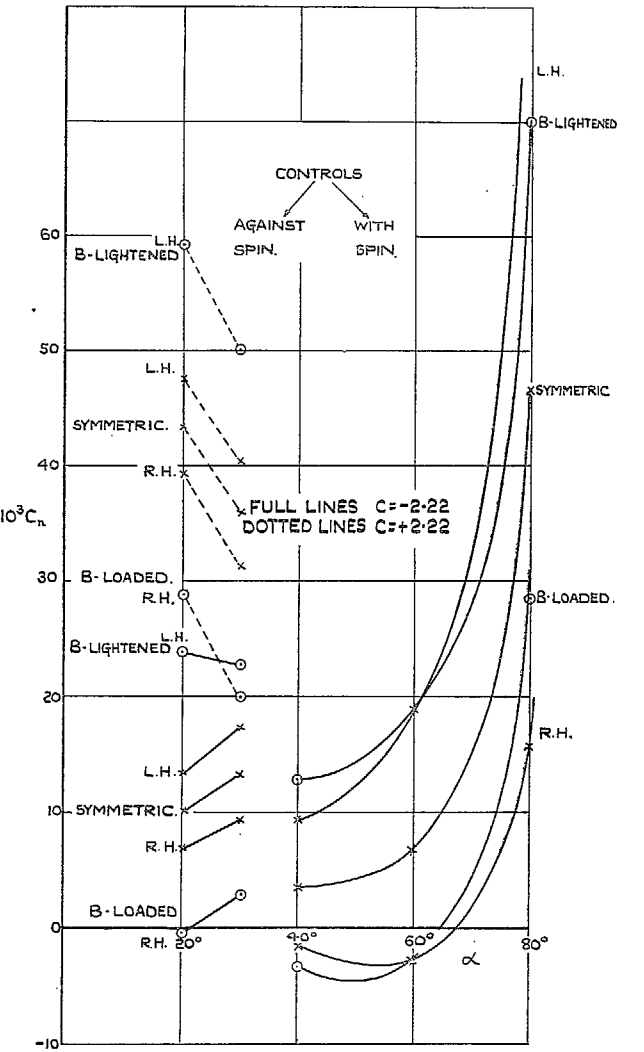

FIG. 8.3. Unbalanced yawing moments.

FIGS. 8.1 to 8.3. Specimen calculations of gyroscopic effects and representation by mass re-distribution.

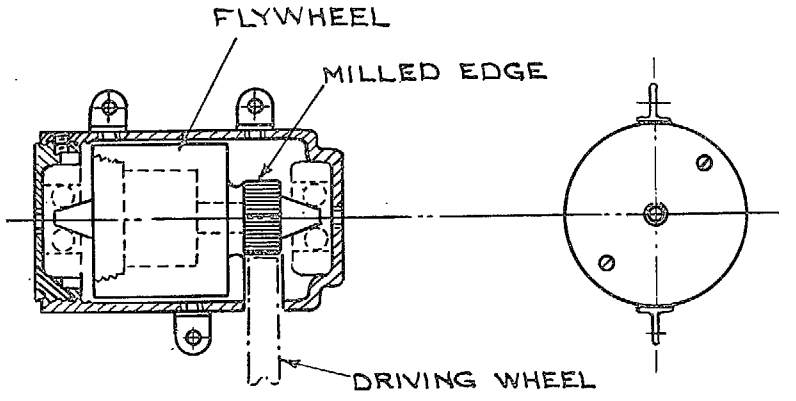

FIG. 8.4a. Flywheel used as model gyroscope.

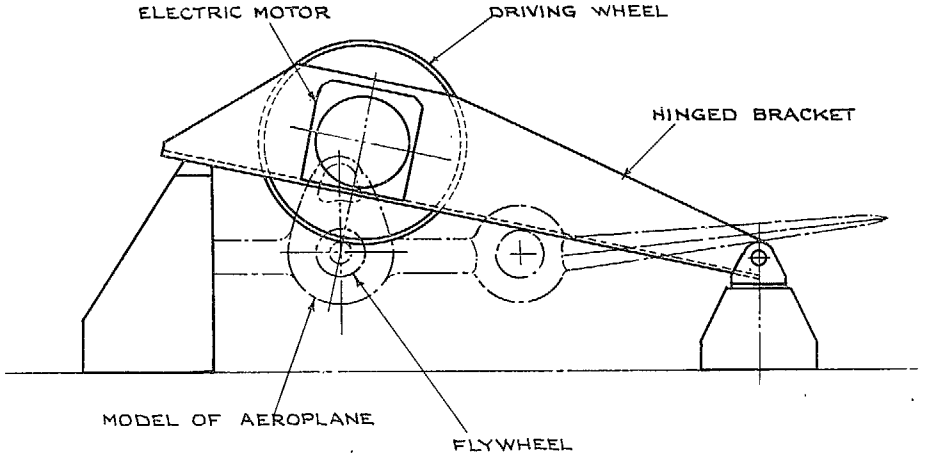

FIG. 8.4b. Method of accelerating the flywheel.

FIG. 8.4. Installation of flywheel in spinning model.

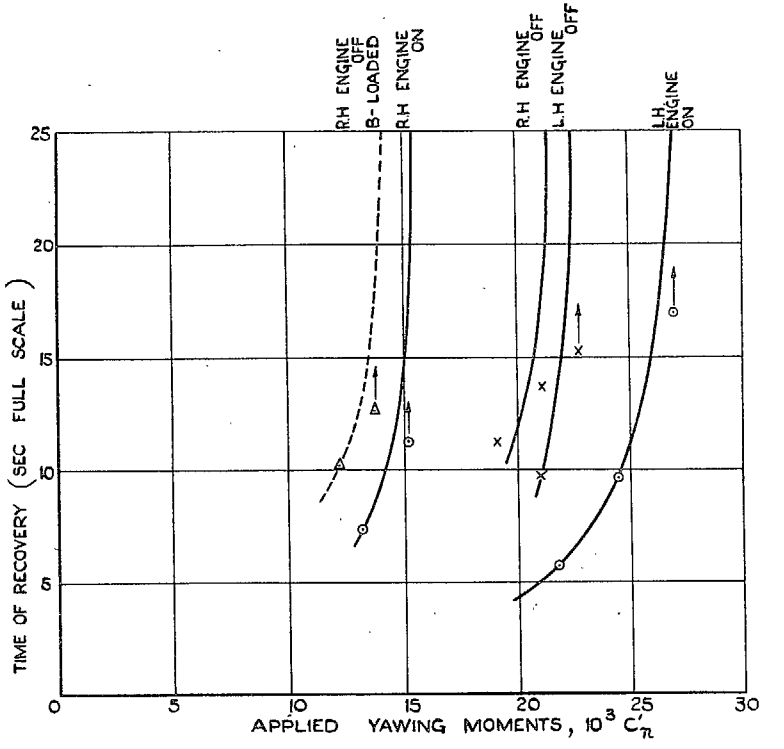

FIG. 8.5a. Recovery.

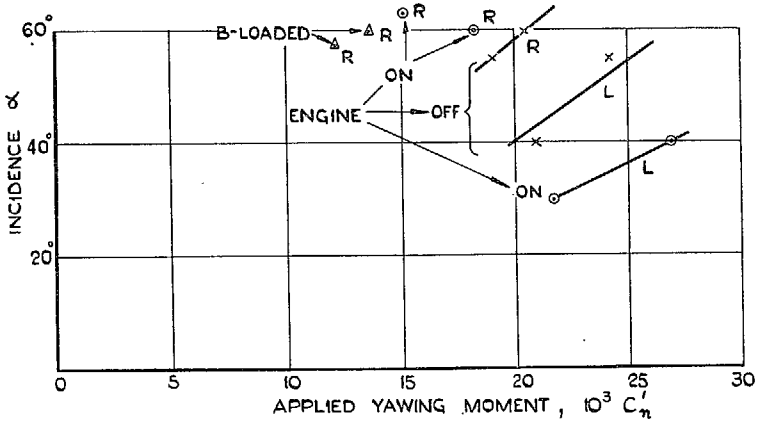

FIG. 8.5b. Incidence in the steady spin.

FIG. 8.5. Effect of gyroscopic moments on recovery and incidence: *Meteor*.

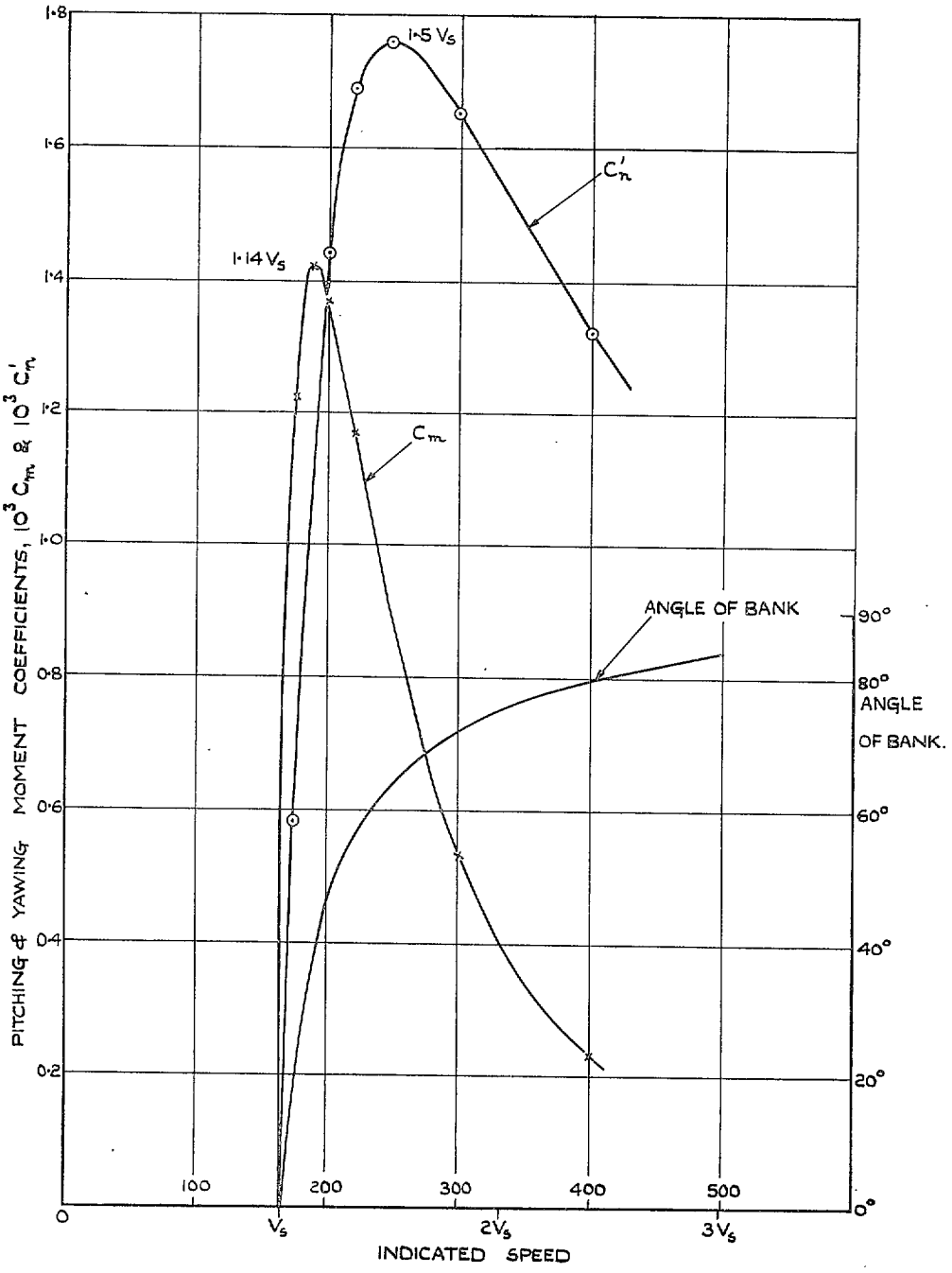

FIG. 8.6. Pitching and yawing gyroscopic moments in turns at the stall (*see* Chapter VIII, section 7).

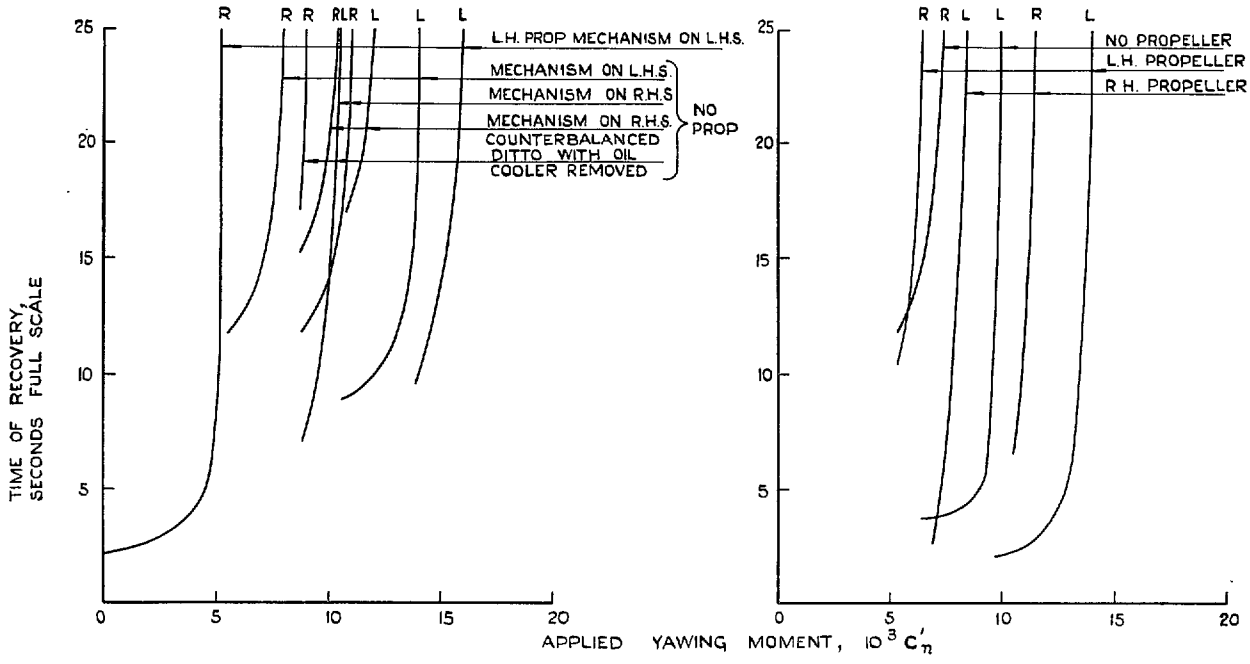

FIG. 8.7a. Effects of mechanism and oil cooler.

FIG. 8.7b. Effect of propeller.

FIG. 8.7. Factors affecting symmetry of model recovery: *Sea Fury*.

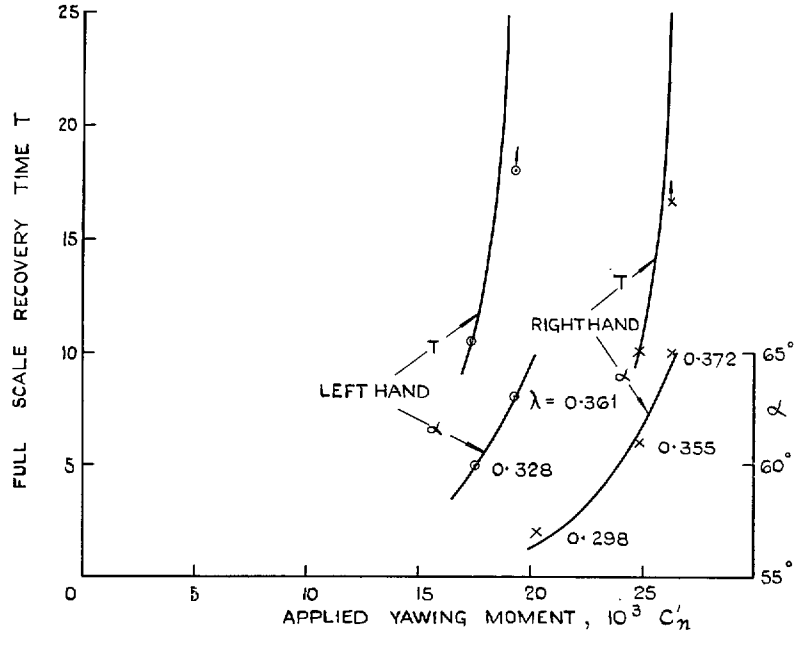

FIG. 8.8. Recovery and steady spin of *Hornet* model.

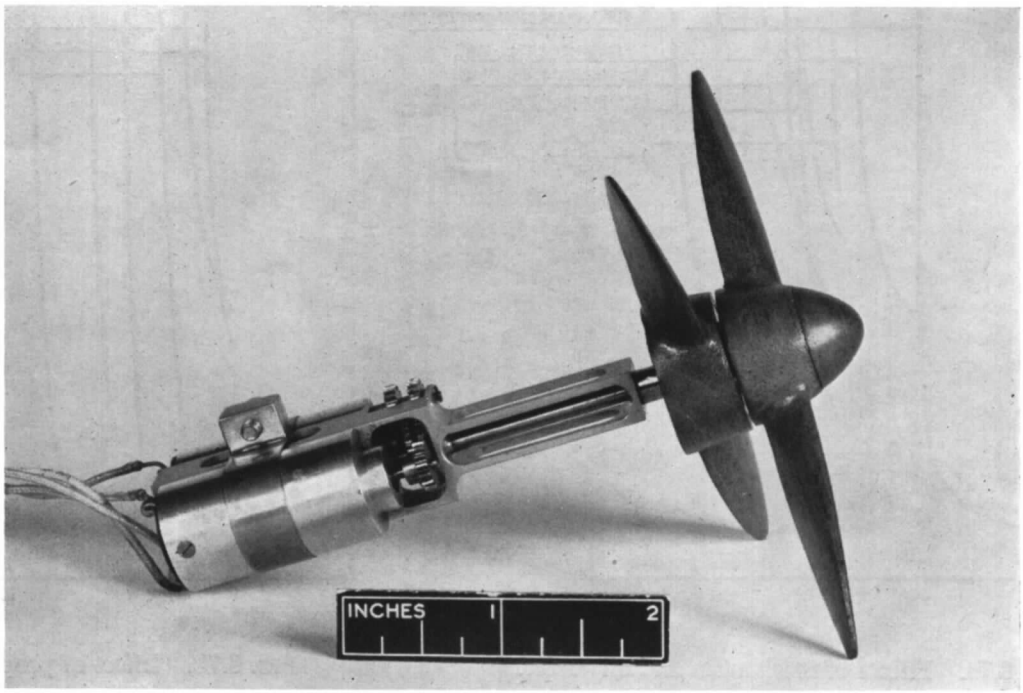

FIG. 8.9. Initial power unit—two motors.

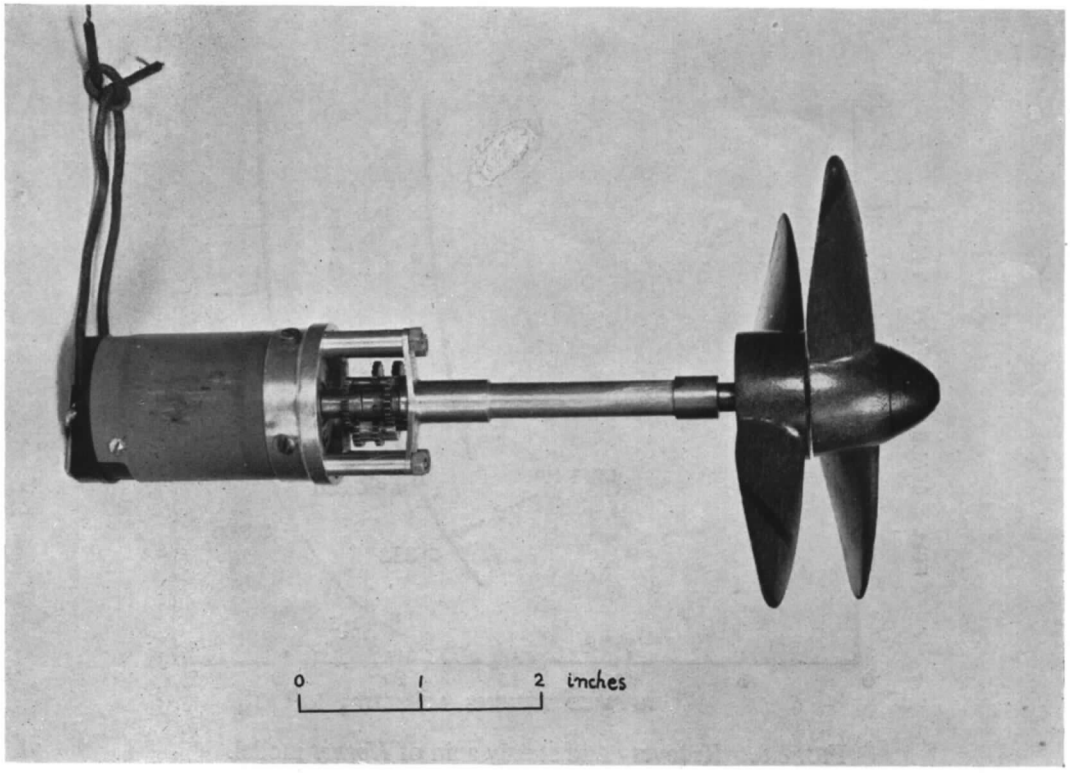

FIG. 8.10. Final power unit—single motor.

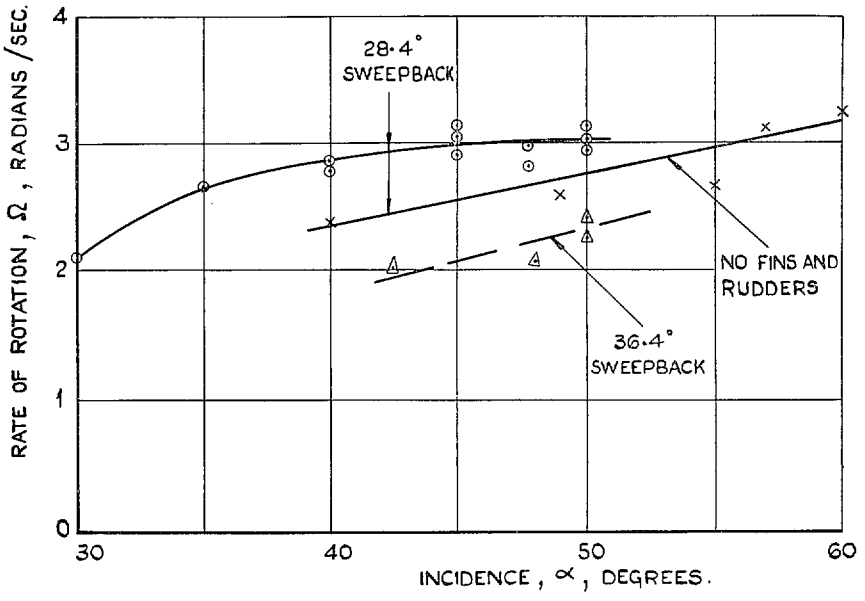

FIG. 9.1. Rate of rotation of G.A.L. tailless glider models.

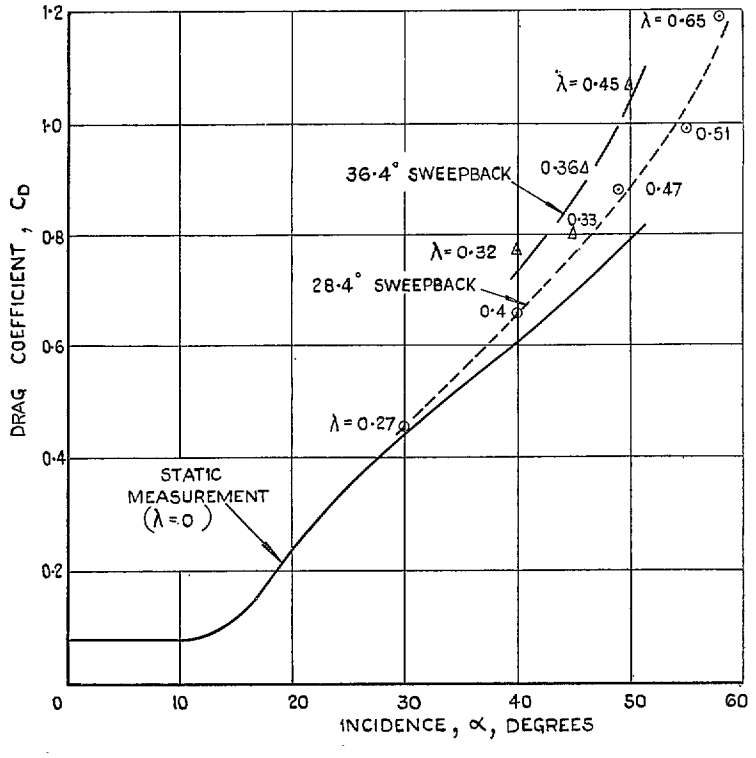

FIG. 9.3. Variation of drag with incidence, rate of rotation and sweepback for G.A.L. tailless glider models.

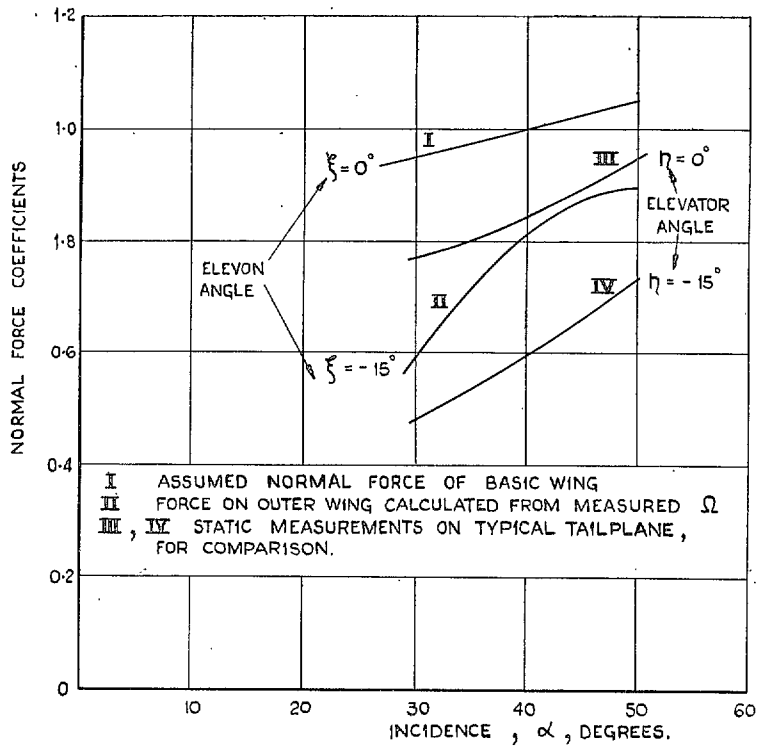

FIG. 9.4. Comparison of normal forces on wing of tailless aircraft with typical tailplane values.

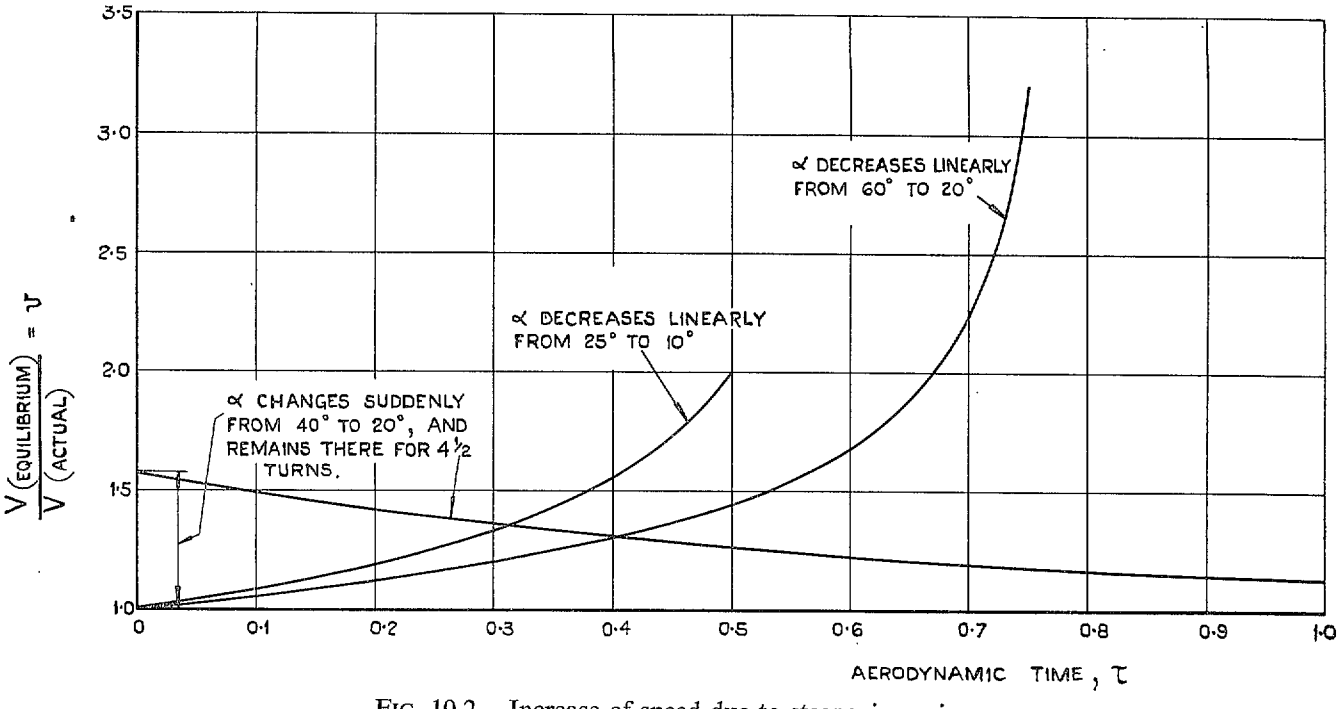

FIG. 10.2. Increase of speed due to steepening spin.

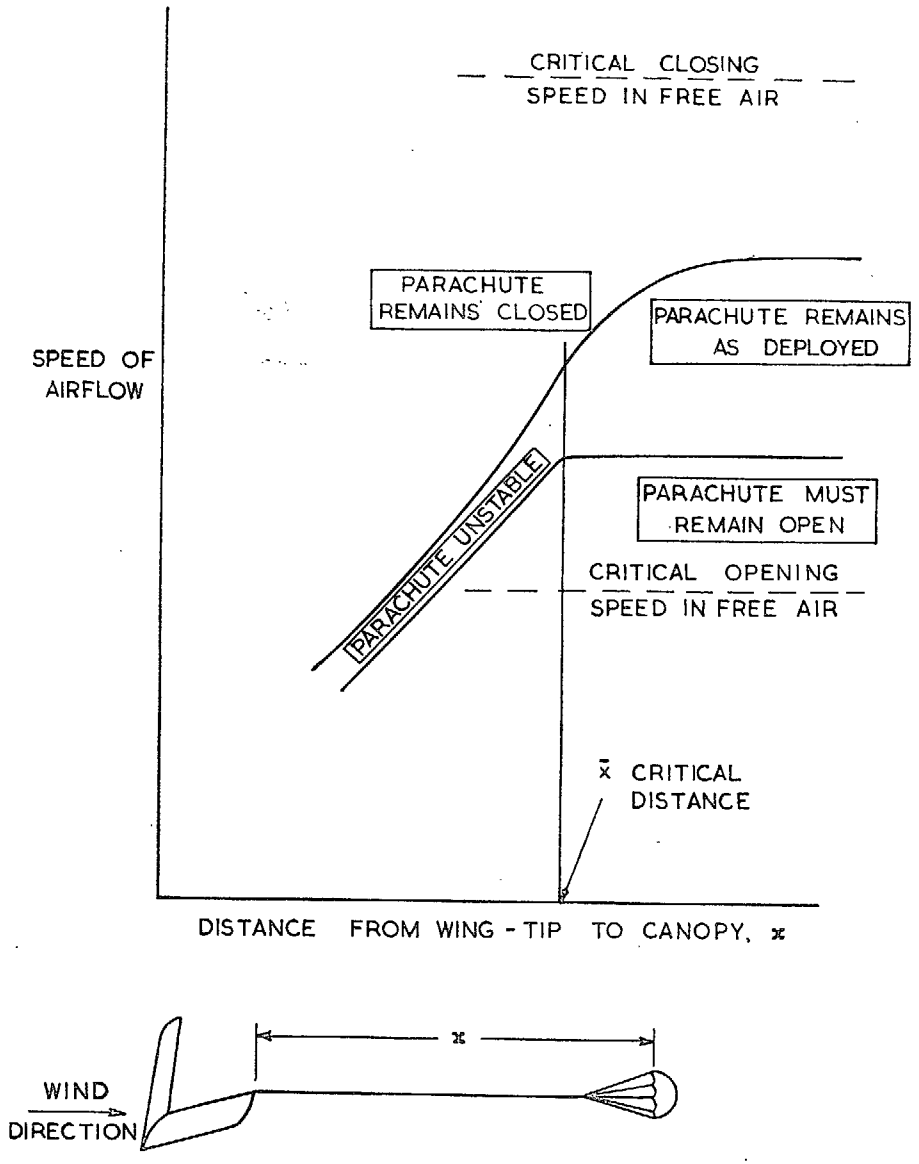

FIG. 10.3. Diagram showing effect of wing wake on critical speeds of anti-spin wing parachutes.

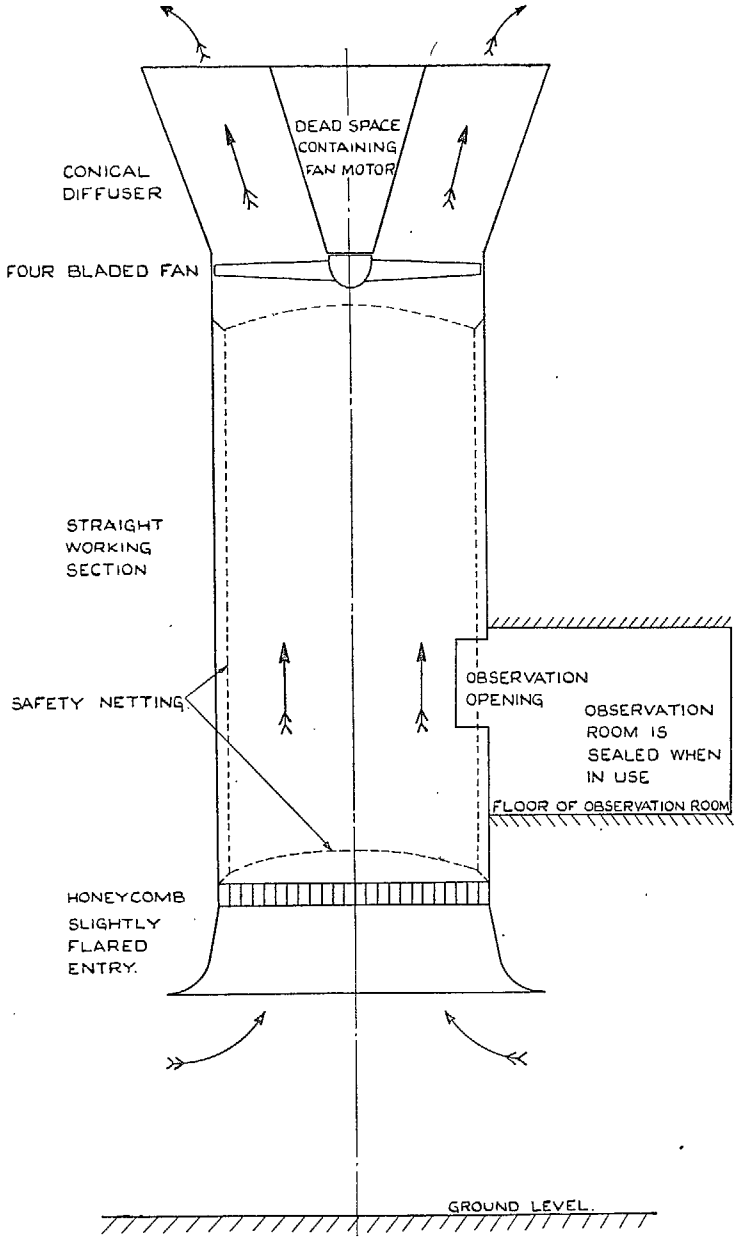

FIG. 11.1. Sketch showing arrangement of R.A.E. 12-ft diameter Vertical Wind Tunnel.

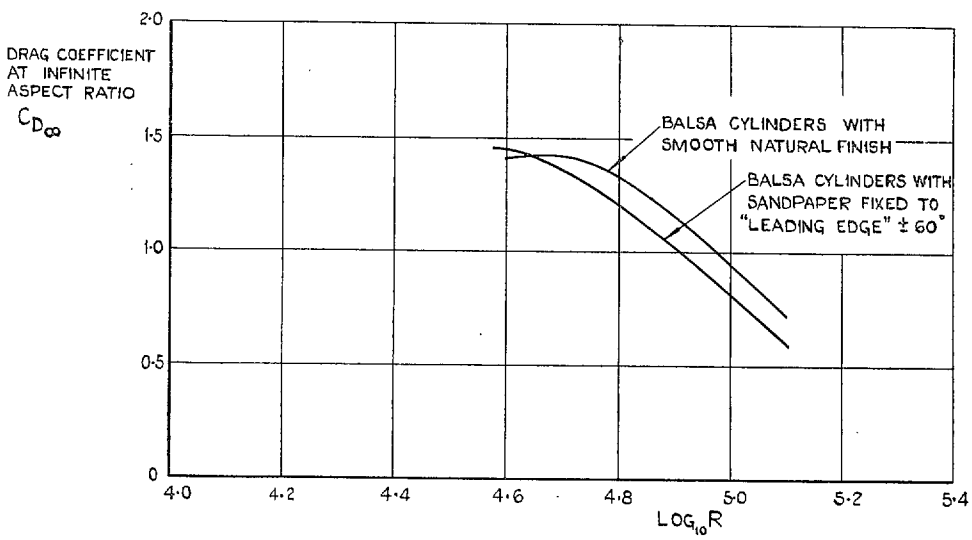

FIG. 11.2. Drag of circular cylinders in vertical tunnel.

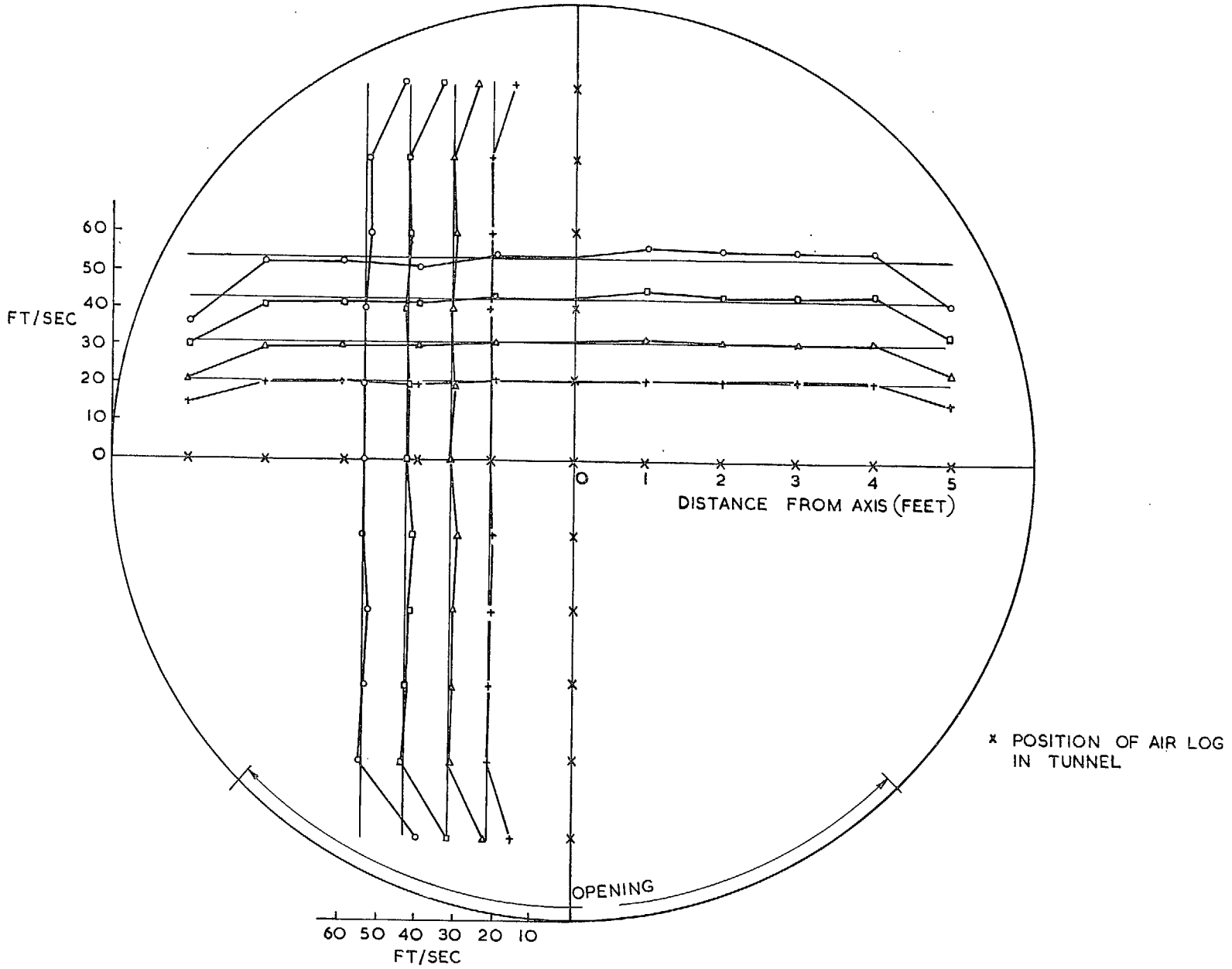

FIG. 11.3. R.A.E. Spinning Tunnel : velocity distribution at working-section.

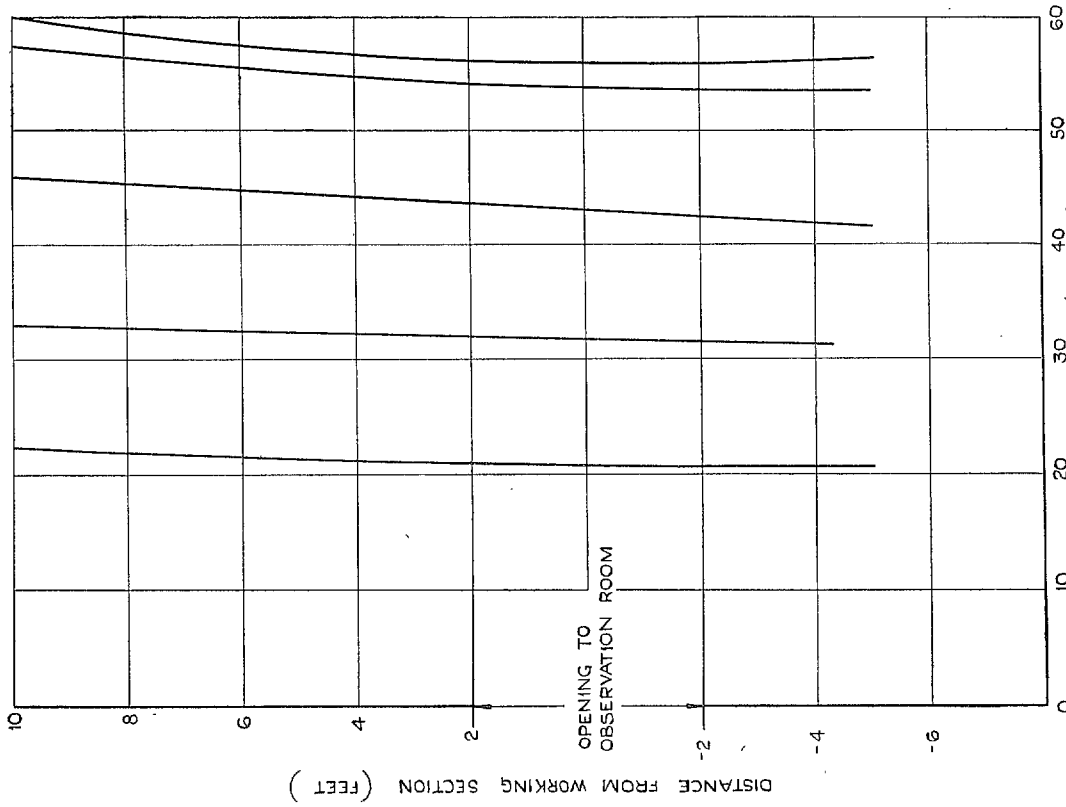

FIG. 11.4. R.A.E. spinning tunnel : velocity gradient.

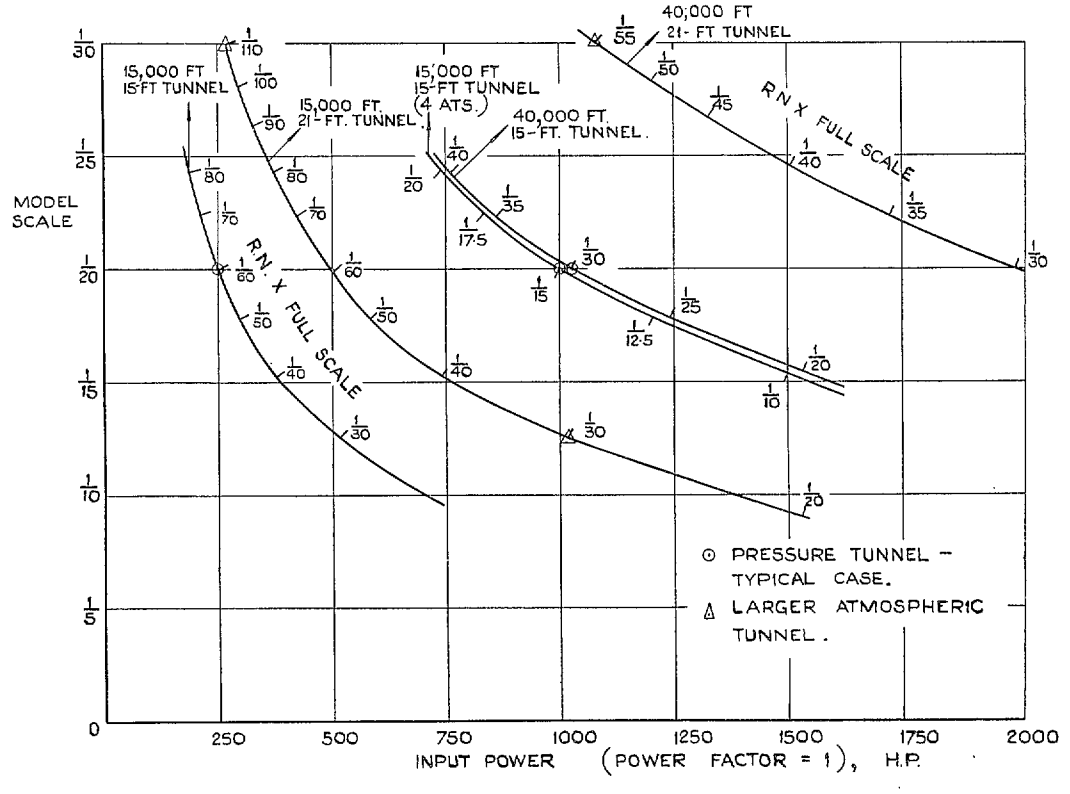

FIG. 11.5. Reynolds number of model spinning tests.

(2778) Wt. 19/8411 K.5 9/56 Hw.

S.O. Code No. 23-2906